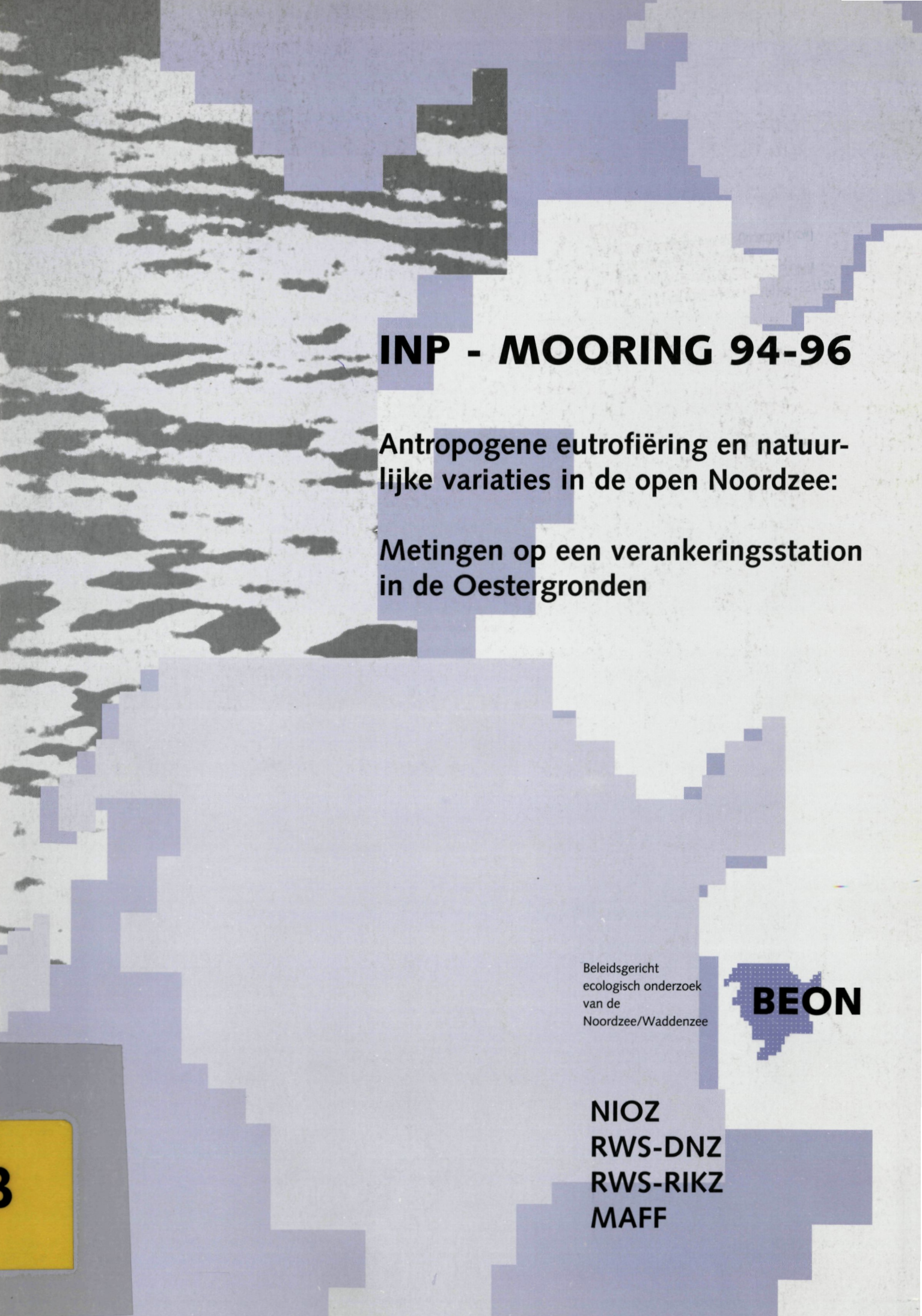


INP - MOORING 94-96

Antropogene eutrofiëring en natuurlijke variaties in de open Noordzee:

Metingen op een verankeringsstation in de Oestergronden

Beleidsgericht ecologisch onderzoek van de Noordzee/Waddenzee

BEON

NIOZ
RWS-DNZ
RWS-RIKZ
MAFF

IZWO
Instituut voor Zeewetenschappelijk Onderzoek (vzw)
Institute for Marine Scientific Research
VICTORIALAAN 3 - B-8400 OOSTENDE BELGIUM
Tel. +32-(0)59-321045 – Fax: +32-(0)59-3211

INP - MOORING 94-96

Antropogene eutrofiëring en natuurlijke variaties in de open Noordzee:

Metingen op een verankeringsstation in de Oestergronden

687

W. Van Raaphorst (NIOZ)

December 1996

BEON Rapport nr. 96-16

BEON project NIOZ 95 E 01 (Dit project is mede gefinancierd door NWO (NOP-VvA en GOA), EG (EC-MAST ERSEM II)

ISSN 0924-6576

Inhoudsopgave

1. INP - Mooring 94 - 96: "Executive summary" 1
W. van Raaphorst
1.1 Samenvatting 1
1.2 Conclusies 4
1.3 Producten en bijdrage van de partners aan het project 4
1.4 Beleidsrelevantie 5
1.5 Context van het onderwerp 5
1.6 Aanbevelingen 6

2. INP - Mooring: Scientific summary. 7
J.J.M. van Haren, F.C. van Duyl, D. Mills, W. van Raaphorst, H. Ridderinkhof, P. Ruardij.

Appendices

I. *W. van Raaphorst, J.F.P. Malschaert & J.J.M. van Haren.* Tidal resuspension and deposition of particulate matter in the Oyster Grounds, North Sea.
II. *F.C. van Duyl, G.C.A. Duineveld, A.J. Kop & G. Kraay.* Pelagic-benthic coupling in the North Sea: short-term dynamics in phytopigment sedimentation and response of benthic bacteria.
III. *P. Ruardij, H. Van Haren & H. Ridderinkhof.* The impact of the thermal stratification on production, succession and grazing on phytoplankton in shelf seas: a model study.
IV. *L. Lohse, H.T. Kloosterhuis, W. Van Raaphorst & W. Helder.* Denitrification rates as measured by the isotope pairing method and by the acetylene inhibition technique in continental shelf sediments of the North Sea.

1. "EXECUTIVE SUMMARY"

Wim van Raaphorst

1.1. Samenvatting

Achtergrond en Doelstelling

Dit rapport bevat de resultaten en conclusies van een uitgebreid onderzoek dat in het kader van het "Integrated North Sea Programme" (INP) is uitgevoerd in de Oestergronden, Noordzee. De metingen zijn begonnen direct na de start van het INP in juli 1991 mede op initiatief van het samenwerkingsverband BEON. Het zwaartepunt van het onderzoek lag in 1994. De hier beschreven werkzaamheden zijn uitgevoerd door het NIOZ, de RWS/DNZ, het RIKZ en MAFF (UK). Het data rapport met daarin het verslag van de meetaktiviteiten en de voorlopige resultaten van 1994 is verschenen als BEON rapport nr. 95-8, "Antropogene eutrofiëring en natuurlijke variaties: Consequenties voor de productiviteit van de Noordzee" (BEON project NIOZ 94 E 01).

Het voorliggende rapport dient als eindverslag bij het BEON project INP - Mooring 94-96 (NIOZ 95 E 01). De doelstelling van dit project was tweeledig:

- **Verschaffen van inzicht in de effecten op het pelagisch en benthisch ecosysteem van variaties in de vertikale transporten in een gelaagde waterkolom.** De gedachte achter deze doelstelling is dat vertikale transporten door de thermocline en aan het bodem-water grensvlak snel kunnen variëren onder invloed van weersveranderingen, wind en getij en dat daardoor (kort durende) uitwisselingen van nutriënten plaats kunnen vinden tussen de boven- en onderlaag van de waterkolom, die vervolgens weer kunnen leiden tot verhoogde primaire productie.
- **Bijdragen aan een verdere operationalisering van een geautomatiseerde monitoringstechniek die additioneel kan zijn voor het bestaande monitoringssysteem vanaf schepen.** Het onderzoek is uitgevoerd met behulp van uitgebreide verankeringssystemen met daarin nagenoeg continu registrerende fysische, chemische en biologische meetinstrumenten. De ervaring die met dit soort geavanceerde technieken is opgedaan kan van grote waarde zijn voor een eventuele invoering van routinematige geautomatiseerde meetmethoden op zee.

Meetlocatie

Het INP verankeringsstation bevond zich in de Oestergronden in de centrale Noordzee, 54° 25' Noord en 04° 02' Oost, waar het water ongeveer 45 m diep is. De waterkolom is in de zomer thermisch gestratificeerd met een warme bovenlaag van ongeveer 10-15 m dik, een tussenlaag met verminderde turbulentie op een diepte tussen 10 en 25 m, en een koude laag in de onderste 20 m boven de bodem. Slib en particulair organisch materiaal afkomstig uit de zuidelijke Noordzee, inclusief de Belgische, Nederlandse en de Engelse kust, kunnen in de Oestergronden uitzakken en zich tijdelijk ophopen in het sediment, vooral in de zomer. Tijdens herfst- en winterstormen vindt waarschijnlijk erosie plaats van het in de zomer gedeponeerde slib dat vervolgens verder getransporteerd wordt naar uiteindelijk het Skagerrak.

Werkzaamheden

De hier beschreven metingen zijn begonnen in november 1993 en geëindigd in februari 1995. In deze periode van totaal 15 maanden zijn voortdurend fysische, chemische en biologische waarnemingen verricht middels in verankeringen aangebrachte sensoren. Eens per maand werd een bezoek gebracht aan het station met de onderzoekvaartuigen Pelagia (NIOZ) en Holland (RWS/DNZ) voor inspectie van de verankeringen, onderhoud van de sensoren, uitlezen van de verzamelde data, calibratiemetingen en additionele bemonsteringen van m.n. de waterkolom. De bodem werd in detail bemonsterd tijdens de 18 daagse STED expeditie met de Pelagia in juli 1994, toen bodem-water interacties werden bestudeerd op 17 sub-stations binnen een afstand van 500 m van de verankeringen. Een enigszins apart onderdeel van STED was het analyseren en vergelijken van "klassieke" en geavanceerde technieken om de stikstofverwijdering door denitrificate in de bodem te meten.

Tijdens het INP - Mooring project zijn geïntegreerde waarnemingsreeksen verzameld van o.a. wind, stroomsnelheid, temperatuur en chlorofiel, die uniek zijn voor een open-zeestation wat betreft hun lengte en resolutie in de tijd. Deze reeksen zijn gebruikt als invoer voor en ten behoeve van de calibratie van het 1-dimensionale kolommodel STRAECOS. Het doel van dit model was de factoren te ontrafelen die de productie en biomassa van fytoplankton in een in de zomer gelaagde waterkolom bepalen. STRAECOS is gebaseerd op een fysisch menglaag-model dat ontwikkeld is op het NIOZ in combinatie met het ERSEM II ecosysteem model dat ontwikkeld is in een samenwerkingsverband tussen meerdere Europese instituten binnen het EC MAST programma.

Resultaten

Het seizoenspatroon van chlorofiel werd gedomineerd door een voorjaars- en een najaarsbloei van fytoplankton. Opvallend was dat de bloei zich ontwikkelde in het voorjaar voordat de gelaagdheid in de waterkolom zich definitief instelde. In deze periode was er een directe koppeling tussen de mate van turbulentie en de concentratie aan chlorofiel, hier (hier gebruikt als maat voor de algenbiomassa). De verzamelde meetreeksen laten zien dat verhoogde chlorofielconcentraties in het voorjaar alleen kunnen bestaan bij voldoende menging van de waterkolom. Kortdurende perioden met rustig weer die leiden tot premature en instabiele stratificatie hebben als direct gevolg dat de "voorjaarsalgen", vooral diatomeeën, uitzakken naar de bodem. Een daarop volgende, opnieuw kortdurende, periode met verhoogde turbulentie t.g.v. bijvoorbeeld wind, brengt de diatomeeën terug naar de fotische zone in de waterkolom, waar dan weer productie kan plaatsvinden. Wanneer de stratificatie uiteindelijk stabiliseert kunnen de diatomeeën en de daarin opgenomen nutriënten niet meer terug naar de bovenste, lichtrijke laag in het water en komt de bloei min of meer abrupt tot een einde. De consequentie van dit scenario is dat in het vervolg van het groeiseizoen nagenoeg alle nutriënten zich onder de thermocline bevinden. Inderdaad was in de zomer van 1994 de bovenlaag zeer helder zonder noemenswaardige hoeveelheden chlorofiel en vond de primaire productie vooral onder de thermocline plaats.

De subtiele wisselwerking tussen turbulentie en chlorofiel is niet alleen van belang voor de duur van de voorjaarsbloei en de vertikale positie van de zomerproductie in de waterkolom, maar ook voor de soortensamenstelling van het fytoplankton en de verdere structuur van het voedselweb in de zomer. Juist in het voorjaar vindt een snelle successie plaats van relatief snel zinkende diatomeeën naar minder zware soorten zoals flagellaten. Zet de stratificatie door tijdens de dominantie van diatomeeën dan krijgen flagellaten geen kans om tot bloei te komen omdat alle voedingsstoffen met de diatomeeën uitzakken naar de bodem. Is het begin van stabiele gelaagdheid iets (enkele dagen tot 1-2 weken) later in het jaar en bestaat een voldoende groot deel van de

algenpopulatie al uit flagellaten dan zinkt niet alles naar de bodemlaag en kan de bloei zich wel verder in het jaar doorzetten in de bovenste deel van de waterkolom.

De najaarsbloei ontwikkelde zich aan het eind van de zomer terwijl de gelaagdheid nog stabiel aanwezig was. In deze periode was de windsterkte matig zonder enige stormaktiviteit. Het STRAECOS model dat vertikale uitwisseling van nutriënten berekent op grond van door wind en getij geïnduceerde menging kon het begin van deze bloei niet reproduceren. Analyse van de fysische tijdreeksen laat echter zien dat in deze periode de vertikale menging, en daarmee de aanvoer van voedingsstoffen naar de bovenlaag van de waterkolom, vooral plaats vindt onder invloed van interne golven die, mogelijk onder invloed van stormen, aan de rand van de Noordzee en de Atlantische Oceaan worden opgewekt.

Tijdens de STED expeditie in juli 1994 is vastgesteld dat slibaccumulatie inderdaad kan plaatsvinden in de Oestergronden. Deze accumulatie wordt in de zomer gevoed door aanvoer vanuit het zuid-oosten, d.w.z. uit de richting van het Friese Front en, mogelijk, de Nederlandse kust. Accumulatie is echter geen statisch proces maar de netto resultante van gelijktijdig optredende maar gemiddeld iets grotere depositie- dan resuspensiefluxen. Hoewel de slibdeeltjes die aan de depositie-resuspensie sequentie deelnamen verrijkt waren met organisch materiaal t.o.v. het materiaal in de bovenste mm's van de bodem en aantoonbaar soms ook vers algenmateriaal bevatten, kon geen directe respons van de benthische microfauna op de depositiefluxen worden aangetoond. De gevonden netto (zomer)accumulatie van organisch materiaal op de bodem was echter ruim voldoende om de bacteriële productie in het sediment te kunnen onderhouden. Bovendien dienen ook de organische componenten in de slibdeeltjes die niet "de hele zomer" blijven liggen maar na gemiddeld 1-2 weken weer resuspenderen, als voedselbron voor de lokale bodemfauna. Deze waarnemingen gelden voor een tijdschaal van enkele weken. Gemiddeld over enkele jaren is de netto accumulatie van sediment in de Oestergronden waarschijnlijk nihil, omdat veel materiaal geërodeerd wordt tijdens herfst- en winterstormen en vervolgens verder getransporteerd naar naar het uiteindelijke depositiegebied in het Skagerrak. In zekere zin functioneren de Oestergronden dus als een doorgangshuis voor particulair materiaal. Echter, tijdens het verblijf in "dit huis" blijft het slib niet ongewijzigd en wordt een substantieel deel van het geassocieerde organisch materiaal microbiologisch afgebroken. Transport en tijdelijke depositie van particulair organisch materiaal heeft dus een belangrijke ecologische betekenis in de Oestergronden.

Tijdens STED zijn ook de denitrificatiesnelheden in de bodem van het verankeringsstation gemeten met de acetyleen inhibitiemethode en de "isotope pairing" techniek. De meeste experimentele denitrificatie getallen die tot nu toe gehanteerd werden voor de Noordzee zijn op de eerste methode gebaseerd. De resultaten van de vergelijkende metingen laten echter zien dat de op de klassieke acetyleen inhibitie methode gebaseerde snelheden de werkelijke denitrificatie flink onderschatten.

Tot slot. Tijdens het project is gewerkt met geavanceerde meettechnieken waarvan sommige, bijvoorbeeld de in situ nitraat autoanalyser, nog in een ontwikkelingsfase verkeerden. Dit betekende dat tijdens de maandelijkse tochten naar het station steeds allerlei grote en kleine problemen moesten worden opgelost. Al met al is ongeveer 30% van de geplande registraties mislukt, waarvan ongeveer 10% door het verlies van een complete verankering of een instrument. Als algemene lijn kwam naar voren dat sensoren voor fysische parameters (o.a. stroommeters, temperatuur) ongeveer 3-12 maanden onbeheerd kunnen worden gelaten. Bio-optische instrumenten (o.a. chlorofiel) vragen daarentegen maandelijke verzorging, en geautomatiseerde nutrienten analyse apparatuur moet eigenlijk (nog) dagelijks worden bijgesteld. Ook het bewerken van de uitgebreide meetreeeksen bleek geen sinecure maar specialistisch werk dat onvermoed veel tijd heeft gekost. Zelfs nu, ongeveer 2 jaar na de laatste vaartocht, wordt nog gewerkt aan het in detail analyseren en corrigeren van de door de stroommters

gegenereerde tijdreeksen. Een routinematig gebruik van verankeringssystemen als monitoringtechniek in de. open Noordzee lijkt daarom voorlopig nog niet zinvol.

1.2. Conclusies

- Kortdurende variaties in de intensiteit van de menging van de waterkolom in de Oestergronden bepalen mede de ontwikkeling van de algenbloei in het voorjaar. De preciese timing van het begin van de stabiele (zomer)stratificatie heeft consequenties voor de algenproductie en -soortensamenstelling in het gehele groeiseizoen.
- Aan het eind van de zomer van 1994 ontwikkelde zich een algenbloei op de Oestergronden, waarschijnlijk als gevolg van door interne golven gedreven uitwisseling van nutriënten door de thermocline. De dynamiek en duur van een dergelijke algenbloei kon gedecteerd worden dankzij de toegepaste continu registratie van zowel fysische als biologische parameters.
- De bodem van de Oestergronden functioneert als een doorgangshuis van slib afkomstig uit de zuidelijke Noordzee. De tijdelijke depositie van organisch materiaal is voldoende om de benthische fauna te voeden. Als eutrofiëring in de zuidelijke Noorzee leidt tot verhoogde productie van organisch materiaal zal een deel hiervan waarschijnlijk terecht komen in de Oestergronden.
- Maandelijkse bemonstering is onvoldoende om de variaties in chlorofiel in de zomer goed vast te stellen. Ook voor een goede beschrijving van de voorjaarsbloei zijn hoog-frequente waarnemingen noodzakelijk. Vanuit dit perspectief is de toepassing van geautomatiseerde monitoringstechnieken m.b.v. verankerde sensoren een veelbelovende ontwikkeling.
- Op dit moment, echter, zijn geavanceerde meettechnieken m.b.v. verankeringen nog niet geschikt voor routinematig gebruik voor monitoringsdoeleinden in open-zeegebieden, omdat de sensoren nog te veel en te regelmatig onderhoud vereisen.

1.3 Producten en bijdrage van de partners aan het project

De volgende producten zijn tot stand gekomen in het kader van het INP-Mooring project.

1. LOHSE, L., H.T. KLOOSTERHUIS, W. VAN RAAPHORST & W. HELDER (1996). Denitrification rates as measured by the isotope pairing method and by the acetylene inhibition technique in continental shelf sediments of the North Sea. Mar. Ecol. Prog. Ser. **132**: 169-179.
2. RUARDIJ, P., H. VAN HAREN & H. RIDDERINKHOF (1996). The impact of the thermal stratification on production, succession and grazing on phytoplankton in shelf seas: a model study. Submitted to J. Sea Res.
3. VAN BOSTELEN, A.J., K.H.M. SCHRADER & W. ZEVENBOOM (1995). Characterization of macro-and meiobenthos at the INP-mooring site in the Oyster Grounds and surrounding areas. North Sea Directorate Report, NZ-95.06.
4. VAN DUYL, F.C., G.C.A. DUINEVELD, A.J. KOP & G. KRAAY (1996). Pelagic-benthic coupling in the North Sea: short-term dynamics in phytopigment sedimentation and response of benthic bacteria. Submitted to Aquat. Microb. Ecol.
5. VAN HAREN, H. (1996). Correcting false thermistor string data. Cont. Shelf Res. **16**: 1871-1883.
6. VAN 't HART, R., M. LAGERWERF, M. & W. ZEVENBOOM (1995). Field survey report INP-Mooring 1994: On-line measurements with m.s. Holland and m.s. Smal Agt. North Sea Directorate Report, NZ-95.07.
7. VAN RAAPHORST, W., F.C. VAN DUYL, H. RIDDERINKHOF, R. RIEGMAN & P. RUARDIJ (1995). Antropogene eutrofiëring en natuurlijke variaties. Consequenties voor de productiviteit van de Noordzee. BEON Rapport nr. 95-8.

8. VAN RAAPHORST, W., J.F.P. MALSCHAERT & J.J.M. VAN HAREN (1996). Tidal resuspension and deposition of particulate matter in the Oyster Grounds, North Sea. Submitted to J. Mar. Res.
9. ZEVENBOOM, W., ALTHUIS, IJ.A., WETSTEYN, L.M.F.J. & D.K. MILLS (1993). INP-Mooring: A joint study on the effects of physical processes on nutrients and phytopankton. Report 93.9-NZ-N (NUT 8/12/INFO 2).
10. Althuis, IJ. (1996). INP fluorescentiemetingen op T135. Continue registratie van algenbiomassa: wat is de meerwaarde. RIKZ werkdocument ter voorbereiding van publicatie. pp 1-7.

De publicaties met de nummers 1, 2, 4 en 8 zijn als appendix aan dit rapport toegevoegd. Ook de producten met de nummers 3, 6 en 9 die door RWS/DNZ zijn verzorgd moeten gezien worden als een integraal onderdeel van deze eindrapportage.

Het INP-Mooring project is uitgevoerd als een samenwerking tussen NIOZ, RWS/DNZ, RIKZ en MAFF(UK). Het grootste deel van het werk is verzorgd door het NIOZ (producten 1,2,4,5, 7 en 8). De bijdrage van RWS/DNZ heeft bestaan uit het verzamelen en uitwerken van de gegevens die met de Holland en Smal Agt verzameld zijn op het verankeringsstation (product 6, 9) en uit het bewerken van meio- en macro-benthos gegevens van de Oestergronden (product 3). Met name de "on-line" gegevens van de Holland zijn van grote waarde geweest voor het project, o.a. voor het calibreren van de fluorometers en voor het afregelen van het STRAECOS model. Daarnaast heeft RWS/DNZ een deel van de logistieke taken voor haar rekening genomen. Voor het RIKZ is een aantal malen een plankton deskundige meegeweest tijdens een van de tochten met de Pelagia naar het station en heeft IJ Althuis de resultaten van de fluorescentiemetingen vergeleken met de standaard chlorofielbepalingen die gedaan zijn in het kader van het reguliere RWS monitoring programma. D.K. Mills van het MAFF (UK) heeft een onschatbare bijdrage geleverd aan het uitwerken van de fluorescentiemetingen.

1.4 beleidsrelevantie

Het uitgevoerde onderzoek is relevant voor het beheer en beleid van de noordzee omdat het inzicht verschaft in de processen die sturend zijn voor de algen-soorten-samenstelling en de primaire productie in het Nederlands deel van de centrale Noordzee. De resultaten laten zien dat natuurlijke variaties leidend tot een iets vervroegd of verlaat begin van de stratificatie in het voorjaar, of tot een verhoogde vertikale menging door interne golven en wind in de zomer een belangrijke rol spelen in de Oestergronden. Omdat het gebied dient als tijdelijke opslag van particulair materiaal afkomstig uit de (geëutrofiëerde) zuidelijke Noordzee kunnen maatregelen ter reductie van de N en P afvoer van de grote rivieren gevolg hebben voor de depositie van organisch materiaal in de Oestergronden en daarmee voor de beschikbaarheid van voedsel voor de lokale bodemfauna.

De verzamelde tijdreeksen zullen een belangrijk hulpmiddel kunnen zijn bij het verder ontwikkelen, calibreren en interpreteren van eutrofiëringsmodellen voor de Noordzee.

De ervaringen die zijn opgedaan tijdens dit onderzoek geven aan dat het gebruik van geavanceerde verankeringssystemen als monitoringstechniek in de centrale Noordzee nog te moeilijk en daarom, voorlopig, nog niet aan te bevelen is.

1.4. Context van het onderwerp

Het project INP - Mooring 94-96 is uitgevoerd onder de BEON speerpunt "eutrofiëring". Refererend naar het 2e MJP BEON zijn de volgende trefwoorden op dit onderzoek van

toepassing: *Monitoringstechnieken, voedselwebrelaties (natuurlijke vs antropogene factoren).*

Het onderzoek heeft bijgedragen aan het inzicht in de mechanismen die de productie en beschikbaarheid van voedsel in de Noordzee bepalen. Als zodanig heeft het zich gericht op de laatste schakel in de bron-effect keten: Reductie van de nutriëntenafvoer van de rivieren - sanering eutrofiëring Zuidelijke Noordzee - effect voor het voedselweb in de gestratificeerde centrale Noordzee.

1.5 Aanbevelingen

- Omdat enerzijds een hogere waarnemingsfrequentie vereist is om de ontwikkeling van de algenbiomassa en soortensamenstelling in de centrale Noordzee goed in kaart te brengen, en anderzijds geautomatiseerde meettechnieken voorlopig nog niet geschikt lijken voor routinematige toepassing, wordt aanbevolen om in belangrijke perioden van het jaar, bijvoorbeeld rond het begin van stratificatie in het voorjaar, 2 of 3 keer per maand een conventionele bemonstering (monitoring) vanaf een schip uit te voeren.
- Om in de nabije toekomst wel zinvol gebruik te kunnen maken van routinematige bemonsteringen m.b.v. verankerde sensoren, is voortgaand onderzoek naar de optimalisering van slimme in situ sensoren noodzakelijk.
- Lateraal transport van kleine slibdeeltjes en particulair organisch materiaal,gevolgd door depositie en resuspensie, verder transport etc., speelt een cruciale rol in de zogenaamde benthisch-pelagische koppeling en de beschikbaarheid van voedsel voor de bodemfauna in de Noordzee. Nader onderzoek vanuit het oogpunt van het functioneren van het ecosysteem naar de dynamiek van fijn particulair materiaal in de Noordzee is gewenst.
- Fysisch, chemisch en biologisch onderzoek wordt veelal nog gescheiden uitgevoerd. Het INP- Mooring project laat duidelijk zien dat vooral geïntegreerd multidisciplinair onderzoek in een gecompliceerd systeem als de Noordzee kan bijdragen aan het geven van antwoorden op zowel wetenschappelijke als beleidsrelevante vragen. Directe combinatie van modelontwikkeling met experimenteel werk geeft een meerwaarde aan beide typen van onderzoek. Aanbevolen wordt om dit soort multidisciplinair onderzoek te stimuleren.

2. INP - MOORING: SCIENTIFIC SUMMARY

Hans van Haren[1], Fleur C. van Duyl[1], Dave Mills[2], Wim van Raaphorst[1], Herman Ridderinkhof[1], Piet Ruardij[1]
and RWS-DNZ, RIKZ

[1]NIOZ, P.O. Box 59, 1790 AB Den Burg, the Netherlands
[2]MAFF Fisheries Lab, Lowestoft, Suffolk NR33 OHT, UK

2.1. The project

Although the North Sea is claimed to be one of the marine ecosystems most intensively studied ever, detailed descriptions of the seasonal cycle of phytoplankton are limited. Most studies are based on sampling insufficient to resolve even the main features of the annual cycle or on measurements in coastal stations close to marine laboratories and therefore not representative for the offshore environment. Until the end of the eigthies, the technology of oceanographic instrumentation prevented a comprehensive data set from being constructed, because moorable instruments capable of measuring biological parameters were not available.

In July 1991 the Integrated North Sea Programme (INP) was launched to carry out an extensive field study to establish properly the variability of phytoplankton abundance in the central North Sea covering a full annual cycle. In contrast with shallower parts of the North Sea, which are well-mixed from surface to bottom throughout the year, this part of the North Sea becomes statically stably stratified in spring, after a period of sufficient insolation, which lasts through the summer. In this area the water depth exceeds the sum of the depth of a wind mixed near-surface layer (typically 10-15 m) and that of a tidally mixed near-bottom layer (typically 10-30 m, depending on the current speed).

At the start of the project, the established idea was that the onset of a large phytoplankton bloom in spring will not occur before stratification is established and the surface mixed layer is shallower than the critical optical depth. For the open ocean on the other hand, some researchers predicted a spring bloom prior to, and even advancing in time, the onset of stratification. For the summer one assumed that in the central North Sea the two well-mixed layers are separated by a sharp and thin density jump (pycnocline), which acts as a barrier for vertical exchange of solutes. As nutrients are to be supplied mainly from the bottom in addition to local regeneration, such physical system implies, under the assumption that the critical optical depth is not larger than the local water depth, a near-bottom mixed layer which is relatively light limited and a near-surface mixed layer which is relatively nutrient limited. Then, the maximum amount of phytoplankton is to be found not in the photic zone proper, but rather near the pycnocline, i.e. roughly in the middle of the water column.

The main aim of INP was to verify this concept and to study the influence of atmospheric disturbances on the vertical exchange across the pycnocline. It was expected that such diapycnal mixing events and the associated short-term bursts of fluxes of nutrients (and perhaps phytoplankton) between the near-bottom and the near-surface mixed layers would happen irregularly in time, and might have longer-term impact on the pelagic biology, especially the phytoplankton species composition, abundance, productivity and sedimentation.

In addition, further aims of the project were to use newly developed moorable instruments to sample the relevant physical, biological and chemical data over long periods of time (up to a year) and at a sufficiently high rate (at least once an hour). This provided a test for future long-term unmanned oceanographic monitoring. Finally, the

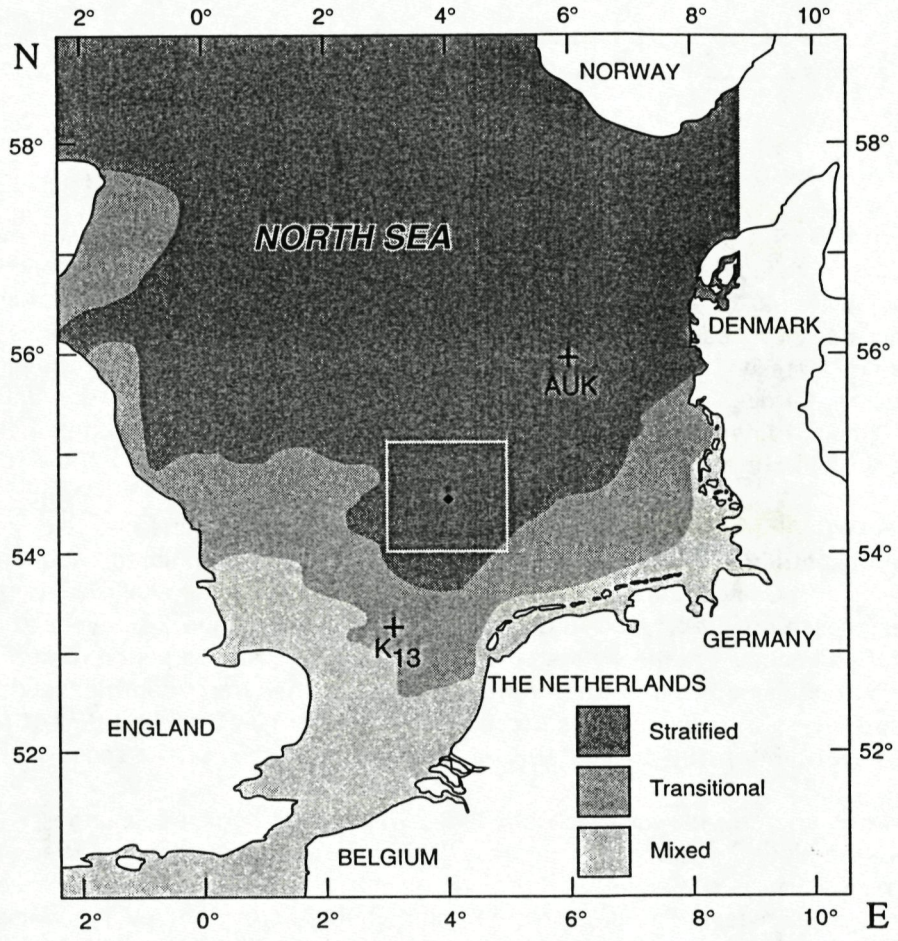


Figure 1. Map of the INP research area (rectangle), the mooring site (•) and the platforms for meteorological data superposed on a general indication of the summer stratification extent.

data should be used to initiate and calibrate a new coupled model for the lower trophic levels in the pelagic system.

2.2. Logistics and technology

The INP mooring site is located in the central North Sea, Oyster Grounds, at 54° 25' N and 04° 02' E, where the waterdepth is about 45 m (Fig. 1). The location is well within the region of seasonal (thermal) stratification. The site has been chosen with care to be well away from frontal zones marking the transition between stratified and totally mixed waters. Nevertheless, frontal meandering and the advection of patches of phytoplankton and suspended matter were detected at times during the study, thereby complicating the analysis. Sedimentologically, the area may be characterized as a temporal depocentre where sediment may be deposited during periods of calm weather and, especially in winter, erosion prevails during stormy periods.

The site has been studied between July 1991 and February 1995, with instruments in place during about 29 months. In 1991 the summer period has been covered, in 1992 the late winter and summer periods, in 1993 the spring period (with bad data return) and from november 1993 onward the site has been occupied for fifteen consecutive months. During 18 days in July 1994 an extensive study of the pelagic-benthic coupling was performed under the separate code name STED (Short TErm Dynamics).

In 1991 every two weeks, and, lateron, at least once a month the mooring site was visited by the R.V. Pelagia (NIOZ) or the R.V. Holland (RWS-DNZ) for instrument servicing and additional sampling for calibration and hydrographic purposes. During STED extensive sediment sampling was performed using ship-borne instrumentation in addition to moored sediment traps. Through very careful ship handling by the crew of the R.V. Pelagia, a grid of 17 benthic stations was sampled within 500 m of the moorings at different phases of the tidal cycle.

Moored self-contained instruments were to sample physical parameters (oceanographical, current, density (temperature), radiation as well as meteorological) and bio-geochemical parameters (chlorophyll-a, nutrients, suspended matter). This data acquisition required some techniques recently developed (especially for bio-optical and acoustic instruments) and technology development (in-situ nutrient auto analyzers). Adopting the two-layer model for the stratified water column, the mooring of two instruments of every type is at minimum, when one instrument is moored in the near-surface layer and the other in the near-bottom mixed layer.

During the full period of the study the water temperature was monitored at every 2 m from surface to bottom using coupled thermistor strings suspended from a surface buoy (Fig. 2). All other moorings contained a sub-surface buoy that became moored at a depth of about 10 m to avoid too severe wind-induced current and wave action, typical for the North Sea, thereby omitting the monitoring of the upper 12 m of the water column. From early 1994 onward, after a grant from NWO, the instrumentation became more suitable for the aim of the study as it was supplemented, a.o., by acoustic Doppler current profilers (ADCP) which can sample all three velocity components every 0.5 m between 3 m above the bottom and about 7 m from the surface, a wave-tide recorder, moorable transmissometers, additional fluorometers and in-situ nutrient (NOx) auto analyzers.

The sampling rate varied from once per minute (ADCP) to once per hour (optical instruments), so that a hitherto unachieved detailed set of data was obtained spanning long periods of time. Although relevant biological time scales typically are about one day, and largest forcing is expected on synoptic scales of one to five days, the relatively high sampling rate was needed to resolve (internal) tidal effects. The fast sampling of the ADCP was used in an attempt to estimate directly vertical fluxes of matter and

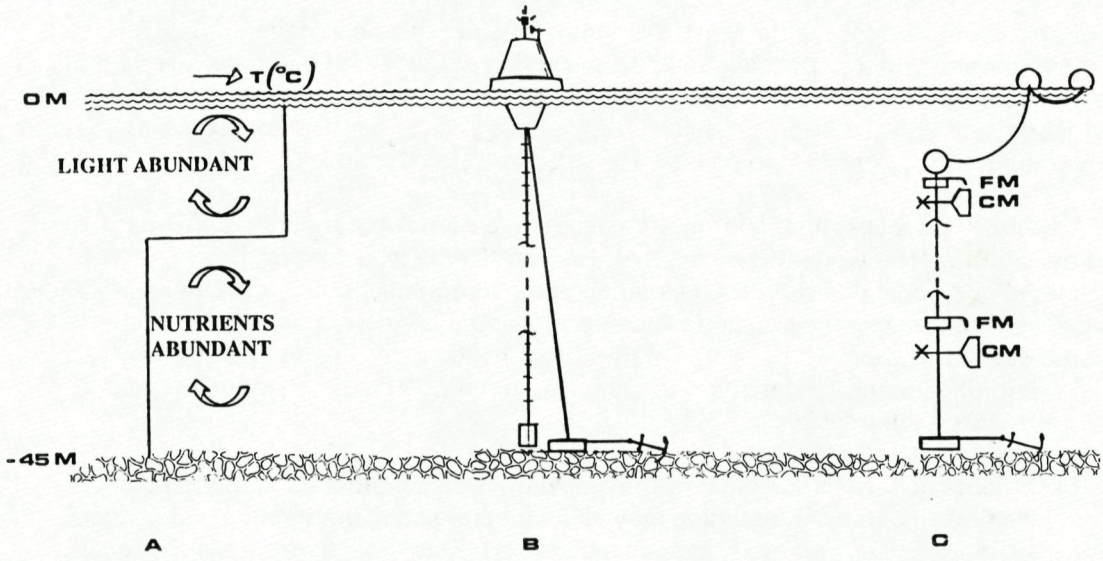


Figure 2. Schematic of the types of mooring used during INP and a sketch of the "classic" two-layer stratification, indicated by the temperature profile as a function of depth in a/. b/ Surface mooring with meteorological data buoy and thermistor strings. c/ general mooring with current meters and fluorometers (~chl-a).

momentum, but due to the problems with this instrument only a limited span of time became covered with good data.

Similarly, the additional development and the many troubles, which needed to be solved during the study, resulted in little good data harvest from the in-situ nutrient auto analyzers. Overall, the loss of data amounted for the moored instruments about 30%, of which some 10% was due to complete mooring and/or instrument loss. Due to bad weather conditions about half of the hydrographic surveys scheduled could not be completed.

The general conclusion after the field study was that such sophisticated moorings are not yet adequate for long-term, routine oceanographic monitoring purposes, as most instruments need too much attendance by regular in-situ calibration and servicing. Instruments measuring physical parameters may remain unattended for a period of a year (thermistor string, ADCP) or three months (current meters, meteorological instruments). Biological parameters can be obtained without servicing and in-situ calibration data for two to four weeks (bio-optical instruments), whereas almost permanent attendance is, still, needed for instruments measuring chemical parameters such as nutrients.

2.3. Modelling

A reduced set of daily averaged observations has been invoked to initiate and calibrate a one-dimensional integrated ecosystem model, which was forced with meteorological and current data measured at the INP site. The purpose of the modeling was to further unravel the relevant factors contributing to phytoplankton dynamics during the annual cycle.

In the physical submodel an integrated mixed layer model is used in which the exchange between the surface and bottom layers and the (initially non-turbulent) pycnocline is governed by en-/detrainment. After calibration some background diffusivity had to be invoked for the pycnocline in order to simulate the gradual increase of temperature in the near-bottom mixed layer. By its one-dimensional nature, horizontal advection is not accounted for in the model.

The rather sophisticated ecosystem component, which has been based upon the ERSEM model, describes biological and chemical processes in the water column as well as in the sediment and consists of nine functional groups to describe pelagic biology, ranging from bacteria to carnivorous zooplankton. The dynamics of chemical variables like nutrients are fully coupled to the biologically driven processes. Early diagenetic transformations and fluxes of organic matter and nutrients in the sediment and across the sediment-water interface are included explicitly.

2.4. Results

The 1994 yearlong series of near-surface chlorophyll-a (chl-a), as extracted from fluorescence observations is shown in Fig. 3, along with the variation with time of the thermal stratification and the wind speed (cubed). The familiar two phytoplankton blooms per year are seen, one in spring and the other in late summer/early autumn. The spring bloom develops before stratification becomes established, and the summer bloom clearly starts out while the water column is still strongly stratified and no strong wind events occur. During winter observed and modelled chl-a levels occasionally exceed well above background level.

Detailed data analysis, fuelled by the numerical model results, shows that indeed the spring bloom disappears from the near-surface layer as soon as the stratification becomes solidly established. It shows, however, also a dependence of the chl-a distribution on the

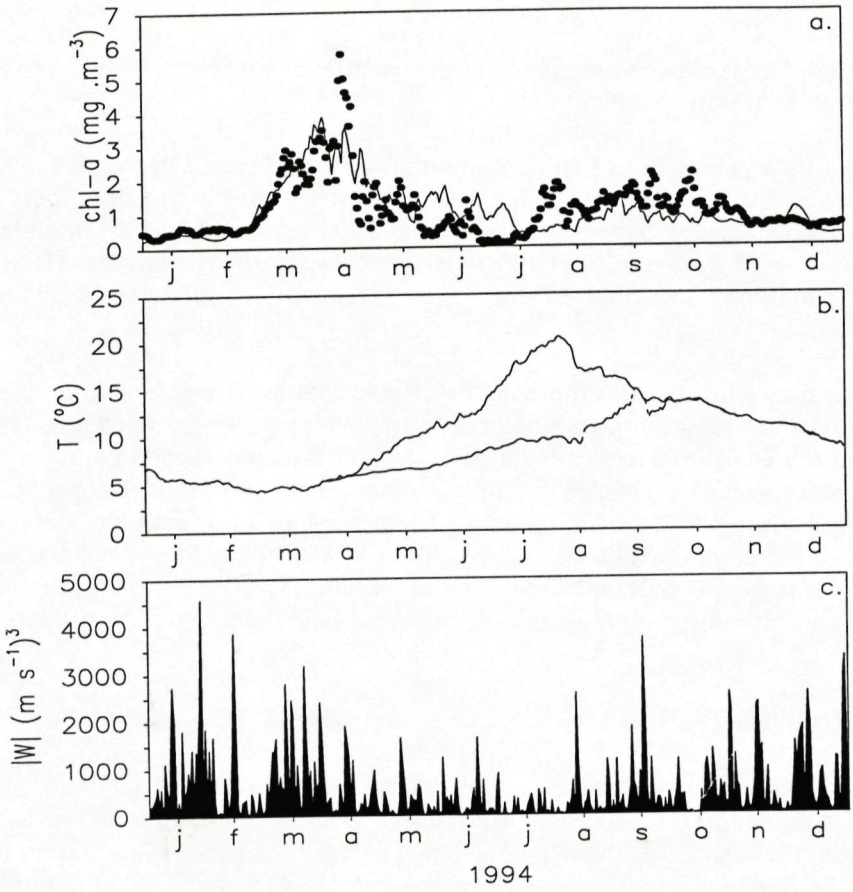


Figure 3. Some of the yearlong 1994 data. a/ chl-a at 13 m depth from fluorescence data (dots) and from the numerical model (solid line). b/ Temperature measured at 2 m from the surface (solid line) and at 2 m from the bottom (dashed line). c/ Wind speed (cubed) measured at AUK.

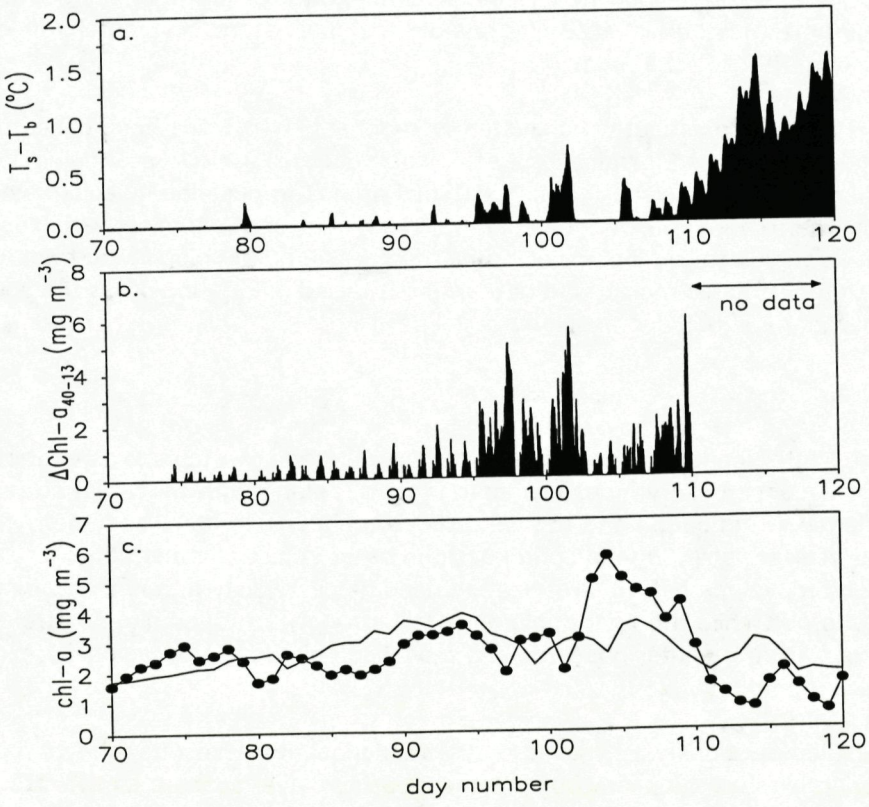


Figure 4. Spring 1994. a/ Hourly averaged observed water temperature difference between 2 and 43 m depth. b/ Hourly averaged observed chl-a difference between 40 and 13 m depth. c/ Daily averaged chl-a at 13 m as observed (dots) and modelled (thick solid line).

turbulence intensity in the water column prior to stable stratification, as is inversely inferred from, short-lived, weakly stratified periods during which the near-surface values of chl-a decrease at the expense of increasing near-bottom values (Fig. 4).

The spring bloom starts around the beginning of March, as soon as irradiation is sufficiently high and suspended matter content is low enough to allow light to penetrate sufficiently deep. The bloom comprises basically relatively heavy plankton species, i.e. mainly diatoms, as is inferred from the negligible phase differences between stratification rate and the rate of chl-a variation with time. The full use of available nutrients and the extent of the bloom in this time of the year thus depend on subtle variations in time between short periods of stratification, when diatoms and suspended matter sink to the bottom and the water column becomes clearer, and short periods of mixing, by which diatoms are brought back into the photic zone.

No observational evidence has been found for the spring bloom to enhance the (onset of) stratification, which seems typical for the open ocean. No evidence has also been found for the opposite situation, in which the stratification favours the spring bloom, which seems typical for shallow seas like the central North Sea. The analysis does show that the turbulence intensity critically influences the growth and that the spring bloom declines as soon as the stratification becomes well established. Curiously, one thus could use the phytoplankton as an indicator for the turbulence intensity in the water column.

The numerical model further showed the important role of the background light extinction in the water and the implications of the timing of the onset of the stratification, not just for the spring bloom, but also for the plankton growth in the rest of the year. It became clear that variations in this timing have major consequences for the production and the succession of the different plankton species and the structure of the pelagic food web during the entire growth season. A different timing of the onset of stratification implies a different ratio of the main phytoplankton species (e.g. diatoms vs flagellates) developing during spring and, accordingly, a different amount of sedimenting diatoms and thus differences in the availability of nutrients in the mixed layers.

Temperature observations made in 1994 show a multiply layered water column over most of the summer suggesting limited nutrient input from the near-bottom mixed layer, and yet, a summer bloom initiation during that period (Fig. 5). This may have been due to horizontal advection as the hydrographic survey at the time showed strong frontal activity. On the other hand, from the ADCP data it became clear that the stability of the water column in terms of Richardson number frequently became critical during that period, due to strong current shear across the pycnocline induced by indirect atmospheric effects, i.e. inertial oscillations. Some support for exchange across the pycnocline, though statistically barely significant, was provided by the observations of periods of enhanced vertical matter fluxes as directly estimated from the ADCP data.

The early summer bloom was not confirmed by the numerical model, which simulated only a late summer bloom some three weeks later, when after a strong wind event the multiple layers reduced to a sharp and thin pycnocline and the classic two-layer system became established (Fig. 5c). This discrepancy between model and observations is explained by the lack of the physical mechanism, causing increased vertical mixing in the model, and possibly, by the role of horizontal advection. Nonetheless, from both the model and the observations atmospherically induced exchange has been inferred across the pycnocline during late summer. The development of the late summer bloom is more strongly governed by convective mixing rather than wind mixing, as has been found after examination of the 1991 and 1992 observations.

From the 1994 observations it was also concluded that light is not limiting production in the near-bottom layer during summer. At the INP location no, or just weak, sub-surface maxima in chl-a content are found near the pycnocline. Prior to the onset of the late

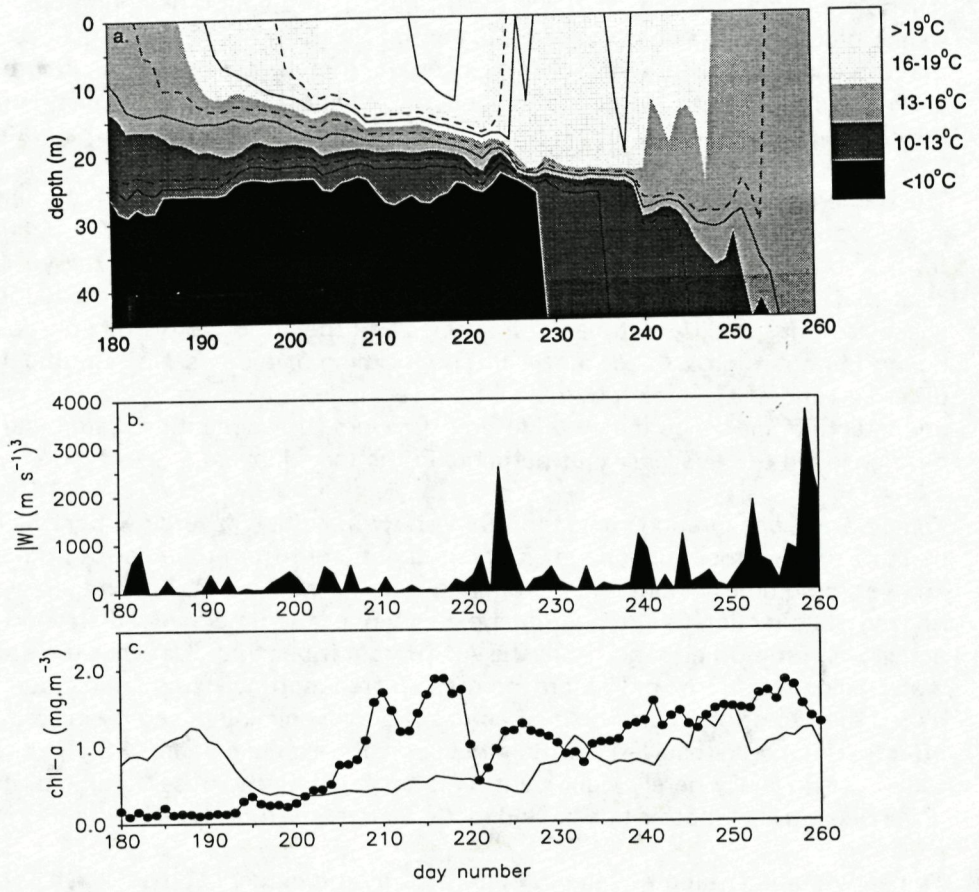


Figure 5. Summer 1994. a/ Daily averaged isotherms, as inferred from temperature data, and drawn every 1 °C between 9°C and 20 °C. b/ Wind speed (cubed) measured at AUK.. c/ Chl-a at 13 m from observations (dots) and the model (thick solid line).

summer bloom, the highest concentrations of chl-a are found evenly distributed over the entire near-bottom mixed layer. This has been supported by the outcome of the numerical model (Fig. 6).

During July 1994 an extensive study has been made of the particle accumulation on the sediment and resuspension and the response of microbenthos upon changes in net sedimentation of organic matter/ phytodetritus. The study on the pelagic-benthic coupling revealed that, indeed, the INP site functions as an area where sediment is accumulated in summer, but most likely re-eroded during severe storms in autumn and winter. Although the full period of measurements was undisturbed by any severe weather, resuspension of bottom fluff material occurred at maximum current during spring tide. This fluff was strongly enriched with organic carbon compared to the bulk sediment and, as has been inferred from the C/N ratio, it contained fresh plankton material at some occasions. Mass fluxes in the sediment trap moored a few meters above the bottom almost completely consisted of resuspended fluff that resettled to the bottom. These trap fluxes showed a distinct tidal cycle with highest fluxes directly after low water slack tide, when low current speeds and high concentrations of suspended and phytoplankton stimulated floc formation.

These deposition fluxes did not entice measurable responses of the microbenthos, probably because variations in benthic bacterial production due to the heterogeneity of the bottom exceeded all other variations. The input of the phytopigments chloropyll-a and fucoxanthin (which are indicators for fresh phytodetritus) to the sediment was less than the degradation of these pigments in the sediment. Thus, phytopigments disappeared from the sediment during the STED period at a rate of $\sim 0.06\ d^{-1}$ corresponding to a turnover period of ~ 17 days. The fact that this decrease in phytopigments was not reflected by a decrease in benthic bacterial production, implies that the turnover of total available bacterial food must have been slower than that of the phytopigments (Fig. 7). It is concluded that phytopigments may be good spatial indicators of food for bacteria, but rather poor indicators of the quantity of food available for bacterial uptake in sediments.

The deposition of total suspended matter and organic carbon has been further analysed with a simple advection-deposition-resuspension model (Fig. 8). From the model, a net accumulation of 75 g m^{-2} has been calculated for a two weeks period, corresponding to a sediment accretion rate of 1.5 mm $year^{-1}$. The input of organic carbon associated with this accumulation was 115 mgC $m^{-2}\ d^{-1}$, which is sufficient to fuel the benthic bacterial production in the surface sediment (32 mgC $m^{-2}\ d^{-1}$). It has been also inferred from the model that, in addition to the net accumulation, material is deposited temporarily on the sediment and resuspended again after 1-2 weeks. During this retention in the sediment, organic matter may provide an additional source of food to the benthic community, and thus may be decomposed substantially before resuspension and further transport across the North Sea.

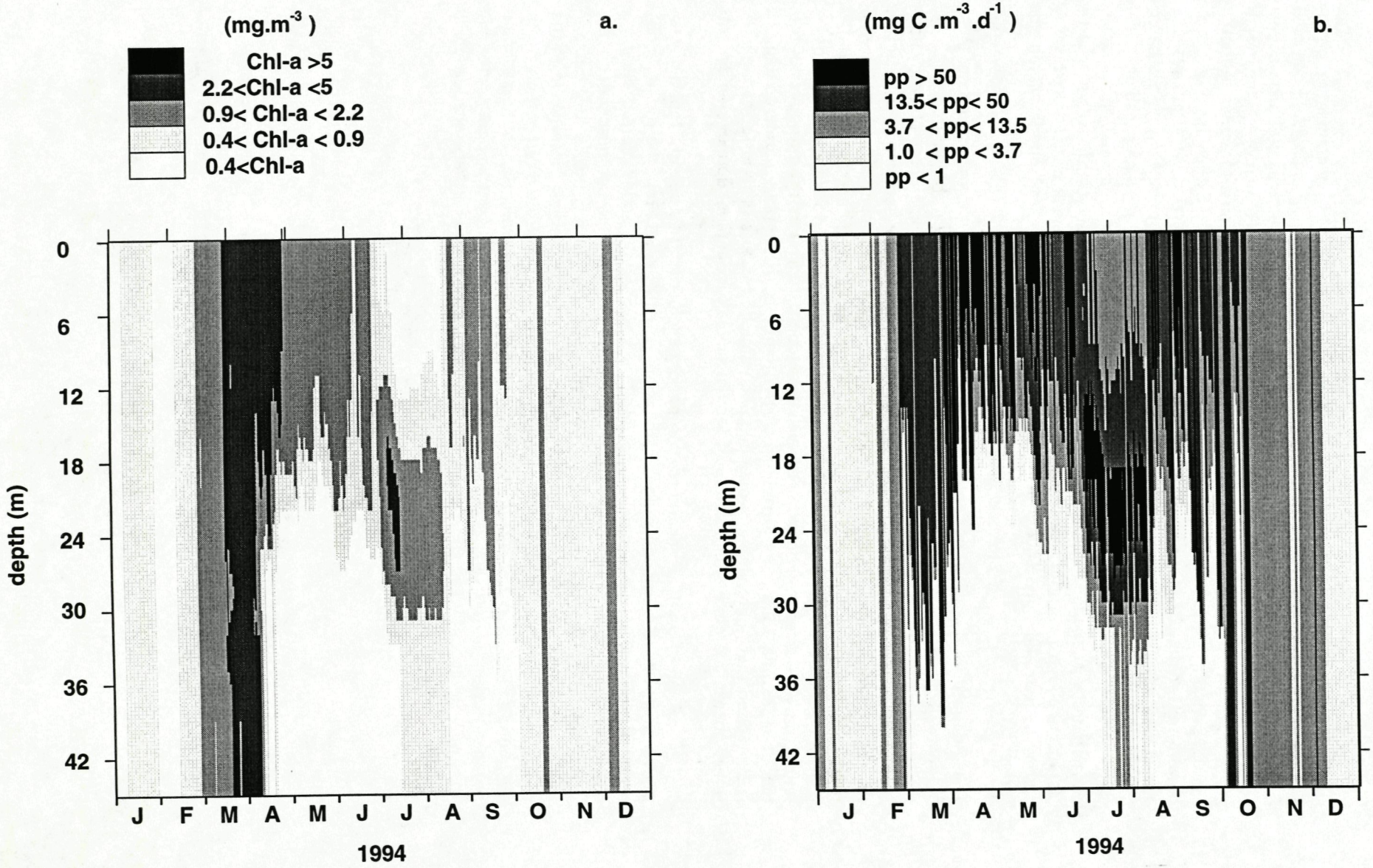


Figure 6. a/ Simulated vertical distribution of chl-a in 1994. Note that only during spring a sub-surface chl-a maximum is found. b/ Simulated vertical distribution of primary production in 1994, which shows a maximum near the pycnocline during summer.

2.5. Conclusions

- Sophisticated moorings are not yet adequate for long-term, routine oceanographic monitoring purposes, as the instruments generally need too much attendance by regular in-situ calibration and servicing.
- No observational evidence has been found for the spring bloom to enhance the (onset of) stratification or vice versa for the stratification to favour the spring bloom. Instead, a spring bloom is found before the stratification becomes well established and, prior to that, a subtle dependance of the evolution of the spring bloom has been found on the turbulence intensity in the water column. The timing of the onset of stratification is critical for the entire growth season.
- In summer no sub-surface maximum in chl-a was observed at INP, because sufficient irradiation reached to the bottom. Despite the strong stratification, a bloom developed after a strong (convective) mixing event in late summer, and another one also prior to that, probably after internal mixing events induced by strong current shear across the pycnocline, although the role of horizontal advection could not be ruled out entirely.
- Given the fact that the period of measurements on pelagic-benthic coupling was undisturbed by any severe weather, the bottom at the INP location has been found to accumulate suspended material during summer. The input of organic carbon is sufficient to sustain the benthic bacterial production. Phytopigments have been found good spatial indicators of food for bacteria but rather poor indicators of the quantity of food available for bacterial uptake in sediments.

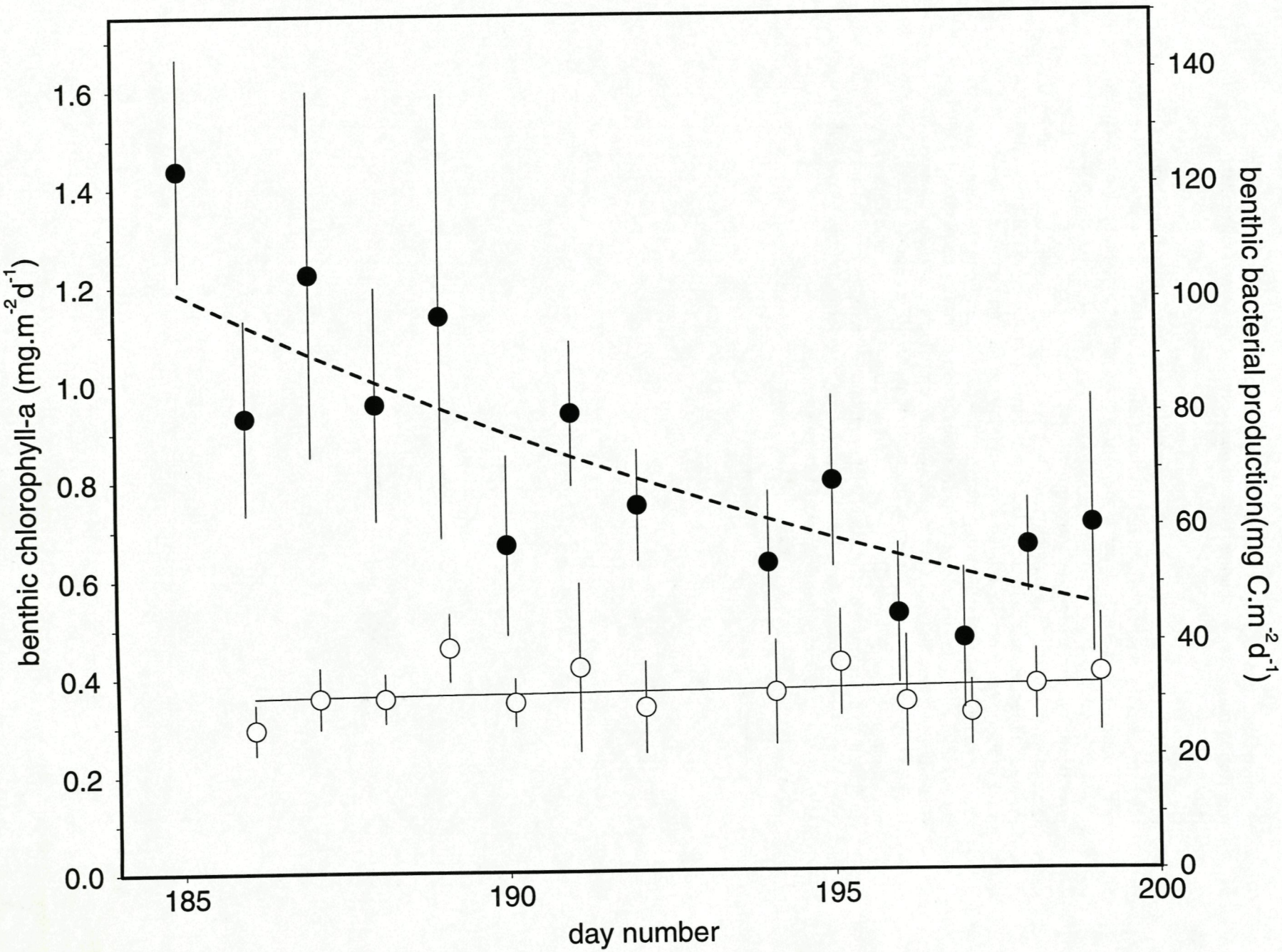


Figure 7. Summer 1994. Daily averaged chl-a concentrations (•) and benthic bacterial production (o) in the 3 mm sediment surface layer.

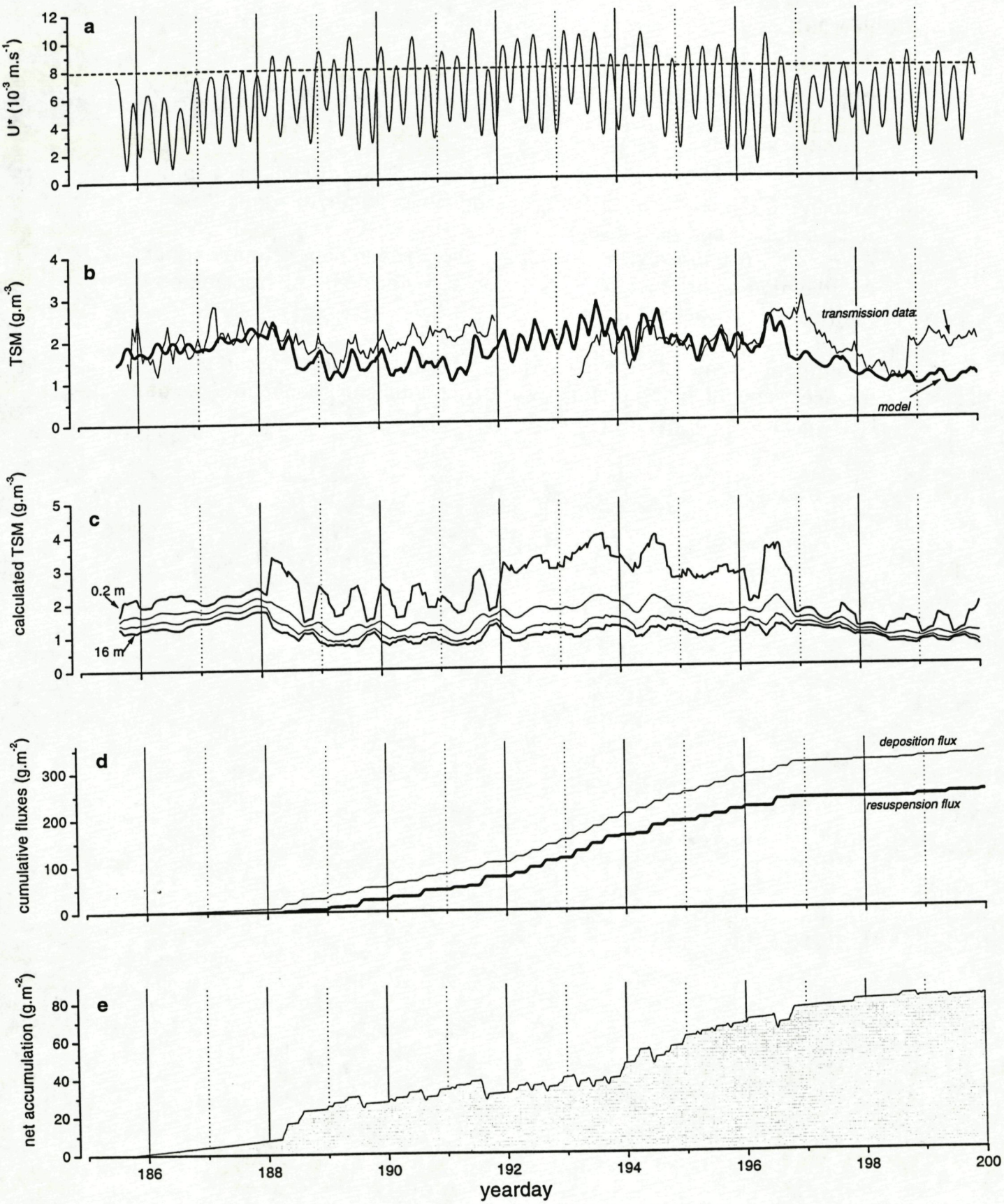


Figure 8. Results of the advection-deposition-resuspension model for Total Suspended Matter (TSM) in July 1994; a/ Friction velocity U at te seabed calculated from current meter data, b/ TSM calculated at 4.5 m above the seabed (thick line, 3 h moving average) and measured (thin line, I data point per hour), c/ TSM calculated at different depths in the lower water column (0.2, 6, 11 and 16 m above the bottom), d/ calculated cumulative fluxes of deposition and resuspension, e/ Calculated cumulative net accumulation of particulate matter on the sea floor.*

APPENDICES

I. *W. van Raaphorst, J.F.P. Malschaert & J.J.M. van Haren.* Tidal resuspension and deposition of particulate matter in the Oyster Grounds, North Sea.

II. *F.C. van Duyl, G.C.A. Duineveld, A.J. Kop & G. Kraay.* Pelagic-benthic coupling in the North Sea: short-term dynamics in phytopigment sedimentation and response of benthic bacteria.

III. *P. Ruardij, H. Van Haren & H. Ridderinkhof.* The impact of the thermal stratification on production, succession and grazing on phytoplankton in shelf seas: a model study.

IV. *L. Lohse, H.T. Kloosterhuis, W. Van Raaphorst & W. Helder.* Denitrification rates as measured by the isotope pairing method and by the acetylene inhibition technique in continental shelf sediments of the North Sea.

APPENDIX 1

Tidal resuspension and deposition of particulate matter in the Oyster Ground, North Sea[1]

Wim van Raaphorst[2], J. (Hans) F.P. Malschaert & J. (Hans) J.M. van Haren

Netherlands Institute for Sea Research (NIOZ)
PO box 59, 1790 AB Den Burg, The Netherlands

688

[1]NIOZ contribution No. 3108; [2]E-mail address: wimvr@nioz.nl

ABSTRACT

Moored instruments (current meters, fluorometers and transmissometer) were used in combination with sediment traps (aspect ratio > 4) operating at hourly opening intervals and shipborn sampling to determine the fluxes of deposition and resuspension of Total Suspended Matter (TSM) under influence of tidal action in the 45 m deep Oyster Ground, North Sea. Here, we present data from the mixed layer below the major thermocline at 20 m above the bottom (mab) obtained during a 14 days period with calm weather in July 1994. Around neap tide near bottom current velocity remained < 0.15 $m.s^{-1}$ and TSM was dominated by slow settling of particles advected from a relatively turbid area south-east of the study site. At the onset of spring tide current speed increased with maximum values > 0.20 $m.s^{-1}$ and sea bed friction velocities exceeding the threshold for resuspension. Particles resuspended were strongly enriched with organic carbon compared to the bulk sediment, suggesting that not the bed proper but a fine grained fluff fraction was eroded. This resuspended fluff was by far the dominating source to the mass fluxes in the sediment trap (3.2 mab), which showed a distinct tidal cycle with highest fluxes directly after low water slack tide and lowest fluxes during maximum ebb current. This pattern was caused by variations in apparent settling velocity of TSM, presumably due to floc forming at periods in the tidal cycle with low current speed and relatively high concentrations of both chlorophyll-a and TSM. From a simple model on advection, deposition and resuspension of TSM, we calculated a net accumulation on the sediment of 75 $g.m^{-2}$ during the 14 days study period, being the difference between

simultaneously operating gross fluxes of deposition and resuspension. Upon deposition the average retention time of particles until their next resuspension and futher transport across the shelf is calculated at 1-2 weeks, which may be sufficient for substantial decomposition of organic matter associated with TSM. The model showed that the saltative particle exchange between the sea bed and the water column is intensified by storms, resulting in net erosion during the storms and bulk resettling thereafter. It is concluded that the Oyster Ground serves as a mid-shelf temporary depocentre and that mineralisation at this and similar areas may play a crucial role in the carbon budget of the North Sea.

1. Introduction

Deposition of organic carbon and other elements associated with total suspended matter (TSM) forms the major link between processes in the water column and the underlying sediment. In shallow shelf seas time necessary for vertical transport from the productive surface layer to the sea floor is relatively short, and a considerable portion of primary production may reach the bottom (Jørgensen 1983). For the North Sea it has been estimated that 17-45% of the primarily produced organic C is mineralised in the sediments of the upper shelf (Postma & Rommets 1984, Nedwell et al. 1993). Shelf seas are, however, highly energetic and a portion of detrital particles is kept in suspension for longer time or is resuspended from the bottom by wave action and tidal currents (Jago et al. 1993, Churchill et al. 1994). As a consequence, a considerable amount of particulate organic matter may be swept from the shelf to the depocentres on the continental slope where it is further mineralised or buried in the sedimentary record (Walsh 1991). In the North Sea the main depocentre is found in the Skagerrak/Norwegian Channel (SNC, Fig. 1) where ~50-70% of the total mass accumulation occurs (Eisma & Kalf 1987).

The average time-scale for water transport from the southern and central North Sea to the SNC is several months to essentially < 1 year (Hainbucher et al. 1987, Otto et al. 1990). Since 'fresh' marine phytoplankton debris typically has first order decomposition rates in the order of ~10 y^{-1} (Walsh et al. 1988, Middelburg 1989) such a transport time would be sufficient to enable almost complete loss of organic matter: ~99% of the organic matter would be mineralised at this rate during 6 months of travelling. Even when taking into account that the decomposition rate decreases as the substrate ages (Middelburg 1989) most of the original organic matter would be mineralised during transport across the North Sea. Using the power-model of

Middelburg (1989) with an initial 'age' of the organic matter of 10^{-4} y and a power of 0.16, ~10% would remain after 6 months. This supports earlier conclusions that, apart from local production (Kempe & Jennerjahn 1988), the organic matter deposited finally in the SNC is largely of refractory nature (Van Weering et al. 1987, Kempe et al. 1988, Lohse et al. 1995).

Particulate matter passes through many cycles of settling and resuspension during transport along the shelf (Eisma & Kalf 1987, Van Weering et al. 1987, Kempe et al. 1988). Depending on the hydrodynamic conditions particles are stored for shorter or longer time in what may be called temporary depocentres on the shelf. Puls & Sündermann (1990) and Sündermann (1993) demonstrated that particles derived from the East Anglian turbidity plume and the southern North Sea can settle in the Oyster Ground in spring and summer although net annual accumulation probably is of minor importance in that area (Cadée 1984, Eisma & Kalf 1987). By considering tidal currents only, Creutzberg & Postma (1979) concluded that it should be possible for fine particles to settle in the Oyster Ground. The absence of net accumulation then suggests that such settlement can only be temporary and that particles are entrained again during periods of erosion, e.g during autumn and winter storms (Kempe et al. 1988, Puls & Sündermann 1990).

Transient deposition contains relatively fresh plankton debris that may serve as food to the local benthic fauna (Jenness & Duineveld 1985). Upon settlement organic C is mineralised and nutrients are largely recycled to the water column (Nedwell et all. 1993, Gehlen et al. 1995, Lohse et al. 1995) stimulating primairy production in the area of temporary deposition. On the other hand, upon resuspension turbidity of the water increases thus putting limits to the local primary production (Tett & Walne 1995). Rather than the permanent depocentre on the slope which are being fuelled by aged materials, the temporary depocenters on the shelf represent key areas in the turnover of organic matter in the North Sea (Gehlen et al. 1995, Lohse et al. 1995).

Deposition and resuspension of TSM in the temporary depocentres have to be considered to understand the carbon budget of shelf seas. Field studies on this subject mostly focus on sediment movement during periods of erosion (Moody et al. 1987, Churchill et al. 1988, 1994, Drake & Cacchione 1989, Lyne et al. 1990a,b). Less attention seems to be paid to the tidal dynamics of TSM during no-storm conditions when settlement may prevail (e.g. Jago et al. 1993). Here we present such data collected during the integrated North Sea Mooring Project (INP-Mooring) at a station in the Oyster Ground area in July 1994. Experiments included sediment trap

deployments with high time-resolution to reveal the tidal frequency and observations with moored sensors on transmission, fluorescence and current velocity. A simple model describing advection, deposition and resuspension of TSM was constructed to guide the discussion of the experimental data. The aim of our study was (1) to determine deposition and resuspension of TSM under influence of tidal action and (2) to evaluate the implications for transport and temporary deposition of TSM in the North Sea.

2. Materials and methods

2.1 Study site

The measurements were performed during a cruise with RV Pelagia in a small grid between 54°24'9" - 54°25'5" N and 4°01'9" - 4°02'9" E in the Oyster Ground on the transition between the southern and the central North Sea (Fig.1). Water depth at the site is 45.5 ± 0.5 m, with the major thermocline around 25-27 m depth. Data were collected between 5 (julian day 185) and 19 July 1994 (julian day 199). An additional survey was made covering 55 CTD casts in a larger grid between 54°15' - 54°35' N and 3°45' - 4°19' E on 7 and 8 July 1994.

The experimental site is in the area where Sündermann (1993) predicted deposition of TSM. Tidal mixing fronts frequently occur ~ 90 km south of the mooring grid where water masses from the southern and northern/central North Sea meet (Pingree & Griffiths 1978, Van Haren & Joordens 1990). According to the Wenthworth scale the upper 5 mm of the bottom sediment consists of very fine sand with a median grain size of ~100 μm (Lohse et al. 1995), a fraction ~15% < 63 μm and a fraction ~5% < 6 μm (Van Raaphorst & Malschaert 1996). Most of the fine particles present have been identified as 'relicts' from Holocene origin (Cadée 1984, Eisma & Kalf 1987). TSM in the bottom water consists of particles with a mean diameter of 5 - 10 μm aggregating to flocs of 100 - 300 μm, depending on the season and weather conditions (Chen 1995). POC content of TSM is normally between 10 and 20% below the thermocline during summer (Postma & Rommets 1984, Hölemann & Wirth 1988).

2.2 Field techniques

Wind velocity and direction and data on the significant wave height were obtained from platform F3 ~60 km NE of the mooring grid.

Water samples were collected with 25 l Niskin bottles at 6, 11, 21, 31 and 41 m above the bottom (mab) spread over the study period at different phases of the tidal cycle. Additional samples were drawn from 0.2 mab using a membrane pump. The first ~200 l pumped on deck were discarded before filling carboys of 25 l. Rate of pumping was 12 - 18 $l.min^{-1}$ resulting in vertical flow velocities through the tubing > 1 $m.s^{-1}$. All materials were made of polypropylene or polythene and cleaned before use. The carboys were carefully homogenised and TSM was collected by low-pressure filtration of 0.5 l subsamples over pre-weighed 0.4 µm polycarbonate filters (25 mm diameter), rinsing the filters with milliQ water to remove the salt. Additional volumes of 0.5 l were filtered (25 mm GF/F, pre-heated at 400°C) for analysing POC and PON in TSM.

CTD casts were performed normally once or twice a day, and with 1 h intervals during a full tidal cycle on 5 and 6 July 1994. The Seabird CTD was equipped with a Sea-Tech transmissometer (660-670 nm, 0.25 m light path). The light attenuation coefficient was calculated from c_0 = ln(transmission) / light path and calibrated against TSM measured by filtration. All transmission data will be expressed as TSM in $mg.l^{-1}$. The fluorometer mounted on the CTD was a Chelsea Aquatracka with a excitation wavelength of 440 nm and band with of 80 nm, and an emission wavelength of 670 nm and band with of 30 nm. All fluorescence data were converted to units of chlorophyll-a using the in situ concentrations of chlorophyll-a measured on HPLC by Van Duyl et al. (1996) for calibration.

At the site an extensive set of moored sensors was deployed. Details of the mooring arrays will be given elsewhere (Van Haren et al. 1996). For this study relevant equipment consisted of current meters, transmissometers, fluorometers and sediment traps. Six NBA-DNC 2M current meters were placed in a single array anchored on the sea floor and with a float on top ~10 m below the water surface. Here we present data based on 10 min. ensembles from the meter placed at 1.5 mab. Accuracy of the current data is ± 1 $cm.s^{-1}$ and ± 5° TN for speed and direction, respectively. We have no data from 'normal' transmissometers moored below the thermocline during the study period. Therefore the light attenuation coefficient was obtained from the 'transmission blank' measured by the WS Ocean NAS 1 submersible nitrate analyser (1 h intervals, 560 nm, 0.02 m light path) mounted at 4.5 mab in a second mooring array. The attenuation data from the NAS 1 were calibrated against those obtained with the Sea-Tech on the CTD. Fluorometers (Chelsea Aquatracka) were placed in a third mooring array. Filters used were selected to measure chlorophyll-a and had a bandwidth of 100

nm at a wavelength of 430 nm for excitation and a bandwidth of 30 nm at 685 nm for emission. Only data from 5 mab will be discussed here.

A Technicap PPS4/3 sediment trap (unbaffled, height 1.2 m, collecting area 0.05 m^2) was bottom-moored to collect TSM at 3.2 mab. A tilt meter combined with a pressure sensor with was mounted on the mooring chain just below the trap. The trap has an cylindrical upper part of 0.55 cm length and a 0.45 m excentric conical part (maximum angle 30°) below, ending in a funnel to the carrousel with 12 sample cups (250 ml). Aspect ratio of the trap is 2.2 based on the cylindrical part only, and > 4 taking the full length into account. The trap was programmed daily to collect during 1 h intervals, opening the first cup at 19.00 h local time and closing the last cup at 7.00 h local time the next day. Recovery of the trap was between 8 and 10 h local time. The cups were filled with filtered sea water (0.4 µm polycarbonate) from the study area before deployment, without addition of preservatives. After retrieval on deck the sample cups were transferred to a climate room at in situ bottom water temperature (9-10° C) for subsequent filtration over 200 µm plankton gauze and pre-weighed 0.45 µm HAc filters (45 mm diameter) within 1-2 h. The filters were stored at -20° C before further processing in the laboratory.

Sediment samples were obtained by gently pushing acrylic liners into the sediment retrieved on deck by a cylindrical boxcorer (for details see Van Raaphorst & Malschaert 1996) at 13 locations at a distance of ~180 m from each other along the eastern and northern boundaries of the mooring grid, i.e. not in between the moorings. Before the cruise we nominated 17 locations for boxcoring. The 13 locations actually visited and their sequence in time were selected by lottery drawing from the pool of 17 nominates during the cruise. The subcores were sliced in layers of 2.5 to 20 mm at in situ temperature, and stored at -20°C. Here, only data from the upper 2 layers (0-2.5 mm, 2.5-5 mm) will be discussed.

2.3 Laboratory analysis

Water content of the sediment samples was obtained from the loss of weight after drying at 60° for 48h. Filters containing TSM and trap material were dried (60° C, 24 h) and re-weighed for mass calculation. POC and PON content of sediment samples and trap material scraped carefully from the filters (under binocular, harvest ~95%) was determined on a Carlo Erba NA 1500-2 elemental analyzer following the procedure of Verardo et al. (1990). Inorganic C was removed from the samples by addition of sulphurous acid. For the POC and PON content of TSM the complete

GF/F filters were used. Accuracy expressed as coefficient of variation for replicate samples was ~2.5% for POC, ~7% for PON and ~4% for CN ratio.

2.4 The model

The concentration of particles in the water column is determined by advection, deposition, resuspension, vertical mixing and internal sources and sinks:

$$\frac{\partial C}{\partial t} + \frac{\partial (uC)}{\partial x} + \frac{\partial (vC)}{\partial y} + \frac{\partial (\omega C)}{\partial z} = \frac{\partial}{\partial z}\left(K \frac{\partial C}{\partial z} \right) + S \qquad (1)$$

where C is mass concentration ($g.m^{-3}$), t is time (s), u,v are fluid velocities ($m.s^{-1}$) in the x (west-east) and y direction (north-south), respectively, ω is the settling rate of suspended particles ($m.s^{-1}$), K is the vertical eddy diffusivity ($m^2.s^{-1}$) and S is a source/sink term ($g.m^{-3}.s^{-1}$). Vertical fluid velocity and horizontal dispersion are neglected in this equation and all parameters may, in principle, be variable in time and x,y,z direction. The term S includes phytoplankton production of POC but also, for a given size class of particles, losses to and gains from other size classes through flocculation and de-flocculation (Hill & Nowell 1995). If, as a first approximation, it is assumed that the dynamics of suspended particles can be described in terms of quantities averaged over all size classes, and if it is further assumed that net production of POC is small on the time-scales considered, (1) is valid for TSM with S = 0.

As a next simplification we assume that the velocities u and v are essentially constant on the x,y length scales of the mooring grid and that the advection terms in (1) may be replaced by the products of u,v and the horizontal concentration gradients at the location. Further taking the average of (1) over the bottom layer yields

$$\frac{\partial \langle C \rangle}{\partial t} + \left\langle u \frac{dC}{dx} \right\rangle + \left\langle v \frac{dC}{dy} \right\rangle = \frac{1}{h} \cdot \left((\omega C)_b - K_b \left(\frac{\partial C}{\partial z} \right)_b \right) + \frac{1}{h} \cdot \left(K_h \left(\frac{\partial C}{\partial z} \right)_h - (\omega C)_h \right)$$

(2)

where $\langle\ \rangle$ is the layer average, h is the depth of the bottom mixed layer (in metres), dC/dx and dC/dy are the horizontal concentration gradients ($g.m^{-4}$) and the subscripts h and b point at the upper (thermocline) and lower boundary (bottom), respectively.

At the bottom the boundary condition reads:

$$(\omega C)_b - K_b\left(\frac{\partial C}{\partial z}\right)_b = Q_b - E_b \qquad (3)$$

where Q_b is the rate of deposition on the bottom ($g.m^{-2}.s^{-1}$) and E_b is the resuspension flux ($g.m^{-2}.s^{-1}$). A similar condition may be formulated for the upper boundary. In our model, however, we assume that the vertical fluxes across the thermocline can be neglected. This assumption is justified from the consideration that in the study area by far the largest portion of TSM in the bottom layer originates from the sediment or is advected in suspension (Jago et al. 1993). Further support follows from the data of Van Duyl et al. (1996) showing that only minor quantities of phytoplankton pigments settled from the surface layer to the bottom layer during the experimental period. Thus, the last term in brackets on the right-hand site of (2) is set at zero.

Application of the model is intended to demonstrate the influence of the main processes, advection, deposition and resuspension on the particle concentrations in the bottom layer. Following the results of Jago et al. (1993) a constant background concentration C_{back} of TSM is assumed in the model, consisting of particles with such a small settling velocity that they are uniformly distributed with depth and do not settle on the sea floor. This backgound concentration is one of the fitting parameters of the model. The model details outlined below refer to TSM corrected for the background concentration.

Advection. The velocities u,v are taken from the current data at 1.5 mab, the gradients dC/dx and dC/dy are based on transmission data of 6 mab obtained during the survey around the mooring grid at 7 and 8 July. Since normally the largest portion of suspended particles is present in the lower part of the bottom layer we believe that this approximation to estimate the layer averaged advection is sufficiently accurate for our purpose. To calculate the concentration at a certain depth z above the bottom downward settling fluxes and upward diffusive transport are assumed to balance:

$$C_z = \langle C \rangle \cdot \frac{h\omega}{K} \cdot \frac{\exp\left(\frac{-\omega}{K} z\right)}{1 - \exp\left(\frac{-\omega}{K} h\right)} \qquad (4)$$

The vertically constant eddy diffusivity K is related to the friction velocity: $K = 0.16 \cdot U_*$ (Puls & Sündermann 1993) where U_* ($m.s^{-1}$) is calculated from the velocities u,v applying a drag coefficient of $2.5\ 10^{-3}$. Equation (4) yields similar profiles as the often used inverse power relation in the logarithmic bottom layer (e.g. Drake & Cacchione 1989, Wright 1995) but it has the advantage that it predicts finite concentrations at $z = 0$. For the settling velocity ω a value of $2\ 10^{-5}$ $m.s^{-1}$ is chosen as an average for suspended fine particles in this part of the North Sea (Jago et al. 1993, Pohlman & Puls 1995, Tett & Walne 1995). Applying Stokes law this settling velocity corresponds to a spherical diameter of ~ 6 μm, in accordance with the size of the non-flocculated particles observed by Chen (1995) in the Oyster Ground area.

Deposition. The settling flux is assumed to be proportional to the TSM concentration C_b at the sea floor

$$Q_b = \omega C_b \qquad (5)$$

in which C_b is calculated after inserting $z = 0$ in (4). The dependency of C_b on K and U_* implies that deposition is most effective at slack tides when current velocity is lowest. The above equation neglects the effect of a critical shear stress reducing the portion of particles effectively settling on the sea floor (*cf.* Krone 1962). In other words, it is assumed that the shear stress prevailing during the experiments is essentially low enough to facilitate complete deposition.

Resuspension. The formulation for resuspension includes a threshold friction velocity below which no entrainment of particles from the sea floor can occur

$$E_b = \beta_r \cdot M_r \cdot \left(\frac{U_*^2}{U_{*,r}} - 1 \right) \qquad \text{for } U_* \geq U_{*,r} \qquad (6a)$$

and

$$E_b = 0 \qquad \text{for } U_* < U_{*,r} \qquad (6b)$$

where β_r (s^{-1}) is the entrainment rate constant, M_r ($g.m^{-2}$) is the total mass of particles on the seabed available for resuspension and $U_{*,r}$ is the threshold friction velocity. Values for this threshold vary considerably between sediments types and depend on several environmental factors (e.g. water content, bed form, biological activity). Here a low value of $8\ 10^{-3}$ $m.s^{-1}$ is chosen, slightly below the value applied by Tett & Walne (1993) but much lower than the threshold velocity applied by Puls & Sündermann (1993) and in several other erosion studies (e.g. Moody et al. 1987, Drake &

Cacchione 1989, Churchill et al. 1994). We assume, however, that only a loose layer of freshly settled fluff material is resuspended by tidal currents in the Oyster Ground, and not material from the underlying bed (Jago et al. 1993). Consequently, M_0 is the mass of particles present in this fluff layer, calculated at each time step from the cumulative difference between deposition and resuspension during the previous period.

In the model resuspension causes a temporary increase in the average settling velocity of TSM lasting for 30 min after the resuspension event. Thereafter ω returns to the basic $2\ 10^{-5}$ $m.s^{-1}$ until the next event. This increase is included to take into account the larger average floc size of the presumably flocculated particles from the fluff layer. The increased settling velocity finally applied is estimated by fitting the model outcomes to the experimental data.

The erosion rate β_r is not easily quantified from the literature, particularly not for the fluff particles involved here (Jago et al. 1993). Therefore, this parameter has also been quantified from fitting the data against the field data.

3 Results

At the site, ebb current runs in a westerly direction and flood current to the east. Accordingly we will refer to the time when the current turns from west to east as low water slack tide (LW slack), and when it turns from east to west as high water slack tide (HW slack).

3.1 Sediment

Visual inspection of the sediment cores showed brown-greenish fine sand in the upper cm's with a thin darker brown fluffy layer on top, particularly in surface depressions, burrrows and excavation mounds of the benthic fauna (mainly *Amphiura filiformis*, *Chaetopterus variopedatus* and *Calianassa subterranea)*. This fluffy layer was most pronounced during the first days and almost disappeared later on.

Water content of the sediment was 0.29 $g.g^{-1}$ (st.d. = 0.02, n = 13) in the upper 2.5 mm and 0.27 $g.g^{-1}$ (st.d. = 0.01, n = 13) in the 2.5-5 mm depth interval (Fig. 2a). There was a tendency of decreasing water content during the experimental period, with maximum values observed at days 187-189. POC content of the sediment

showed the same tendency around an average of 0.24% (st.d = 0.04, n = 13) in the upper 2.5 mm and 0.22% (st.d = 0.04, n = 13) in the 2.5 mm below (Fig. 2b). The maximum content was measured at day 189 and the minimum at day 198. The average CN ratio of the sediment was 10.8 (st.d = 0.8, n = 13) in both depth intervals, without any visible trend in time (Fig. 2c).

3.2. Spatial distribution of chlorophyll-a and TSM

The survey around the mooring grid revealed an approximately west-east gradient in chlorophyll-a at 6 mab with the highest values west from the grid (Fig. 3a). Along a north-south transect a maximum in chlorophyll-a concentration in the bottom layer was present just north of the mooring site (Fig. 3c). Above the thermocline the spatial distribution of chlorophyll-a was more patchy without a clear gradient. In the bottom layer TSM concentration showed a gradient decreasing from south-east to north-west (Fig. 3b,d). A similar distribution, though with lower concentrations, was present above the thermocline.

3.3. Vertical distribution of chlorophyll-a and TSM

The water column was stratified with a series of temperature transitions between 10 and 25 m depth on top of the major thermocline at 25-27 m depth (19-21 mab). Temperature increased from 15 °C at day 185 to 18 °C at day 199 in the upper 10 m of the water column and from 9.2 to 9.8 °C at 1.5 mab. Semi-diurnal variation of temperature was apparent, however small compared to the gradual increase of the mean temperature during the study period. Salinity varied between 34.3 and 34.7, the highest values occurring at the end of the study period.

Chlorophyll-a and TSM were considerably higher in the bottom layer than above the thermocline (Fig. 3c,d, 4a,b), particularly TSM increased with depth and reached maximum concentrations close to the bottom (0.2 mab) where concentrations were between 5 and 12 $mg.l^{-1}$ around LW slack, ~ 5 $mg.l^{-1}$ around maximum ebb current, and between 1 and 3 $mg.l^{-1}$ during the rest of the tidal cycle (Fig. 5). One exceptionally high value of 20 $mg.l^{-1}$ was measured just before maximum flood current at 0.2 mab. At all other depths TSM was less variable around 1 - 2 $mg.l^{-1}$ (Table 1, Fig. 5).

The POC content of the suspended matter was highest above the thermocline (Table 1). The CN ratio of the organic matter showed much less variation with depth and was

also rather constant during the tidal cycle at values close to 10.5 (Table 1). At 21 mab the CN ratio appeared to be slightly lower, but the difference with the other depths is statistically not significant at $p = 0.1$.

3.4 Time series of wind, current velocity, chlorophyll-a and TSM

Wind velocities were mostly between 2.5 and 7.5 $m.s^{-1}$, velocities > 7.5 $m.s^{-1}$ occurred, however, during periods of several hours from day 190 to 193 (Fig. 6a). During most days the wind was directed to the north, only at days 188-189 and 197-199 wind blew in a southerly direction. Wave action was of minor importance with significant heights < 1 m throughout the study period.

Current velocity showed a classic semi-diurnal rhythm superimposed on the spring-neap cycle, with maximum velocities > 0.20 $m.s^{-1}$ at 1.5 mab around spring tide (day 189-194) and < 0.15 $m.s^{-1}$ around neap tide (day 186 and 197). The main axis of the tidal ellipse was approximately in the west-east direction, ~90° to N for the flood current and ~300° to N for the ebb current. Along this axis the current pattern was regular (Fig. 6b) with minor net tidal displacement over the 14 days experimental period (Fig 6c). In accordance with the lateral gradient in chlorophyll-a (Fig. 3a) the west-east current was responsible for advecting chlorophyll-a to the mooring site. From day 186 to 196 peaks in chlorophyll-a coincided with maximum displacement to the east around HW slack (Figs. 4a, 6f). After day 196 chlorophyll-a had a major peak around midnight, with only a minor peak during the day. The moving average of the chlorophyll-a time series showed an increasing trend until day 189 followed by a gradual decrease until day 199 (Fig. 6f).

The north-south component of the current was shifted 90° in phase, smaller and less regular than its west-east counterpart (Fig. 6d). Superimposed on the regular tidal sinusoidal form, the north-south current showed an additional minimum velocity at HW slack when the west-east current was zero (Fig. 8a,b). Net tidal displacement was much larger to the north than to the west (Fig. 6e). Time series of TSM showed moderate peaks occurring mostly at LW slack or at maximum current speed (Fig. 6g). From the moving average of TSM we observed an slightly increasing trend until day 188 followed by a minimum at day 189. A more pronounced decrease occurred from day 197 to 198 corresponding with the few days of wind blowing to the south, a decreased rate of net tidal displacement to the north and a low maximum current speeds at neap-tide (Fig. 6e).

3.5 Sediment traps

Outcomes of the tilt meter recordings indicated that inclinations of the trap were < 25° from the vertical, the highest tilts measured at maximum current velocities. Vertical displacements of the trap as measured by the pressure sensor mounted on the tilt meter were neglectable. Here we give the trap results uncorrected for tilt, but we will come back to this point in the discussion.

Inspection under the microscope showed that the material caught in the trap consisted mainly of fine grained sediment particles (silt). Diatoms or their remains were visible and one or two copepods had entered some of the sample cups. Total mass fluxes (dry weight) were between 390 an 2700 $mg.m^{-2}.h^{-1}$, with the maximum tidal mean fluxes occurring at day 188 and the lowest after day 192 (Fig. 7a). The average mass flux was 973 $mg.m^{-2}.h^{-1}$ (st.d. 368 $mg.m^{-2}.h^{-1}$, n = 131). Although this trend was also visible in the mass flux of POC (Fig. 7b), it was much less clear due to the opposite trend in POC content (% of dry weight) that varied between 1.3% on day 189 to one extremely high value of 5.0% on day 194 (Fig. 7c). The average POC content of all samples was 2.4% (st.d. 0.5%, n = 131) and the average CN ratio in the mass fluxes was 9.4 (st.d. 0.7, n = 131) with a maximum value of 11.5 (Fig. 7d). Two exceptionally low ratios were measured on day 189 (6.3), and day 194 (6.5) indicating a substantial contribution of fresh planktonic material on these days. In general the tidal mean CN ratio in the mass fluxes showed a slight decrease from ~10 in the first days to ~9 at the end of the measurements.

The box-whisker plots in Fig. 7 point at considerable variability within a single tidal cycle. To clarify this variability we divided the tidal cycle in 12 phase intervals of 30° each (corresponding to ~ 1h) and positioned the 1 h interval trap data according to these phase intervals. Subsequently we subtracted the median mass flux (POC, CN ratio) of each tidal cycle from the 1 h interval values of that cycle. Thus we obtained 11 data points corresponding to 11 days of trap deployment in each of the 12 phase intervals, corrected for the 14 days trend. For reference, similar plots were constructed for current velocity after selecting and integrating the 1 h trap intervals from the 'continuous' current velocity time series (Fig. 8a,b). The plots in Fig. 8 represent the effect of the 'mean' tidal cycle relative to the tidal mean mass fluxes in the traps, and thus are complementary to the data in Fig. 7.

In the mean tidal cycle total mass flux (dry weight, Fig. 8c) peaked in the first hour after LW slack and had its lowest value around maximum ebb current. On average the mass fluxes were higher during the flood current than during ebb. The flux of POC had peak values in the first hour after both slack tides (Fig. 8d) and, as for total mass flux, the total flux of POC was highest during flood current. During both flood and ebb tide minimum fluxes of POC occurred around maximum current velocity. Expressed as percentage of the total mass flux, POC content of the particles trapped showed a slight decrease from LW slack to maximum flood current followed by a sharp increase to high contents in the 2 h around HW slack (Fig. 8e). After this peak POC content decreased to its lowest value at maximum current velocity to the west (ebb) and subsequently increased again when approaching LW slack. The 2 extreme values in Fig. 8e around HW slack correspond to the samples with relatively low CN ratios on days 189 and 194. On average the CN ratio showed only minor variation during the tidal cycle, although there was a slight tendency for lower ratios during HW slack and higher ratios during maximum current velocity (Fig. 8f).

3.6. Model results

The model was tuned by comparing TSM calculated for 4.5 mab with the transmission data at the same depth (Fig. 9b). Starting values were 1 $g.m^{-3}$ for the column averaged TSM concentration $\langle C \rangle$ and 30 $g.m^{-2}$ for the mass of particles M_r in the fluff sediment layer. Parameter values are summarised in Table 2. The enhanced settling rate of 2.5 10^{-4} $m.s^{-1}$ after resuspension of particles from the fluff layer (Table 2) agrees with the range of values given by Jago et al. (1993) for their station B near our mooring site. With $\beta_r = 5\ 10^{-5}\ s^{-1}$ and M_r typically between 10 and 100 $g.m^{-2}$ (Fig. 9c), the term $\beta_r \cdot M_r = 0.5\ 10^{-3} - 5\ 10^{-3}\ g.m^{-2}.s^{-1}$, again within the range given by Jago et al. (1993).

Friction velocities exceeding the resuspension threshold of $8\ 10^{-3}$ $m.s^{-1}$ were not reached before day 188, around maximum ebb current from day 188 to 192, around both maximum ebb and maximum flood current between day 192 and 196 and irregularly after day 196 (Fig. 9a). Thus the increase of TSM predicted by the model and observed in the data between day 186 and 188 (Fig. 9b) is caused by advection of particles with a low settling velocity and not by local resuspension. The first resuspension event on day 188 causes a peak in TSM followed by enhanced sedimentation. Together with the decreased tidally averaged advection of turbid waters from the south (Fig. 6d,e) this explains the low TSM concentrations on day 189. Although the model accurately predicts the resuspension peaks between day 189

and 192 the overall increase in TSM due to a combination of advection and resuspension is lagging behind the observational data in this period. A similar discrepancy is present after day 198. Between day 194 and 198 the model predicts the TSM concentrations reasonably well, including the strong decrease around day 197, which similar to day 189 seems to be caused by the absence of resuspension together with a lower net tidal advection of water from the south.

In line with the in situ data, the model simulated strong vertical gradients in TSM, particularly close to the sediment surface (Fig. 9c). Distinct peaks of friction velocity between day 188 and 192 and at day 196 are well reflected in corresponding peaks of TSM calculated for 0.2 mab. These resuspension maxima are, however, smoothed out considerably higher up in the water column. Also between day 192 and 196 when friction velocity was above the threshold for resuspension most frequently, TSM above 6 mab remained relatively low indicating that resuspended particles stayed close to the bottom. Averaged over the entire period the deposition flux is slightly higher than the flux caused by resuspension (Fig. 9d). In total ~ 75 $g.m^{-2}$ had cumulated on the sea floor, the bulk of the accumulation occurring on day 188 and 194-195.

4. Discussion

4.1. Sources of TSM

The mooring site in the Oyster Ground is just north of the transition from the vertically well mixed southern North Sea with high TSM concentrations to the Central North Sea which is stratified during summer and is less turbid (Eisma & Kalf 1987). In the Oyster Ground TSM mostly shows a gradient from south-east to north-west in the summer months, with concentrations between 0.5 and 2 $mg.l^{-1}$ below the thermocline (Fig. 3; Wirth & Seifert 1988, Hölemann & Wirth 1988, Dyer & Moffat 1993). The highest turbidity is probably present ~ 90 km south-west of the mooring grid in the vicinity of a tidal mixing front ('Frisian Front') at slightly shallower depth, 30-40 m, than the Oyster Ground proper (Van Haren & Joordens 1990). Close to this front is a mud patch (Creutzberg et al. 1984) from which particles may be resuspended and contribute to TSM at the mooring site. Contribution of other sources further away can, however, not be excluded. Moreover, the mud patch it self has been identified as an area where particles can be deposited originating from the entire Southern Bight and the English coast (Creutzberg & Postma 1979, Creutzberg et al. 1984). Thus, the

ultimate, longer-term sources of TSM observed at the mooring site are likely to be found in a large area south of the Oyster Ground.

Current meter data indicated a ~2 $km.d^{-1}$ northward residual drift at 1.5 mab, which is in line with the 2 - 3.5 $km.d^{-1}$ tidal displacement from the Frisian Front to the north observed previously during the summer season (Tijssen & Wetsteyn 1984, Van Haren & Joordens 1990) and also with the current pattern in the area modelled by Pohlman & Puls (1995) for a 'climatological mean' summer period. Thus, even from a relatively short distance as from the Frisian Front mud patch it may take several weeks for a suspended particle to reach the mooring grid. The vertical distribution of TSM along the north-south transect across the mooring site (Fig. 3d) gives direct evidence for deposition in the Oyster Ground of particles advected from the south. If we, as a crude simplification, treat the lines of constant concentration in Fig. 3d as the lines along which particles settle to the sea floor, it is calculated that they sink ~1 m for every km travelled to the north. This implies that they may be advected for 50 km at most before reaching the sediment. Maximum time-scales for settling from the water column can be calculated from $\tau = h/\omega$ (see last part of discussion), where h is the depth of the bottom layer (~ 20m) or the entire water column (~ 50m). For particles with a sinking velocity of 2 10^{-5} $m.s^{-1}$ (Table 2) $\tau \approx$ 10-25 days. Comparing the time scales for lateral transport and settling it is concluded that particles can reach the Oyster Ground only after having passed a continuous saltation process of settling from the water column and rebouncing from the sea floor.

To determine whether the particles resuspended have the same properties as the top 2.5 mm of the sediment we follow the approach of Jago et al. (1993) and apply the two-component mixing model of Morris et al. (1987). In this model it is assumed that TSM consists of a constant background S_0 with carbon content C_0 and a variable amount of particles S_r resuspended from the sediment and having a carbon content C_r. Taking into account that $TSM = S_0 + S_r$ an inverse relationship follows between the organic carbon content of the mixture suspended in the water column (POC) and the total mass of that mixture (TSM):

$$POC = (C_0 - C_r) \cdot \frac{S_0}{TSM} + C_r \qquad (7)$$

Regression of POC against TSM in samples from the bottom mixed layer (0.2, 6, 11 mab) yields a significant relationship (Fig. 10a) from which C_r is calculated at 2.4%

(SD = 1.5%). This carbon content is ~10 times higher than in the upper mm's of the sediment, ~ 5 times lower than on average in the water column, but equal to the average organic carbon content in the sediment trap mass fluxes. If we do a similar analysis for organic N (Fig. 10b) it follows that the resuspension flux has an N content of 0.44% (SD = 0.14%) which again is close to the trap materials (0.30%). The organic carbon content in the resuspension flux found here confirms the data of Jago et al. (1993) who found C_r varying between 1.9% and 4.5% at 2 sites in the North Sea and in different months of the year. It is concluded that particles available for resuspension under no-storm conditions are carbon-enriched compared with the bulk sediment. This corroborates the view of Jago et al. (1993) and validates our modelling assumption that the materials resuspended are derived from a surficial fluff layer and not from the sea bed proper. From the similarity of the C and N contents in the fluff material and in the sediment traps it is further concluded that deposition of resuspended fluff materials is by far the dominating contributor to the trap mass fluxes.

Most of the labile carbon in the sediment originating from summer production is likely to be mineralised in winter or washed from the sediment (Van Raaphorst et al. 1992). Thus, we estimated the 'base-line' POC content of the sediment on the basis of the 0.17% organic C measured by Van Raaphorst & Malschaert (1996) in the upper 5 mm of the sediment at the mooring site in February 1992. Using this value and POC = 0.24% and 2.4% in the bulk sediment and the fluff material, respectively, it follows that only ~3% of the sediment in the Oyster Ground consists of fluff available for resuspension under the hydrodynamic conditions that prevailed during our study.

Not only POC in the resuspension flux can be estimated from the regression line in Figure 10a, but, if S_0 is known, also the C content in the suspended background (C_0). The steepness of the hyperbolic regression curve at low TSM values, however, makes the reliability of such estimate very sensitive to the accuracy of S_0. Using the background TSM concentration of 0.3 $mg.l^{-1}$ estimated from our modelling exercise (Table 2) C_0 is calculated at 53% which is a rather high percentage. If, instead, we assume a slightly higher background of 0.5 $mg.l^{-1}$ a more realistic POC content of 33% is found. Comparing this latter percentage with the average POC content of TSM (Table 1) and the 2.4% carbon content calculated for the resuspension component, it is concluded that, on average, resuspended fluff contributes as much as 70-80% to TSM in the bottom mixed layer.

4.2. Phytoplankton

A small part of TSM in the bottom mixed layer consisted of phytoplankton. At the average chlorophyll-a concentration of ~800 ng.l^{-1} (Fig. 6f) and assuming an algal POC:chlorophyll-a ratio of 50-100:1 (Reid et al., 1990) we estimate the average phytoplankton concentration at 0.04-0.08 mg-C.l^{-1}, corresponding to 0.1-0.2 mg.l^{-1} total biomass. Thus, the contribution of phytoplankton biomass to TSM is 10-20% in the lower part of the water column, but the contribution of phytoplankton C to total POC may be as large as 25-50%. Although these percentages are crude averages they demonstrate that living biomass and pigment containing detritus can not be neglected as part of TSM, which, consequently, not only consists of 'old' fluff materials but also, although for a minor part, of 'fresh' organic matter.

The relationships in Fig. 10a,b obscure any further partition of TSM into old and fresh materials. Plotting the CN ratio of the suspended particles as a function of TSM, however, shows that the CN ratio at TSM = 1-3 mg.l^{-1} is less than at either lower or higher suspended matter concentrations (Fig. 10c). This indicates that labile, presumably plankton derived material dominates POC at low to moderate TSM concentrations, probably because phytoplankton production is stimulated in water masses with low TSM where light conditions are most favourable. Indeed, highest chlorophyll-a concentrations were measured west of the mooring site where TSM was lowest and, in accordance, the tidal variability of chlorophyll-a is mainly due to west-east advective transport, which renders the semi-diurnal pattern with major peaks in fluorescence at HW slack. This is in contrast to TSM that is advected from the south-east and shows its peak values mainly during ebb current and LW slack, albeit additional maxima occurred around HW slack sometimes (e.g. Fig. 4).

Although the time series of TSM and chlorophyl-a are controlled by different processes and by advection from different directions, this does not mean that they behave completely separated without mutual influences. Superimposed on the semi-diurnal pattern in chlorophyll-a Van Duyl et al. (1996) found a quarter-diurnal pattern related to deposition of phytoplankton occurring at HW slack tide followed by resuspension at increasing current velocity. Because some time passes between settling on the sea floor and re-entrainment in the water column, resuspended phytoplankton enters a new water mass enriched with TSM, thus providing conditions favourable for aggregation and floc-forming during the next LW slack. Flocculation may be further stimulated through binding of fluff particles with organic compounds derived from the phytoplankton (Eisma 1992, Chen 1995). This explains why

sediment trap mass fluxes of phytopigments (Van Duyl et al. 1996) and organic carbon (Fig. 8) are so high at LW slack despite the low phytoplankton concentrations in the water column in that phase of the tidal cycle.

4.3. Sediment trap fluxes

Even though wind and wave activity were low during our experimental period, the C and N content of the sediment trap mass fluxes indicated that these fluxes were due primarily to resuspension and resettling of bottom fluff, a situation which is characteristic for high-energy environments (e.g. Gardner et al. 1983). Thus, by no means the trap fluxes can be used to directly determine the rate of mass accumulation on the sediment. Instead, they will be evaluated with the aim to further discuss the tidal dynamics of both resuspension and resettling fluxes.

There is overwhelming evidence that the efficiency of sediment traps is controlled by their geometry, the mooring design and the hydrodynamic conditions during deployment (e.g. Gardner 1985, Butman 1986, Butman et al. 1986, Baker et al. 1988, Gust et al. 1994). A general conclusion of these studies is that 'a sediment trap is a tool that cannot be accurately calibrated at this time' (Gust et al. 1994), and, consequently, that 'knowledge of the collection efficiency of sediment traps, particularly under conditions of varying current speed, is presently more a matter of hope than confidence' (Baker et al. 1988). Despite this high level of uncertainty several recommendations have been made for optimal design and deployment that seem widely accepted. We took into account these recommendations and applied a bottom-moored array containing a cylindrical trap with a relatively high aspect ratio > 4. As the current speed essentially varied between 2 and 20 $cm.s^{-1}$ the trap Reynolds number was $4\ 10^3$ - $4\ 10^4$. In this range of Reynolds numbers the collection efficiency of the trap probably is relatively insensitive to varying flow speed (Butman 1986), although a later study of Baker et al. (1988) revealed that lower efficiencies may be expected at the highest current velocities encountered during our study. The dimensionless fall velocity of the particles collected in the trap (ω/U = fall velocity / current velocity) cannot be quantified accurately from our data. Taking the tidal range in current speed and assuming that the fall velocities estimated from the model (Table 2) are a good approximation for the real world ω/U may vary over two orders of magnitude between 10^{-2} and 10^{-4}. There are both theoretical and experimental indications that the collection efficiency decreases with decreasing dimensionless fall velocity (Butman et al. 1986, Baker et al. 1988), thus suggesting that slowly settling

particles may be under-collected at maximum current speed in the tidal cycle. Gardner (1985), on the other hand, showed that smaller particles are collected more efficiently than larger ones when the trap is tilted in the direction of the current, which was always the case during our deployments.

Tilted traps collect more particles than traps held vertical (Gardner 1985). It can, however, not be concluded whether, at a given current speed and trap Reynolds number, tilted traps are over-collectors or vertical traps are under-collectors. To investigate the possible effect of tilt on our trap mass fluxes we applied the tilt-correction determined for baffled cylinders with aspect ratio 5.2 by Gardner (1985):

$$F = \frac{F_T}{1 + 1.4 \cdot \sin 2\theta} \qquad (8)$$

where F is the corrected mass flux expected in a vertical trap, F_T is the flux measured in the tilted trap and θ is the degree of tilt from the vertical. Correction for tilt lowers the mass fluxes considerably, but the overall picture with highest fluxes in the first week of our measurements remains intact (Fig. 11a). For the mean tidal cycle correction of the mass fluxes had a relatively minor effect (Fig. 11b) giving support to the conclusion that particularly the high mass fluxes shortly after LW slack are realistic.

Downward particle fluxes can increase for two reasons. First, increasing the particle concentration should cause an enhanced flux if particle settling velocities remain unchanged. Second, larger fluxes may be due to increased settling velocities through flocculation or addition to the water column of larger, rapidly sinking particles. Enhanced tidal mean total mass fluxes were measured on day 188 to 190 when also the highest fluxes were collected in individual sample cups (Fig 7a, 11a). These high fluxes correspond to the massive deposition simulated by the model on day 188 (Fig. 9d). Although TSM increased in the first week this increase seems not sufficient to explain the high trap fluxes, certainly not when taking into account that TSM between day 191 and 197 was similarly high as on day 188 and even higher than on day 189. Thus, it seems that the average settling velocity had increased from day 188 to 190. This is evidenced by the ratio between the mass fluxes and the TSM concentration, which can be viewed as the apparent settling velocity of the particles collected in the trap (Fig. 12). Assuming the tilt-corrected fluxes as being representative the apparent tidal mean settling velocity was ~1 10^{-4} $m.s^{-1}$ which is in between the low and high settling velocity estimated from our model. Higher median values of ~ 1.5 10^{-4} $m.s^{-1}$ were calculated for day 188 and 189 while velocities between 2.5 10^{-4} and 5 10^{-4} ms^{-1}

occurred during 4 trap opening hours on day 188 to 190 at the onset of the spring tide-related period with enhanced bottom friction velocities. The same calculation shows a minimum tidal mean settling velocity on day 196 just before neap-tide.

Any further statement on the effect of the spring-neap cycle on the trap fluxes has to remain speculative because we sampled only one such cycle. The trap data span, however, a total of 11 semi-diurnal cycles and for these more definite conclusions can be drawn. In the mean tidal cycle total mass flux was strongly elevated in the first hour after LW slack and lowest during maximum ebb current. The similarity of this pattern with that of the apparent settling velocity (Fig. 12b) demonstrates the importance of changes in particle settling velocity during the tidal cycle. Around maximum ebb current particles are resuspended from the sea floor and maximally advected from the south-east. At the relatively high current speed during that phase of the tidal cycle flocs are not likely to be formed and may even be broken up (e.g. Chen 1995). The organic carbon content of the mass fluxes is relatively low at maximum ebb current indicating a poor association with detritus and phytoplankton derived compounds. This association increases upon approaching LW slack, indicated by the higher POC content and lower CN ratio, consistent with the conclusion made earlier that the high mass fluxes shortly after LW slack are caused by flocculation processes. Flocculation effects on the apparent settling velocity are more pronounced at LW slack than at HW slack. We conclude that floc forming is stimulated most efficiently at times of low current speed directly after maximum concentrations of both chlorophyll-a and TSM have been advected to the mooring site, thus providing sufficient possibility for particle collision and aggregation.

4.4. Sediment

Resuspension, advection and redeposition alter the properties of the surface layers of the sediment. During periods of resuspension sediment stratification and laminations may disappear, particularly close to the sediment surface (Aller 1989). We observed a fluffy layer on top of the sediment in our box-core only during the first days of the cruise, i.e. during neap tide when the current velocity remained low. The disappearance of this layer coincides with the first day the bottom friction velocity exceeded the threshold for resuspension assumed in the model. Other sediment properties as water content and organic carbon content in the top 5 mm reached their highest values at the moment of massive deposition on day 188 shortly after the first resuspension event (Fig. 2, 9) when also the trap fluxes were at maximum (Fig. 7),

and decreased continuously in the period thereafter. (Fig. 2). We interpret these observations as evidence for resuspension starting at day 188 at the onset of spring tide following steady deposition around neap tide.

The decrease in the water and organic carbon content at the beginning of spring-tide suggests that fluff is washed out from the sediment. This contradicts with the model outcome and the trap data showing that resuspended fluff resettled during slack current following resuspension. Apparently, this intermittent deposition did not lead to a watery fluff layer recognisable in the box-cores. An important mechanism by which fluffy layers are created is by feeding, locomotion and habitat development of the benthic fauna that, amongst other effects, leads to rhythmic fluff expulsions related to faeces production and caving (Davis 1993). It may be that the benthic fauna changed its behaviour during the spring-neap cycle. Suspension feeders probably diminish their activity at the high current speed at spring tide, thus having to take all their food at the subsequent slack current, whereas they may show an approximately constant activity around neap-tide (Davoult & Gounin 1995). In addition, some species may change from bed destabilising (Davis 1993) deposit feeding at low current velocity to passive suspension feeding at higher velocities (Thomsen et al. 1995 and references cited therein). This may have promoted an efficient burial of resettled material during spring-tide. According to Davis (1993) both the bed stabilising and destabilising effects caused by different species of benthic fauna increase with increasing seabed shear stress. The disappearance of the fluff layer on top of the sediment then may simply reflect the high turn-over rate of resuspendable particles due to the increased gross fluxes of both resuspension and deposition during spring-tide.

4.5. Advection, resuspension and deposition in the Oyster Ground

There are no good estimates available on the net transport time of TSM through the southern North Sea. The residence time of water, < 1year (see introduction), may serve as a minimum estimate only because temporary deposition and retention on the sea floor should lengthen the average travelling time of particulate matter. It has been suggested (Kempe et al. 1988) that the fine fraction of the sediment requires 10 to 15 years for the journey from the Elbe Estuary in the German Bight to the Skagerrak. Such a long travelling time would guarantee almost complete oxidation of the labile organic matter before final deposition in the Skagerrak-Norwegian Channel. Thus, an important question to be answered is to what extent deposition and resuspension in the Oyster Ground and similar areas influence the overall lateral transport of TSM and the

fate of organic matter. We will firstly address the time that particles deposited may be retained in the sediment before their next resuspension under calm weather conditions, then discuss the possible influence of storms, and finally the role of mid-shelf depocentres in the carbon budget of the North Sea.

Residence times of particulate matter. The time scale for settling, $\tau = h/\omega$, estimated in the first part of the discussion is an overestimate because it does not take into account the vertical profile of TSM with high concentrations close to the bottom, thus shortening the average settling distance of the particles. A more accurate estimate can be obtained from the model result on the gross deposition flux Q_b (eq. 5) yielding a total of 325 $g.m^{-2}$ in 14 days (Fig. 9), corresponding to an average flux of 23 $g.m^{-2}.d^{-1}$. At a mean concentration of 1.5 - 2 $g.l^{-1}$ the inventory of TSM in the lower mixed layer of the water column is 30 - 40 $g.m^{-2}$, from which follows a settling time of ~ 1.5 day. If, alternatively, the apparent sinking velocities calculated from the sediment trap data are used and we assume an average settling distance of 10 m (half the thickness of the lower mixed layer), the time needed for settling out is estimated at ~10 /1 $10^{-4} = 10^5$ s = 1.2 day. It is concluded that the residence time of particulate matter in the lower mixed layer is in the order of only 1 - 2 days.

The residence time in the water column should be compared to the time particles are retained in the sediment upon deposition. The model simulates a net accumulation of ~75 $g.m^{-2}$ in the 14 days study period, suggesting that, at prolonged deposition for some weeks, the total inventory on the bottom can be several hundreds of grams per square meter. From the organic carbon content in the sediment and resuspended fluff we have calculated earlier that about 3% of the mass present in the upper 5 mm of the sediment is available for resuspension. With this percentage and taking into account the volume occupied by pores (45%, calculated from the water content) and further assuming a specific density of the sediment grains of 2.5 $g.cm^{-3}$, it is calculated that approximately 250 $g.m^{-2}$ of resuspendable fluff is present in the surface 5 mm of the sediment. Although this value directly depends on the depth of the sediment layer assumed to be involved in resuspension, the order of magnitude strongly supports the model results. From the comparison of these estimates with the inventory of TSM in the overlying water it is concluded that by far the largest portion of the total pool of particles taking part in the saltation process between the sea bed and the water column is present in the sediment.

The gross resuspension rate is taken from the model and amounts 250 $g.m^{-2}$ in 14 days (Fig. 9). Taking a range of 100 - 250 $g.m^{-2}$ as a best guess for the pool of

resuspendable fluff in the sediment, this means that the average residence time of particles between deposition and resuspension is in the order of 1 - 2 weeks under the calm weather conditions that prevailed during our study.

Influence of storms. The 14 days accumulation of ~75 $g.m^{-2}$ would, if valid outside the study period, lead to a sediment accretion of approximately 1.5 mm per year. Previous studies have indicated that net accumulation is not likely to occur in the Oyster Ground on time scales larger than decades to centuries (Cadée 1984, Eisma & Kalf 1987). The summer deposition predicted by the laboratory experiments of Creutzberg & Postma (1979) and the models of Puls & Sündermann (1990) and Sündermann (1993) is, however, confirmed by our study. Here, we will question whether such deposition can lead to accumulation during stormy periods in autumn and winter. Therefore we conducted additonal simulations with our model, inserting current velocities measured at the mooring site in December 1994. Thus, we createded 'storms' between day 190 and 195 with bottom friction velocities well above 10-15 10^{-3} m s^{-1} (Fig. 13). For comparability we left all parameters unchanged compared to the summer simulation, except for the depth of the bottom mixed layer that we assumed now to occupy the whole water column of 46 m (i.e. no stratification as normal during winter). With this set of parameters the model reproduced the development of TSM concentration as revealed by ADCP reasonably well, particularly the timing of the strong peaks in TSM associated with maximum friction velocities (Fig. 13). It should be noted that this result was obtained without taking the effect of waves into account.

The picture that emerges from the model is a highly dynamic exchange of particles between the sediment and the water column at increased friction velocity. Compared to the calm-weather simulation (Fig. 9) the gross fluxes of both resuspension and deposition were ~5 times higher in the stormy winter situation. These fluxes are probably even underestimated due to the absence of the effect of wave action in our calculations. Therefore we expect that in the stormy period the resuspension flux and the exhaustion of the bottom layer available for resuspension were more pronounced than suggested by the model, particularly at the moments when wind speed (and waves) was at maximum. Both the data from the ADCP and the model results show that rapid resettling occurs after passage of the storms, albeit that concentrations after the storms remained slightly higher than before. As a consequence, the fluff layer that was almost completely eroded at maximum current speeds quickly re-established when wind and current velocity slowed down. In conclusion, the model results suggest a net accumulation on the bottom in between storms also during autumn and winter.

The role of temporary depocentres in North Sea carbon cycling. During their retention in the sediment upon deposition, particles can loose a substantial portion of their organic carbon content. Thomsen et al. (1995) reported results from an *in situ* experiment on a several km's long transect occupied by macrofauna feeding at the sediment-water interface along the continental slope of the Barents Sea, and showed that POC laterally advected was the most important source of labile carbon to the benthic community. In the Oyster Ground, a similar importance of advection of organic matter may exist. In the absence of sufficient deposition from local primary production in the water column, TSM and POC advected to the Oyster Ground may sustain deposition fluxes and provide organic matter to the benthos. The calculated net deposition of 75 $g.m^{-2}$ corresponds to a daily input of organic carbon of ~115 $g.m^{-2}$ to the sediment (assuming a labile carbon content of 2.4 - 0.2 = 2.2%), which is sufficient to fuel the local benthic bacterial production (32 $gC.m^{-2}.d^{-1}$ in the top 3 mm, Van Duyl et al. 1996). This comparison is biased as it assumes complete availability for the bacterial population of the organic matter accumulated within the time-scale considered and because it ignores the carbon utilisation by meiofauna and macrofauna. It does, however, also not into account the amount of organic matter that is not accumulated but which is deposited temporarily and during its stay in the sediment is available as carbon source for the benthic organisms. An average retention time in the sediment of 1 - 2 weeks may allow for substantial decomposition of relatively fresh organic matter (Middelburg 1989, Van Raaphorst et al. 1992). According to the measurements of Van Duyl et al. (1996) sediment concentrations of the phytopigments chlorophyll-a, fucoxantine and pheophytin-a decreased at a first order rate of ~ 0.06 d^{-1} between day 185 and 199, corresponding to a turn-over time of 17 days. This turn-over is determined by a balance of decomposition and new input of phytopigments from the water column. Consequently, the average life-time of phytopigments in the sediment is lower than indicated by the above rate of disappearance. Although the degradation of pigments may be more rapid than other sedimentary organic compounds that may serve as food for the benthos (Van Duyl et al. 1993), it is strongly suggested that the largest portion of the organic matter deposited is mineralised in a few weeks only, i.e. at time scales comparable to the average retention of fluff particles in the sediment between deposition and resuspension.

A rapid mineralisation of organic matter shortly after deposition is in accordance with sediment-water exchange fluxes and pore water profiles of inorganic nutrients at this station and in comparable areas with transient deposition in the North Sea (Gehlen et

al. 1995, Lohse et al. 1995, Van Raaphorst & Malschaert 1996). Such rapid microbial decomposition is probably promoted by frequent resuspension and physical stirring of the sediment (Aller 1989). Furthermore, the rich macrofauna assemblage at the site may provide an additional stimulus for particle reworking and organic breakdown. We conclude that substantial decomposition can occur of the organic matter settled in the Oyster Ground before re-entrainment into the cross-shelf transport route towards the Skagerrak-Norwegian Channel. Taking into account that repeated deposition and resuspension may occur on this route, this conclusion implies that mid-shelf temporary depocentres play a crucial role the carbon budget of the North.

Acknowledgements. We are grateful to Willem Polman and the crew of RV Pelagia for their help during the cruise. Lutz Lohse joint our lab container on board and did part of the sediment sampling. Fleur van Duyl is acknowledged for putting her data at our disposal. She, Willem Helder and Herman Ridderinkhof critically read early drafts of the manuscript. This study was funded by the Dutch BEON programme (grant 94/95 E-01) and by the Nertherlands Marine Research Foundation (grant 39104).

REFERENCES

Aller, J.Y. 1989. Quantfying sediment disturbance by bottom currents and its effect on benthic communities in a deep-sea western boundary zone.Deep-Sea Res. **36**: 901-934.

Baker, E.T., H.B. Milburn & D.A. Tennant 1988. Field assessment of sediment traps under varying flow conditions. J. Mar. Res. **46**: 573-592.

Butman, C.A. 1986. Sediment trap biases in turbulent flows: Results from a laboratory flume study. J. Mar. Res. **44**: 645-693.

Butman, C.A., W.D. Grant & K.D. Stolzenbach 1986. Predictions of sediment trap biases in turbulent flows: A theoretical analysis based on observations from the literature. J. Mar. Es. **44**: 601-644.

Cadée, G.C. 1984. Macrobenthos and macrobenthic remains on the Oyster Ground, central North Sea. Neth. J. Sea Res. **18:** 160-178.

Chen, S. 1995. Floc size and aspects of flocculation processes of suspended particulate matter in the North Sea area. Ph.D. thesis, University of Utrecht, NL.

Churchill, J.H., P.E. Biscaye & F.Aikman III 1988. The character and motion of suspended particulate matter over the shelf edge and upper slope off Cape Cod. Cont. Shelf Res. **8:** 789-890.

Churchill, J.H., C.D. Wirick, C.N. Flagg & L.J. Pietrafesa 1994. Sediment resuspension over the continental shelf east of the Delmarva Peninsula. Deep-Sea Res. II **41:** 341-363.

Creutzberg, F. & H. Postma 1979. An experimental approach to the distribution of mud in the southern North Sea. Neth. J. Sea Res. **13:** 99-116.

Creutzberg, F., P. Wapenaar, G. Duineveld & N. Lopez Lopez 1984. Distribution and density of the benthic fauna in the southern North Sea in relation to bottom characteristics and hydrographic conditions. Rapp. P.-v. Réun. Conts. int. Explor. Mer. **183:** 101-110.

Davis, W.R. 1993. The role of bioturbation in sediment resuspension and its interaction with physical shearing. J. Exp. Mar, Biol. Ecol. **171**: 187-200.

Davoult, D. & F. Gounin 1995. Suspension-feeding activity of a dense *Ophiuthrix fragilis* (Abildgaard) population at the water-sediment interface: time coupling of food availability and feeding behaviour of the species. Estuar. Coast. Shelf Sci. **41:** 567-577.

Drake, D.E. & D.A. Cacchione 1989. Estimates of the suspended sediment reference concentration and resuspension coefficient (γ_0) from near-bottom observations on the California shelf. Cont. Shelf Res. **9:** 51-64.

Dyer, K.R. & T.J. Moffat 1993. Suspended sediment distributions in the North Sea. Inst. Marine Studies Report, Univ. of Plymouth.

Eisma, D. 1992. Suspended matter in the aquatic environment. Springer, Berlin.

Eisma, D. & J. Kalf 1987. Dispersal, concentration and deposition of suspended matter in the North Sea. J. Geol. Soc. **144:** 161-178.

Gardner, W.D. 1985. The effect of tilt on sediment trap efficiency. Deep-Sea Res. **32**: 349-361.

Gardner, W.D., M.J. Richardson, K.R. Hinga & P.E. Biscaye 1983. Resuspension measured with sediment traps in a high-energy environment. Earth Planet. Sci. Lett. **66**: 262-278.

Gehlen, M., J.F.P. Malschaert & W. Van Raaphorst 1995. Spatial and temporal variability of benthic sislica fluxes in the southeastern North Sea. Cont. Shelf Res. **15:** 1675-1696.

Gust, G., A.F. Michaels, R. Johnson, W.G. Deuser & W. Bowles 1994. Mooring line motions and sediment trap hydromechanics: *in situ* intercomparison of three common deployment designs. Deep-Sea Res. **41**: 831-857.

Hainbucher, D., T. Pohlmann & J. Backhaus 1987. Transport of conservative passive tracers in the North Sea: first results of a circulation and transport model. Cont. Shelf Res. **7:** 1161-1179.

Hill, P.S. & A.R.M. Nowell 1995. Comparison of two models of aggregation in continental-shelf bottom boundary layers. J. Geophys. Res. **100:** 22,749-22,763.

Hölemann, J. & H. Wirth 1988. Concentration, major element ratios and scanning electron microscopy of suspended particulate matter from the North Sea, spring 1986. Mitt. Geol.-Paläont. Inst. Univ. Hamburg, SCOPE/UNEP Sonderband **65:** 183-206.

Jago, C.F., A.J. Bale, M.O. Green, M.J. Howarth, S.E. Jones, I.N. McCave, G.E. Millward, A.W. Morris, A.A. Rowden & J.J. Williams 1993. Resuspension processes and seston dynamics, southern North Sea. Phil. Trans. R. Soc. Lond. **A343:** 475-491.

Jenness, M.I. & G.C.A. Duineveld 1985. Effects of tidal currents on chlorophyll-a content of sandy sediments in the southern North Sea. Mar. Ecol. Prog. Ser. **21:** 283-287.

Jørgensen, B.B. 1983. Processes at the sediment-water interface. In: B. Bolin & R.B. Cook (eds.), The major biogeochemical cycles and their interactions. Wiley, Chichester, pp. 477-515.

Kempe, S. & T. Jennerjahn 1988. The verticle particle flux in the northern North Sea, its seasonality and composition. Mitt. Geol.-Paläont. Inst. Univ. Hamburg, SCOPE/UNEP Sonderband **65:** 229-268.

Kempe, S., G. Liebezeit, V. Dethlefsen & U. Harms 1988. Biogeochemistry and distribution of suspended matter in the North Sea and implications to fisheries biology. Synopsis. Mitt. Geol.-Paläont. Inst. Univ. Hamburg, SCOPE/UNEP Sonderband **65:** XI-XXIV.

Krone, R.B. 1962. Flume studies of the transport of sediment in estuarial shoaling processes. Hydr. Engr. Lab. and Sanitary Engr. Res. Lab., Univ. of California, Berkeley, 110 pp.

Lohse, L., J.F.P. Malschaert, C.P. Slomp, W. Helder & W. Van Raaphorst 1995. Sediment-water fluxes of inorganic nitrogen compounds along the transport route of organic matter in the North Sea. Ophelia **41:** 173-197.

Lyne, V.D., B. Butman & W.D. Grant 1990a. Sediment movement along the U.S. east coast continental shelf-I. Estimates of bottom stress using the Grant-Madsen model and near-bottom wave and current measurements. Cont. Shelf Res. **10:** 429-460.

Lyne, V.D., B. Butman & W.D. Grant 1990b. Sediment movement along the U.S. east coast continental shelf-II. Modelling suspended sediment concentration and transport rate during storms. Cont. Shelf Res. **10:** 397-428.

McCave, I. 1987. Fine sediment sources and sinks around the East Anglian coast (UK). J. Geol. Soc. Lond. **144:** 149-152.

Middelburg, J.J. 1989. A simple rate model for organic matter decomposition in marine sediments. Geochim. Cosmochim. Acta **53:** 1577-1581.

Moody, J.A., B.A. Butman & M.H. Bothner 1987. Near-bottom suspended matter on the continental shelf during storms: estimates based on *in situ* observations of light transmission and a particle size dependent transmissometer calibration. Cont. Shelf Res. **7:** 609-628.

Morris, A.W., A.J. Bale, R.J.M. Howland, R.F.C. Mantoura & E.M.S. Woodward 1987. Controls of the chemical composition of particle populations in a macrotidal estuary (Tamar estuary, UK). Cont. Shelf Res. **7**: 1351-1355.

Nedwell, D.B., R.J. Parkes, A.C. Upton & D.J. Assinder 1993. Seasonal fluxes across the sediment-water interface , and processes within sediments. Phil. Trans. R. Soc. Lond. **A343:** 519-529.

Otto, L., J.T.F. Zimmerman, G.K. Furness, M. Mork, R. Saetre & G. Becker 1990. Review of the physical oceanography of the North Sea. Neth. J. Sea Res. **26:** 161-238.

Pingree, R.D. & D.K. Griffiths 1978. Tidal fronts on the shelf seas around the British Isles. J. Geophys. Res. **83:** 4615-4622.

Pohlman & Puls 1995. Currents and transport in water. In: J. Sündermann (ed.), Circulation and contamination fluxes in the North Sea, Springer, Berlin, pp. 345-402.

Postma, H. & J.W. Rommets 1984. Variations of particulate organic carbon in the central North Sea. Neth. J. Sea Res. **18:** 31-50.

Puls, W. & J. Sündermann 1990. Simulation of suspended sediment dispersion in the North Sea. In: R.T. Cheng (ed.) Residual currents and long-term transport. Coastal and Estuarine Studies **38**, Springer New York, pp. 356-372.

Puls & J. Sündermann 1993. Modeling the distribution of suspended matter and lead in the North Sea. In: A.J. Mehta (ed.). Nearshore and estuarine cohesive sediment transport. Coastal and Estuarine Studies **42**, Springer New York, pp. 520-540.

Reid, C.P., C. Lancelot, W.W.C. Gieskes, E. Hagmeier & G. Weichart 1990. Phytoplankton of the North Sea and its dynamics: A review. Neth. J. Sea. Res. **26**: 295-331.

Ruardij, P., J.J.F. Van Haren & H. Ridderinkhof 1996. The impact of timing of the thermal stratification on production, succession and grazing of phytoplankton in shelf seas: A model study. Submitted to J. Sea. Res.

Sündermann, J. 1993. Suspended particulate matter in the North Sea: field observations and modelling. Phil. Trans. R. Soc. Lond. **A343:** 45-52.

Tett, P. & A. Walne 1995. Observations and simulations of hydrography, nutrients and plankton in the southern North Sea. Ophelia **42:** 371-416.

Thomsen, L., G. Graf, K. von Juterzenka & U. Witte 1995. An *in situ* experiment to investigate the depletion of seston above an interface feeder field on the continental slope of the western Barents Sea. Mar. Ecol. Prog. Ser. **123**: 295-300.

Tijssen, S.B. & F.J. Wetsteyn 1984. Hydrographic observations near a subsurface drifter in the Oyster Ground, North Sea. Neth. J. Sea Res. **18:** 1-12.

Van Duyl, F.C., G.C.A. Duineveld, A.J. Kop, & G. Kraay 1996 Pelagic-benthic coupling in the North Sea: short-term dynamics in phytopigment sedimentation and the response of benthic bacteria. Submitted to:

Van Haren, J.J.M. & J.C.A. Joordens 1990. Observations of physical and biological parameters at the transition between the southern and the northern North Sea. Neth. J. Sea Res. **25:** 331-350.

Van Raaphorst W., H.T. Kloosterhuis, E.M. Berghuis, A.J. Gieles, J.F.P. Malschaert & G.J. van Noort 1992. Nitrogen cycling in two types of sediments of the southern North Sea (Frisian Front, Broad Fourteens): Field data and mesocosm results. Neth. J. Sea Res. 28: 293-316.

Van Raaphorst, W. & J.J.F. Malschaert 1996. Ammonium adsorption in superficial North Sea sediments. Cont. Shelf Res. **16**: 1415-1435.

Van Weering, T.C.E., G.W. Berger &J. Kalf 1987. Recent sediment accumulation in the Skagerrak, north eastern North Sea. Neth. J. Sea Res. **21:** 177-189.

Verardo, D.J., P.N. Froelich & A. McIntyre 1990. Determination of organic carbon and nitrogen in sediments using the Carlo Erba NA-1500 analyzer. Deep-Sea Res. **37:** 157-165.

Walsh, I.J., J. Dymond & R. Collier 1988. Rates of recycling of biogenic components of settling particles in the ocean derived from sediment trap experiments. Deep-Sea Res. **35:** 43-58.

Walsh, J.J.1991. Importance of continental margins in the marine biogeochemical cycling of carbon and nitrogen. Nature **350:** 53-55.

Wirth, H. & R. Seifert 1988. Mineralogy, geochemistry and SEM-observations of suspended particulate matter from the North Sea, spring 1984. Mitt. Geol.-Paläont. Inst. Univ. Hamburg, SCOPE/UNEP Sonderband **65:** 163-181.

Wright, L.D. 1995. Morphodynamics of inner continental shelves. CRC Marine science series, CRC Press, Boca Raton, Florida, USA, pp.241.

Table 1: Average concentration of TSM, POC content and CN ratio measured in the bottle samples from different depths in the water column. The data of 0.2 mab represent bottom water sampled with a membrane pump, 6 - 11 mab represents the lower water column, 21 mab is at the lower part of the thermocline, and 31-41 mab is in the surface water. The number of data varies from n = 11 (POC, 21 mab) to n = 24 (TSM, 6-11 and 31-41 mab).

Depth mab	TSM $mg.l^{-1}$	POC %	CN ratio
0.2	4.1 (3.4)	9.4 (5.1)	10.6 (2.9)
6-11	1.7 (0.6)	11.0 (5.8)	10.0 (3.0)
21	1.4 (0.7)	16.6 (8.5)	8.8 (1.9)
31-41	0.9 (0.5)	18.8 (8.5)	10.8 (4.5)

Table 2: Parameter values applied in the advection-deposition-resuspension model of TSM (equation 1-6). [(1), (2)] calculated from the spatial distribution of TSM at 6 mab (Fig. 3); [(3)] based on Tett & Walne (1995); [(4)] based on Jago et al. (1993), Pohlman & Puls (1995) and Tett & Walne (1995); [(5), (6), (7)] estimated by fitting the model outcome against the field data; Settling velocity 2 represents the increased average settling rate of TSM after a resuspension event.

Name	Symbol	Unit	value	
west-east gradient of TSM	dC/dx	$g.m^{-4}$	$1\ 10^{-4}$	(1)
north-south gradient of TSM	dC/dy	$g.m^{-4}$	$1\ 10^{-4}$	(2)
threshold friction velocity	$U_{*,r}$	$m.s^{-1}$	$8\ 10^{-3}$	(3)
settling velocity 1	ω	$m.s^{-1}$	$2\ 10^{-5}$	(4)
settling velocity 2	ω	$m.s^{-1}$	$2.5\ 10^{-4}$	(5)
entrainment rate constant	β_r	s^{-1}	$5\ 10^{-5}$	(6)
background concentration	C_{back}	$g.m^{-3}$	0.3	(7)

CAPTIONS ON FIGURES

Figure 1. Map of the North Sea showing the position of the study site.

Figure 2. Properties of the upper sediment layers (0-2.5 mm, 2.5-5 mm) at the mooring site from 5 (day 185) to 19 July 1994 (day 199). A: water content ($g.g^{-1}$); B: POC content of the solid particles (%); C: atomic CN ratio of the sedimentary organic matter.

Figure 3. Spatial distribution of chlorophyll-a and TSM in the bottom layer around the mooring grid on 7 and 8 July 1994. Dots indicate sampling points, boxes (A,B) and vertical line (C,D) the mooring grid. A,B: Distribution of chlorophyll-a ($\mu g.l^{-1}$) and TSM ($mg.l^{-1}$), respectively, at 6 mab. C,D: chlorophyll-a and TSM, respectively, along a south-north cross-section through the mooring grid. Arrows in A,B indicate the position of the cross-section.

Figure 4. Vertical distribution of chlorophyll-a and TSM and the current velocity (1.5 mab) at the mooring site during a 24 h period on 7 and 8 July 1994. Dots indicate sampling points. A: Chlorophyll-a ($\mu g.l^{-1}$) ; B: TSM ($mg.l^{-1}$); C: current velocity ($m.s^{-1}$).

Figure 5. TSM ($mg.l^{-1}$) in water samples obtained from 0.2 and 6 mab at different phases of the tidal cycle. Samples from several days were positioned in a mean tidal cycle relative to the moment of LW slack to convert the time of sampling into degrees with LW slack = 0°, 360° and HW slack = 180°. ($mg.l^{-1}$). See Fig. 8a,b for tidal mean current velocity.

Figure 6. Time series between 5 July 1994 (day 185) and 19 July 1994 (day 199) of A: wind speed ($m.s^{-1}$) at 10 m above the water surface, B: current velocity ($m.s^{-1}$) in west-east direction at 1.5 mab, C: net tidal displacement (km) in west-east direction at 1.5 mab, D: current velocity ($m.s^{-1}$) in north-south direction at 1.5 mab, E: net tidal displacement (km) in north-south direction at 1.5 mab, F: chlorophyll-a ($ng.l^{-1}$) at 5 mab, and G: TSM ($mg.l^{-1}$) at 4.5 mab. Thick lines are 12 h moving averages of the data.

Figure 7. Time series of the tidally averaged mass fluxes in the sediment trap at 3.2 mab between 5 July 1994 (day 185) and 19 July 1994 (day 199). In the box-whisker plots the horizontal line is the median value, the lower and upper side of

the boxes are the 25th and 75th percentiles, respectively and the whiskers point at the 5th and 96th percentiles, respectively. Exceptionally high and low individual data are indicated with an asterisk or an open circle, depending on the distance from the median value(approximately 2 and 3.5 times the box size, respectively). A: Total mass flux of dry weight ($g.m^{-2}.h^{-1}$); B: mass flux of POC ($mg.m^{-2}.h^{-1}$); C: POC content of particles trapped (% of dry weight); D: atomic CN ratio of the organic matter trapped.

Figure 8. Box-whisker plots of the mean tidal cycle of A,B: current velocity; C: total mass flux of dry weight in the sediment trap ($g.m^{-2}.h^{-1}$); D: mass flux of POC ($mg.m^{-2}.h^{-1}$); E: POC content of particles trapped (% of dry weight); F: atomic CN ratio of the organic matter trapped. All data are relative to the tidally averaged data in Fig. 7.

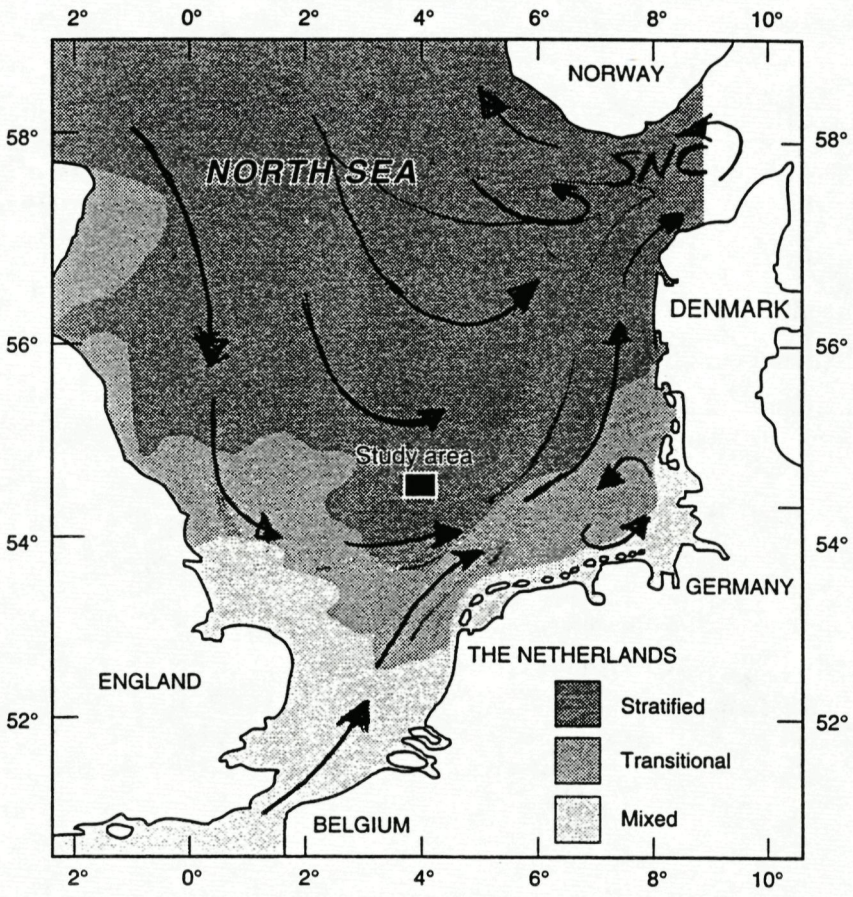
Figure 9. Results of the advection-deposition-resuspension model. A: Friction velocity U_* calculated from current meter data. Note the spring-neap cycle with high velocities around day 192-194 and lower velocities on days 186 and 198. B: TSM calculated at 4.5 mab (thick line, 3 h moving average) and estimated from transmission data at the same depth (thin line, 1 data point per hour). C: TSM calculated at different depths in the lower water column (0.2, 6, 11 and 16 mab). D: Calculated cumulative fluxes of deposition, resuspension and net accumulation (= deposition - resuspension) of particulate matter on the sea floor.

Figure 10. Relationships between A: organic carbon content, B; organic nitrogen content, and C: CN ratio of TSM and the concentration of TSM in pump (0.2 mab) and bottle samples from the lower water column (6 and 11 mab). The regression line in A represents the relation $POC = 15.2_{(SD=2.5)} / TSM + 2.4_{(SD=1.5)}$, n = 36, R = 0.72; in B: $PON = 1.37_{(SD=0.25)} / TSM + 0.44_{(SD=0.14)}$, n = 36, R = 0.71. Error bars in A,B indicate the POC, PON contents ± standard deviation estimated for very large values of TSM. Lines in C are tentative and show the general trend (solid) and the dip in CN ratio around TSM = 2 $mg.l^{-1}$ (dashed).

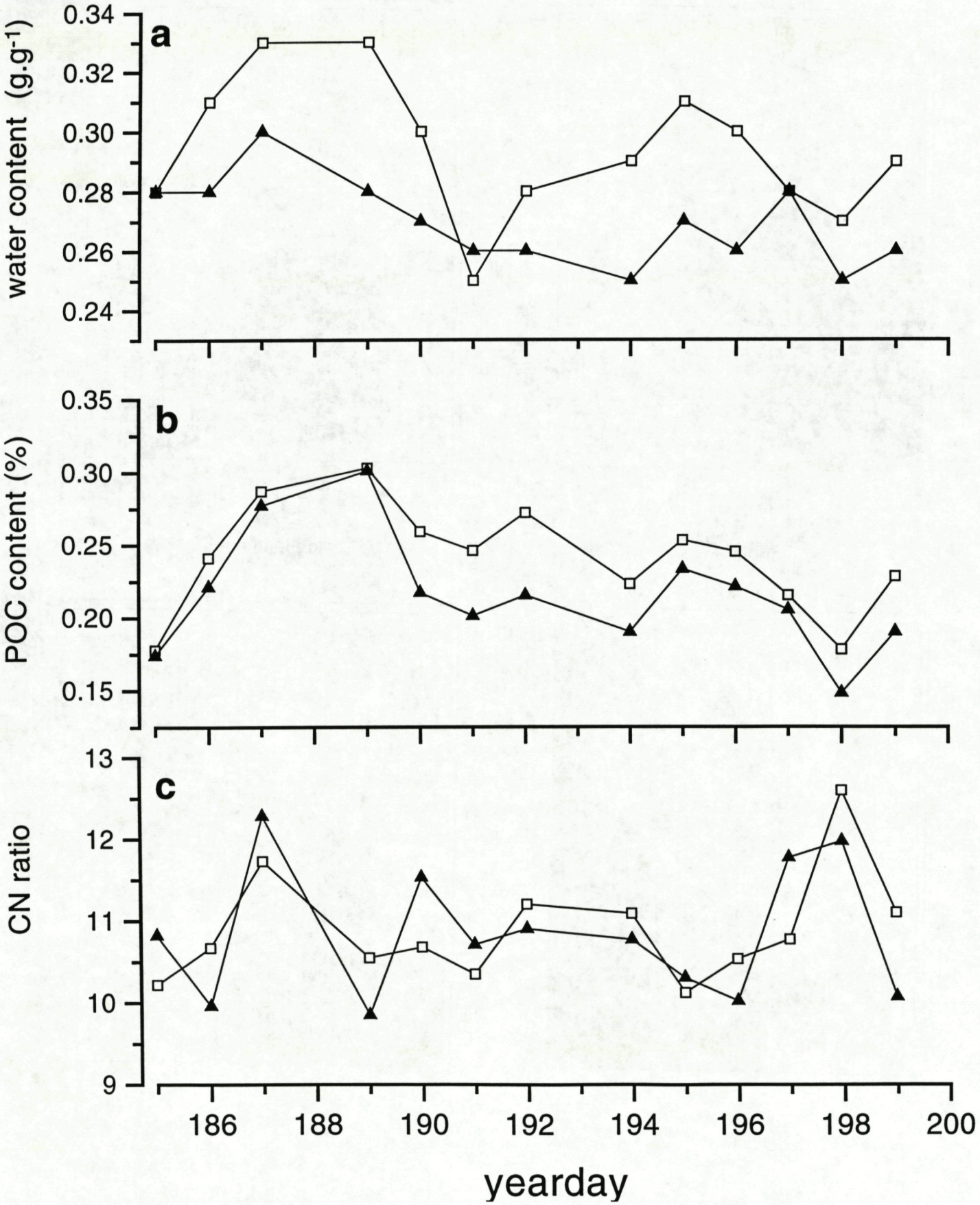
Figure 11. Total mass fluxes in the sediment trap corrected for tilt (box-whiskers) and median fluxes not corrected for tilt (solid line) obtained from Fig. 7 and 8. A: tidally averaged fluxes; B: mean tidal cycle of the fluxes corrected for the 14 days trend.

Figure 12. Apparent settling velocity of the particles collected with the sediment trap calculated as the ratio between the total mass flux in the trap and the TSM concentration measured at 4.5 mab with the transmissometer. Box-whiskers are based on mass fluxes corrected for tilt, solid line on the uncorrected mass fluxes. A: tidally mean velocity; B: mean tidal cycle of settling speed corrected for the 14 days trend.

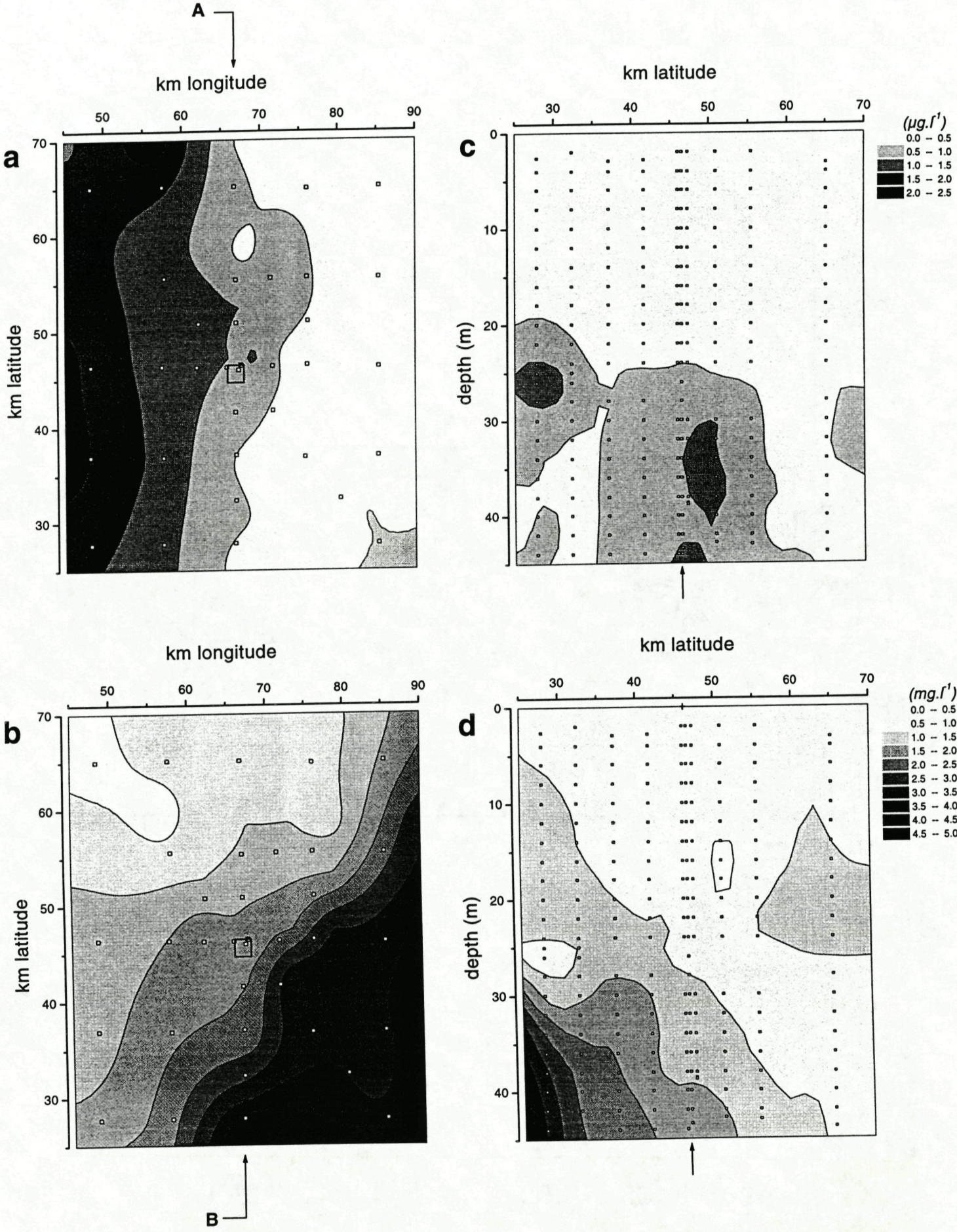
Figure 13. Results of a model simulation with storms. Wind and current velocities measured in December 1994 were inserted in the original data set (Fig. 6) starting day 190. A: wind speed ($m.s^{-1}$) at 10 m above the water surface, B: current velocity ($m.s^{-1}$), C: ADCP echo signal (relative units) indicating TSM concentrations at 4 mab, D: calculated TSM concentrations ($mg.l^{-1}$) at 4.5 mab, E: calculated cumulative gross fluxes of resuspension and deposition ($g.m^{-2}$), F: calculated net accumulation on the sediment ($g.m^{-2}$).



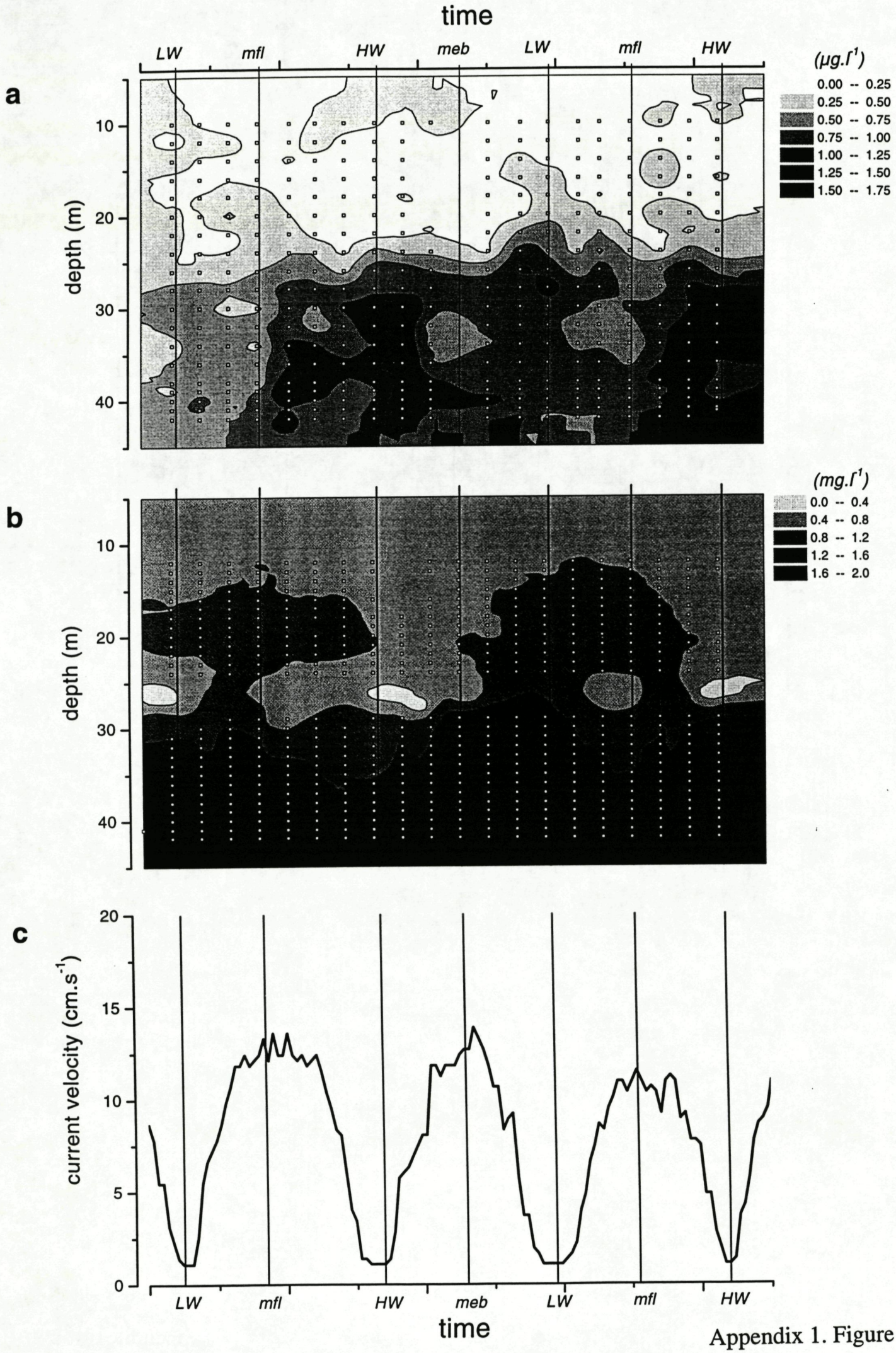
Appendix 1. Figure 1



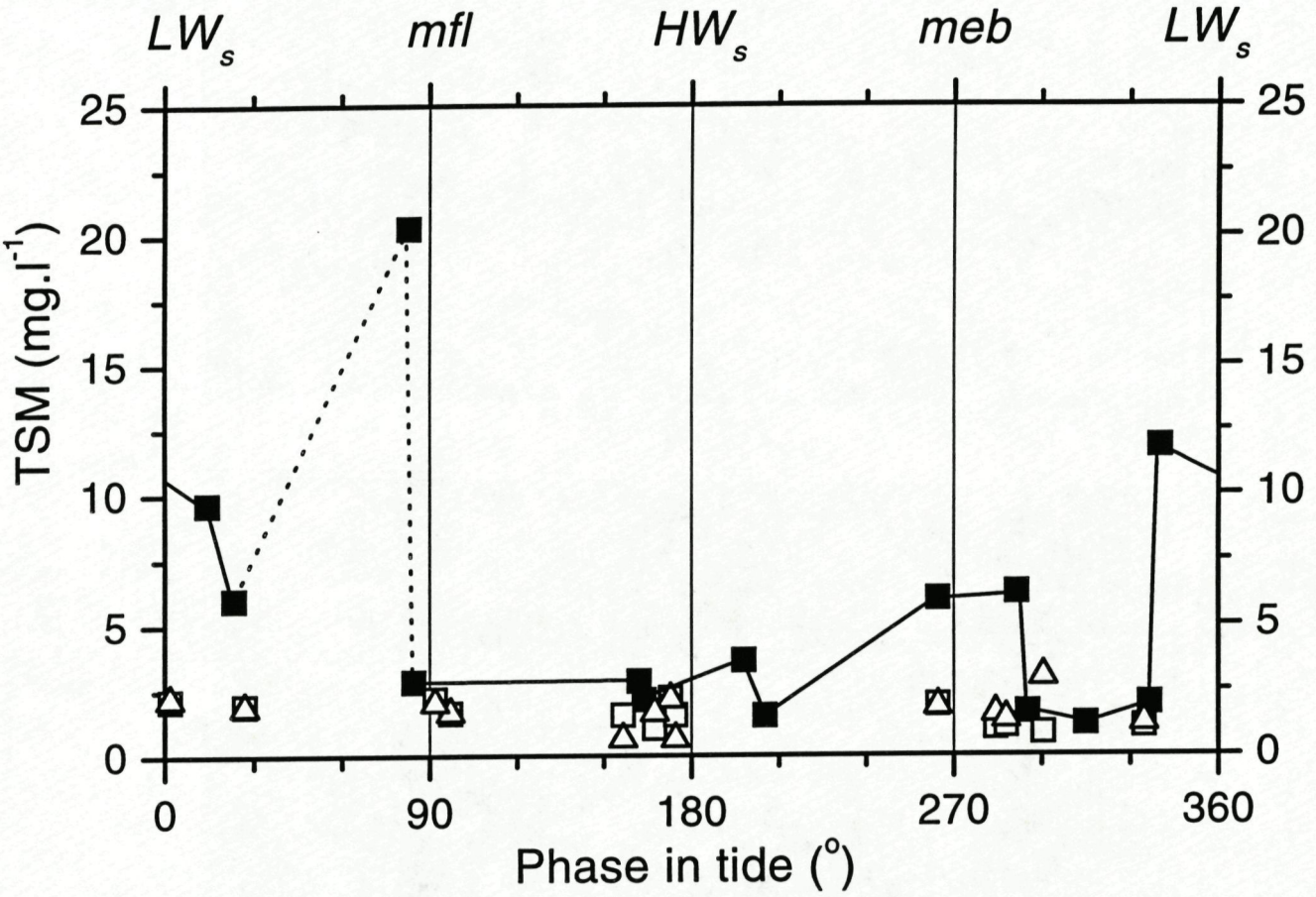
Appendix 1. Figure 2



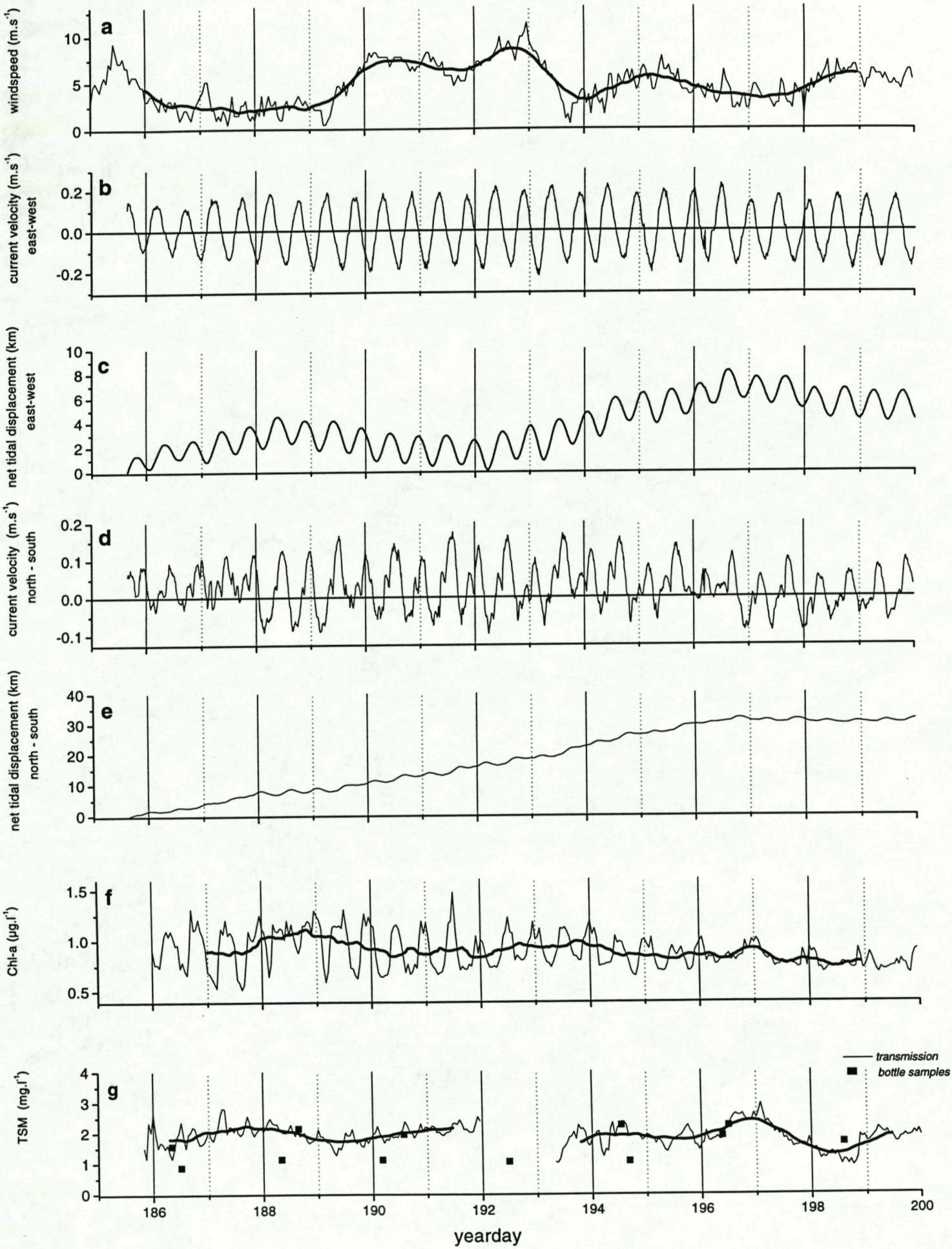
Appendix 1. Figure 3



Appendix 1. Figure 4

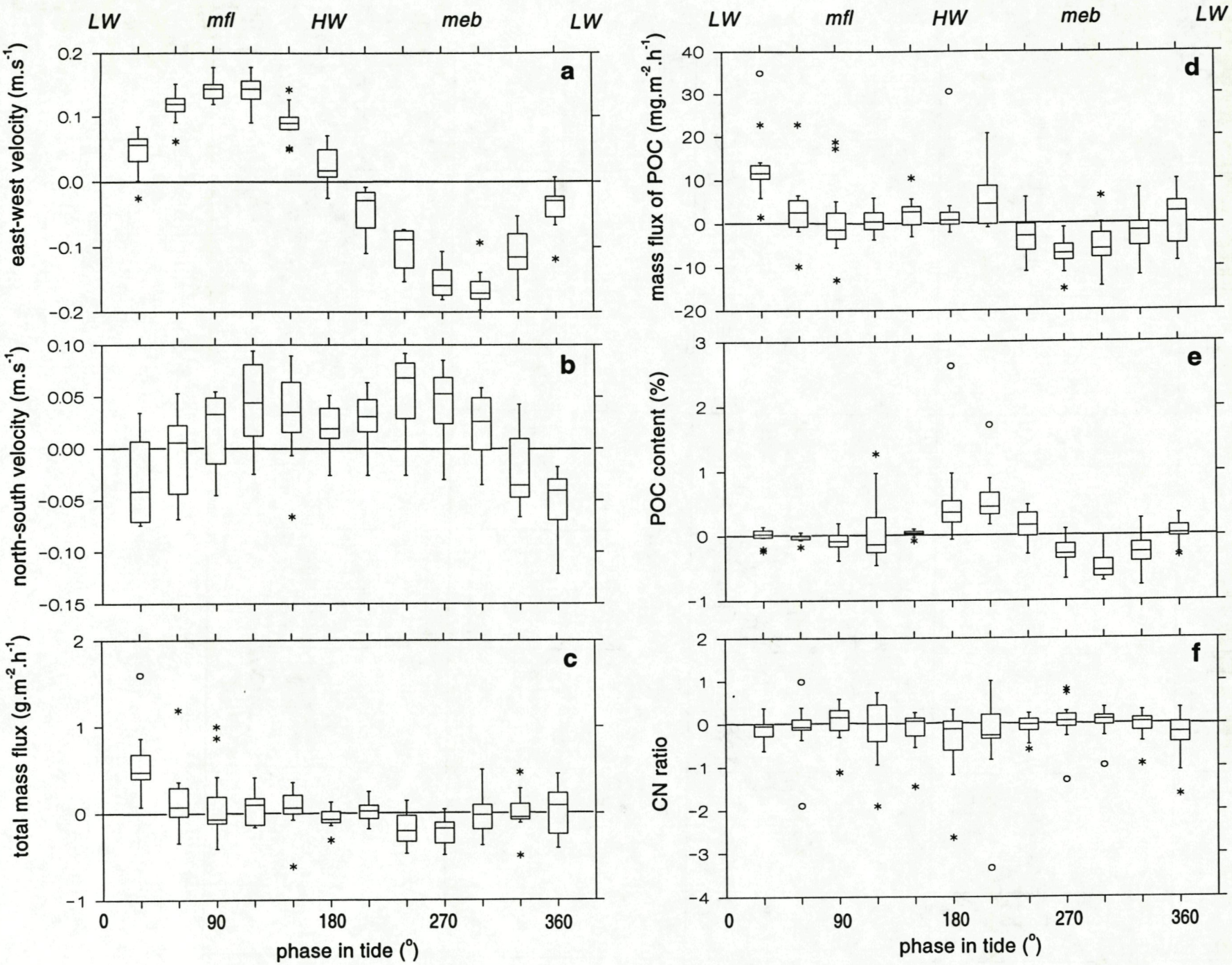


Appendix 1. Figure 5

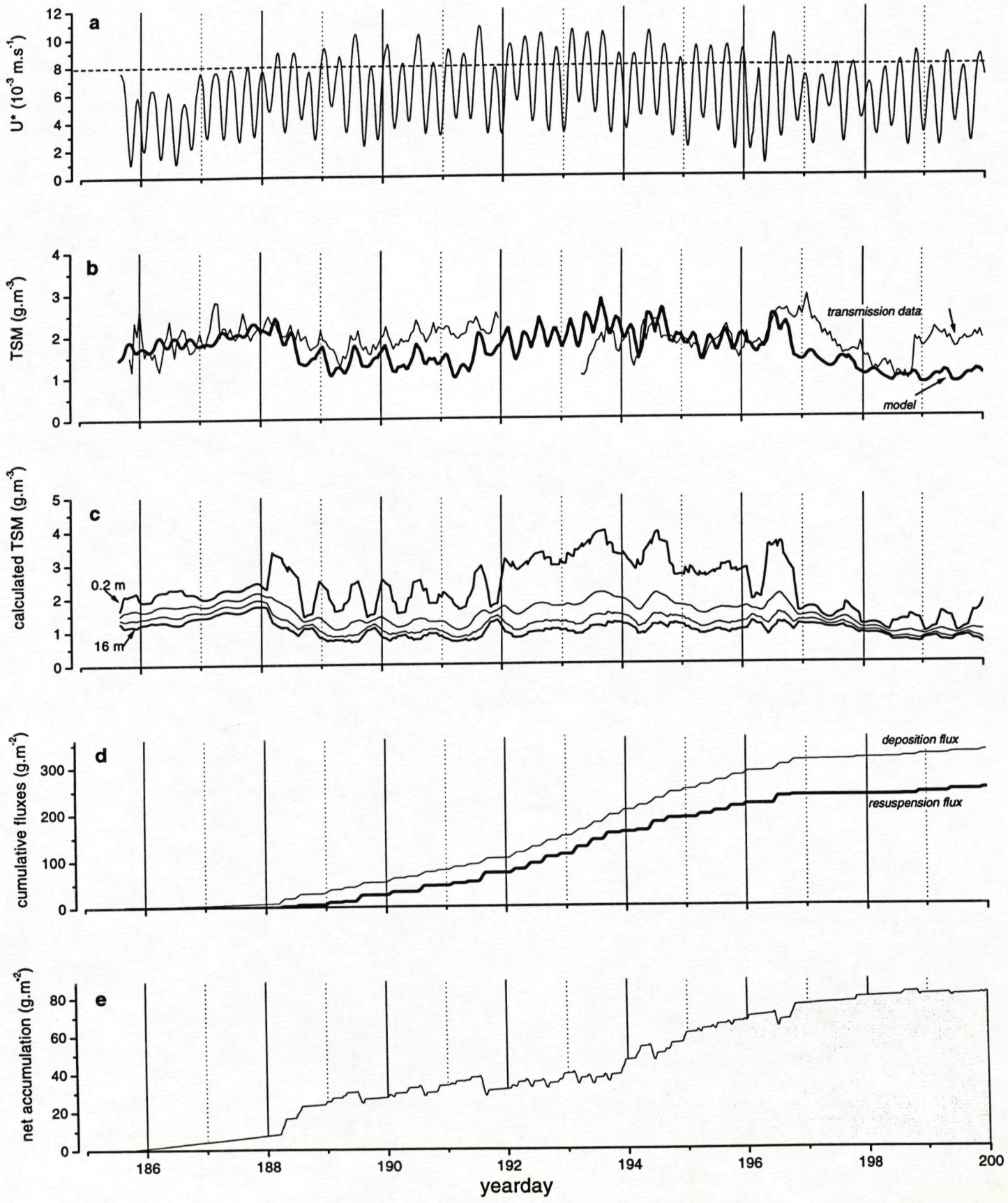


Appendix 1. Figure 6

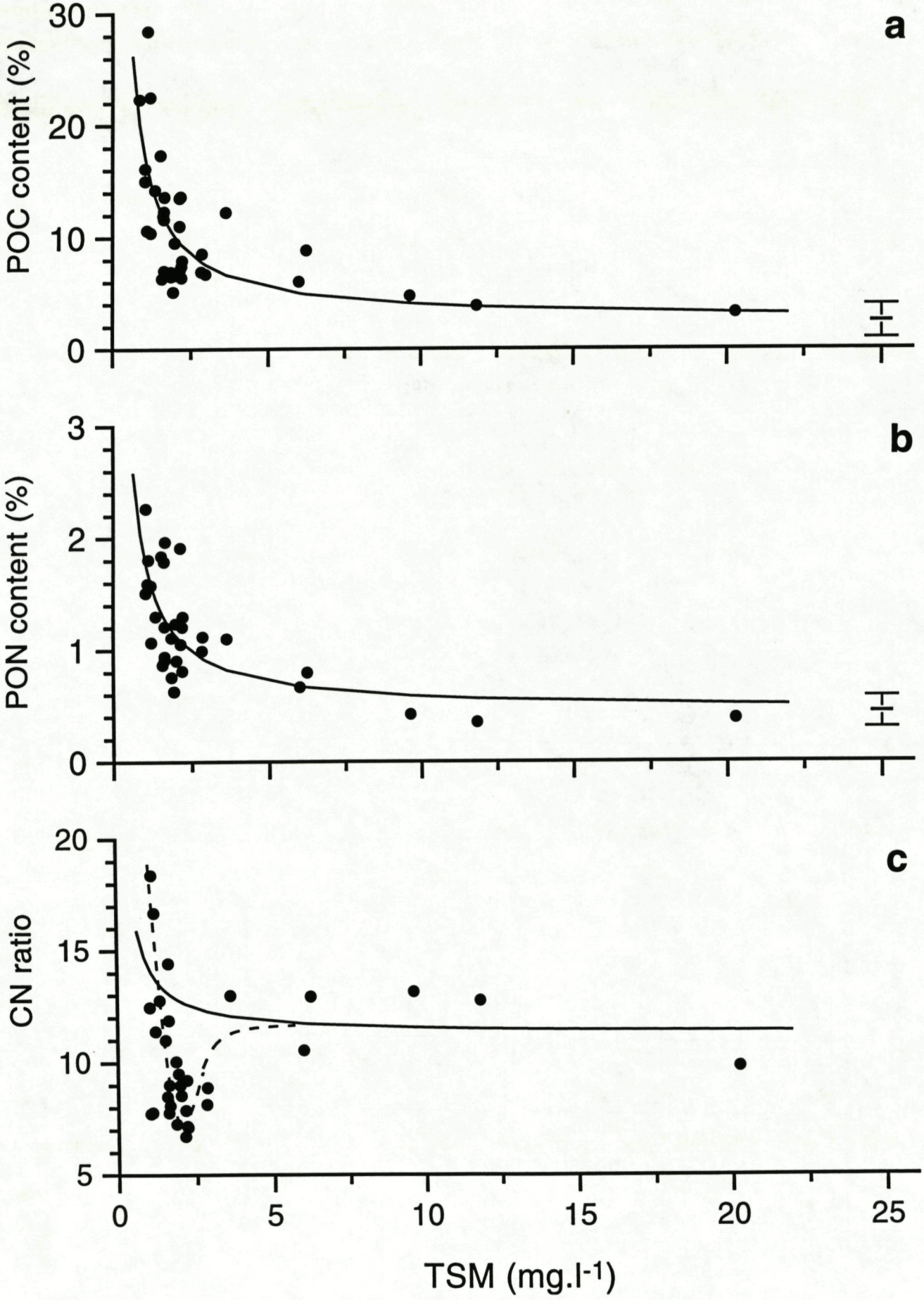
Appendix 1. Figure 7



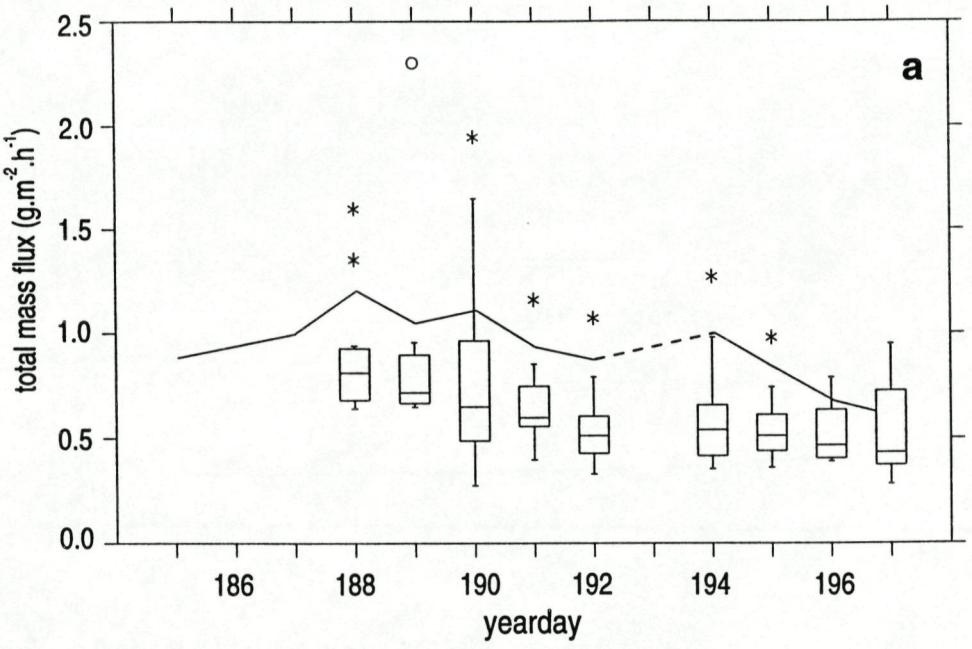
Appendix 1. Figure 8

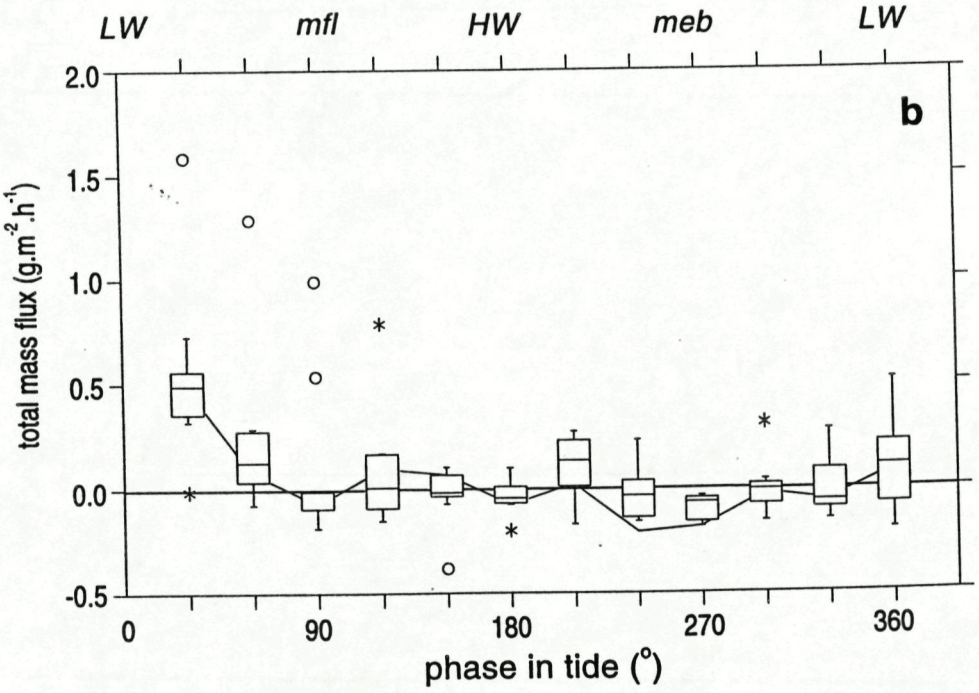


Appendix 1. Figure 9

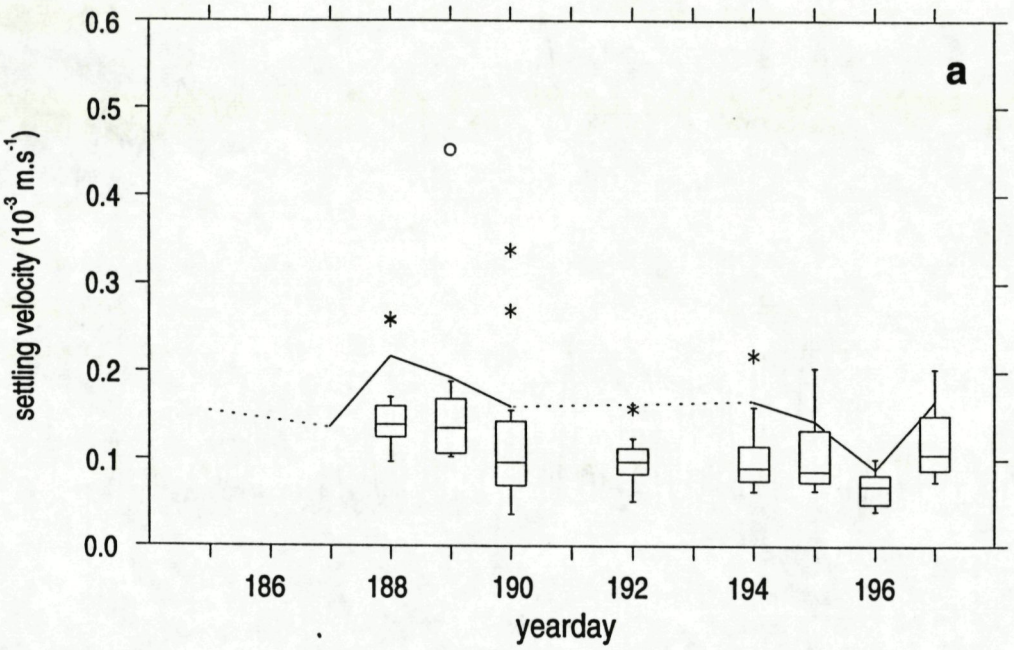


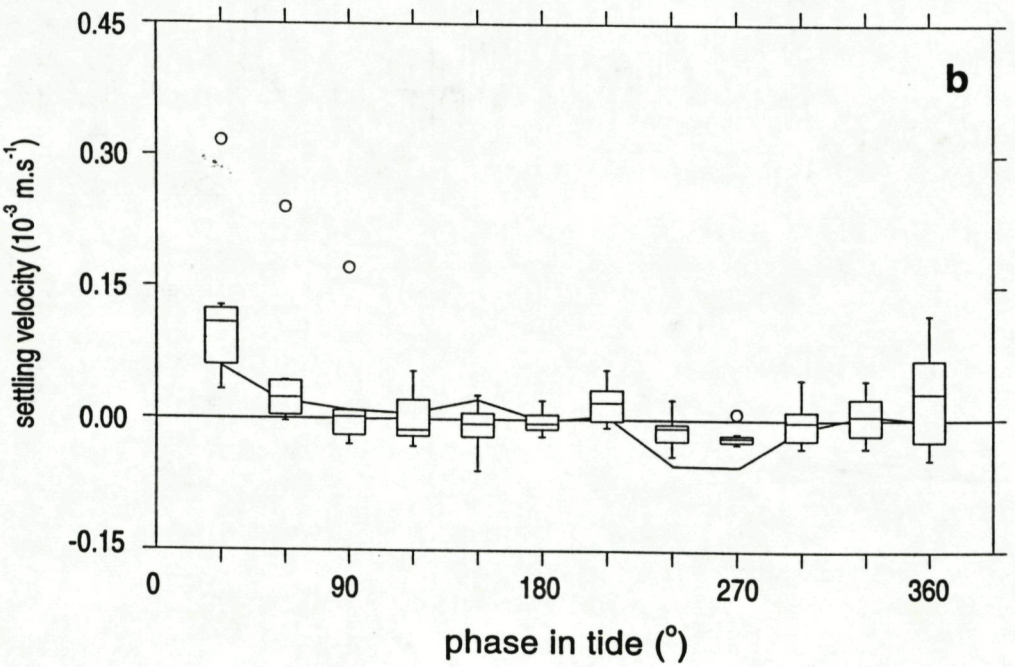
Appendix 1. Figure 10



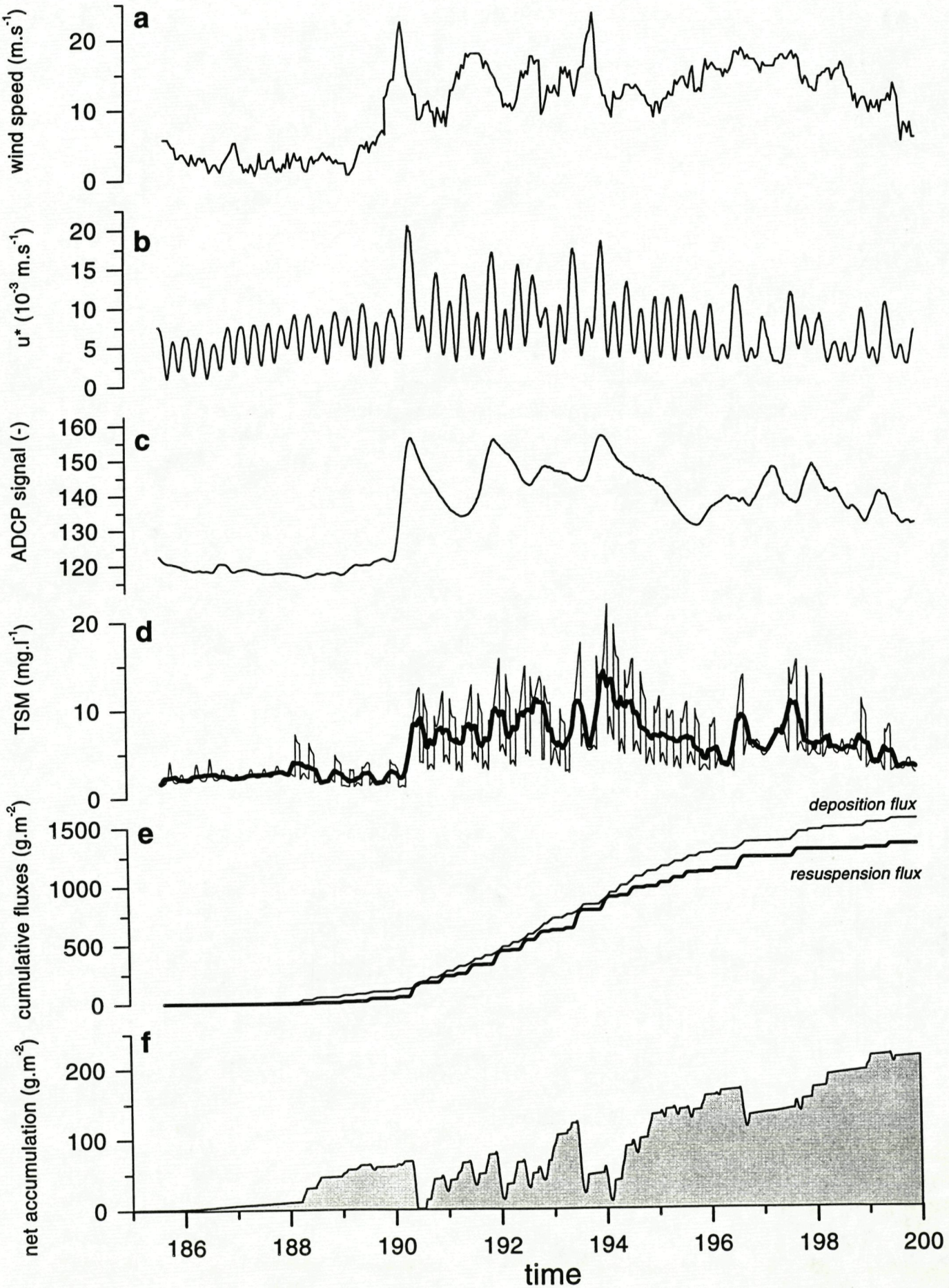


Appendix 1. Figure 11





Appendix 1. Figure 12



Appendix 1. Figure 13

APPENDIX 2

Pelagic-benthic coupling in the North Sea: short-term dynamics in phytopigment sedimentation and the response of benthic bacteria

696

Fleur C. van Duyl, Gerard C. A. Duineveld, Arjen J. Kop, Gijsbert Kraay

Netherlands Institute for Sea Research, P.O.Box 59, 1790 AB Den Burg, Texel, The Netherlands

Abstract

A temperature stratified water column including the sediment surface layer in the Oyster Ground, North Sea was studied in July 1994. Twice a day (once during slack tide and once during full tide) samples were taken for phytopigments at different depths, sedimentation of phytopigments was assessed just above the bottom, and the phytopigment content in the 3 mm sediment surface layer was determined. In addition benthic bacterial production and abundance were measured. Semi-permanent registration of current velocity and direction was conducted close to the bottom, and fluorescence was measured intermittently at 13 and 38 m depth. The aim of the study was to assess the pelagic-benthic coupling for phytopigments and the response of benthic bacteria to changes in phytopigment input in the bottom. During the cruise mixing events which resulted in enhancement of the phytopigment content in the bottom mixed layer did not occur. There were no evident indications of net sedimentation of phytopigments on the bottom. The bulk of the material which settled during slack tide was resuspended during full tide. Due to the absence of substantial variations in net pigment input in the bottom, the benthic phytopigment inventory gradually decreased during the cruise (half-life of 10-13 days). This was not reflected by benthic bacterial variables which did not significantly change. As a consequence short-term temporal relations between bacterial variables and phytopigments in the sediment were not found. The pigment content apparently lost its role of indicator of available substrate for bacteria in the absence of substantial input of fresh algal material. However the benthic spatial variations in phytopigments due to the heterogeneity of the study were significantly reflected by the bacterial variables. It was concluded that bacterial variables are spatially related to phytopigments in North Sea sediments in an area with a comparable recent history of phytodetritus sedimentation. Benthic bacterial production may only be temporally related to phytopigments when fresh algal material is available in the sediment.

Introduction

Several studies have been dedicated to the response of benthic bacteria upon the deposition of algae (Meyer-Reil 1987, Graf 1992). Under manipulated conditions response rates have been shown to be fast when fresh algal material is concerned (e.g.

Graf 1987, Turley & Lochte 1990, van Duyl et al. 1992, a, b, Osinga et al. 1996). Little is known however of the response rate of bacteria to natural pulsed inputs in the field. Most studies roughly related benthic bacterial responses to large sedimentation events such as the spring and autumn algal bloom sedimentation in temperate regions (e.g. Graf et al. 1982, 1983, Meyer-Reil 1987). However the importance of small short-term sedimentation events of algal material for benthic bacteria activities and the bacterial response to such events is poorly known (Meyer-Reil 1987, van Duyl et al. 1993).

In temperature stratified shelf waters sedimentation events have been shown to be indirectly related to vertical mixing events (Noji et al. 1986, Olesen 1995). Mixing events change the physical structure of the water column with respect to, among others, light penetration, turbulence and temperature and generate vertical fluxes of nutrients across the thermocline triggering fluctuations in phytoplankton growth and biomass (e.g. Walsh et al. 1978, Hitchcock et al. 1987, Kiørboe & Nielssen 1990, Ridderinkhof 1992, Kiørboe 1993, Tett & Walne 1995). Mixing events in temperature stratified shelf waters usually result in algal biomass increases.

It is generally assumed that enhanced primary production and algal biomass result in enhanced sedimentation (e.g. Suess 1980, Ambrose & Renaud 1995). At increasing algal densities the chances for collision between algae and between algae and other particles will increase. This may result in flocculation and larger particles will sink faster than smaller particles do. So sedimentation is likely to increase with increasing algal densities in the water column (Kiørboe 1993). In shelf seas like the North Sea fluctuations in phytoplankton biomass are presumably reflected by variations in phytoplankton sedimentation and activities in the benthic compartment (Billen et al. 1990).

Limited attention has been paid to the time scales of coupling between the mixing event, enhanced algal biomass, sedimentation and benthic bacterial response under natural conditions (Graf 1992). For exact determination of response rates and sizes, time scales of sampling were usually insufficient. Such a study requires simultaneous and frequent sampling of physical, chemical and biological variables for several weeks at one station. Moreover it requires distinction between spatial and temporal variations of bottom variables in particular.

We carried out such a sampling programme for 2 weeks at a temperature stratified station in the North Sea and we investigated the response rate of benthic bacteria in relation to variations in algal biomass in the water column and in the sediment surface layer. Algal pigments were determined, as they have been shown to be good indicators of labile compounds regulating sediment bacterial production and abundance (e.g. Bird & Kalff 1984, Cole et al. 1988, Sander & Kalff 1993, van Duyl & Kop 1994). The aim of the study was to increase the understanding of the pelagic-

benthic coupling on short time scales (hrs, days, weeks) with respect to phytopigments and benthic microbial variables.

The following questions were addressed:

1. are variations in water column algal pigment concentrations reflected by variations in pigment sedimentation and by variations in pigment concentrations in the sediment surface layer?
2. do benthic bacteria in numbers and production reflect temporal variations in pigment concentrations in the sediment, and pigment sedimentation?
3. what is the time scale and size of the response of bacteria in relation to the pigment input?

Acknowledgements: We are grateful for the help of Ronald Osinga, Mathieu Starink, Jos Thieme, Henk Franken, Ruud Groenewegen, Evaline van Weerlee, Annette van Koutrik, Willem Polman and the crew of the MS Pelagia. Wim van Raaphorst and Hans van Haren are gratefully acknowledged for putting unpublished data with respect to POC , nutrients, meteorological, current velocities and temperature and fluorescence data at our disposal. Jaap van der Meer is acknowledged for the statistical advice. We thank Wim van Raaphorst and Arjen Boon for critically reading the manuscript. This research was partly funded by BEON (grant 94/95 E-01,) and by the Netherlands Marine Research Foundation (grant 39104).

Material and methods

Study area. The study area was located on the Oyster Ground in the North Sea (**Fig.1**). The size of the study area was approximately 900 by 900 m. Waterdepth is 46 m and the water column was temperature stratified with a thermocline around 25-27 m depth. All samples were collected between 5 and 19 July 1994 aboard the RV Pelagia.

A geographic scheme of the organization of the sampling area is given in **Fig. 2**. The dashed line surrounds the mooring site of ca 600 by 600 m with moored instruments. The area is marked by 4 conspicuous buoys (R1-R4) to warn ships. Along the north and east side of the mooring a grid of 17 sampling stations is indicated. The distance between stations was based on the need to have 17 non-overlapping anchor stations for the RV to eliminate sampling in disturbed sediments either disturbed by benthic sampling or by anchoring. Sediment remains after sampling were retained on board and discharged several nautic miles outside the study area, to reduce unneccesary disturbance in the small study area. The study area was kept as small as possible to minimize the horizontal spatial variability of water column characteristics and of benthic variables in the study area. Moreover the spatial variability in the

benthic compartment was assessed to be able to distinguish between spatial and temporal variability.

Sampling methods and frequency. In the framework of the Integrated North Sea Programme (INP) semi-permanent moorings measured discontinuously meteorological (e.g. windforce and direction, wave height), physical (e.g. temperature, currents), chemical (salinity) and biological (e.g. fluorescence) variables over the water column in the study area (van Haren 1993). Data applied for this study comprise windspeed, wave height, temperature throughout the entire water column, fluorescence at 13 and 38 m depth, current velocities and direction at 1.5 m above the bottom.

The sedimentation/resuspension of phytodetritus and organic matter (POC) was determined in cylindrical Technicap multi-sample sediment traps (aspect ratio 120/25) located 3.5 m above the bottom at the mooring site (Fig. 2). These kind of traps have been recommended in situations where the water is not stagnant (Hargrave & Burns 1979, Butman 1986). One trap was programmed to collect phytodetritus during daytime for 2 hrs around slack tide and 2 hrs around full tide. Full tide is defined as the period with the highest current velocities during the tidal cycle, which occur on average 3h before (in the ebb tide) or 3h after LW slack tide (in the flood tide). Material collected in periods between full tide and slack tide was trapped as well to estimate daily sedimentation/resuspension. Organic matter for POC was collected in another trap, programmed to collect material every h during nighttime (19.00-7.00h next day) (van Raaphorst et al. 1996). Traps were emptied once a day between 8 and 9.00h a.m..

The water column and the sediment surface were sampled twice a day in approximately 45 mins during slack tide and 45 mins during full tide. In principal daily sampling occurred in one of the 17 sampling stations with the research vessel anchored in the middle of the station (GPS navigation). All samples were taken within the boundary of the station (see circles Fig. 2). The sequence at which the stations were sampled from day to day was random.

Twice every day phytodetritus was sampled at 5 and 40 m depth with a combined CTD-Rosette sampler. Phytodetritus samples from just below the thermocline between 22 and 30 m depth were collected every other day in different tidal phases (slack and full tide). Every other day dissolved inorganic nutrients and POC were sampled at 6 different depths (5, 15, 25, 35, 40 and 45 m) two times a day, once around slack tide and once during full tide. Inorganic nutrients (NH4, NO3, PO4, SiO2) were determined on autoanalysers (Traacs). POC was determined on a HCN-analyser (Verardo et al. 1990).

Bottom water was collected from 20 cm above the bottom (0.2 mab) by means of a membrane pump. Bottom water was sampled for bacterioplankton production on 6 days during the cruise.

Intact sediment cores for the analysis of phytopigments, bacterial production and abundance and organic matter were collected with a modified cylindrical Reineck type boxcorer (Reineck 1963) with an inner diameter of 31 cm. Each day 6 sediment boxcores were sampled at one particular station number, i.e. 3 around slack tide and 3 during high bottom current velocities. The spatial variance within one station was determined.

Spatial heterogeneity of the different sediment variables in the study area was determined by collecting 9 sediment boxcores within 2 hrs in 9 randomly selected stations of the 17 predetermined stations and directly subsampled for different analyses. This exercise was performed two times, once around slack tide (7 July) and once during full tide (9 July). Variance between sampling stations was determined.

Statistics

To distinguish changes in time (every day another station was sampled) from spatial variability in the sediment variables the spatial variance between stations was compared with the residual variance, which was based on changes of variables in time during the cruise. The heterogeneity sampling excercise rendered the sum of variances of variables within and between stations. The sediment samples collected at one station rendered the spatial variation within one station. Subtracting these two variances yields the real spatial variance between stations. When the residual variance of the time series was in the same order of magnitude as the variance between sampling stations and autocorrelation was absent (multiple) regressions were applied to assess significant changes in time.

In addition paired observations of different variables were tested on relations with t-tests and one way ANOVAS (Sokal & Rohlf 1981).

Measurements of phytopigments and bacteria

Phytopigments. Concentrations of the phytopigments chlorophyll-a (CH) and fucoxanthin (FU) and its degradation product pheophytin-a (PH) were determined in the water column, in the material collected in the sediment traps and in the sediment. Pheophytin-a was selected, because it is an important early product of fresh CH degradation and it is presumed to be a microbially formed (Sun et al. 1993a and references therein). For qualitative analysis of the algal species composition in the water column additional pigments were analysed such as peridinin, zeaxanthin chlorophyll b, c2 and c3. Water samples for pigments were filtered over GF/F (Whatman filters, 47 mm diameter). After filtration filters were transferred to plastic

tubes with stoppers, rapidly frozen in liquid nitrogen and stored in a -80°C freezer until processing. Sediment samples were obtained by subsampling each sediment boxcore with 10 acrylic liners (2.5 cm i.d.). The upper 3 mm section of the sediment cores was collected and pooled to reduce heterogeneity within one boxcore. Sediment slurries were made by adding 10 cm^3 wet sediment to 10 cm^3 filter sterilized seawater from the overlying water of the boxcosm. Slurries were kept at field temperature and were subsampled for phytopigments, bacterial production and bacterial abundance within 2 hrs. Sediment slurry samples of 5 cm^3 for pigment analyses were pipetted with a cut-off pipette in plastic tubes with stoppers and treated similarly before storage as pigments concentrated on filters. All pigment samples were freeze dried and stored at -50°C until analysis on a HPLC (see Wright et al. 1991). The pigment content in sediments was expressed per unit volume wet sediment. Sediment dry weight was 2.65 $g.cm^{-3}$ and porosity of the sediment surface layer was on the average 0.52 (v/v) (e.g. van Raaphorst et al. 1996).

Bacterial production. Bacterial production was determined with L-[4,5-^{3}H]leucine with a specific activity of 164 Ci/mmol (Amersham) following van Duyl & Kop (1994) for measurements in sediment and Simon & Azam (1989) for measurements in the water column. For bacterial production 200 µl sediment slurry (see above) was incubated for 1 h with 27 µl leucine solution (containing 0.02 nmol ^{3}H leucine and 0.18 nmol leucine). Isotopic dilution was determined routinely in all slurries (Moriarty & Pollard 1981). To samples 0.2, 0.4 and 0.6 nmol leucine was added respectively with similar amounts of labelled leucine to determine isotopic dilution.

Bacterioplankton production in bottom water (0.2 mab) was performed on 20 ml bottom water samples. After the incubation the sample was split in 2 samples of 10 ml each and one was fractionated over 3 µm filters. The incorporated leucine was determined in the unfiltered water sample and in the 10 ml filtrate. The difference between incorporation in the unfiltered samples and in the filtrate was contributed to the leucine incorporation of bacteria attached to particles > 3 µm. Analyses were conducted in triplicate. The 10 nM leucine added saturated the uptake system of bacteria. No corrections were made for internal isotopic dilution according to Simon & Azam (1989).

Bacterial numbers. In each sediment slurry bacterial numbers were counted after staining with acridine orange (van Duyl & Kop 1994). One cm^3 slurry was fixed with 50 µl buffered 37% 0.2 µm filtered formaldehyde. Slides for total counts were prepared the same day and stored at -80°C until analyses. Fixed slurries were stored at 4°C and used for later preparations of slides for repetitive counting of bacteria.

Results

Physical and chemical characteristics

The weather was extremely calm during the expedition on the Oyster Ground. Wind velocities varied between 0 and 8 $m.s^{-1}$ with a few shortlasting increases to 10 $m.s^{-1}$. Wave heights did not exceed 1 m during the cruise and were usually less than 50 cm.

The study site on the Oyster Ground was temperature stratified with the thermocline initially around 27 m depth and gradually moving upwards in the course of the cruise to 23 m depth (**Fig 3**). In the surface mixed layer (SML: 0-10/15 m) at 5 m depth temperature rose from 15 to 17.8 °C and in the bottom mixed layer (BML: 25-46 m) at 40 m depth from 8.5 to 9.6°C during the cruise. There was a 10-15 m thick non-turbulent intermediate waterlayer present during the cruise, extending from 10/15 to 25 m depth. During the cruise gradients in temperature became steeper in this waterlayer and it narrowed down to a thickness of 10 m. Light penetrated in the entire water column down to the bottom (van Haren et al. unpublished).

The water column was characterized by nutrient poor surface waters and slightly nutrient enhanced bottom waters (**Fig. 4**). From 8 to 10 July (day 188 to 190) increases in DIN , PO_4 and SiO_2 were observed in the water column, followed by decreases from 10 to 12 or 14 July (day 190, 192, 194). From 14 to 16 July (day 194-196) a slight increase in DIN, PO_4 and SiO_2 was recorded at 25 m depth. The PO_4 increase was traced into the surface mixed layer.

Current velocities ranged between 1 and 26 $cm.s^{-1}$ at 1.5 mab. The highest current velocities were measured between 9 and 11 July (day 189 to 191), which were related to spring tide (8 July). Current speeds during sampling around slack tide (HW or LW) ranged from 1 to 8.7 $cm.s^{-1}$ and during full tide (ebb or flood tide) from 13.2 to 26 $cm.s^{-1}$, with the smallest amplitude of current velocities on 17-18 July after neap tide (15 July). The highest current velocities during sampling were measured around 290° (WNW direction, ebb stream) and around 90° (E direction, flood stream). Around slack tide current direction during sampling was variable.

Phytopigments in the water column

Chlorophyll-a (CH) in the water column ranged from 100 to 400 $ng.l^{-1}$ in the SML at 5 m depth and from 650 to 1300 $ng.l^{-1}$ in the BML at 25 and 40 m depth. These data were used to calibrate the fluorescence measurements of the fluorometers deployed at 13 and 38 m depth. Variations in fluorescence were related to the daily cycle in the SML, and roughly to the tidal cycle in the BML (**Fig. 5a,b**). Peaks in fluorescence in the BML appeared after the onset of the flood current until the decrease of the ebb current. During high water slack tide fluorescence remained usually high. Lowest fluorescence usually occurred during low water slack tide. This pattern was evident from day 185 to day 196. From day 196 onwards to the end of the cruise (day 200) the day-night cycle dominated the diurnal cycle. Fluctuations and concentrations of CH in the BML decreased from 14 July (day 194) onwards.

Fucoxanthin (FU) in the water column showed comparable variations as chlorophyll-a, but its concentration was significantly lower (**Fig. 5c**). The ratios between FU and CH were significantly different in the SML and BML with a significant proportionate increase in FU compared to CH in the BML (**Fig. 8, lower part**). Zeaxanthin was the dominant carotenoid in the SML (25-65 $ng.l^{-1}$) and was virtually absent in the BML. Peridinin was usually absent in the SML but well represented in the BML (20-40 $ng.l^{-1}$). The chlorophyll c3/c2 ratio was close to 1 in the BML and less than 1 in the SML.

There was a distinct increase in chlorophyll-a on 14 July in the SML (5 m depth, day 194), which coincided with a small increase in nutrients (Fig. 5). The enhanced pigment content was traced until 25-30 m depth. Variations in pigments at 40 m depth were too large to be ascribed to the event. However the FU/CH ratio suddenly increased in the entire water column and other changes in pigment composition occurred in the SML (slight increase in chlorophyll-b in relation to chlorophyll-a) and in the BML (peridinin slightly decreased and zeaxanthin slightly increased in the BML). The pheophytin-a content was below the detection limit in the water column samples.

The POC content did not vary over the vertical and fluctuated between 100 and 400 $\mu gC.l^{-1}$ (**Fig 9a**). During the cruise the POC content varied but did not significantly change in time except for a POC decrease in the BML from 6 to 10 July. The POC/chlorophyll-a ratio was significantly higher in the SML (POC/CH of ca 1000 at 5 m depth) than in the BML (POC/CH of ca 200 at 22-40 m depth).

Sediment trap results

The trapping of phytodetritus in the BML was significantly larger around slack tide than during full tide (t-test: DF=8, $P<0.01$) (**Fig. 6a, b, c**). During high water slack tide the pigment content in the BML was usually larger than during low water slack tide (see Fig. 5b), but this difference was not reflected in the sedimentation. The variations in average daily fluorescence (CH) in the BML were significantly reflected by the sedimentation of CH and FU during slack tide (adjusted $R^2=0.34$, $P=0.05$ for CH and $R^2=0.44$, $P<0.05$ for FU). These relations were not found with sedimentation during full tide or with daily sedimentation of phytodetritus.

The highest sedimentation of chlorophyll-a was measured during low water slack tide on 8 July (day 198), and was on the average 0.08 mg $chl\text{-}a.m^{-2}.2h^{-1}$. During full tide this was on the average 0.04 mg $chl\text{-}a.m^{-2}.2h^{-1}$. The daily accumulation of phytodetritus in traps ranged from 0.1 to 1.2 for chlorophyll-a, from 0.1 to 0.8 for fucoxanthin and from 0.01 to 0.08 $mg.m^{-2}.d^{-1}$ for pheophytin-a (**Fig. 6d**). Daily POC accumulation in traps varied between 400 and 600 $mgC.\ m^{-2}$ (**Fig. 9b**). The enhanced phytopigment concentrations in the SML and at 25-30 m depth on 14-16 July (day

194-196) were not reflected in the sedimentation pattern of phytopigments. From July 10 (day 190) onwards the pigment accumulation in traps tended to decrease while the POC content remained stable (Fig. 6c, 9b). The FU/CH ratio in the traps was significantly higher than this ratio in the ambient water (Fig. 8). The POC/chlorophyll-a ratio of the sedimented material was also significantly higher than this ratio in the ambient BML water (Fig. 9a, b).

Spatial heterogeneity

There was a considerable spatial heterogeneity in benthic variables (phytopigment concentrations, bacterial production (BBP) and abundance (BBN)) in the study area (**Table 1**) despite the small distance between sampling sites (Fig. 2). The coefficients of variations for the benthic variables ranged from 28-41% for phytopigments and from 12-20% for bacterial numbers and 20-38% for benthic bacterial production. Spatial heterogeneity in benthic variables was less during high current velocities than during slack tide.

Pelagic-benthic coupling in relation to tidal dynamics

Despite the evident tidal periodicity in sedimentation there were no significant differences between the benthic data (bacterial abundance, production and phytopigments) collected during different tidal phases characterized by significantly different tidal currents, not during the heterogeneity measurements (Table 1), nor during the daily measurements in slack and full tide periods (t-test: DF=11, P>0.3).

However, the amount of fucoxanthin trapped in different slack tide periods was positively related to the sediment fucoxanthin content during slack tide periods (0-3 mm; adjusted R^2=0.25, P<0.1). This relation was not found for data collected in full tides. For the samples collected in full tide only a significant inverse relation between the sedimentation of pheophytin-a in traps and the sediment content of pheophytin-a (adjusted R^2=0.56, P<0.05) was found.

Sedimentation of phytodetritus (CH, FU, PH) during slack tide periods was positively related to the benthic bacterial numbers and explained 32 to 58% of the variation in numbers (P<0.1). In the BML average total counts of 0.4 * 10^6 bacteria.ml^{-1} were determined of which the part attached to sinking algal particles (not counted) may have settled on the sediment surface during slack tide. This temporal enrichment of the sediment by bacteria did not result in enhancement of the benthic bacterial production. The total bacterioplankton production in the BML ranged from 0.6 to 1.4 µg $C.l^{-1}.d^{-1}$ with approximately 45% of the bacterioplankton production in the fraction > 3 µm. The bacterioplankton production in the fraction >3 µm did not significantly vary in the tidal cycle (t-test, DF=5, P>0.5). Based on trap results it was estimated that the material with associated bacterioplankton production in the fraction > 3 µm in

approximately 45 lts of BML water may settle during 2 hours around slack tide on a meter square. This may enhance the BBP with approximately 15 to 30 μg $C.m^{-2}.d^{-1}$ during slack tide as compared to similar calculations during full tide. This enhancement is too low to result in a measurable increase in BBP in the upper 3 mm of the sediment.

Pelagic-benthic coupling in relation to day-to-day dynamics in benthic variables

The different phytopigments in the sediment showed a significant concentration decrease in time (adjusted R^2=0.30 (CH), R^2=0.27 (FU), R^2=0.26 (PH), n=14, P< 0.04 in all cases, **Fig. 7a, b**). The disappearance of phytopigments in the sediment coincided with a slight decrease in phytodetritus concentrations in the water column (based on fluorescence, Fig 5) and a slight decrease in sedimentation of phytopigments (Fig. 6). The POC concentrations did not show evident decreases during the cruise (Fig. 9a,b,c). The POC/chlorophyll-a ratio in the sediment traps and in the sediment increased in time. The input rate of phytopigments is less than the disappearance rate of phytopigments in the sediment. In case the disappearance of phytopigments is solely attributed to decay of pigments the first order decay constants for pigments in the sediment would be respectively 0.056 d^{-1} for chlorophyll-a (half-life of 12 days), $0.068.d^{-1}$ for fucoxanthin (half-life 10 d) and 0.055 d^{-1} for pheophytin-a of (half life of 13 days).

The variations in daily sedimentation of fucoxanthin were significantly reflected by its concentration in the sediment; 34% of the variation in the relation could be attributed to sedimentation (adjusted R^2=0.34, P<0.05). The FU/CH ratio in the sediment was significantly higher than the ratio in sediment traps and in the water column and varied between 1 and 2 (Fig.8).

Significant day-to-day variations in benthic bacterial production and bacterial numbers were not established. These variables did not exceed the spatial heterogeneity of the study area during the cruise (**Fig. 10a, b**). So the decrease in phytopigments was not reflected by a decrease in the bacterial variables. The BBP and the BBN remained constant during the cruise and were 32 $mgC.m^{-2}.d^{-1}$ (sd 8) and $2.505*10^9$ $bacteria.cm^{-3}$ wet sediment (sd $0.273 * 10^9$). The rise in bottom temperature from 8.5 to 9.6°C during the cruise was not reflected by an increase in the BBP (Fig. 10a).

Relationships between bacterial variables and phytopigments in the sediment

Benthic bacterial production (daily averages) was significantly correlated with the pigment concentrations (daily averages) of pheophytin-a and the pheophytin-a/chlorophyll-a ratio in the sediment (adjusted R^2=0.50, 0.40, P<0.05). Significant correlations between BBP and benthic chlorophyll-a and fucoxanthin respectively

were absent. Only when time as well as benthic phytopigments were taken as independent variables in the multiple regression 47 and 70% of the variation of BBP was explained by variation in chlorophyll-a, fucoxanthin and pheophytin-a respectively (CH: adjusted R^2=0.47, FU: R^2=0.64, PH: R^2=0.70, n=13, P<0.05). In case the factor time is not involved in the variability such as in the heterogeneity sampling exercise, in which the variability of different variables is completely due to spatial variability, weakly significant relations were also found between BBP and the phytopigments fucoxanthin and chlorophyll-a samples collected in singular during full tide (adjusted R^2=0.21-0.32, n=9, P<0.1). During slack tide sampling this relationship was not found.

Variations in BBN (on basis of daily averages) were significantly correlated to the pheophytin-a content of the sediment (adjusted R^2=0.23, n=14, P<0.05). Relations between BBN and the other benthic pigments were absent (P>0.1 in all cases). When all BBN data of the time series (1-2 per day) were tested 13 to 37% of the variations could be attributed to variations in phytopigments in the bottom (CH: adjusted R^2=0.133, n=27, P= 0.035; FU: R^2=0.16, n=27 P=0.022; PH: R^2=0.365, n=27, P=0.001). No significant relations were found between BBN and benthic phytopigments in the samples collected for the determination of heterogeneity on 7 (slack tide) and 9 July (high current velocities). Significant relations between BBP and BBN were absent.

Discussion

The weather conditions were exceptionally calm and sunny throughout the cruise. In July normally small changes in the weather (cold front, summer storm) can be expected which induce small mixing events in the water column (van Haren pers. comm, Ridderinkhof 1992). This turbulence may extend to the depth of the thermocline and induce sufficient entrainment of the thermocline (Ruardij et al. 1996) to result in redistributions of nutrients and stimulation of algal growth and increase of algal biomass. Such short mixing events due to short summer storms, cold fronts or other events leading to substantial increases of algal biomass in the water column however did not take place from 4 to 19 July 1994 (**Fig. 11**). Fig. 11 shows that such events, resulting in enhanced fluorescence, occurred 2 wks before and just after the cruise. During the cruise fluorescence and phytopigment concentrations showed only minor variations, largely coupled to tidal advection and day-night cycles of phytoplankton.

Vertical exchange in the water column

Exchange between the surface mixed layer (SML) and the benthic mixed layer (BML) was limited. The strong temperature stratification around 25 m depth and the temperature gradient in the SML on top of the thermocline (non-turbulent

intermediate layer, Ruardij et al. 1996) were indicative of the limited vertical heat exchange. It is evident that turbulent diffusion was low during the cruise. The limited exchange resulted in concentration differences in inorganic nutrients and phytopigments between the SML and the BML. The inorganic nutrient concentrations were low enough (particularly PO4) to limit primary production in the SML. In the BML nutrient concentrations were almost 2-3 times higher than in the SML. The differences in phytopigment concentrations between the SML and BML were large for chlorophyll-a with concentrations of 100 to 400 $ng.l^{-1}$ in the SML and 550 to 1400 $ng.l^{-1}$ in the BML, and even larger for fucoxanthin. Comparable differences in pigment concentrations between the SML and BML have been found in the North Sea in summer, but our absolute values were considerably lower (e.g. Gieskes & Kraay 1984, Peeters et al. 1995, Karlson et al. 1996).

Another effect of limited exchange between water layers were the differences in pigment composition. The occurrence of zeaxanthin in the SML suggest presence of cyanobacteria, prochlorophyta and green algae (see Wright et al. 1991). Considering the size of these small organisms it is unlikely that they sink into the BML. The FU/CH-a ratio was in the BML significantly larger than in the SML. Fucoxanthin is an indicator of diatoms and prymnesiophytes (Jeffrey 1974). In combination with the found chlorophyll c3/c2 ratio of about 1 and the fact that chlorophyll c3 is generally absent in diatoms (Stauber & Jeffrey 1988) it is most likely that prymnesiophytes such as Phaeocystis (Jeffrey & Wright 1994) occur in the water column. This pigment finger print is also characteristic for some dinophytes (see Jeffrey & Wright 1994). In combination with peridinin a major signature pigment for autotrophic dinoflagellates, which is consistently present in the BML and absent in the SML, it is likely that these dinoflagellates are relatively abundant in the BML and absent in the SML. Turbulence in the BML was probably larger than in the SML and possibly sufficient to keep the much larger sized dinoflagellates suspended. So it is most probable that completely different algal communities persisted in the different water layers.

During the cruise there was sufficient light penetration to allow primary production in the BML (PAR of ca 10 $\mu E.m^{-2}.s^{-1}$, van Haren unpublished data). One week after the cruise primary production was measured at the same station by Riegman (pers. comm.). He measured a primary production of approximately 200 $mgC.m^{-2}.d^{-1}$ in the BML. In the summer of 1989 and 1990 Peeters et al. (1995) measured primary productions in the BML of up to 800 $mgC.m^{-2}.d^{-1}$.

The increase in phytopigments on 14 July (day 194) in the SML and the thermocline (25 m depth) coincided with/was preceeded by a slight increase in PO_4. Significant increases in inorganic N were not established, but uptake by algae of these components, particularly NH_4, may be very fast in summer (e.g. Le Corre et al. 1996). Moreover the increase in fluorescence in the SML (13 m) coincided with a slight

decrease in the BML (38 m). In combination with the observation that the FU/CH ratio was higher on this day than on previous days suggests that an event may have occurred, which triggered some exchange between the BML and SML. The increase of the FU/CH ratio in the BML might have been due to enhanced resuspension during the event. A sudden and short-lasting vertical mixing event induced by internal waves creating shear stress between water masses in the thermocline might have been responsible (van Haren pers.comm.). However advective transport cannot really be excluded in being responsible for the event. It appeared that the increase in phytopigments in the SML was not related to the increase in nutrients around 10 July (day 190). The time lag between the decrease in nutrients and the increase in fluorescence was too long (ca 4 days). It was obvious that the event did not enhance the pigment concentrations in the BML.

We conclude that there was negligible exchange of pigments between the SML and BML during the cruise. The pigment content and composition in the BML may have largely developed in the BML, which functioned biologically independent of the SML with respect to organic matter and mineralization. So our study of the pelagic-benthic coupling will be restricted to the BML and the benthic compartment.

Coupling between pigments in the water column and sedimentation

The question addressed here is whether the phytopigment concentrations in the BML are related to the sedimentation of phytopigments. Variations of phytopigments in the BML were quite large. Similar observations were made by Peeters et al. (1995). Such large variations appear to be mainly due to advective transport, which renders the semi-diurnal pattern with 2 major peaks in fluorescence. Currents from the west to the east (predominantly flood streams) tended to convey more phytopigments in the BML over the study area than ebb streams. This is in accordance with the spatial gradients in fluorescence in a more extended area around the station (Van Raaphorst et al. 1996). Superimposed on this pattern a different quarter-diurnal pattern occurred related to resuspension and sedimentation of phytopigments. We assumed that most of the material deposited during slack tide is resuspended again at increasing current velocities. These patterns are in accordance with other observations in the North Sea (Jago et al. 1994).

The tidal variations in water column pigments in the BML were only partly reflected by variations in pigment sedimentation. Decreases in fluorescence around slack tide usually coincided with increases in sedimentation compared to amounts trapped during full tide. The observation that fluorescence was significantly higher at the onset of HW than at the onset of LW slack tide was not reflected in the amounts op phytopigments trapped. This suggests decoupling between concentrations in the water column and sedimentation of phytopigments. Algal sedimentation is not necessarily

determined by algal density only, but is often related to the algal life cycle (e.g. Noiji et al. 1986, Wassman 1994, Brussaard et al. 1995) and other characteristics such as size and stickiness (Kiørboe 1993). Changes in current velocities and turbulence around slack tide may enhance the flocculation of algae, which increases their sinking rate (e.g. Kiørboe & Hansen 1993). Conditions for flocculation might have been more suitable around low water slack tide than around high water slack tide. Van Raaphorst et al. (1996) demonstrated that the total seston content is higher around LW than HW slack tide and this may have stimulated flocculation and sedimentation. This phenomenon may explain the comparable amounts of pigment sedimentation during low and high water slack tide in the tidal sedimentation pattern. The close relation between daily average fluorescence (CH) and CH and FU sedimentation during slack tide emphasizes the coupling between water column concentrations and sedimentation on a day-to-day basis. Moreover the decrease of CH in the BML in the last week of the cruise was reflected by a slight decrease in sedimentation

The FU/CH ratio of the material trapped during slack tide could not be distinguished from the ratio of the material trapped during full tide. The FU/CH ratio was significantly higher in traps than in surrounding water and lower than the ratio in sediment. This may imply that traps selected for material rich in FU compared to CH.

So we observed absence of coupling between concentration in the water column and sedimentation of phytopigments on a tidal scale, but coupling on a daily/weekly scale.

Coupling between sedimentation and benthic variables

The next question is: are tidal, day-to-day and weekly variations in phytopigment sedimentation reflected by variations in benthic phytopigments and bacteria? The significant differences between sedimentation during slack tide and during full tide were not reflected by the phytopigment concentrations and the bacterial variables in the sediment surface layer. The benthic phytopigment and bacterial variables were not significantly higher during slack tide than during full tide. Only the standard variations were larger when measured during slack tide (table 1). This indicates that phytodetritus and bacteria settled patchy on the bottom during slack tide, probably due to irregularities of the bottom surface such as molds and burrows created by benthic fauna. Moreover insufficient resolution of sample analysis (sections of 3 mm thick were probably too thick to show tidal variations of phytopigment concentrations in the sediment) may have been due to the absence of significant differences in benthic phytopigment concentrations related to the tidal cycle. In the traps on the other hand material accumulated for 2 hrs in the different tidal phases emphasizing

the differences between slack tide and full tide sedimentation. Once trapped the material cannot be easily resuspended again.

Nevertheless some indications for coupling between sedimentation and accumulation on the bottom were found. Fucoxanthin and bacteria accumulated in slack tide periods, considering the positive relationships between FU sedimentation and its content in the sediment and considering the relationships between phytopigment sedimentation and benthic bacteria. Net sedimentation during slack tide must have been low, however, because accumulation could not be demonstrated for chlorophyll-a and accumulation of particle-associated bacteria did not result in measurable enhancement of the BBP. The inverse relationship between pheophytin-a sedimentation and its content in the sediment during high current velocities suggests that resuspension of fluffy material, which was deposited during slack tide, occurs and that this results in disappearance of most of the material which settled during slack tide. The consistent difference between the FU/CH ratios in traps and in the sediment surface layer, which was independent of the tidal phase, indicate that trap contents were not due to entrapment of resuspended bottom material only. The higher FU/CH ratio in the sediment surface may have been the result of diatom sedimentation events preceeding our cruise. Diatoms are particularly rich in fucoxanthin (Jeffrey 1974).

On a daily basis sedimentation of phytodetritus on the sediment must have exceeded resuspension. The variations in fluorescence related to tidally induced advective transport indicate that there was a gradient with higher fluorescence at the W side and lower fluorescence at the E side in a larger area encompassing the study area (van Raaphorst et al. 1996). This gradient persisted until day 196 (Fig. 6b) implying that sedimentation exceeded resuspension of phytodetritus. The variations in net sedimentation were however insufficient to result in subsequent variations in benthic variables. POC, BBP and BBN did not significantly change and the benthic phytopigments decreased during the cruise. The input was insufficient to compensate for the decrease in benthic phytopigments.

Aspects of pelagic-benthic coupling in the tidal cycle were demonstrated, but the net sedimentation of phytodetritus was too small and varied insufficiently to be reflected by the day-to-day and weekly variations in benthic variables.

Coupling between pigments and bacterial variables in the sediment

The next question is: Why did the benthic bacteria in the sediment surface layer did not respond to the variations in benthic phytopigments?

Algal pigments, such as chlorophyll-a and pheopigments, have been shown to be indicators of available food for bacteria and significant relations between the variables are usually found (e.g. Cole et al. 1988, Sander & Kalff 1993, van Duyl & Kop

1994). Most of these studies refer to spatial variability based on a wide range of sediment types. Chlorophyll-a and pheopigments in North Sea sediments usually covary with bacterial biomass and benthic pheopigment content is a good predictor of benthic bacterial production beside temperature (van Duyl & Kop 1994).

In the present study the significant decreases in benthic phytopigments were however not reflected by benthic bacterial variables. The temporal variations in BBP and BBN in the confined study area did not exceed the spatial variations. So BBP and BBN did not significantly change and remained equal for 2 weeks. Apparently a decoupling of bacterial production and chlorophyll-a and fucoxanthin as indicators of food availability occurred in time. The decrease in benthic phytopigments might be due to selective burial by mixing activities of macrofauna, but it is more likely that the decrease was due to decomposition/transformation reactions in situ. Pigment degradation following first-order kinetics resulted in decay rates, which are of the same order of magnitude as found by others (Leavitt & Carpenter 1990, Abele-Oeschger 1991, Sun et al. 1993b). Contrary to chlorophyll and fucoxanthin, pheophytin-a (PH) and the PH/chlorophyll-a ratio were significantly related to BBP and BBN, respectively. The temporal decrease of PH was apparently insufficient to mask its spatial relations with bacterial variables. This may be related to the observations that CH degradation to PH under oxic conditions is probably induced by microorganisms (Sun et al. 1993a and references therein), which may also point to a closer relation between bacterial variables and PH than with the other pigments.

It appears that the spatial relation between BBP and CH and FU in the sediment are masked by the time, possibly by time passed since the last substantial algal sedimentation. This may imply that spatial relations between BBP and benthic CH and FU can be found always in an area with a comparable recent history of phytopigment input in the sediment surface. Only the ratio between BBP and these pigments will increase with time passed since the last substantial phytodetritus sedimentation event. Apparently CH and FU are only markers of food availability but poor indicators of the amount of available food for bacteria. The degradation/ disappearance rate of these pigments may be faster in the sediment than the decomposition of most of the food they are representing.

Despite the decrease in phytopigments there was sufficient food available to maintain an average BBP of 32 $mgC.m^{-2}.d^{-1}$ in the 3 mm surface layer of the sediment. Although this production was almost half as much as the production at the same stn in July 1988 (15 July 53 $mgC.m^{-2}.d^{-1}$, van Duyl et al. 1993) and in August 1991 (55 $mgC.m^{-2}.d^{-1}$), it was significantly higher than winter values (Feb 1992, 13 $mgC.m^{-2}.d^{-1}$, van Duyl & Kop 1994). Considering the consistency and the height of the BBP it is improbable that input of directly utilizable organic matter of low molecular weight originating from the lysis of algal cells was sufficient as a food source. It is more

likely that enzymatic hydrolysis of higher molecular-weight material was the limiting step in bacterial production (Meyer-Reil 1991, Kristensen et al. 1995). This is probably the reason why temporal relations between bacterial variables and phytopigments were not established in the sediment. So there was no effect of the pelagic-benthic coupling of phytopigments on sedimentary bacteria on a day-to-day and weekly scale.

Concluding remarks

Events which resulted in significant enhancements of algal biomass in the water column and of algal input in the sediment did not occur during the cruise. The vertical exchange in the water column was limited. Pelagic-benthic coupling was demonstrated, but without any significant variations in net enrichment of the sediment with phytodetritus in time. The decrease in algal pigments in the sediment was predominantly due to natural decay in situ. Spatial relations between phytopigments and benthic bacterial production were decoupled in time implicating that chlorophyll a and fucoxanthin are poor indicators of the amount of bacterial substrate in the absence of fresh algal input (directly utilizable organic matter). The spatial relations between BBP, BBN and benthic phytopigments however indicate that the dominant source of food for bacteria in the Oyster Ground is phytodetritus.

LITERATURE CITED

Abele-Oeschger D (1991) Potential of some carotenoids in two recent sediments of Kiel Bight as biogenic indicators of phytodetritus. Mar Ecol Prog Ser 70:83-92

Ambrose Jr WG, Renaud PE (1995). Benthic response to water column productivity patterns: Evidence for benthic-pelagic coupling in the Northeast Polynya. J Geophys Res 100:4411-4421

Bird DF, Kalff J (1984) Empirical relationships between bacterial abundance and chlorophyll concentration in fresh and marine waters. Can J Fish aquat Sci 41:1015-1023

Billen G, Joiris C, Meyer-Reil L-A, Lindeboom HJ (1990). Role of bacteria in the North Sea ecosystem. Neth J Sea Res 26:265-293

Brussaard CPD, Riegman R, Noordeloos AAM, Cadée GC, Witte H, Kop AJ, Nieuwland G, van Duyl FC, Bak RPM (1995) Effects of grazing, sedimentation and phytoplankton cell lysis on the structure of a coastal pelagic food web. Mar Ecol Prog Ser 123:259-271

Butman CA (1986) Sediment trap biases in turbulent flows: results from a laboratory flume study. J Mar Res 44:645-693

Cole JJ, Findlay S, Pace ML (1988) Bacterial production in fresh and saltwater ecosystems: a cross-system overview. Mar Ecol Prog. Ser 43:1-10

Gieskes WWC, Kraay GW (1984) Phytoplankton, its pigments, and primary production at a central North Sea station in May, July and September 1981. Neth J Sea Res 18:51-70

Graf G, Bengtsson W, Diesner U, Schulz R, Theede H (1982) Benthic response to sedimentation of a spring phytoplankton bloom: process and budget. Mar Biol 67:201-208

Graf G, Schulz R, Peinert R, Meyer-Reil L-A (1983) Benthic response to sedimentation events during autumn to spring at a shallow-water station in the Western Kiel Bight. Mar Biol 77:235-246

Graf G (1987) Benthic energy flow during a simulated autumnn bloom sedimentation. Mar Ecol Prog Ser 39:23-29

Graf G (1992) Benthic-pelagic coupling: a benthic review. In M Barnes, AD Ansell, RN Gibson (Eds.) Oceanography and marine biology (pp. 149-190). London, England: UCL Press.

Hargrave BT, Burns NM (1979) Assessment of sediment trap collection efficiency. Limnol Oceanogr 24:1124-1136

Hitchcock GL, Langdon C, Smayda TJ (1987) Short-term changes in the bioloy of a Gulf Stream warm-core ring: Phytoplankton biomass and productivity. Limnol Oceanogr 32:919-928

Jago CF, Bale AJ, Green O, Howarth MJ, Jones SE, McNave IN, Millward GE, Morris AW, Rowden AA, Williams JJ (1994) Resuspension processes and seston dynamics, southern North Sea. In H Charnock, KR Dyer, JM Huthnance, PS. Liss, JH Simpson, PB Tett (Eds.) Understanding the North Sea System (pp. 97-113). London: Chapman & Hall, Royal Society.

Jeffrey SW (1974) Profiles of photosynthetic pigments in the ocean using thin-layer chromatography. Mar Biol 26:101-110

Jeffrey S. W, Wright SW (1994) Photosynthetic pigments in the Haptophyta. In JC Green, BSC Leadbeater (Eds.) The Haptophyte alga pp 111-132. Oxford: Clarendon Press.

Karlson B, Edler L, Granéli W, Sahlstein E, Kuylenstierna M (1996). Subsurface chlorophyll maxima in the Skagerrak-processes and phytoplankton community structure. J Sea Res 35:139-158

Kiørboe T (1993) Turbulence, phytoplankton cell size, and the structure of pelagic food webs. In JHS Blaxter, AJ Southward (Eds) Advances in Marine Biology (pp. 1-72). London: Academic press

Kiørboe T, Hansen JLS (1993) Phytoplankton aggregate formation: observations of patterns and mechanisms of cell sticking and the significance of exopolymeric material. J Plankton Res 15:993-1018

Kiørboe T, Nielsen TG (1990) Effects of wind stress on vertical water column structure phytoplankton growth and productivity of plankton copepods. In M &. RNG Barnes (Eds.) Trophic relationships in the marine environment (pp. 28-40). Aberdeen: Aberdeen Univ. Press

Kristensen E, Ahmed SI, Devol AD (1995) Aerobic and anaerobic decomposition of organic matter in marine sediment: which is fastest? Limnol Oceanogr 40:1430-1437

Leavitt PR, Carpenter SR (1990). Aphotic pigment degradation in the hypolimnion: Implications for sedimentation studies and paleolimnology. Limnol Oceanogr 35:520-534

Le Corre P, Wafar M, 'Helguen SL, Maguer JF (1996) Ammonium assimilation and regeneration by size-fractionated plankton in permanently well-mixed temperature waters. J. plankton Res. 18:355-370

Meyer-Reil L-A (1987) Seasonal and spatial distribution of extracellular enzymatic activities and microbial incorporation of dissolved organic substrates in marine sediments. Appl environ Microbiol 53:748-1755

Meyer-Reil L-A(1991) Ecological aspects of enzymatic activity in marine sediment. In RJ Chrost (Eds.), Microbial enzymes in

aquatic environments (pp. 84-94). New York: Springer-Verlag.
Moriarty DJW, Pollard PC (1981) DNA synthesis as a measure of bacterial productivity in seagrass sediments. Mar Biol Prog Ser 5: 151-156
Noji T, Passow U, Smetacek V (1986) Interaction between pelagial and benthial during autumn in Kiel Bight. I. Development and sedimentation of phytoplankton blooms. Ophelia 26:333-349
Olesen M (1995) Comparison of the sedimentation of a ditom spring bloom and of a subsurface chlorophyll maximum. Mar Biol 121:541-547
Osinga R, Kop AJ, Malschaert FP, van Duyl FC (1996) Effects of the sea urchin *Echinocardium cordatum* on bacterial production and carbon flow in experimental benthic systems under increasing organic loading. J Sea Res (in press)
Peeters JCH, Los FJ, Jansen R, Haas HA, Peperzak L, Vries I de (1995) The oxygen dynamics of the Oyster Ground, North Sea. Impact of eutrophication and environmental conditions. Ophelia 42: 257-288
Reineck HE (1963) Der Kastengreifer. Natur u. Museum 93:102-108
Ridderinkhof H (1992) On the effects of variability in meteorological forcing on the vertical structure of a stratified watercolumn. Cont Shelf Res 12:25-36
Ruardij P, Haren H van, Ridderinkhof H (1996) The impact of timing of the thermal stratification on production succession and grazing of phytoplankton in shelf seas: a model study. submitted to J. Sea Res..
Sander BC, Kalff J (1993) Factors controlling bacterial production in marine and freshwater sediments. Microb Ecol 26:79-99
Simon M, Azam F (1989) Protein content and protein synthesis rates of planktonic marine bacteria. Mar Ecol Prog Ser 51: 201-213
Sokal R, Rohlf FJ (1981) Biometry: The principles and practice of statistics in biological research (2 ed.). San Francisco: Freeman WH
Stauber JL, Jeffrey SW (1988). Photosynthetic pigments in fifty-one species of marine diatoms. J. Phycology 24:158-172.
Suess E (1980) Particulate organic carbon flux in the oceans: surface productivity and oxygen utilization. Nature 288:260-263
Sun M-Y, Lee C, Aller RC (1993a) Anoxic and oxic degradation of 14C-labeled chloropigments and a 14C-labeled diatom in Long Island Sound sediments. Limnol Oceanogr 38:1438-1451

Sun M-Y, Lee C, Aller RC (1993b) Laboratory studies of oxic and anoxic degradation of chlorophyll-a in Long Island Sound sediments. Geochim Cosmochim Acta 57:147-157

Tett P, Walne A (1995) Observations and simulations of hydrography, nutrients and plankton in the southern North Sea. Ophelia 42: 371-416

Turley CM, Lochte K (1990) Microbial response to the input of fresh detritus to the deep-sea bed. Palaeogr Palaeoclim Palaeoecol 89: 3-23

Van Duyl FC, Bak RPM, Kop AJ, Nieuwland G, Berghuis EM, Kok A (1992a) Mesocosm experiments: mimicking seasonal developments of microbial variables in North Sea sediments. Hydrobiologia 235/236:267-281

Van Duyl FC, Kop AJ (1994) Bacterial production in North Sea sediments: clues to seasonal and spatial variations. Mar Biol 120: 323-337

Van Duyl FC, Kop AJ, Kok A, Sandee AJJ (1992b) The impact of organic matter and macrozoobenthos on bacterial and oxygen variables in marine sediment boxcosms. Neth J Sea Res 29:343-355

Van Duyl FC, Van Raaphorst W, Kop AJ (1993) Benthic bacterial production and nutrient sediment-water exchange in sandy North Sea sediments. Mar Ecol Prog Ser 100:85-95

Van Haren JJM (1993). Theme I: Mooring. In W van Raaphorst JP Boon Eds The Integrated North Sea Programme 1991-1992. Preliminary results. Neth Inst Sea Res Texel NL. NIOZ-Report 1993-9:1-5

Van Raaphorst W, Malschaert JFP, Van Haren JJM (1996). Tidal resuspension and deposition of particulate matter in the Oyster Ground, North Sea continental shelf. J Mar Res submitted

Verardo DJ, Froelich PN, Macintyre A (1990) Determination of organic carbon and nitrogen in sediments using the Carlo Erba Na-1500 analyser. Deep-Sea Res 37: 157-165

Walsh JJ, Whitledge TE, Barvenik FW, Wirick CD, Howe SO, Esaias WE, Scott JT (1978) Wind events and food chain dynamics within the New York Bight. Limnol Oceanogr 23:659-683

Wassmann P (1994) Significance of sedimentation for the termination of *Phaeocystis* blooms. J Mar Syst 5:81-100

Wright SW, Jeffrey SW, Mantoura RFC, Llewellyn CA, Bjørnland T, Repeta D, Welschmeyer N (1991) Improved HPLC method for the analysis of chlorophylls and carotenoids from marine phytoplankton. Mar Ecol Prog Ser 77:183-196

Fig. 1. Location of the study site in summer temperature stratified waters on the Oyster Ground, North Sea.

Fig. 2. Detail of the study area (ca 900 by 900 m) with a mooring site with equipment (ST sediment traps, T thermistorstring, B fluorescence, A acoustic doppler current profiler, M meteorology station, C current meters, N nitrate autoanalysing system) in the SW part (ca 600 by 600 m, with R1-R4 outline) and bordered at the N and E-side by 17 stations with a diameter of 180 m representing the daily stations for water and sediment sampling.

Fig. 3. The vertical temperature distribution during the cruise (isotherms of 9 to 20°C, 1°C).

Fig. 4. DIN, PO_4 and SiO_2 concentrations at different depths during the cruise.

Fig. 5. a. Chlorophyll-a variations in the SML. __ fluorescence at 13 m depth expressed in chlorophyll-a; HPLC analyses of chlorophyll-a at 5 m depth (•). Note the day-night cycle in the fluorescence.

b. Chlorophyll-a variations in the BML. __ fluorescence at 38 m depth expressed in chlorophyll-a; HPLC analyses of chlorophyll-a at 25-30 m (◇) and at 40 m (●) depth depth. Note the tidal cycle in the fluorescence with increasing concentrations during flood tide, a small drop in fluorescence during HW slack tide, an overall decrease during ebb tide with lowest fluorescence during LW slack tide.

c.Fucoxanthin variations in the watercolumn at 5 m depth in the SML and at 22-30 m and 40 m depth in the BML.

Fig. 6. Phytopigment sedimentation in the BML. Inventory of sedimentation of phytopigments in 2 h periods around high (H) or low (L) water slack tide and in 2 h periods during full tide a. chlorophyll-a, b. fucoxanthin, c. pheophytin-a. d. daily sedimentation of chlorophyll-a, fucoxanthin and pheophytin-a.

Fig. 7. Variations in benthic phytopigments in the 3 mm thick sediment surface layer for (a) chlorophyll-a and fucoxanthin (spatial variability ranges from 0.7-1.4 mg $CH.m^{-2}$ and from 0.9-1.8 mg $FU.m^{-2}$) and for (b) pheophytin-a (spatial variability is indicated).

Fig. 8. The FU/CH ratio at different depths in the water column, in the sediment trap and in the sediment surface layer.

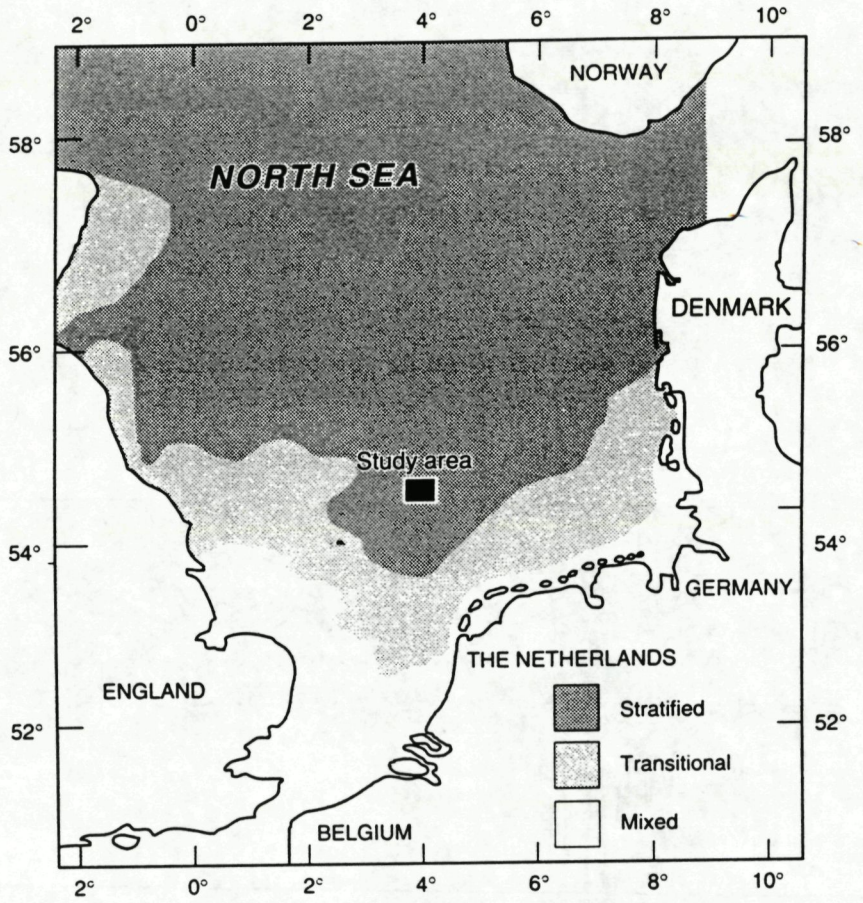
Fig. 9. Variations in the particulate organic carbon content (POC) and the POC/chlorophyll-a ratios (a) in the BML at 40 m depth, (b) in the sediment traps at 43 m depth and (c) in the sediment surface layer at 46 m depth.

Fig. 10. Variations in (a) bacterial production and (b) bacterial abundance in the 3 mm thick sediment surface layer.

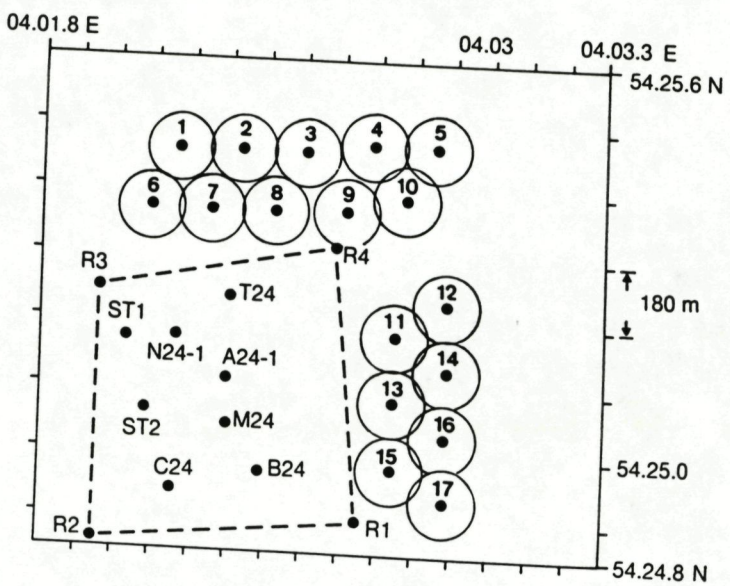
Fig. 11. a. Seasonal fluorescence in 1994, with (b) a detail of the period between yearday 150 and 230 including the indicated STED cruise period.

Table1. Comparison of the spatial variability in the study area during slack tide and full tide for benthic variables (phytopigments, bacterial production and abundance) in the 3 mm sediment surface layer.
There were no significant differences between data collected during slack or full tide (ANOVA).

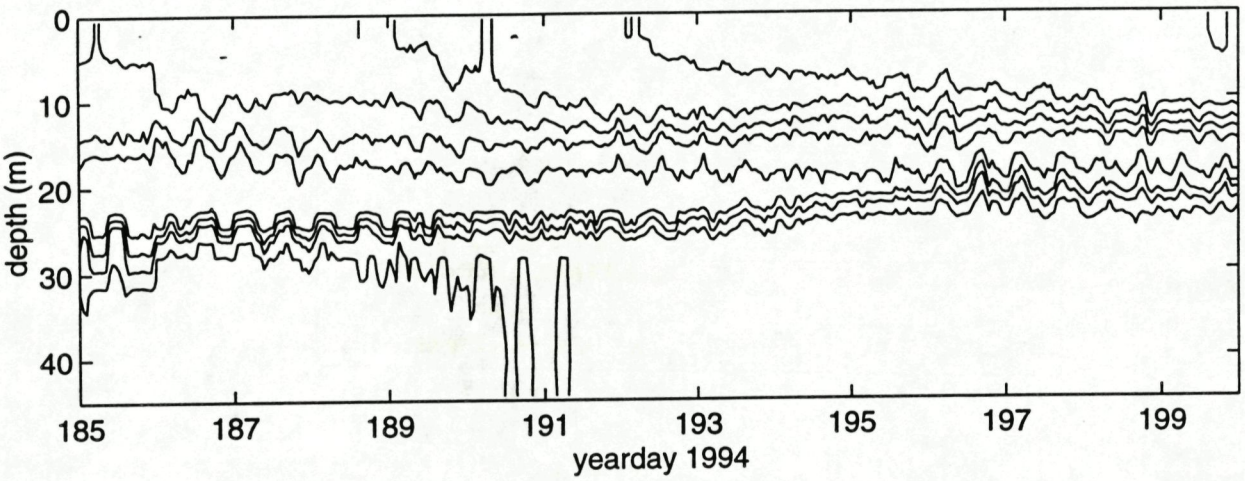
			slack tide		**full tide**			
	dimension	n	average	stdev	average	stdev	P-value	
current speed	*cm.s-1*	*9*	*3.2*	*1.64*	*20.18*	*1.63*		
current direction	*°*	*9*	*126.53*	*123.09*	*301.03*	*6.93*		
date	*Jul-94*		*7*		*9*			
sampling period	*h*		*10:05-11:43*		*14:32-15:59*			
phytopigments								
chlorophyll-a	mg.m-2	9	1.097	0.454	0.950	0.270	0.429	ns
fucoxanthin	mg.m-2	9	1.419	0.494	1.245	0.443	0.407	ns
pheophytin-a	mg.m-2	9	0.358	0.138	0.269	0.108	0.148	ns
bacteria								
bacterial numbers	n.cm-3	9	2.38E+09	4.65E+08	2.40E+09	2.91E+08	0.854	ns
bacterial production	mgC.m-2.d-1	9	30.8	11.8	30.7	6.2	0.972	ns



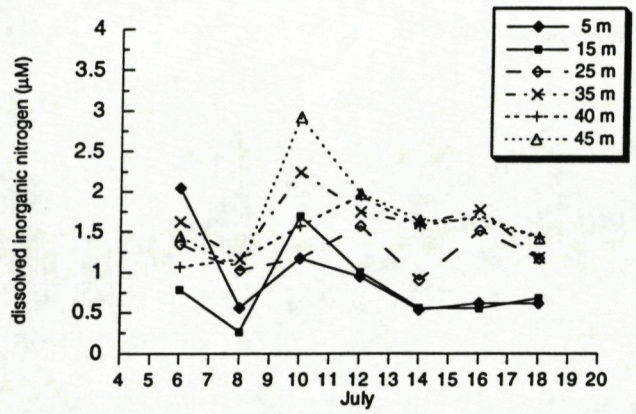
Appendix 2. Figure 1

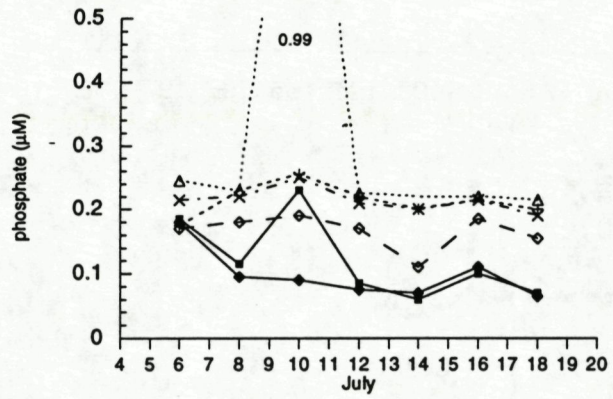


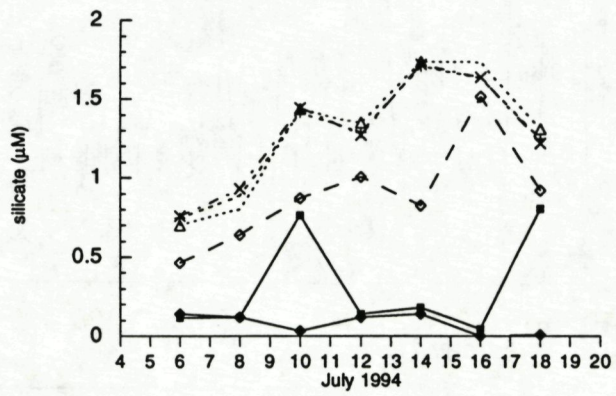
Appendix 2. Figure 2



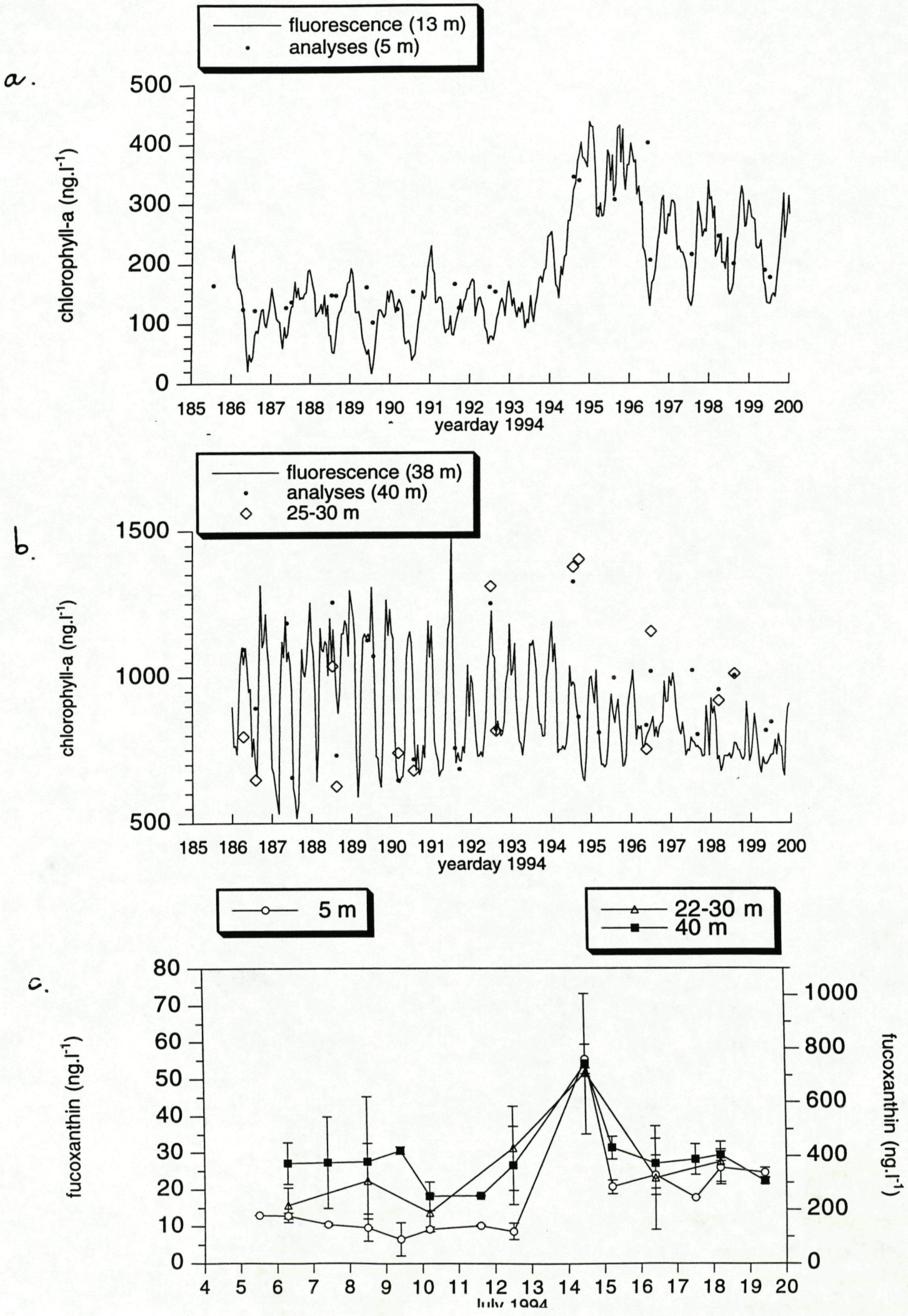
Appendix 2. Figure 3





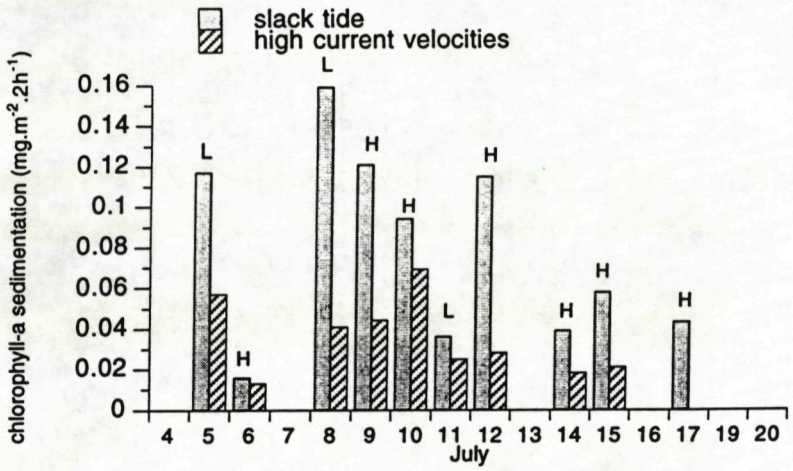


Appendix 2. Figure 4

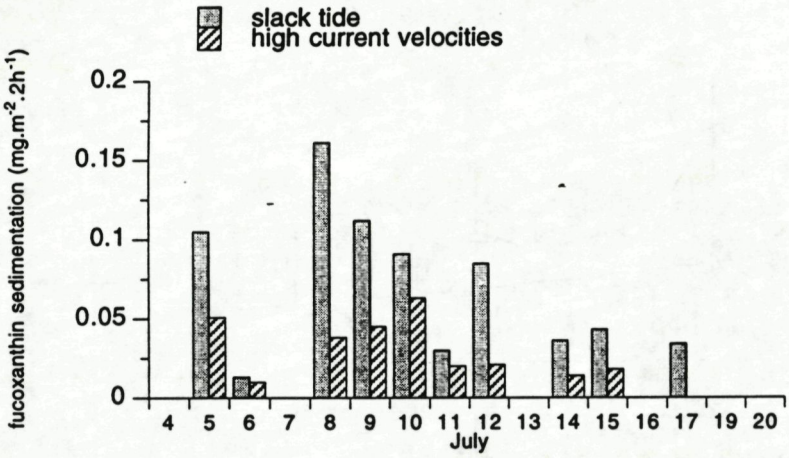


Appendix 2. Figure 5

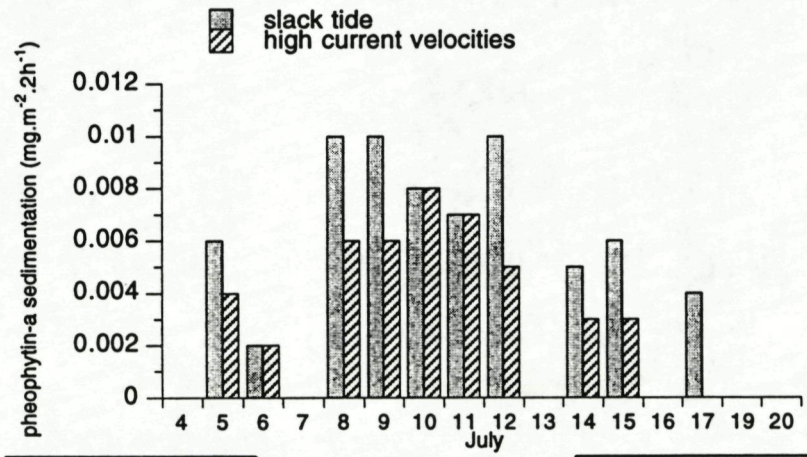
a.



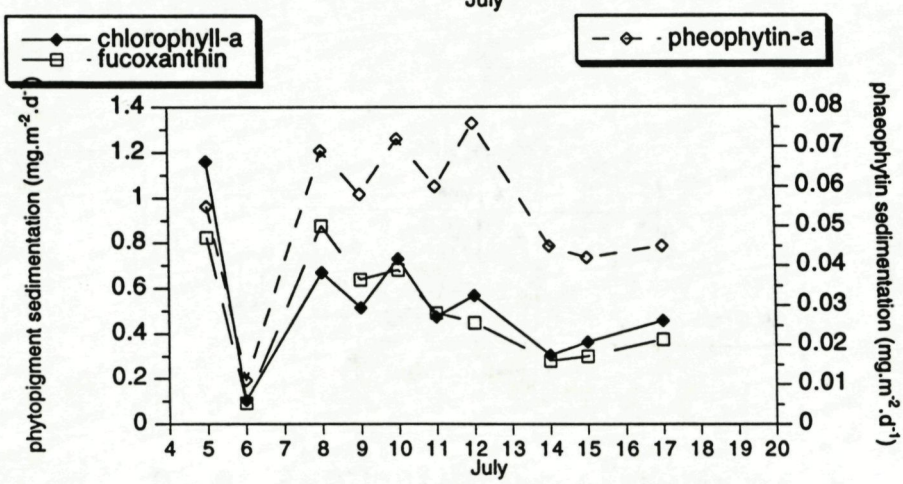
b.



c.

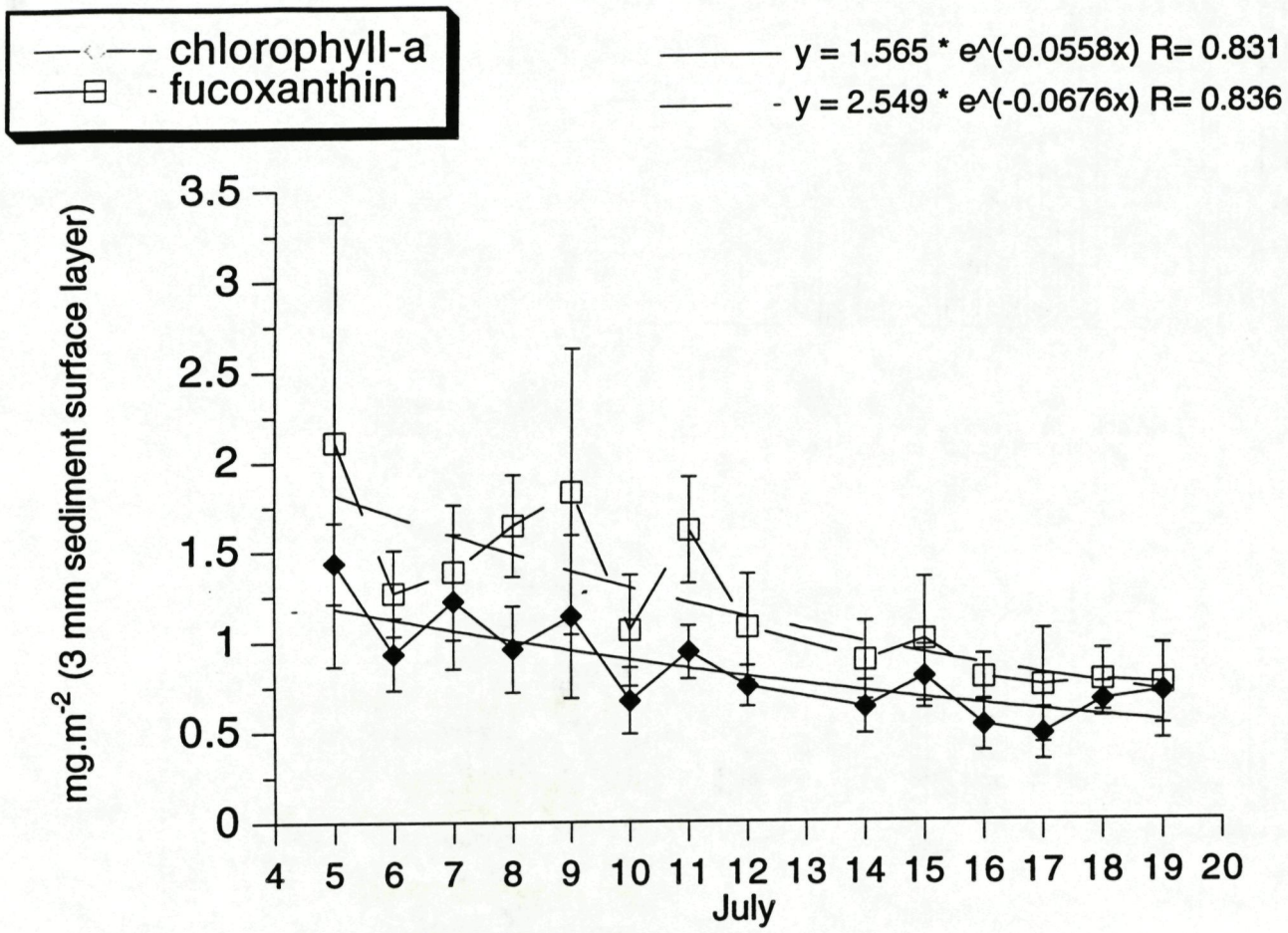


d.

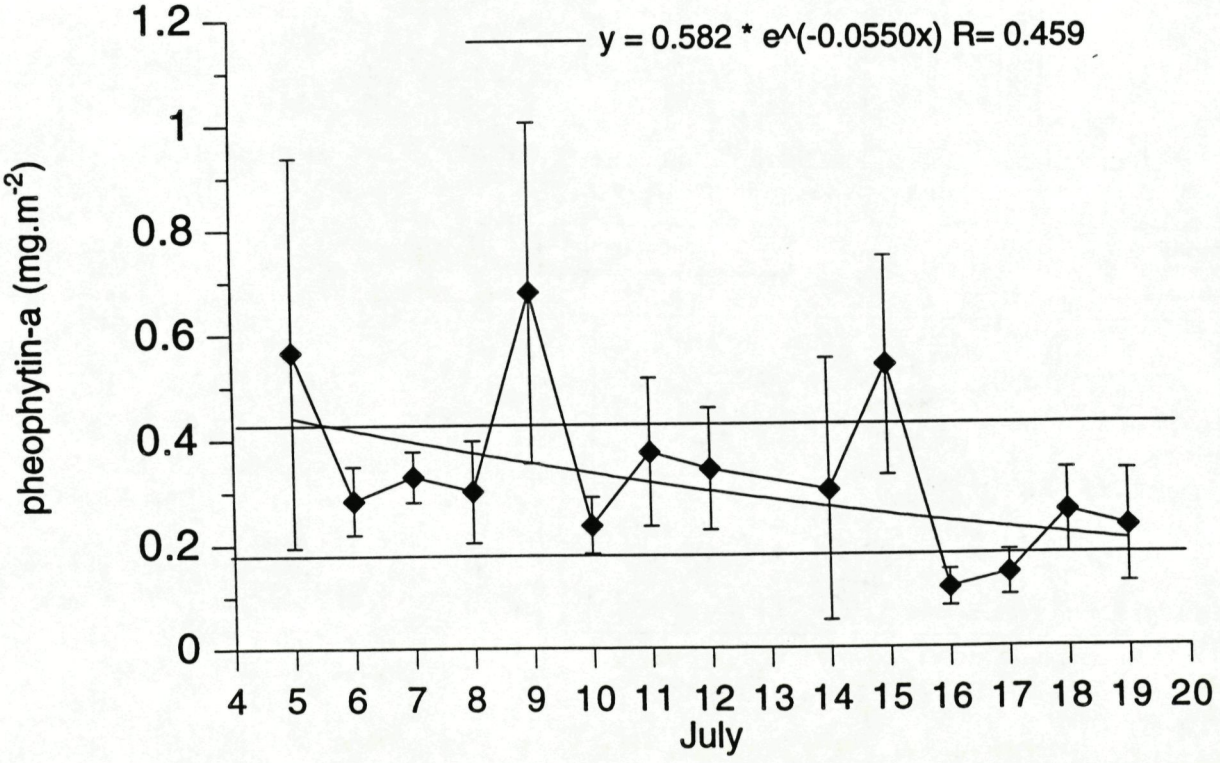


Appendix 2. Figure 6

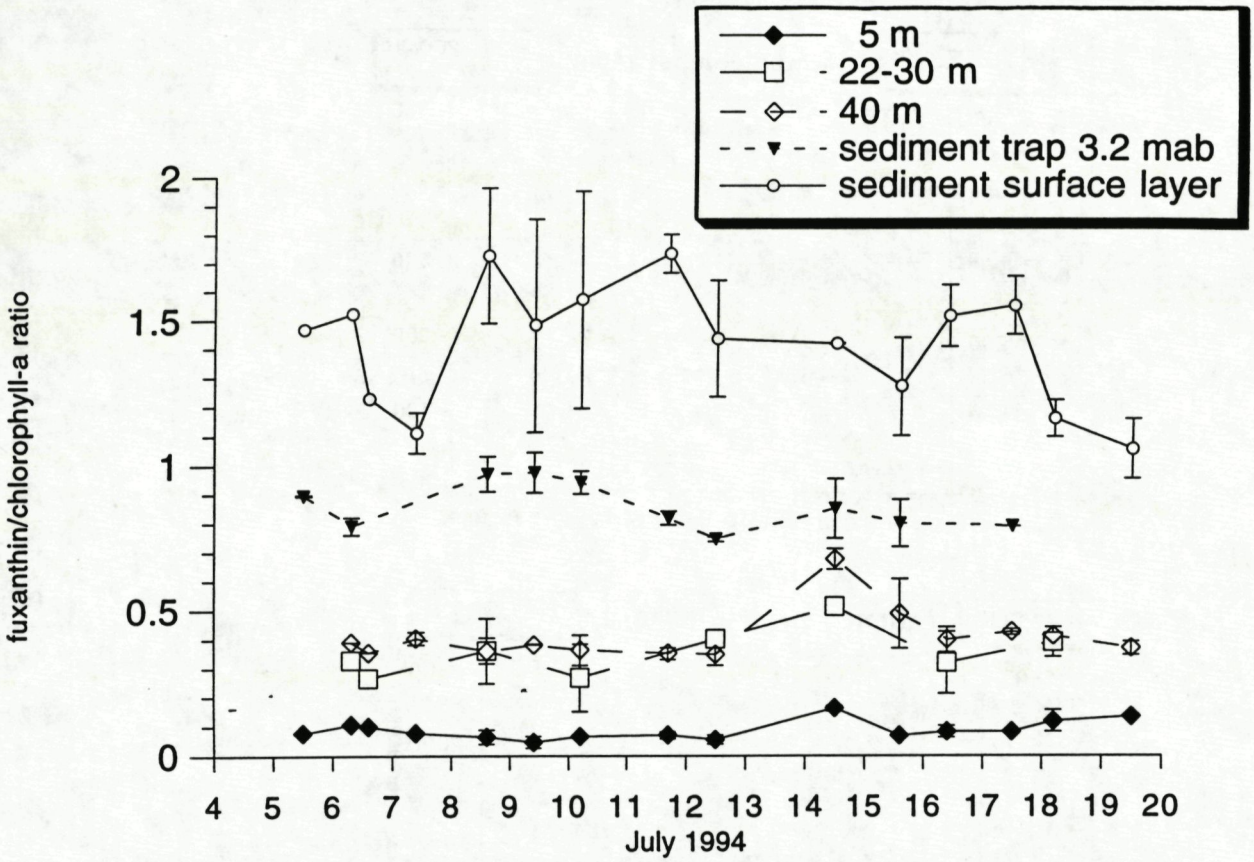
a.



b.

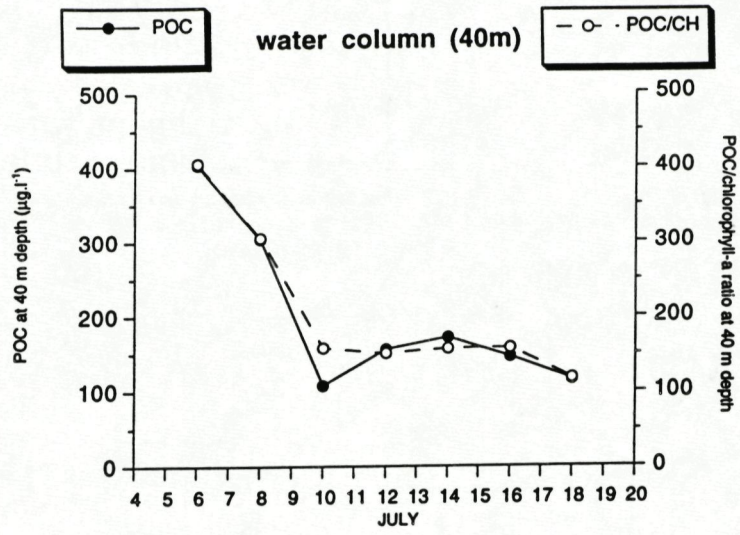


Appendix 2. Figure 7

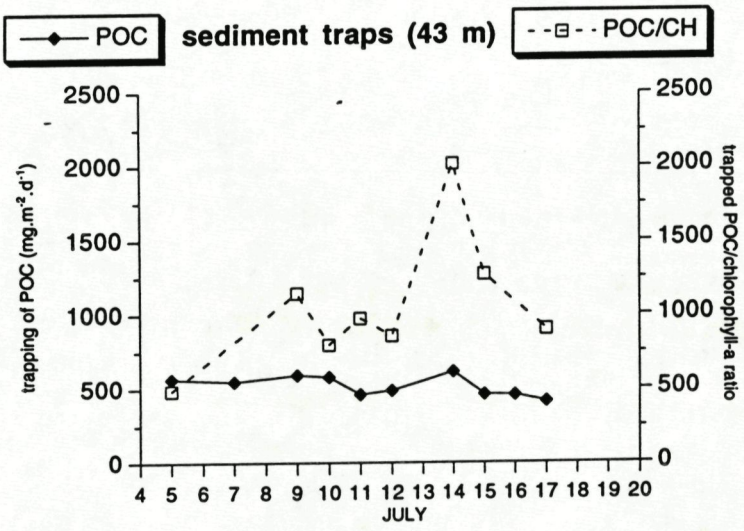


Appendix 2. Figure 8

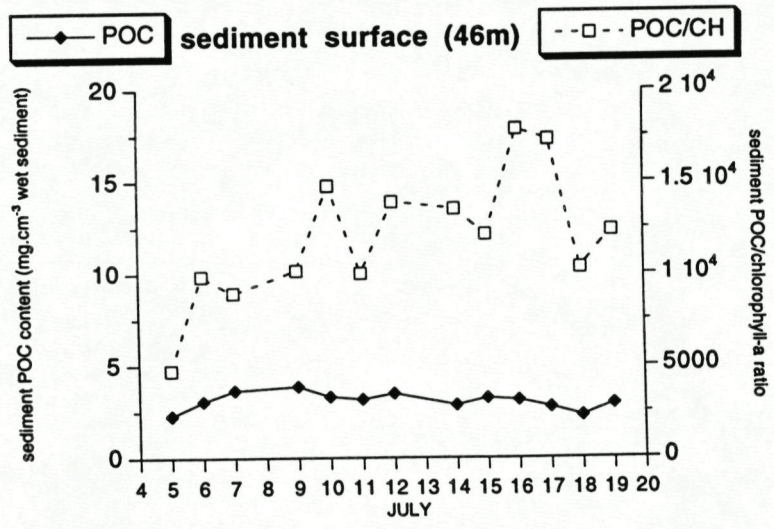
a.



b.

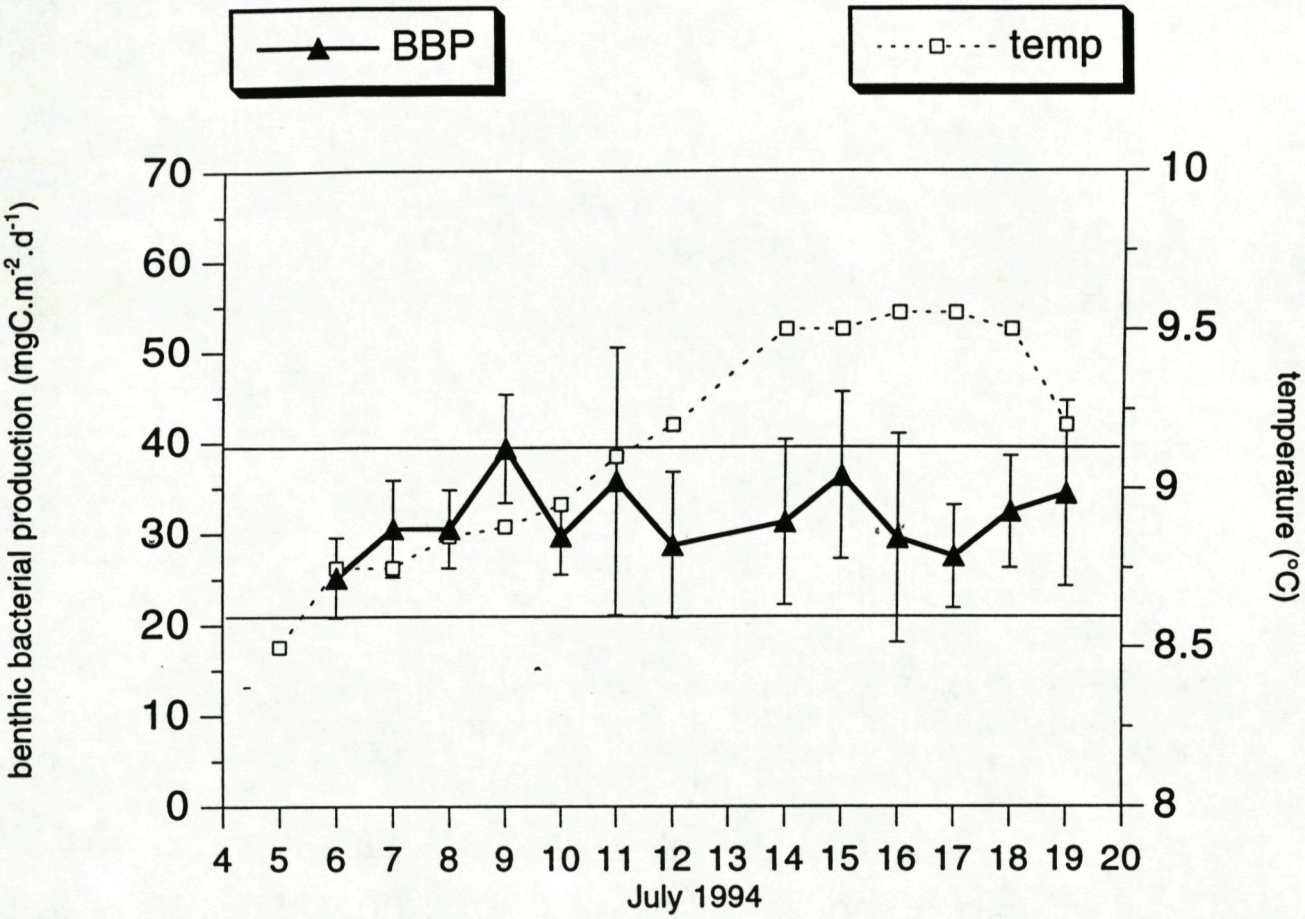


c.

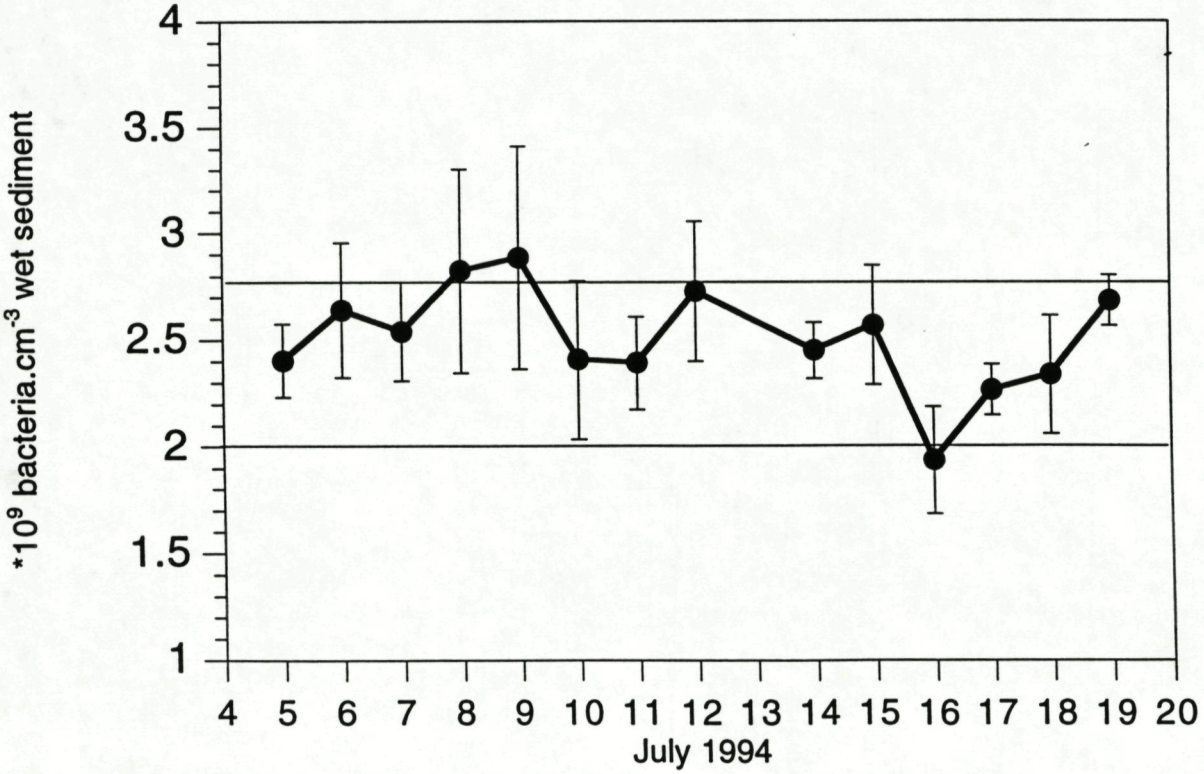


Appendix 2. Figure 9

a.

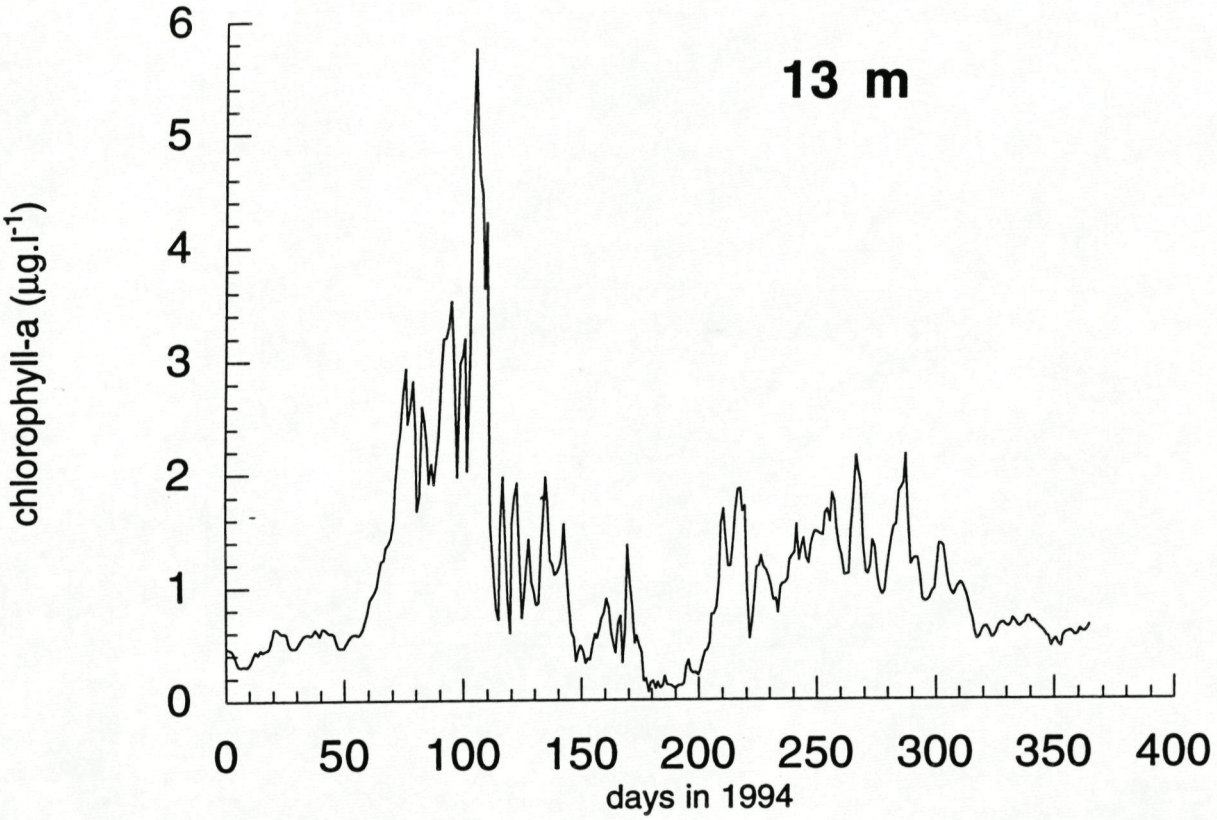


b.

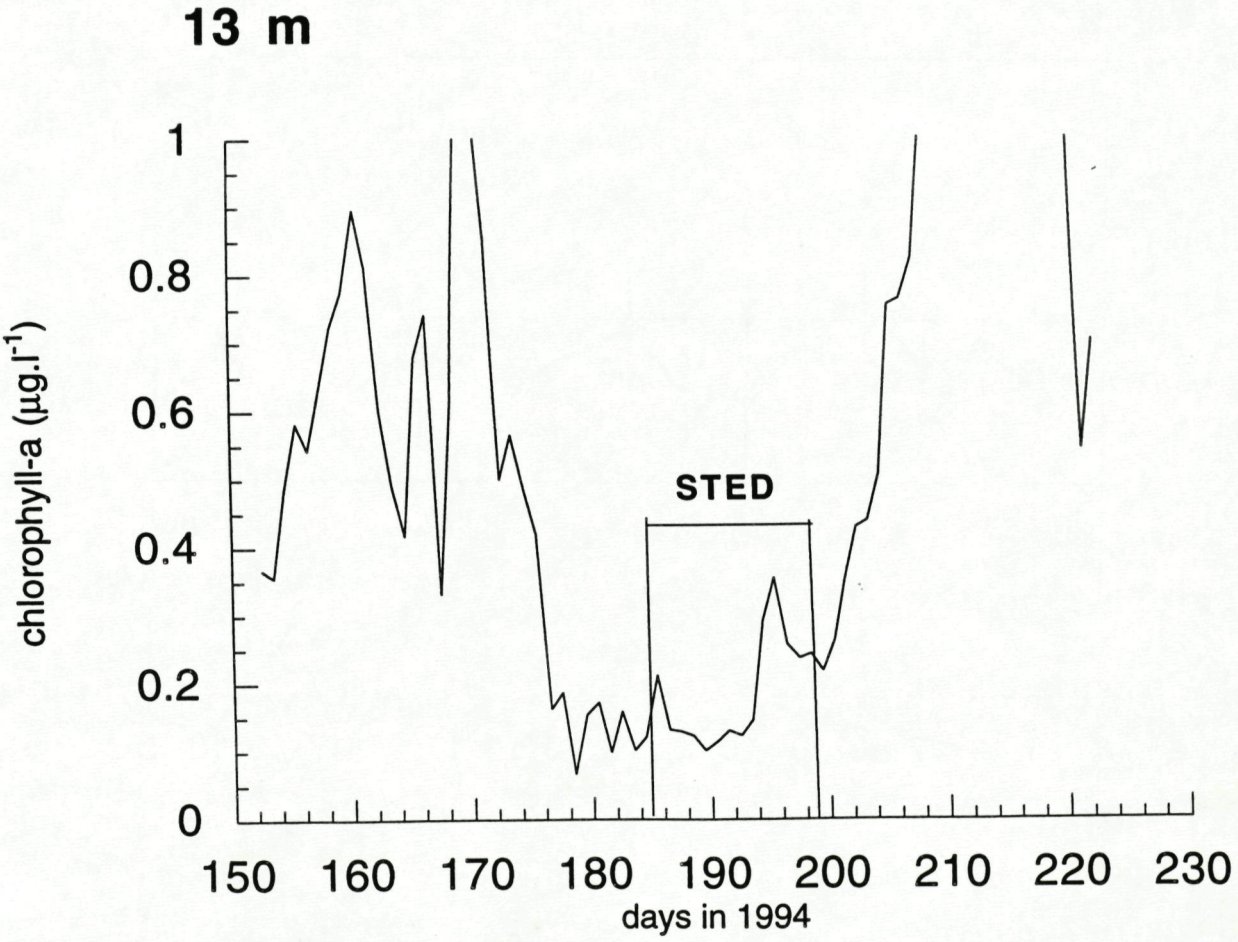


Appendix 2. Figure 10

a.



b.



Appendix 2. Figure 11

APPENDIX 3

The impact of timing of the thermal stratification on production, succession and grazing of phytoplankton in shelf seas: a model study *

PIET RUARDIJ, (HANS) J.M. VAN HAREN & HERMAN RIDDERINKHOF

Netherlands Institute for Sea Research, Postbox 59, 1790 AB Den Burg, Texel, The Netherlands

ABSTRACT

Local heating rate within the water column depends on energy input by solar radiation and heat exchange across the surface as controlled by wind and convection. The heating results in thrmal stratification of the water column, which in turn affects the vertical transport of, for example, nutrients. In this papaer we evaluate the implications of the stratification on the biota by focussing on the time of the onset, its stability in space and its variability in time. Especially the consequences of the stratification on the phytoplankton dynamics and the trophic interactions are shown. For this purpose, an integrated ecosystem model is developed which includes a physical submodel and an ecological model. The model is calibrated with data from a mooring project, during which a large number of physical and biological parameters have been measured at a site on the Oyster Groundsin the North Sea over a 15 months period. The physical model is a one-dimensional entrainemnt/detrainment model. The ecological model consists of submodels which are part of the ERSEM-ecosystem model and which describe the biological and chemical processes in the water column and in the benthos. Results show that stratification has a major impact on the biota. Especially the timing of the onset of the stratification has major consequences for the production and succession of phytoplankton and the structure of the food web during the whole growing season.

1. Introduction

During summer the deeper parts of shelf seas are stably thermally stratified. Since the availability of nutrients and light to the phytoplankton is controlled by the vertical density structure of the water column, such stratification has a major impact on the primary production in the water column (Tett *et al.*, 1993; Tett & Walne,

*Publication no. 3088 ot the Netherlands Institute for Sea Research

1995). This holds not only for the distribution of primary production in the water column, but also for the nutrient dynamics (Tett & Walne, 1995). Until now several two-layer coupled models exists that describe primary production in a stratified shelf sea (*e.g.* Radach & Lenhart (1995); Tett & Walne (1995)). Only a few vertically fully resolved coupled physical-biological models exist in the literature (Radach, 1983; Stramska & Dickey, 1993). None of them however, discusses the consequences of the timing of the onset and the extent of the stratification for the phytoplankton production, the succession and trophic interactions during a full growing season. Nevertheless, one may speculate that the timing of the onset of stratification in spring, when succession of dominating phytoplankton species proceed in a rapid sequence (weeks) (Riegman *et al.*, 1993) may determine the species composition for at least several months. In addition, irregular short-term declines or even breakdowns of stratification, both resulting in enhanced mixing may have a longer-term effect on the physical and biological properties of the water column.

Ridderinkhof (1992), for instance, showed that wind mixing events do not only influence the short-term variability of the surface mixed layer depth, but also the total heat content of a water column on a longer, seasonal, time-scale.

It is our hypothesis that short-term mixing events are responsible for the supply of nutrients to the surface mixed layer during summer, and as such may have a major impact on the summer phytoplankton production. The primary objective of the present study is thus to examine the consequences of the timing of the onset of the stratification in spring and the impact of the variability of the stratification during summer, when forced by wind, air temperature, humidity, irradiation and tidal friction, on primary production, nutrient-phytoplankton interactions and interactions of phytoplankton with higher trophic levels on the continental shelf. To achieve this aim we combined the physical model of van Aken (1984) and Ridderinkhof (1992) with the ERSEM-II ecosystem model (Baretta *et al.*, 1995) and the extensive data set available from a mooring site in the Oyster Grounds, North Sea (Fig. 1). This data set can be applied as forcing for the model (mainly the physical part) and for calibration data, *e.g.* for chlorophyll-a, vertical extinction and nutrients. The ERSEM-model has been jointly developed by six institutes in Europe and it is claimed that the model is generic for shelf seas. The original 2-

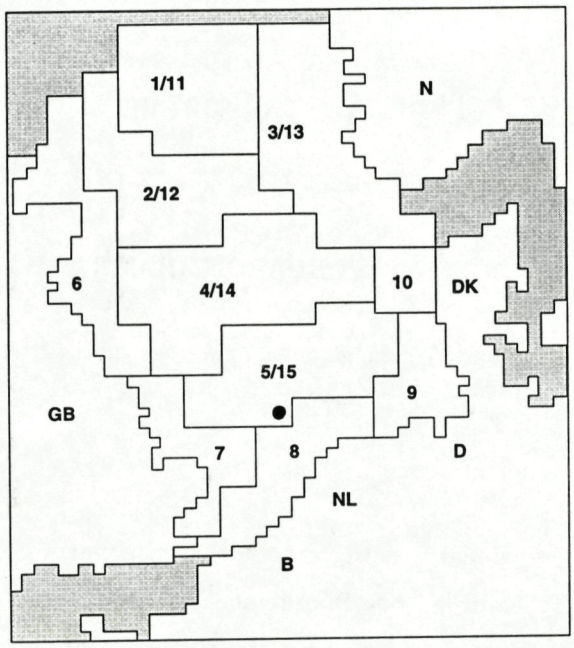


Fig. 1. Schematic map of box division as applied in the original ERSEM model. • indicates the INP-mooring site in the Oyster Grounds.

D version of the model describes in an appropriate way pelagic and benthic processes as well as sediment-water exchanges in the North Sea (Varela *et al.*, 1995; Broekhuizen *et al.*, 1995; Radach & Lenhart, 1995; Ebenhöh *et al.*, 1995; Ruardij & van Raaphorst, 1995). As a secondary objective this study provides an independent test of the ERSEM model for its applicability in a 1-D situation, but with a different physical model component and at another space scale than the 2-D version as developed for the entire North Sea (Fig. 1). Also, the underlying physical model could be tested extensively for the first time in combination with biological sub-models.

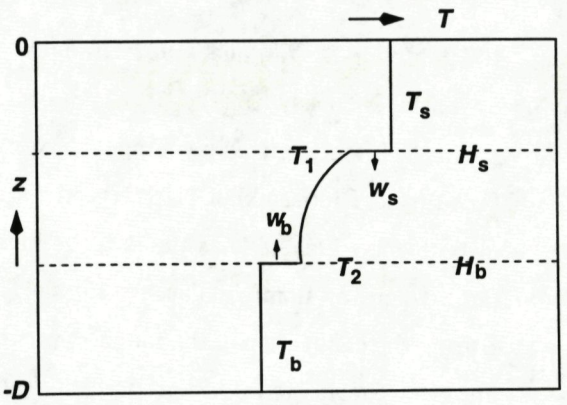


Fig. 2. Schematic picture of the surface mixed layer of depth D (0 - H_s) and bottom mixed layer (H_b - D), separated by a thermocline with weak turbulence. T_s and T_b are the temperatures of the surface and bottom layers, respectively. T_1 and T_2 are the temperatures at the top and bottom of the thermocline. w_s and w_b are the entrainment velocities.

2. The Model

2.1. The physical Model

The physical model used is based on a mixed layer model of van Aken (1984) which has been modified by Ridderinkhof (1992). The main characteristics are summarized in Fig. 2. It is assumed that the physical structure of the water column consists of three different layers:

- The turbulent surface mixed layer (SML) which has a mean temperature T_S and a thickness H_S. The entrainment velocity w_s parameterizes the turbulent fluxes to the layer below. Turbulence in this layer is mainly generated by wind.
- The thermocline layer (WTIL : weak turbulence intermediate layer).
- The turbulent bottom mixed layer (BML) which has a mean temperature T_b and thickness $D - H_b$. The entrainment velocity (w_b) parameterizes the turbulent fluxes at the top of this layer to the WTIL. Turbulence in the bottom layer is assumed to be only generated by the tidal currents.

Temperature changes are caused by heating through irradiation, counteracted by the heat efflux across the air-sea interface. This efflux is controlled by the turbulence in the SML, the air temperature and the humidity (van Aken, 1984). Contrary to the two mixed layers, the WTIL is subdivided in sub-layers with a depth of 1 m.

The vertical transport in the water column is induced by shifting of the layer boundaries. Direct exchange between the SML and the BML is only possible if the boundaries of the WTIL overlap, i.e. when the WTIL disappears. This approach differs from models which solve the advection-diffusion equation on a vertical grid in which the diffusion coefficients are derived from a turbulence-closure scheme. (Mellor & Yamada,

1974; Mellor & Yamada, 1982; Radach, 1983; Stramska & Dickey, 1993).

In the integral mixed layer model of van Aken (1984) and Ridderinkhof (1992) vertical mxing in both mixed layers is assumed to be infinitely large where as nomixing occurs in the WTIL. During the calibration of the model it turned out however, that a weak background diffusivity in the WTIL was necessary to match the model results with the observed data on the vertical temperature distribution. A second modification of the physical model is the extension with a resuspension and deposition processes for suspended particles. Basically, suspended particle dynamics is modelled similarly as by Tett & Walne (1995). Resuspension is assumed to be proportional to the friction at the sea-bed, induced by the tidal current and wave orbital velocity, in excess above a threshold friction. The parameters involved were all calibrated by comparing the model results with the available field data.

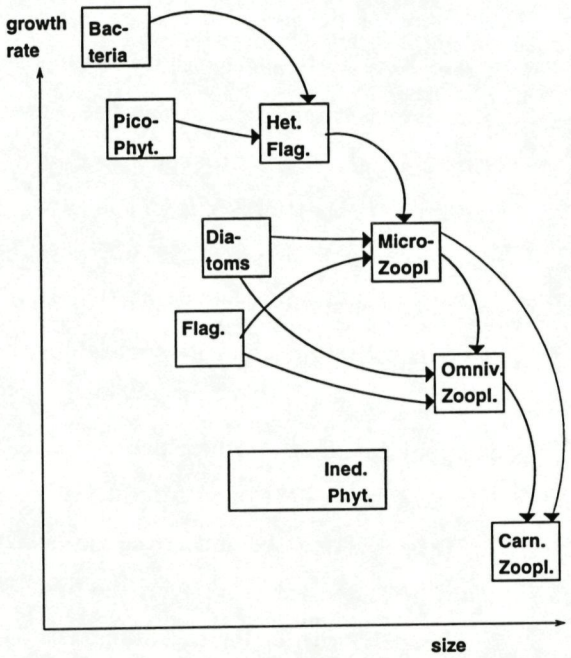


Fig. 3. Schematic outline of the functional groups in the pelagic sub-model in ERSEM. The site of a functional group shows its magnitude and its growth rate (Het.Flag= heterotrophic flagellates, Ined. Phyt. = inedible phytoplankton).

2.2. The ecological Model

The ecological part of the model consists of a number of sub-models of the ERSEM-II model (Baretta *et al.*, 1995). This part consists of an interlinked set of modules describing the biological and chemical processes in the water column and in the benthic system. Each module consists of a coupled set of ordinary differential equations. The structure of ERSEM II is the same as the ERSEM-I model (Blackford & Radford, 1995). The dynamics of the biological functional groups are described by physiological processes (ingestion, respiration, excretion, egestion *etc.*) and population processes (growth, migration and mortality). Biological variables in the model are phytoplankton, variables related to the microbial loop, zooplankton and benthic fauna. (Varela *et al.*, 1995; Ebenhöh *et al.*, 1997; Baretta-bekker & Rasmussen, 1995; Baretta-bekker *et al.*, 1997; Broekhuizen *et al.*, 1995; Ebenhöh *et al.*, 1995; Blackford, 1997) The dynamics of chemical variables like nutrients are fully coupled to the biologically driven carbon dynamics. Early diagenetic transformations and fluxes of organic matter and nutrients in the sediment are included in the model (Ruardij & van Raaphorst, 1995).

The total phytoplankton pool is subdivided in four functional groups. which are based on their size and ecological properties (diatoms, flagellates, picophytoplankton and inedible phy-

toplankton) (Fig. 3). Picophytoplankton rapidly grows and is grazed by heterotrophic flagellates. Despite there larger size, diatoms grow, faster than flagellates (Ebenhöh *et al.*, 1997). Inedible phytoplankton is a slow grower due to the fact that the maintainance of its inedibility is an energy consuming process. All phytoplankton groups contain internal nutrient pools and thus have dynamically varying C:N:P:(Si) ratios. The nutrient uptake by phytoplankton is controlled by the difference between the external nutrient concentration and the internal nutrient pools. The growth rate is dependent on the internal quota (Droop, 1973). The consumers consist of five groups also based on their ecological function and size (see Fig. 3).

An important interaction between physics and biology is the light climate in the water column, where stratification may cause a higher average light availability for the phytoplankton in the SML (Tett *et al.*, 1993). On the other hand a high phytoplankton biomass in the SML will cause a lower the light availability in the BML.

The relation between light and production is described in the ERSEM model with the equation of Steele (1962) to allow for the effect of light inhibition at high irradiance close to the water surface. Here, Steele's equation is replaced by the one of Smith (1936) which seems more appropriate for several reasons. The equation of Smith (See Box 1) assumes light saturation instead of photo-inhibition above a certain irradiance I_0. According to Kirk (1983) photo-inhibition is not as frequent a phenomenon as was originally supposed, and it is likely to be of small or no significance during periods of even small wind speed,

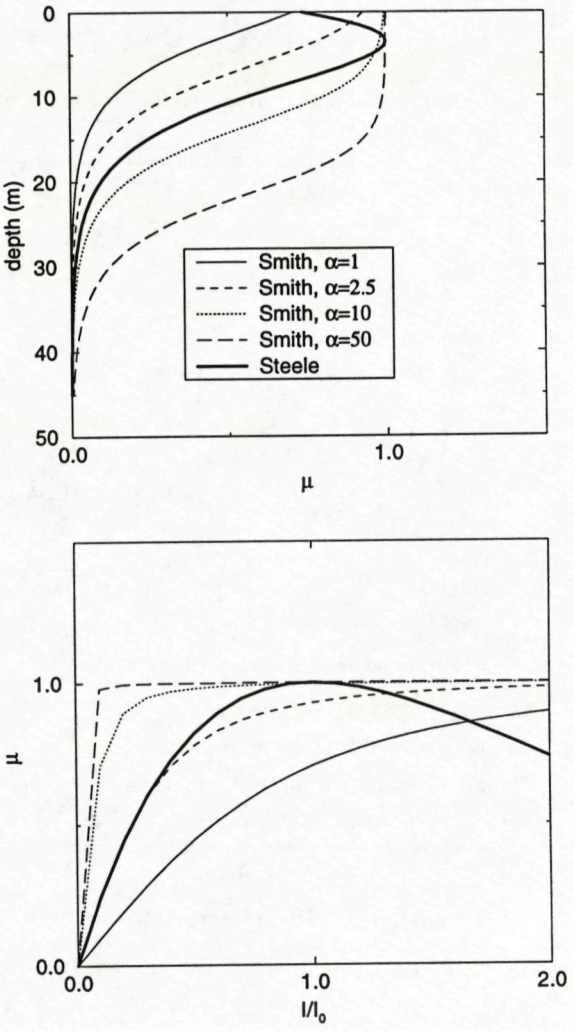


Fig. 4. P/I curve (lower panel) and distribution of primary production as a function of depth (upper panel) as calculated with the equation of Steele (thick line) and the equation of Smith for different α's .

which creates sufficient turbulence to move algae cells away from the sea surface. Jassby & Platt (1976) showed that this equation fits the observed production- irradiation curves better. Following the argument by Kirk (1983) it is assumed in the model that phytoplankton can profit optimally from high irradiance close to the water surface when their residence time at this shallow depth is much smaller than the length of a day. Thus the term I/I_0 in the Smith equation

t

BOX 1 *Equations of irradiance as used in the model*

P/I relation

Steele: $P(I) = \mu \frac{I}{I_o} e^{1-\frac{I}{I_o}}$

Smith: $P(z) = \frac{\mu\alpha\frac{I}{I_o}}{\sqrt{\mu^2 + (\alpha\frac{I}{I_o})^2}}$

Production integrated over z meter

Steele: $P(I,z) = \frac{\mu}{kz}\left(e^{1-\frac{I}{I_o}e^{-kz}} - e^{1-\frac{I}{I_o}}\right)$

Smith: $P(I,z) = \frac{\mu}{kz}\left({}^{e}\log(1+\sqrt{(\frac{\mu I_o}{\alpha I})^2+1}) - {}^{e}\log(e^{-kz}+\sqrt{(\frac{\mu I_o}{\alpha I})^2+e^{-2kz}})\right)$

where:

$P(I)$: actual specific primary production (d^{-1}).

μ: specific growth rate of phtyoplankton. (d^{-1})

I: actual irradiation (Watt m^{-2}).

I_o: irradiation to which phytoplankton is adapted (Watt m^{-2}).

α: correction factor for turbulent mixing.(-)

z: depth of box colomn (m)

k: vertical extincntion (m^{-1}).

is multiplied with a correction factor α that is related to the level of turbulence in the water column (Box 1). The effect is reached at lower irradiance when any turbulent mixing is present (Fig. 4). In the model the α is set to 1 for layers which are part of the WTIL. For the mixed layers α depends on the total net kinetic energy due to wind and the tidal friction near the bottom. The I_{opt}'s by the phytoplankton depend on the average light circumstances of a layer and so decrease with depth. This is in accordance with observations by Ryther & Menzel (1959)

The benthic system is important with respect to the regeneration of nutrients originating from material deposited on the sea floor. The essential process in this sub-model is the mineralization of organic material, coupled to diagenetic processes of nutrients (Ruardij & van Raaphorst, 1995).

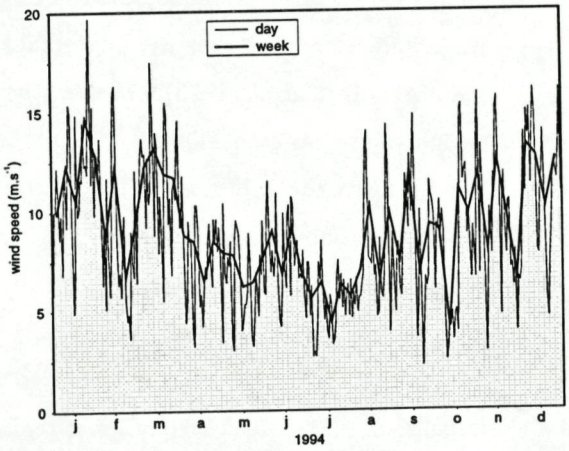


Fig. 5. Wind forcing in the model as measured near the mooring site in 1994. The grey area indicates the surface below the daily averaged wind forcing. The thick line indicates the weekly averaged wind forcing.

3. DATA

All data used in this model study are collected at the mooring site in the Oystergrounds

(54°25′ N, 04°02′) and a large part of the data are sampled by moored instruments at a rate of at least once per hour (van Haren & Mills, 1996). Most of the physical data, are used to force the model with the exception of the temperature data which are used to calibrate the model. All other types of data (of chemical and biological parameters) are used to calibrate the model.

3.1. Forcing data

The forcing data exist of time series of either daily or weekly averages. Normally daily averages are used as forcing data. The model is not forced with hourly data, because the processes defined in the biological model are formulated on a daily averaged basis. All meteorological data were collected on sites near the mooring-site in 1994. The solar radiation was obtained from measurements at the mooring-site. Wind velocity (Fig. 5) was measured on an oil platform in the central North Sea, 150 km Northeast of the mooring site. Other variables necessary to calculate the turbulent heat flux at the sea surface (air temperature, humidity) were measured at the site. To be able to calculate the (vertical) behaviour of the bottom mixed layer we estimated based on local measurements daily averaged values for the vertically averaged velocity of advective water transport corrected for the tides.

3.2. Calibration data

The calibration data can be divided in two groups:

- Daily data.
  Water temperature, chlorophyll-a and vertical extinction are available on a daily basis. Temperature is measured every 2 meter. Chlorophyll and the vertical extinction are derived from fluorescence and transmission measurements and both are measured at 13 meter and 38 meter depth.

- Biweekly data.
  All nutrients were measured every two weeks. Part of the data were measured directly on board by the NIOZ (Malschaert, van Ooyen & van Raaphorst, unpublished data) and another part was measured during the routine monitoring programme of the Dutch ministry of public works (RWS/DNZ, The Hague). The different sources of the nutrient data are identified by different symbols in all figures.

4. Calibration

The availability of a large set of data, measured at the mooring site allows for a proper calibration of the model.

With the temperature data the physical part of the model is evaluated. With the other data (chlorophyll-a, nutrients) at least the most important part of the ecological model can be tested.

As already explained in the introduction the forcing is at least on a daily basis and hence all data applied in the model are transferred to averaged daily values. The reasoning for this is that all ecological processes in the ERSEM model were already defined as daily averaged processes.

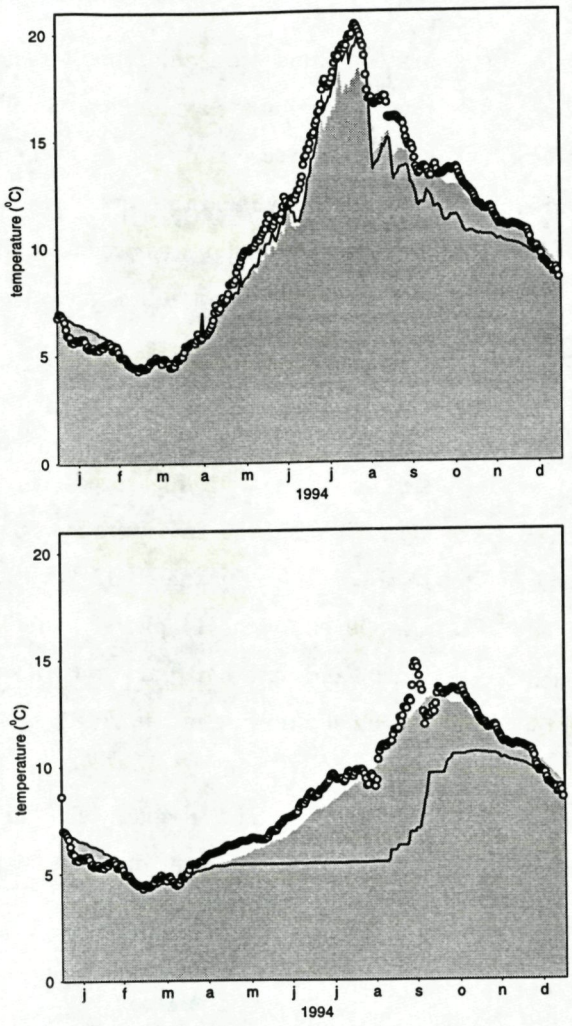


Fig. 6. Seasonal dynamics of temperature at 1 m and 43 meter for a simulation without a constant eddy background diffusion (solid line), a simulation with an eddy background diffusion (=$4.5 \cdot 10^{-5}$ $m^2 s^{-1}$) (grey area) and observations (o's).

Also, Ridderinkhof (1992) showed that the effect of short changes in wind speed (within a day) do not lead to large changes in the stratification when compared to those after the daily averaged forcing. Hence, possible effects of interactions between physical and ecological processes which appear within a day will only be partly covered by the model.

4.1. Initial values

The determination of the initial values is fairly easy. In winter, the entire water column is well mixed and hence all data are equal to each other in all boxes. If present, initial values were taken from the available field data. See the figures in which field data are compared with model results (Figs 8, 9, 10, 11, 12 and 13). Other initial values, especially of the biological components, were set to the end values of a simulation run of the year 1994.

4.2. The physical model

With the data set available we tested whether (heat) transport is governed by entrainment and detrainment , (vertical) mixing or (horizontal) advection. In Fig. 6 the evolution of the temperature is given for 1 and 43 meter depth. It is shown clearly that the model works pretty well for the surface but poor for the bottom layer if transport takes only place through entrainment and detrainment (=no eddy diffusion). By incorporating turbulent diffusion into the model, after estimating a constant diffusion coefficient from the field data, we are able to model reasonably the seasonal temperature at 43 meter. The results show that the model can estimate the seasonal dynamics quite well but does not show the short-term disturbances apparent in the data, especially in the middle layers.

For the calibration of the resuspension process all vertical extinction values of autumn and winter were available. In these periods phytoplankton does not control the the vertical extinc-

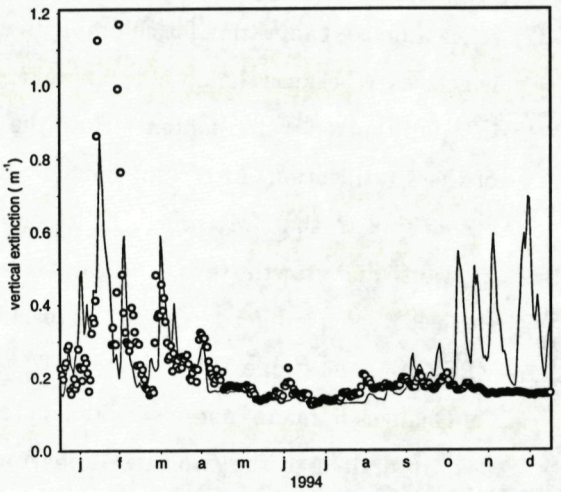


Fig. 7. Seasonal variation of the vertical light extinction in the first 13 meters: model (solid lines) and data (dots). The data are based on light transmission measurements.

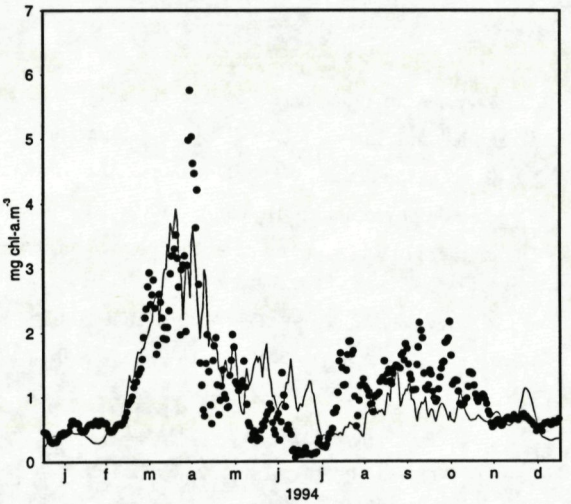


Fig. 8. Seasonal dynamics of chlorophyll-a at 13 meter for the "standard" simulation (solid line), and observations (dots)

tion but the suspended matter. However, only data obtained in the first three months are used, because field observations for this parameters show contradictive results between the first three months and the last three months (Fig. 7).

4.3. The ecological model

To facilitate calibration of the ecological model against the field data we selected two criteria which are ranked in order of importance.

1. The model has to predict the observed chlorophyll-a dynamics in the surface layer (at 13 m) and in the bottom mixed layer (at 38 m) as good as possible (cf. Figs 8 and 9). Prediction of the constant biomass level during the winter months is important for the proper condition at the start of the spring bloom.

2. The model has to reproduce the observed low nutrient concentrations in the surface layer in the summer and possibly also the low values found in the bottom layer. (cf. Figs 10 - 13).

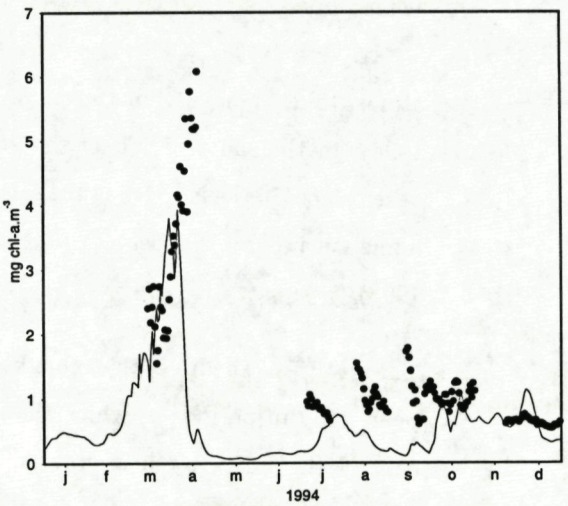


Fig. 9. Seasonal dynamics of chlorophyll-a at 38 meter for the "standard" simulation (solid line), and observations (dots)

However from the data we do have nearly no knowledge about the composition of the phytoplankton. The only certain facts are:

- just before the start of the thermal stratification an important sedimentation of di-

Table 1.

Overview of differences between the original E(RSEM) model and this S(TRAECOS) model parameters. (P= picophytoplankton, F= Flagellates, D= diatoms, I= inedible phytoplankton). The proportional rate is defined as the growth rate relative to the one of flagellates.

		P	F	D	I
proportional	E	2.00	1.00	1.25	0.50
growth rate(-)	S	1.18	1.00	0.73	0.63
C:Chlorophyll-a	E	50	25	25	25
(mg C.(mg Chl)$^{-1}$	S	25	25	25	25
sinking rate	E	-	-	45	5
under stress (m)	S	-	-	22.50	45
sinking rate	E	-	-	-	-
in WTIL (m)	S	-	-	15	-

atoms takes place (van Haren & Mills, 1996). In the same period of the years in other places in the North Sea the same phenomenon has been observed. (Jago *et al.*, 1993).

- The group of inedible phytoplankton appears only in periods in which the grazers control the net growth of phytoplankton (Ebenhöh *et al.*, 1997).

These facts resulted in a more restrictive sinking behaviour for diatoms: as soon as a diatom cell appears in a box with low turbulence (a box of the WTIL) the diatom starts sinking to the bottom mixed layer. A number of parameters were adjusted after recalibration (Table 1). The main changes with respect to the original ERSEM-model appeared for the C/Chla-ratio and the increased light sensitivity. Both changes have been made in order to maximize the uptake of silicate per unit of chlorophyll-a in order to reach a better calibration for chlorophyll-a. This is necessary because the uptake only takes place in a fully mixed water column before the onset of the stratification. After that moment the diatoms sink to the BML where light conditions are worse and growth stops. The growth rates of the other groups differ less from the ones in the ERSEM-model (table 1).

Changes in micro- and mesozooplankton values are limited to the two most important parameters. One describes the maximal uptake. The other one describes the concentration below which the food uptake is food dependent according to a Monod relation (Baretta-bekker *et al.*, 1997). Nothing has been changed in the food web itself. The only aim for this part of the model was to get a seasonal cycle in which initial and end values are of the same order of magnitude.

5. Results

5.1. The physical model

The stratification starts in March, after a small period in February, when the irradiation and the air temperature increase. Between the beginning of March and mid April stratified periods are alternated with well mixed periods. From mid-April onwards a stable WTIL develops with a less variable behaviour. The observed stratification starts about three weeks later, but the moment of the start of the stable stratification fits very well.

At times, the thickness of the WTIL varies in a few days from 30 to 20 m and vice versa (observed and modelled). In July and August

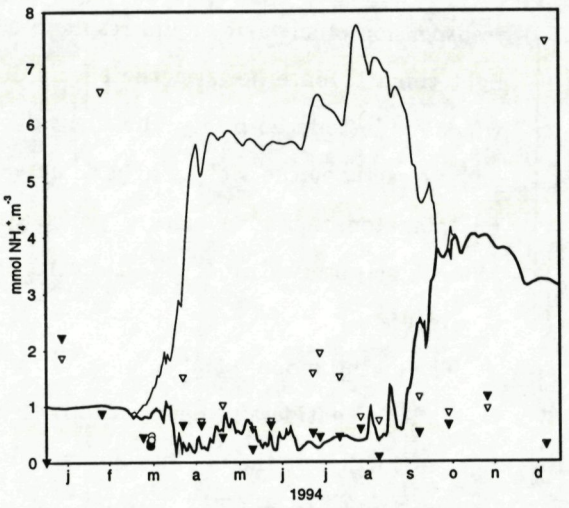


Fig. 10. Comparison between the seasonal variation of ammonium concentration as simulated with the standard model (lines) and observations (points). The solid line and the filled symbol are for 10 meter depth, the dotted line and the open symbols for 40 meter depth. (The △'s are data points measured by RWS, the o by the NIOZ).

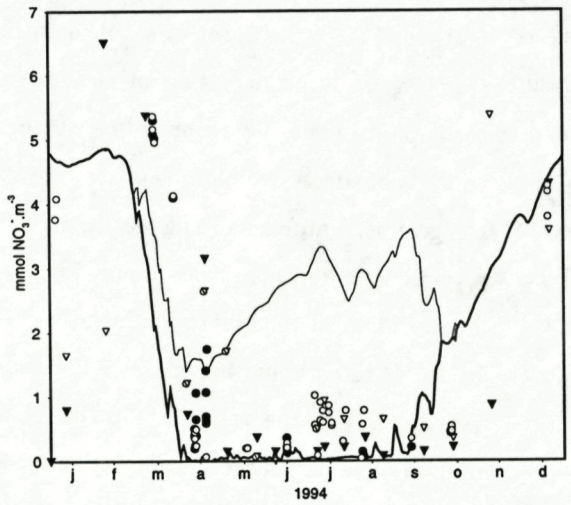


Fig. 11. As Fig. 10 but for the nitrate concentration.

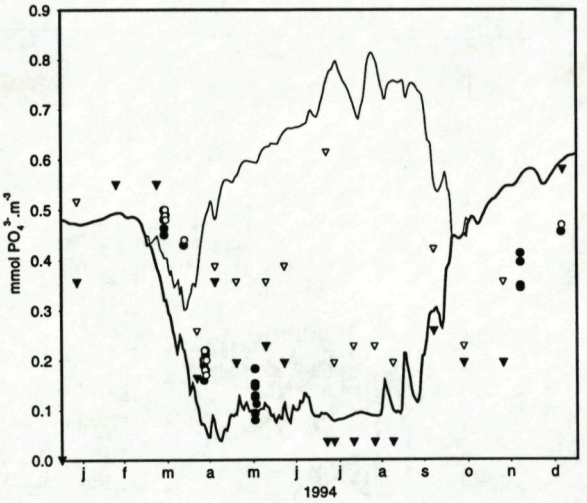


Fig. 12. As Fig. 10 but for the phosphate concentration.

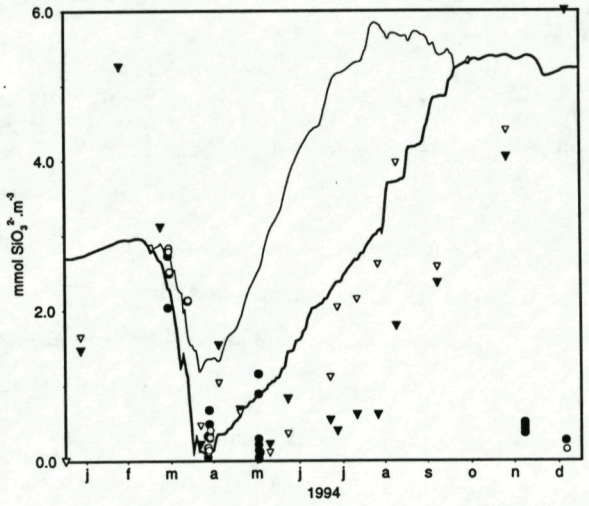


Fig. 13. As Fig. 10 but for the silicate concentration.

the wind speed is considerable lower than in the other months of 1994. In these two months the WTIL is thickest. After the end of the summer a small period with high winds speeds causes the WTIL to disappear for a short period of time but it reappears again during small periods. In the autumn, after two periods with strong winds, the stratification is finally terminated in the model. The field observations show however that until the end of the year the water column is stratified during short periods. It may be concluded that the model shows roughly the same seasonal variation as the field observations. The most clear deviation occurs in July when the observed thickness of the WTIL is much larger than modelled.

The vertical extinction is mainly determined by the resuspension of suspended matter driven

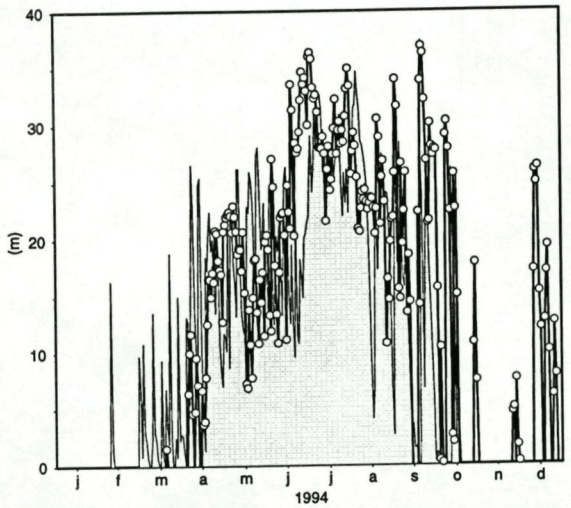


Fig. 14. The thickness of the non turbulent inter layer (WTIL) as modelled (the grey area) and calculated from the data (o's).

by the wind except during the phytoplankton bloom in spring and periods of low wind speeds especially in summer (Fig. 7) The parameterization seems fairly realistic, together with the way in which the resuspension processes are modelled. In autumn the model overestimates the vertical extinction. Apparently, the particulate matter near the sediment surface can not be resuspended after a summer of consolidation of the sediment or it is already exported after resuspension during the last storms in early spring.

5.2. The ecological model

The timing of the spring bloom depends on the physical conditions in the entire water column and on the phytoplankton concentration in the winter period. The field observations of chlorophyll-a show a very stable behaviour in winter despite the high vertical extinction values (van Haren & Mills, 1996). These high vertical extinction values (Fig. 7) are caused by the resuspension of silt and should result in a poor light climate. Since however the effects of high winds are introduced on the turbulent diffusion and indirectly on the average light climate of the phytplankton, the model can reproduce a stable biomass as observed in the field during such a period(Fig. 8).

The spring bloom of phytoplankton is initiated after a considerable decrease of the vertical light extinction at the end of February directly after the last storm (Figs 7 and 15). All phytoplankton groups react to this change according to their functional behaviour which results in a succession of phytoplankton types during the bloom period according to their ecological behaviour in interaction with the physical environment. The bloom and this succession are hated in mid-April after the onset of stable stratification (Fig. 14) and the depletion of the nutrients in the euphotic zone. This month-long spring bloom consists of successive blooms of two phytoplankton groups, diatoms and flagellates, preceeded by a small picophytoplankton bloom (Fig. 17). This small bloom of picophytoplankton is controlled by the heterotrophic flagellates which can react very quickly to the variations in the availability of food. The first large diatom bloom is stopped by the depletion of silicate and the start of the stratification. The uptake of nutrients by phytoplankton in the surface mixed layer in spring and the associated decrease of nutrients seem fairly well modelled, although the response in the model is about one month too early for nitrate and silicate when compared with observations. This difference in timing is the effect of the earlier start of the stratification in the model: the

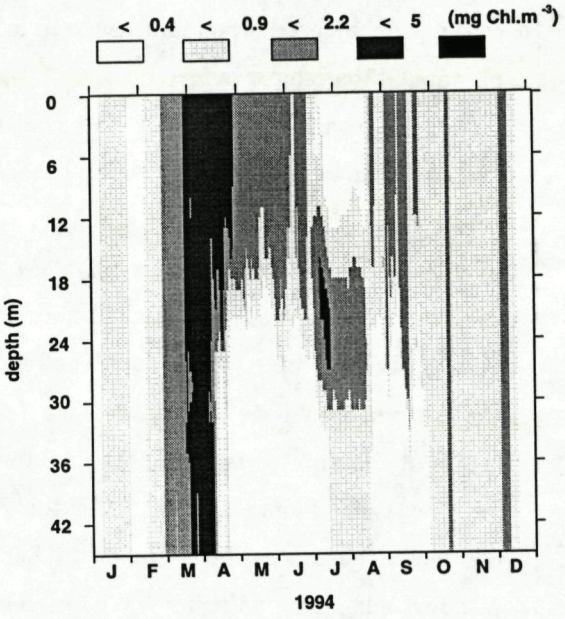


Fig. 15. Seasonal dynamics of the vertical distribution of chlorophyll-a in the water column.

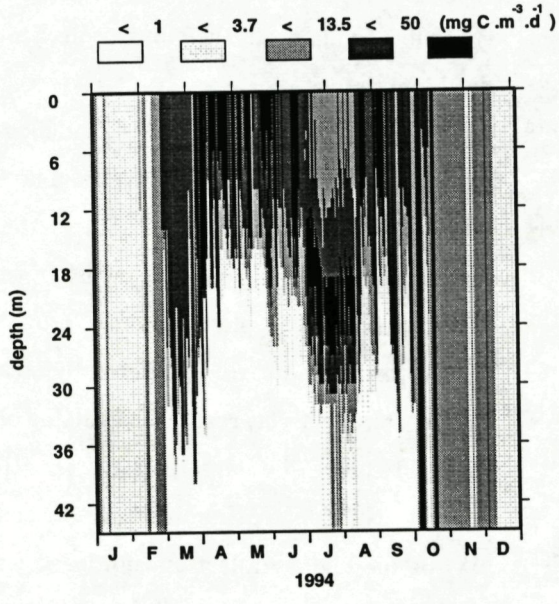


Fig. 16. Seasonal dynamics of the vertical distribution of primary production.

input of nutrients from the bottom mixed layer is too soon decreased.

The successive blooms of diatoms and flagellates respectively are succeeded in the model by a summer biomass minimum when mainly flagellates and picophytoplankton are active. The bloom of inedible phytoplankton appears after mid-august when stratification is disturbed shortly and grazers succeed in controlling the edible phytoplankton.

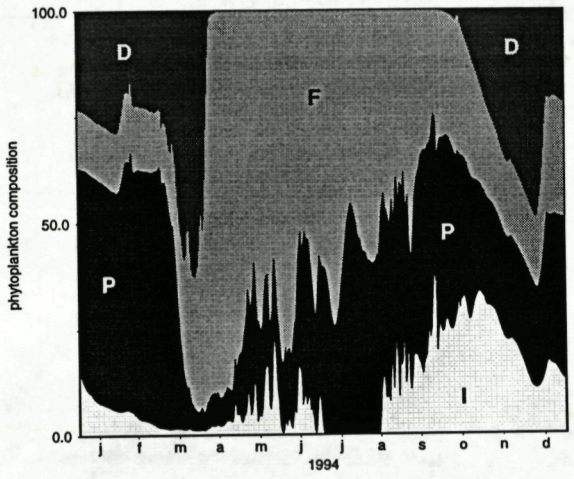


Fig. 17. Seasonal dynamics of the composition of phytoplankton succession at 13 meter for the "standard" simulation. (D= diatoms, F= flagellates, P= picophytoplankton and I= inedible phytoplankton)

The modelled chlorophyll-a content in the the bottom mixed layer (Fig. 9) shows the same peak in mid April as in the field observations. This peak is caused by the sinking of diatoms from the upper layer due to low turbulence levels in the water column at the onset of the stratification. The model value of peak is lower than the observations, probably because the model gives a too early stratification of the water column. The separation of a part of the column leads, firstly, to an unfavourable light climate in the bottom layer and to a reduction of the primary production in this layer and, secondly, to a barrier of the transport of nutrients to the surface mixed layer. The relatively high light extinction in this period (Fig. 7) leads to zero production in the bottom layer (Fig. 16).

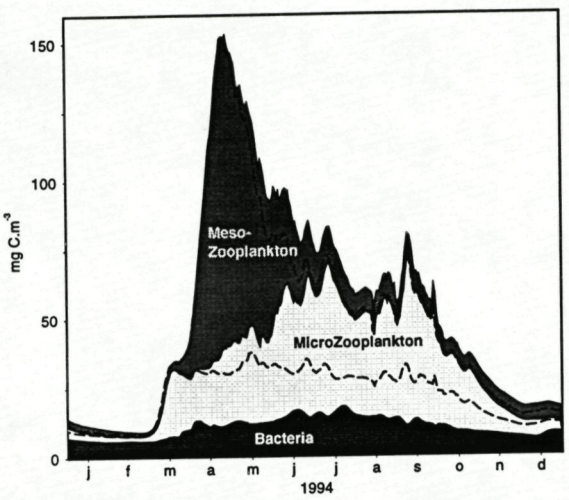


Fig. 18. Cumulative representation of seasonal dynamics of consumers for the "standard" simulation. The dotted lines refer to the subdivision of microzooplankton and mesozooplankton in respectively heterotrophic flagellates and other microzooplankton and omnivorous and carnivorous zooplankton.

During the summer period there is a stable stratification and hence a low input of nutrients from the bottom mixed layer. This leads to a typical summer depression in the phytoplankton (Figs. 15 and 16) and nutrient concentrations in the upper mixed layer. At the end of the summer the stratification is disturbed by high winds speeds which result in an autumn bloom of the phytoplankton. The modelled chlorophyll-a concentration, in the period June-August shows a markable difference with the observed values, which show a period with very low chlorophyll-a concentration and which is succeeded, after a sudden increase by a period with higher values. The model shows nearly a reverse tendency. This difference can be partly explained by the differences in thickness of the WTIL between model and observations (Fig. 14). A larger WTIL thickness leads to a lower diffusive transport of nutrient upwards and this leads to a strong limitation of the primary production and hence to a lower phytoplankton biomass.

The seasonal dynamics of the consumers (Fig. 18) shows a behaviour which can be expected with the modelled succession of phytoplankton. The heterotrophic flagellates, part of the microzooplankton, respond directly to the growth of the picophytoplankton. The bloom of the diatoms and flagellates leads to a fast increase of the omnivorous mesozooplankton. After the spring bloom microzooplankton is the dominant consumer which grazes on bacteria, picophytoplankton, flagellates and on the heterotrophic flagellates. The omnivorous zooplankton is succeeded by carnivorous zooplankton, mainly because the autotrophic part of the food is too low to maintain the omnivorous zooplankton biomass .

The relatively high values of modelled phosphate and silicate in the bottom mixed layer during the summer, as compared with the field observations may have several reasons. In the first place, the modelled phytoplankton growth near the bottom is too early hampered by stratification, which effectively results in a cutting off from the light source. Perhaps the light sensitivity is too low. Nutrient regeneration in the sediment may be too high and, last but not least, horizontal advective transport which is not represented in this model, may lead to a net export of nutrients.

6. Sensitivity analysis

To evaluate the effects of the physical stratification a sensitivity analysis has been performed

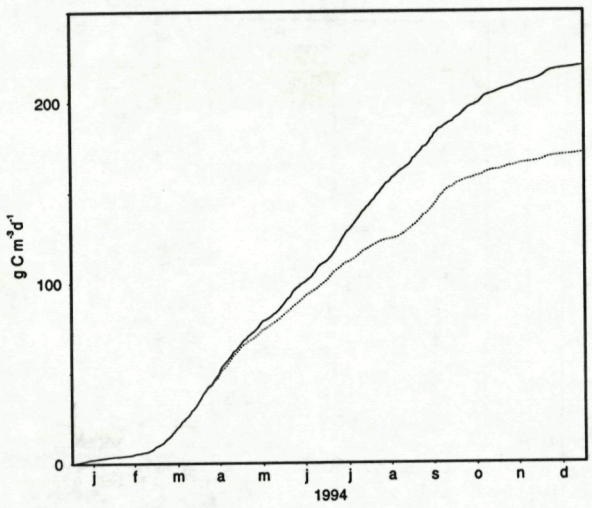


Fig. 19. Primary production integrated over time of the "standard" simulation (solid line) and a run without eddy background diffusion (dotted line).

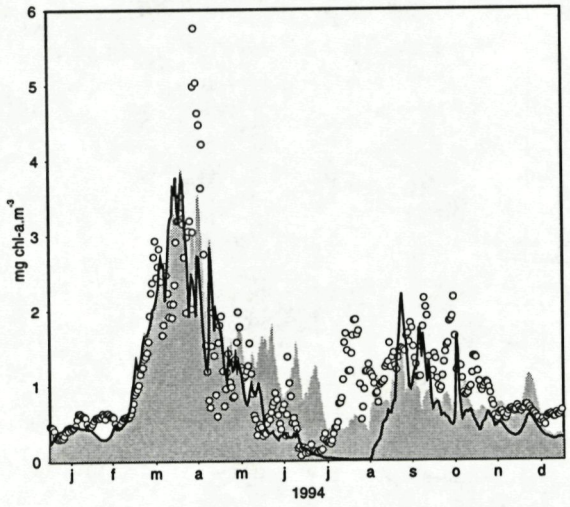


Fig. 20. Seasonal dynamics of chlorophyll-a at 13 meter for the standard run (grey area), a run without background eddy diffusion (solid line), and observations (dots).

for which the control of the physical environment on the biota, the productivity of the ecosystem, the succession of the phytoplankton and the competition between the consumers is monitored. The control on the biota mainly takes place by limiting the vertical transport of nutrients and changes in the light climate (self shading). The stratification itself is determined by physical processes which have a high variability in space and time since these processes are forced by climatological factors like irradiation and wind. The mutual effect of these processes can be summarized as follows:

- the magnitude of the background eddy diffusion in the WTIL.
- the time of onset and the duration of the stratification
- short time disturbances in the stratification
- alternation in time of periods stratification and mixing.

In the following sections the net results of these effects on the functioning of the ecosystem will be shown This will be done by comparing the standard runs with another model run in which one or two changes are made in the code or in the parameters which directly or indirectly describe one of the mechanisms or processes.

6.1. The impact of the background eddy diffusion

In Section 4. it has been shown that the background eddy diffusion is very important in reproducing observed temperature variations in the time. Due to the stratification the transport from the lower layers is limited and hence the nutrient depletion leads to very low chlorophyll-a concentrations in the surface layers. In Fig. 19 the cumulative primary production is given for the standard run and for a run without background diffusion. The diffusion is responsible for an increase of about 25% of the total primary produc-

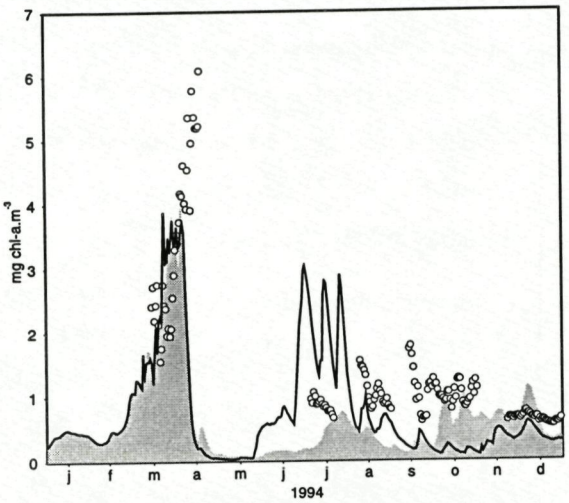


Fig. 21. Seasonal dynamics of chlorophyll-a at 38 meter for the "standard" simulation (grey area), a run without eddy background diffusion (solid line), and observations (dots).

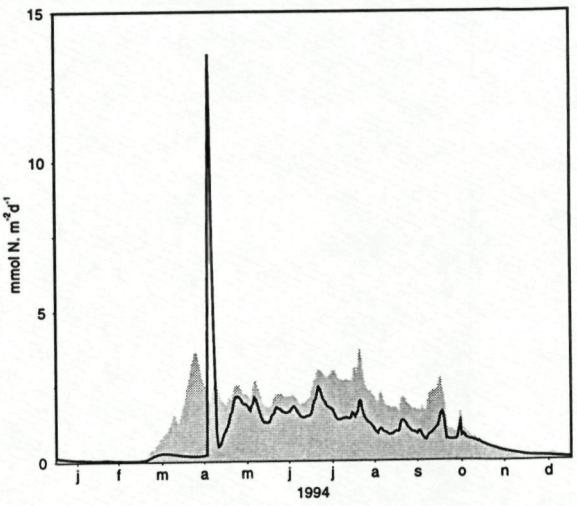


Fig. 23. The comparison between seasonal dynamics of the sedimentation of particulate N (detritus + diatoms) between the "standard" simulation (grey area), a run with a delayed start of the stratification (solid line).

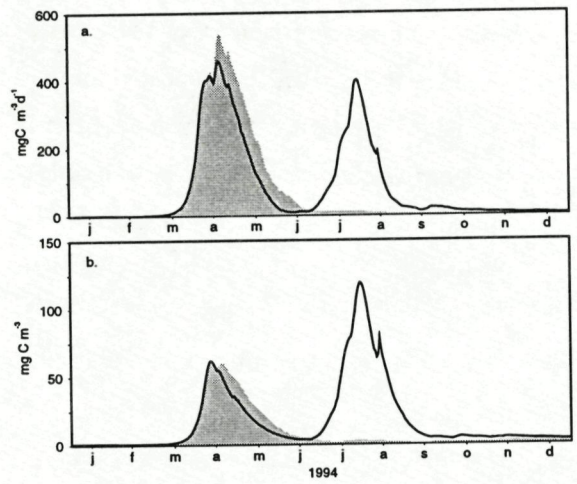


Fig. 22. Seasonal dynamics of (a) mesozooplankton biomass at 38 meter and (b) net column production of zooplankton for the "standard" simulation (grey area), a run without eddy background diffusion (solid line).

tion in the water column. It has a large impact on the phytoplankton biomass in and above the WTIL. In the summer months there are obvious differences between the standard run and the run without diffusion. It also makes clear that the observed low chlorophyll-a concentrations may be caused by intermittently lower vertical diffusion than the background value. A low concentration in the upper layers can have a dramatic effect on the bottom mixed layer especially in a water column of 45 meters where the compensation depth of the primary production (the depth at which gain and loss processes of phytoplankton are in equilibrium) can reach the bottom when phytoplankton near the bottom is not limited by light, it may start production and increase its biomass quickly. (Fig. 21). This has consequences for the consumers in the run without diffusion. Mesozooplankton (Fig. 22) has a second peak during summer and these results in about twice as large productivity in the entire water column.

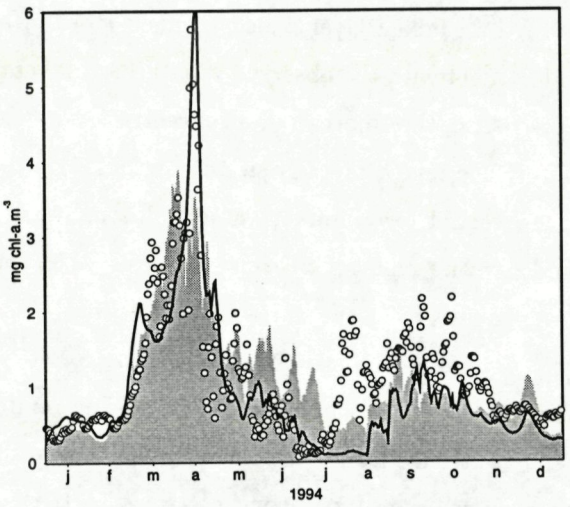


Fig. 24. The comparison between seasonal dynamics of chlorophyll-a at 13 meter between the "standard" simulation (grey area), a run with a delayed start of the stratification (solid line) and observations (dots).

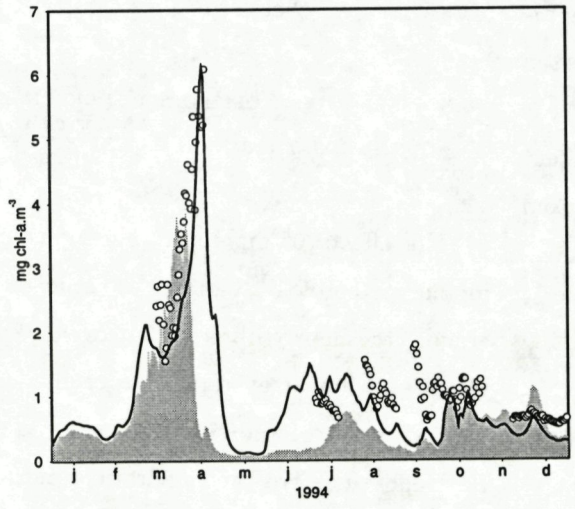


Fig. 25. As Fig. 24 but for chlorophyll at 38 m.

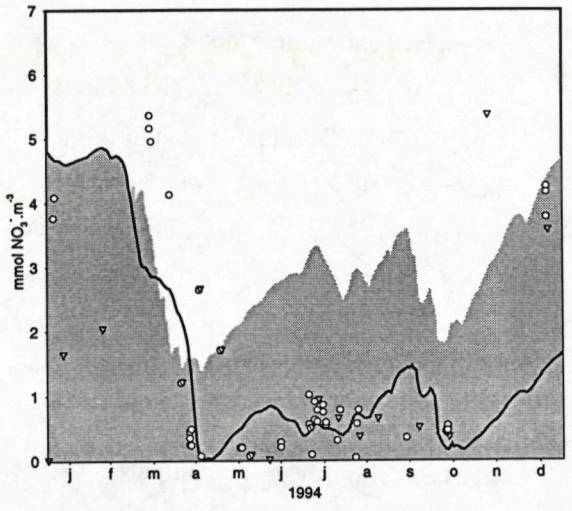


Fig. 26. The comparison between seasonal dynamics of nitrate at 40 meter between the standard run (grey area), a run with a forced delayed start of the stratification (solid line) and observations (o's and △'s). See further in caption of Fig. 10 .

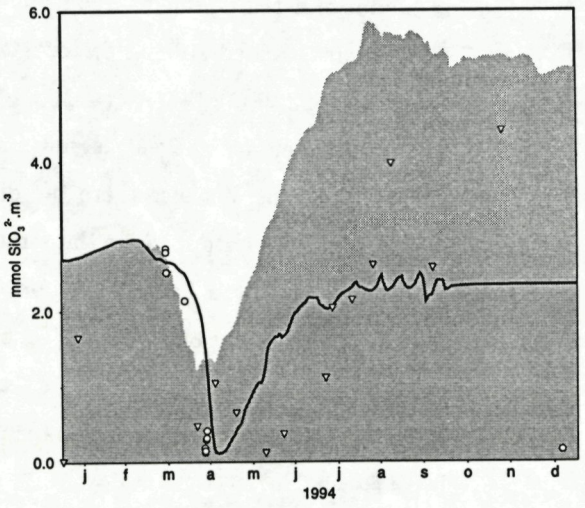


Fig. 27. As Fig. 26 but for silicate at 40 m.

6.2. The impact of the start of the stratification in spring on the phytoplankton bloom and the consequences for the rest of the growing season

In the Section 5.1. it has been noted that the start of the stratification in the model is about three weeks earlier than observed in the field. In this three weeks the stratification is not very stable with time, but during the whole period there is stratification present (Fig. 14). Thus the exchange between bottom and surface mixed layer will be decreased by this stratification. In this sensitivity analysis the consequences of the too early stratification in the model will be tested by conditioning the model such that

the stratification does not start before a certain day (day 115 = 15 April). This large intervention in the model made a recalibration of the diatom growth necessary. By reducing the C/Chla-proportion of diatoms to its original higher value in the ERSEM model (see Table 1) we could avoid that the chlorophyll-a concentration shows a decrease instead of an increase in early spring. After this adaptation, the model shows a remarkable improvement compared to the standard run in both the biotics (chlorophyll-a) and the abiotics (nutrients). These improvements are mainly caused by the better average light climate in a total well-mixed water column, the subsequent higher primary production during the spring bloom and the coupled large sedimentation of nutrient stressed sinking diatoms to the sediment (Figs. 23-25).

Such a sedimentation event is not present in the standard runs, because there the diatom bloom is much earlier stopped by the stratification and succeeded by a flagellate bloom. This bloom does not settle out but is locally consumed or is ended by nutrient depletion. This leads to a production of detritus which in its turn sedimentates slowly.

The sinking of diatoms in this sensitivity run results also in a coupled sedimentation of particulate nutrients which subsequently lead to a removal of the nutrients from the pelagic system for a longer time. The higher primary production in spring leads firstly to a better agreement between modelled and observed chlorophyll-a concentrations at 38 meter (Fig. 25). The large removal of nutrient results in a decrease to low values of the pelagic nutrients concentrations in the bottom mixed layer which is much more in agreement with the observed values (Figs. 26 and 27). Also, the chlorophyll-a concentration in the surface mixed layer (Fig. 24) reaches now the observed low summer values, although still on a wrong moment in time. These low chlorophyll-a values in the surface layer do not lead to a summer bloom in the bottom mixed layer like in the first sensitivity analysis. The removal of nutrients from the pelagic system also results in limiting nutrient concentrations in the bottom mixed layer. It may be concluded that the unrealistic modelling of the stratification structure in the water column during three weeks in spring have lead to consequences for the model results of the biota for the rest of the year.

6.3. The effect of short disturbances of the stratification on the ecosystem

The effects of differently averaging periods for the meteorological forcing are studied by averaging the hourly observations over weekly intervales. A linear averaging procedure was applied. For the windforcing the energy is considered and therefore the quadratic values of the observations are used to calculate the mean. In this way extreme daily values are suppressed and short disturbances are smoothed out. Ridderinkhof (1992) shows that the depth of the surface mixed layer is much less when the forcing of the model is ibased on weekly averaged parameters. Entrainment of the WTIL into the surface mixed layer occurs less frequently and moreover less intensely when the strong wind events are filtered out. This reducing the cross-

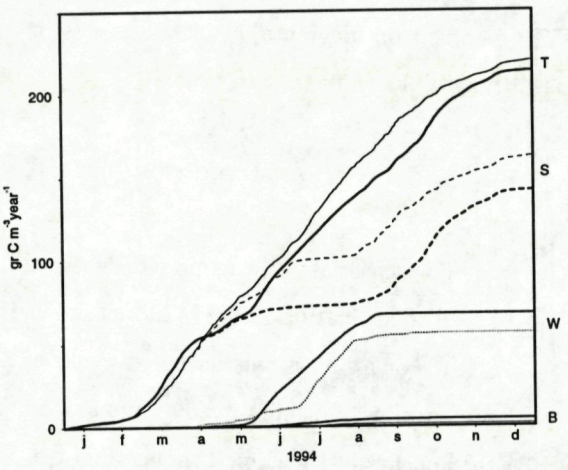


Fig. 28. Cumulative primary production for the Total water column (solid lines), the Surface mixed layer (broken lines), the Weak turbulent intermediate layer (dotted line) and the Bottom-mixed layer (solid line) between the standard run (thine lines) and a run with weekly forcing (thick line).

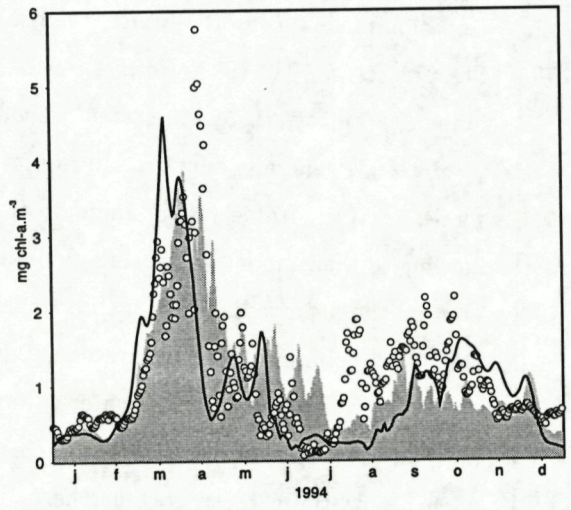


Fig. 29. Seasonal dynamics of chlorophyll-a at 13 meter for the "standard" simulation (grey area) with daily forcing, run with weekly forcing (solid line), and observations (dots).

thermocline exchange results in a larger temperature difference between the surface and bottom mixed layers for weekly averaged forcing. Ridderinkhof (1992) proved this, however, with the original model without background eddy diffusion. Fig. 28 shows the cumulative primary productions for daily (standard run) and weekly averaged forcing for the different main layers. It can be concluded that the forcing with weekly iaveraged data has no significant influence on the total primary production of the water column. The effects which are shown are the same as in the first sensitivity analysis but to a lesser extent. Again there is a shift of the primary production to the lower layers. Also the same effect on the chlorophyll-a concentration as shown in the first sensivity analysis can also be observed. The shift in time of the primary production is explained by the better light climate in the lower layers. It can be concluded that when averaged monthly instedad of weekly values averaged are used the exchange is suppressed and leads to unexpected events in the lower layers.

6.4. The effect of the variability and dynamics of the wind forcing on the system

The wind is an important forcing for the disturbance of the stratification. Also the onset of the stratification requies a period of relatively low winds. Therefore, we compared the standard run (1994) with a run in which the wind forcing is like measured in the year 1986. Especially the spring period of that year included a period with quiet weather (Fig. 30). The results show that the response of chlorophyll-a to the other wind forcing is large (Fig. 31). Due to the quiet weather in early spring, the diatoms are not able to reach high values during the spring bloom. They are replaced by the flagellates which accordingly reach much higher values than in 1994.

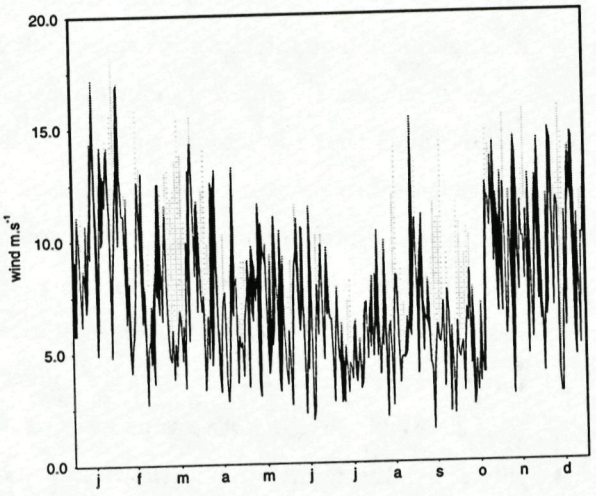


Fig. 30. Seasonal wind of the "standard" simulation (all forcing from 1994) and a run with wind forcing of 1986. In the graph the difference is given between the two wind forcings. A positive difference of the winds between 1994 and 1986 is given as a grey surface. A negative difference is given as a black area.

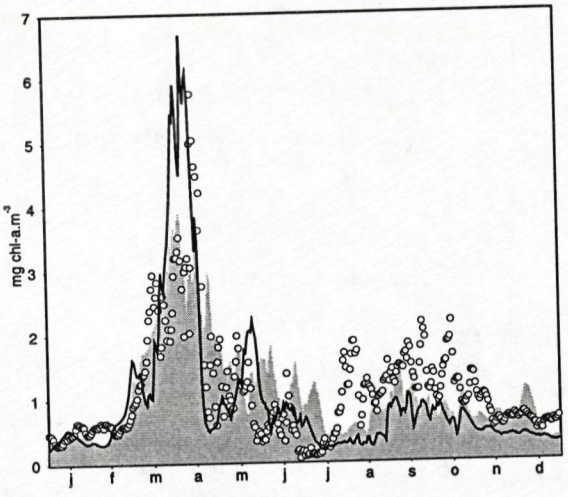


Fig. 31. Seasonal dynamics of chlorophyll-a at 13 meter for the "standard" simulation (grey area) (all forcing from 1994) and a run with wind forcing of 1986 (solid line), and observations (dots).

The timing of the succeeding smaller blooms in the summer period is also different. It can be concluded that the timing of the onset and the maximal concentration of the spring bloom is dependent on incidental events such as storms and may differ from year to year.

7. Discussion

The seasonal cycle as modelled with the combined stratification-ERSEM model shows the existence of a "classical" seasonal cycle of phytoplankton with a short-lived spring diatom bloom that occurs at the same time as the beginning of thermal layering, a summer period of low phytoplankton biomass in the surface layer together with a maximum in the WTIL, and an autumn increase due to the remixing of the entire water column. The chlorophyll-a observations at the mooring site (van Haren & Mills, 1996) and observation made during the NERC English North Sea project in 1988-1989 (Howarth *et al.*, 1993; Joint & Pomroy, 1993; Mills *et al.*, 1983; Tett *et al.*, 1993) generally support the results of the model. Tett & Walne (1995) indicate that, according to their model, the spring bloom is initiated by the net irradiance in the upper layers of the water column. This net irradiance depends on the light extinction of the water column and on the thickness of the surface layer. This model confirms partially these conclusions: a thinner surface mixed layer will show higher concentrations, but would not enhance the total primary production as is shown in the sensitivity analysis. An earlier start of the stratification will also sooner limit the production in the surface layer and will results in a lower production during the spring bloom.

The modelled succession fits well with other observations of the contributions of different size

fractions of the phytoplankton in a water column at mid-latitudes. Durbin *et al.* (1975) showed that in Narragansett Bay (USA) phytoplankton in the size class smaller than 20 μm (= picophytoplankton in our model) is abundant in winter and had an early peak before the spring bloom. The spring bloom mainly consists of large algae (diatoms in this model) and is succeeded in summer by phytoplankton in the smaller size classes (flagellates + picophytoplankton in this model).

The seasonal variations of the microzooplankton fit very well with data of the BODC (Barettabekker & Rasmussen, 1995). The omnivoruous zooplankton showed too soon a larger peak i in comparison with data compiled by Broekhuizen *et al.* (1995). It seems that the parameter change, after the calibration, has not lead to reasonable results for zooplankton. However, if taking in account the seasonal dynamics of the main food sources for zooplankton, flagellates and diatoms (Figs 8 and Fig. 17), it cannot be expected that with this model their maximal biomass could be simulated at such a late moment in time. The only way to model such peak is by assuming a lower growth rate, an active migration of zooplankton to the layers with highest food concentration and a more efficient use of the (scarce) food, especially by microzooplankton during the summer season.

The largest differences between observed and modelled chlorophyll-a values are found during the summer. These could only partially be explained by the differences in the thickness of the WTIL between the model and observations. From other observations it is clear why; it has been shown that sometimes there is a considerable advective transport (van Raaphorst *et al.*, 1996) but also apparently internal mixing induced by inertial stress (van Haren & Mills (1996)). To include these processes in our model we have to replace our physical model by a 3D transport model with turbulence closure included.

We have shown that it is possible to study a water column in a shelf sea with a closed one-dimensional model although at times tidal transport may not be negligble. The remaining problems are the wrong timing of the spring bloom and, secondly, the variable exchange sometimes during the summer period. The first problem is probably caused by the use daily forcing during the period of unstable stratification, where hourly forcing would be better. The second problem is related to the exclusion of a few specific physical processes which cannot be integrated in such a 1D-model. They could induce sometimes disturbances in the vertical stratification and indirectly on the biota.

Finally our model showed that that the winter concentrations of nutrients are the main substrate source for the phytoplankton and that during the rest of the year local regeneration of nutrients is much more important than the advective input from other areas. This is in agreement with results of Radach & Lenhart (1995) who showed that in the ERSEM application for the entire North Sea the advective input of nitrogen in the (large) boxes is only 3% of the annual uptake by primary production.

8. Conclusions

- Diatoms play a crucial role in the ecological system (model). They are probably responsible for the fast decrease of nutrients in spring, which has consequences for the rest of the growing season.
- The role of the microbial loop is predominant during a nutrient limited environment: they recycle a major part of the nutrients in the water column.
- With the physical mixed layer model the stratification processes and the forcing of these processes can be modelled quite well. However, small discrepancies between modelled and observed timing of the onset of the stratification may lead to large discrepancies between observed and modelled biota.
- The introduction of a background eddy diffusion is very relevant for the biological system. In this way nutrients are transported to the upper layers which results in a large total primary production.
- Short disturbances do not have the major impact as suggested by Ridderinkhof (1992). The field observations show that the effects of tides and waves are not implemented well in the original set-up of the mixed layer model and have to be introduced by assuming a background eddy-diffusion.
- Lateral transport of nutrients seems unimportant for the functioning of the ecosystem. Some effects which are induced by physical processes such as inertial shear, horizonatl advective water transports) can only be resolved by a turbulence closure model incoporated in a three -dimensional model .
- Perhaps the most important conclusion is that the physical environment is the determining factor for the seasonal variations of the dynamics of the biota. The wind regime during spring may advance or delay the stratification. In turn this leads to a decrease or increase, respectively, of the primary production in the spring bloom. The presence of silt on the sediment during a windy spring can lead to resuspension of silt, depress the primary production by light limitation and may counteract the positive effects of the wind-delayed onset of the stratification. The magnitude of the primary production during spring has implications for the entire growing season, especially when the spring bloom has resulted in a large sedimentation of phytoplankton. The nutrients in the surface mixed layer as well as in the bottom mixed layer are affected. The consequence may be that from year to year large interannual differences can appear in the magnitude, sesaonal variation and succession of phytoplankton. This effect will be certainly reflected in the secondary production of micro- and mesozooplankton.

Acknowledgements.— This research was partly funded by the European Community under MAST II contract number MAS2-CT92-0031. Additional

funds were supplied by BEON. H. van Haren has been supported by a grant from the Dutch Organization for the advancement of Scientific Research (NWO). Most field data were obtained from cruises financially supported by the Netherlands Marine Research Foundation (grant 39104). We thank Wim van Raaphorst, Job Baretta and Bouwe Kuipers for their critical reading of the manuscript.

References

Baretta, J.W., W. Ebenhöh & P. Ruardij, 1995. The European Regional Seas Ecosystem Model, a complex marine ecocsystem model. –Neth. J. Sea Res. **33:** 233–246.

Baretta-Bekker, J. & J.B..E.K. Rasmussen, 1995. The microbial food web in the European REgional Seas Ecocsystem Model. –Neth. J. Sea Res. **33:** 363–379.

Baretta-Bekker, J.G., J. Baretta, A.S. Hansen & B. Riemann, 1997. An improved model of carbon and nutrient dynamics in the microbial food web in marine enclosures. in preparation.

Blackford, J., 1997. A quatitative analysis of benthic biological dynamics in a North Sea ecosystem model. In preparation.

Blackford, J. & P. Radford, 1995. A structure and methodology for marine ecosystem modelling. –Neth. J. Sea Res. **33:** 247–260.

Broekhuizen, N., M.R. Heath, S.J. Hay & W.S.C. Gurney, 1995. Predicting the Dynamics of the North Sea's Mesozooplankton. –Neth. J. Sea Res. **33:** 381–406.

Droop, M., 1973. Some thoughts on nutrient limitation in algae. –J. phycol. **9:** 264–272.

Durbin, E., G. Krawiec & T. Smayda, 1975. Seasonal studies on the relative importance of different size fractions in Narragansett Bay (U.S.A). –Mar.Biol. **32:** 2710287.

Ebenhöh, W., J.W. Baretta & J.G. Baretta-Bekker, 1997. The primary production module in the marine ecosystem model ERSEM-II. in prepatration.

Ebenhöh, W., C. Kohlmeier & P. Radford, 1995. The benthic biological submodel in the European Regional Seas Ecosystem. –Neth. J. Sea Res. **33:** 423–452.

Howarth, M.J., K.R. Dyer, I.R. Joint, D.J. Hydes, D.A. Purdie, H. Edmonds, J.E. Jones, R.K. Lowry, T.J. Moffat, A.J. Pomroy & R. Proctor, 1993. Seasonal cycles and their spatial variability. –Phil. Trans. R. Soc. **343:** 383–402.

Jago, C.F., A.J. Bale, M.O. Green, M.J. Howarth, S.E. Jones, I.N. McCave, G.E. Millward, A.W. Morris, A.A. Rowden & J.J. Williams, 1993. Resuspension processes and seston dynamics, southern North Sea. –Phil. Trans. R. Soc. **343:** 475–488.

Jassby, A.T. & T. Platt, 1976. Mathematical formulation of the relationship between photosynthesis and light for phytoplankton. –Limnol. Oceanogr. **21:** 540–547.

Joint, I. & A. Pomroy, 1993. Phytoplankton biomass and production in the southern North Sea. –Mar. Ecol. Prog. Ser. **99:** 169–182.

Kirk, J.T.O., 1983. Light and photsysnthesis in aquatic ecosystems. Cambridge University Press, Cambridge. 400 pp.

Mellor, G. & T. Yamada, 1974. A hierarchy of turbulence closure models for plnaetary boundary layers. –J Atmos. Sci. **31:** 1791–1806.

Mellor, G. & T. Yamada, 1982. Development of a turbulence closure models for geophysical fluid problems. –Rev. Geophys. Space Phys. **20:** 851–875.

Mills, D.K., P. Tett & G. Novarino, 1983. The Spring Bloom in the south-western North Sea in 1989.

–Neth. J. Sea Res. **33:** 65–80.

Radach, G., 1983. Simulations of phytoplankton dynamics and their interactions with other system components. In: J.S. amd W. Lenz, North Sea Dynamics. Springer-Verlag, Berlin: 584–610.

Radach, G. & H. Lenhart, 1995. Nutrient dynamics in the North Sea: fluxes and budgets in the water colomn derived from ERSEM. –Neth. J. Sea Res. **33:** 301–335.

Ridderinkhof, H., 1992. On the effects of variability in meteorological forcing on the vertical structure of a stratified water column. –Cont. Shelf Res. **12:** 25–36.

Riegman, R., B.R. Kuipers, A.A.M. Noordeloos & H.J. Witte, 1993. Size-differential control of phytoplankton and the structure of phytoplankton communities. –Neth. J. Sea Res. **31:** 255–265.

Ruardij, P. & W. van Raaphorst, 1995. Benthic nutrient regeneration in the ERSEM ecosystem model of the North Sea. –Neth. J. Sea Res. **33:** 453–483.

Ryther, J. & D. Menzel, 1959. Light adaptation bu marine phytoplankton. –Limnol. Oceanogr. **4:** 492–497.

Smith, E.L., 1936. Photosynthesis in relation to light and carbon dioxide. –Proc. Natl. Acad. Sci. Wash. **22:** 504–511.

Steele, J., 1962. Environmental control of photosynthesis in the Sea. –Limnol. Oceanogr. **7:** 137–150.

Stramska, M. & T. Dickey, 1993. Phytoplankton bloom and the vertical thermal structure of the upper ocean. –J. Mar. Res. **51:** 819–842.

Tett, P., I. Joint, D. Purdie, M. Baars, S. Oosterhuis, G. Danreri, F. Hannah, D. Mills, D. Plummer, A. Pomroy, A. Walne & H.J. Witte, 1993. Biological consequences of tidal stirring gradients in the North Sea. –Phil. Trans. R. Soc. **A343:** 493–508.

Tett, P. & A. Walne, 1995. Observations and simulations of hydrography, nutrients and plankton in the southern North Sea. –Opheilia **42:** 371–416.

van Aken, H., 1984. A one-dimensional mixed-layer model for stratified shelf seas with tide- and wind-induced mixing. –Deutsches Hydrographisches Zeitschrift **37:** 3–27.

van Haren, H. & D.K. Mills, 1996. High frequency long time series measurements of phytoplankton biomass in the central North Sea. In preparation.

van Raaphorst, W., J. Malschaert & J.J. van Haren, 1996. Tidal dynamics of deposition and resuspension of particulate matter on the North Sea continental shelf. In preparation.

Varela, R.A., A. Cruzado & J.E. Gabaldón, 1995. Modelling Primary production in the North Sea using ERSEM. –Neth. J. Sea Res. **33:** 337–361.

APPENDIX 4

Vol. 132: 169–179, 1996 | MARINE ECOLOGY PROGRESS SERIES Mar Ecol Prog Ser | Published February 29

Denitrification rates as measured by the isotope pairing method and by the acetylene inhibition technique in continental shelf sediments of the North Sea

713

Lutz Lohse*, Henderikus T. Kloosterhuis, Wim van Raaphorst, Willem Helder

Netherlands Institute for Sea Research (NIOZ), PO Box 59, 1790 AB Den Burg, Texel, The Netherlands

ABSTRACT: Denitrification rates in continental shelf sediments of the North Sea were measured by the simultaneous application of the acetylene inhibition technique (AIT) and the isotope pairing method (IPM). Nitrification was the predominant source of nitrate in these sediments. Both techniques were able to detect coupled nitrification-denitrification activity. Denitrification rates measured by the AIT were only measurable during the first 60 min of the incubation. Rates obtained by the AIT in this period ranged between 5.4 and 7.3 µmol N m^{-2} h^{-1}. Continued incubation of acetylene amended sediment cores resulted in decreasing denitrification rates, suggesting that accumulated nitrous oxide was consumed despite the presence of acetylene. Denitrification rates obtained by the application of the IPM ranged between 9.8 and 13.2 µmol N m^{-2} h^{-1}. Constant production of single-labelled ($^{14}N^{15}N$) relative to double-labelled ($^{15}N^{15}N$) dinitrogen indicated a homogeneous mixing of both isotopic nitrate species through the denitrification zone. The present results suggest that previously published data severely underestimated denitrification rates in North Sea continental shelf sediments. Concomitant measured fluxes of nitrate and ammonium across the sediment-water interface reveal that in these sediments most of the deposited nitrogen is returned to the water column as ammonium and nitrate.

KEY WORDS: Denitrification · Nitrification · Isotope pairing method · Acetylene inhibition technique · Nitrate fluxes · Continental shelf sediments

INTRODUCTION

Denitrification is the successive reduction of fixed NO_3^- and NO_2^- to gaseous N_2O and to N_2 and can be considered as one of the key processes in global and marine nitrogen cycles. The bacterially mediated process occurs in the absence of oxygen, primarily close to the anoxic-oxic interface as encountered in e.g. coastal sediments. At such a site, denitrifying bacteria receive NO_3^- by diffusion either from the overlying water or from the oxic sediment surface layer, where ammonium is oxidised to nitrate. The latter process, called nitrification, is considered as the predominating nitrate source for denitrification in most coastal sediments (Seitzinger 1988).

Numerous studies demonstrated the significance of benthic denitrification in the nitrogen budget of estuarine, coastal and shelf sea areas (e.g. Nishio et al. 1983, Jensen et al. 1988, Devol & Christensen 1993). It has been estimated that up to 80% of the external nitrogen load to coastal areas can be removed by denitrification (overview in Seitzinger 1990). Therefore, this process not only plays an important role in counteracting eutrophication effects (Rönner 1985), but it may also affect pelagic production (Nixon 1981). In order to measure denitrification rates quantitatively, considerable efforts have been made to develop sophisticated methods which permit their detection in marine sediments under *in situ* conditions.

The most direct approach is to measure the evolution of N_2 and N_2O in the water or gas phase of enclosed benthic chambers (Seitzinger et al. 1980). The major

*E-mail: lutz@nioz.nl

© Inter-Research 1996
Resale of full article not permitted

advantage of this method is that no inhibitors or artificial substrates are required and in principle the method can be applied *in situ* with benthic landers (Devol & Christensen 1993). Normally, the N_2 containing overlying water has to be replaced with He/O_2 flushed water and the sediment cores have to be preincubated for up to 10 d to lower the background N_2 concentrations in the porewater. During the preincubation, the heterotrophic denitrification activity may be influenced by an exhaustion of the labile organic carbon pool. A recent modification diminished the preincubation time to 3 or 4 d, but, due to incomplete removal of N_2 from the porewater, this resulted in relative high background fluxes of N_2 which have to be subtracted from the true denitrification rate (Nowicki 1994). In any case, this approach is sensitive to contamination with atmospheric nitrogen gas. The present detection limit of ~25 µmol N m^{-2} h^{-1} (Seitzinger 1987) excludes the application of this technique in aquatic sediments with low activity.

The most frequently used method up until now has been the acetylene inhibition technique (Sørensen 1978). This method is based on the accumulation of N_2O due to the inhibition of the nitrous oxide reductase enzyme by acetylene (Yoshinari & Knowles 1976). Although far more rapid and easier to apply than the N_2 evolution technique, several methodological constraints must be taken into account. Particularly, the co-inhibition of nitrification by acetylene may lead to an exhaustion of the porewater nitrate pool which in turn can lead to an underestimate of the true denitrification rate. Additionally, studies with combined microsensors for nitrous oxide and oxygen have shown that N_2O may be partly reduced to N_2 despite the presence of acetylene (Christensen et al. 1989). Nevertheless, this technique continues to be applied extensively in marine sediments (Kemp et al. 1990, Law & Owens 1990, Blackburn et al. 1994, Thompson et al. 1995).

The applicability of stable isotopes in denitrification studies was improved by the introduction of the isotope pairing method (Nielsen 1992). This approach facilitates the determination of the reduction of both NO_3^- diffusing downwards from the overlying water and of NO_3^- produced through nitrification. Basically, $^{15}NO_3^-$ added to the overlying water is allowed to diffuse through the oxic sediment layer to the denitrification zone. According to the stoichiometry of denitrification, added $^{15}NO_3^-$ pairs with indigenous $^{14}NO_3^-$ originate either from nitrification or from the overlying water. Reduction of $^{14}NO_3^-$ and $^{15}NO_3^-$ results in the formation of the isotopes $^{14}N^{14}N$, $^{14}N^{15}N$, and $^{15}N^{15}N$. Crucial assumptions in this technique are that (1) the rate of coupled nitrification-denitrification is not influenced by the addition of labelled nitrate and (2) the $^{15}NO_3^-$ added to the overlying water mixes homogeneously with the $^{14}NO_3^-$ pool down to the zone where denitrification occurs. The latter prerequisite is most easily met in sediments where the oxygenated layer is restricted to a few millimetres.

Although the limitations of the methods have been addressed in several denitrification studies, systematic comparisons are rarely performed. Seitzinger et al. (1993) carried out a comparative experiment incubating lake sediments under controlled conditions, in which denitrification rates were measured with the N_2 flux method, the acetylene inhibition technique, and a ^{15}N tracer approach (Nishio et al. 1983). In that particular study, the N_2 flux technique consistently gave highest rates, while rates obtained with the ^{15}N tracer technique were low and more variable. The acetylene block technique, however, failed to detect any nitrous oxide produced by coupled nitrification-denitrification activity.

In this study, we compare results from an experiment carried out on the continental shelf of the North Sea. The acetylene inhibition technique and the isotope pairing technique were used to determine *in situ* denitrification rates in sediments overlain by a well-oxygenated water column with low nitrate concentrations. Our main objective was to compare the outcomes of both techniques and to reexamine previous measurements in this area based on the acetylene inhibition technique only. All experiments were conducted during the STED expedition (Short Term Dynamics of benthic microbial activities and nutrient fluxes related to sedimentation and current velocities) in July 1994 aboard the RV 'Pelagia'.

MATERIALS AND METHODS

Characterisation of the study site. Samples were collected at the Oysterground mooring station (54° 25.46' N, 4° 02.16' E) in the central part of the southern North Sea. The water column was stratified by a thermocline with surface and bottom water temperatures of 17 and 9°C, respectively. The salinity ranged around 34.5‰ throughout the water column. Bottom water oxygen concentrations (~261 µmol l^{-1}) did not differ substantially from saturation values. Nitrate and ammonium concentrations in the bottom water did not exceed concentrations of 1 µM.

According to the Wentworth scale, the sediments consisted of very fine sands, having an average porosity of 0.55 (v/v) in the upper 5 mm. Previous investigations showed that the organic carbon and nitrogen content (averaged over the first 5 mm) were 0.12 and 0.02%, respectively (Lohse et al. 1993).

Sample collection. Sediment cores were obtained by gently pushing acrylic liners into the sediment re-

trieved on deck by a cylindrical boxcorer (for details, see Lohse et al. 1993). Only boxcores without visible disturbance of the sediment water interface were used for subcoring. All processes reported in this study were measured on 3 different days, denoted here as Expts A (8 July), B (14 July), C (7 July) and E (17 July). The distance between the sample location was <200 m. The experiments were carried out in a thermostated container which was adjusted to *in situ* temperature (±0.5°C).

Denitrification assays. Sediment cores were taken with acrylic liners (23 cm length, 3.6 cm i.d.). The sediment was adjusted in height so that the cores contained approximately 5 cm of sediment column and 15 cm of overlying water. The uncapped sediment cores were carefully immersed in an aquarium containing bottom water from the sampling location. The overlying water in the cores was stirred by a small rotating magnet, located 2 cm above the sediment-water interface. The momentum of these magnets was switched from clockwise to anticlockwise rotation every 5 s in order to minimise the effect of pressure gradients at the sediment water interface caused by one-directional flow patterns. All cores were preincubated for 2 to 3 h prior to further treatments.

Acetylene inhibition technique (AIT): The conventional acetylene-block technique (Sørensen 1978) was modified according to Christensen et al. (1989). Commercial grade acetylene gas (Hoekloos Ltd, Amsterdam, The Netherlands) was purified by scrubbing the gas in concentrated sulphuric acid and 5 M NaOH (Hyman & Arp 1987). Four to 10 sediment cores were amended with water saturated with purified acetylene following the procedure previously described in Lohse et al. (1993). The final concentration of acetylene in the overlying water and in the porewater was 10 kPa. Two additional sediment cores received no acetylene and served as control. The cores were then capped and incubated for between 20 and 120 min. Nitrous oxide in the overlying water was analysed after transferring a 10 ml sample into a 30 ml extraction vial. The vial was shaken vigorously for 10 min to achieve equilibrium between headspace and water. A 3 ml sample of the gas phase was transferred into an evacuated vacutainer (Terumo, Belgium). After taking a second water sample (20 ml) for dissolved nutrient analysis, the core was capped again and the remaining overlying water, along with the sediment, was shaken vigorously for 15 min. Again, a gas sample was drawn from the headspace and transferred into an evacuated vacutainer. Nitrous oxide in the vacutainers was analysed on a Packard 438a gas chromatograph equipped with an electron capture detector (for details, see Lohse et al. 1993). The concentration of N_2O in water was calculated using the solubility coefficients of N_2O in seawater (Weiss & Price 1980). The vacutainers contained an elevated background concentration of nitrous oxide (430 ± 25 ppb) which was taken into account for all calculations. The denitrification rate was calculated from the total increase of nitrous oxide in the porewater and overlying water of individual cores.

Isotope pairing method (IPM): Denitrification rates were estimated in 6 to 10 sediment cores by adding 20 ml of a labelled 50 mM $^{15}NO_3^-$ solution (98 atom%, Sigma Ltd, UK) to the bulk water of the aquarium (~19 l). This resulted in a final nitrate concentration in the aquarium water of between 61 and 83 µM $^{15}NO_3^-$. The cores remained uncapped for another 30 min, to facilitate a homogeneous distribution of nitrate between the overlying water of the cores and the surrounding aquarium water. Subsequently, all cores were capped with rubber stoppers and incubated for 25 to 180 min. The formation of ^{15}N labelled dinitrogen was analysed by terminating the incubation of single cores in 20 to 45 min intervals. A subsample of 40 ml was taken from the overlying water with a plastic syringe. Part of this sample was carefully transferred into two 12.6 ml exetainers (Labco Ltd, Bucks, UK) which were closed by a screw cap equipped with a gastight injection septum. The exetainer contained 250 µl of a 50% (w/w) $ZnCl_2$ solution to prevent further microbial activity. The water left in the syringe was used for immediate analysis of nutrients. An additional amount of 3 ml of the $ZnCl_2$ solution was added to the remaining overlying water in the core, which was then mixed gently with the whole sediment column to produce a slurry. Similar to the analysis of the water phase, a subsample of this slurry was transferred into 2 additional exetainers which contained 250 µl of $ZnCl_2$ solution.

In Expt E, designed to assess the potential effect of labelled $^{15}NO_3^-$ on the first-order kinetics of denitrification, 13 cores were enriched with varying concentrations of $^{15}NO_3^-$. This was achieved by adding different aliquots of a 5 mM $^{15}NO_3^-$ stock solution to the water column of single cores, resulting in concentrations between 15 and 180 µM $^{15}NO_3^-$. The incubation was terminated after 150 min, according to the procedure described above. All exetainers were stored at 4°C until analysis, which took place within 5 wk after sampling.

Dissolved labelled and unlabelled N_2 was extracted from the water phase of the exetainer by replacing 4 ml of water in the exetainer with helium gas. By vigorous shaking for 5 min more than 98% of N_2 from the water phase was transferred into the headspace of the exetainer (Weiss 1970). The first set of exetainers was analysed at the National Environmental Research Centre (NERI) in Silkeborg, Denmark. Analysis was performed with a Tracermass stable isotope mass spec-

trometer (Europa Scientific, Crewe, UK) equipped with a triple collector system. The complete sample headspace was injected by an autosampler (RoboPrebG+) equipped with a helium flushed needle system. The gas was purified in a glass column packed with Drierite and Carbosorb. Additionally, the gas flow was lead through a heated copper reduction tube (600°C). The standard error of repeated single injections was less than 1.6%. The denitrification rate was calculated from the increase of labelled isotopes in individual cores.

To establish an intercomparison with data obtained at NERI, we analysed a duplicate set of samples on the stable isotope mass spectrometer (VG Isotech Fisons Optima, Middlewich, UK) at the Netherlands Institute for Sea Research (NIOZ). Both mass spectrometers had essentially the same technical manifold, although at the NIOZ, smaller subsamples (400 µl) of the headspace gas were injected manually using a gas-tight Hamilton syringe. The readings of both mass spectrometers showed excellent agreement (data not shown).

Calculation of denitrification rates. Analysis of the isotopic composition of the injected gases results in currents of $^{14}N^{14}N$ (mass 28), $^{14}N^{15}N$ (mass 29), and $^{15}N^{15}N$ (mass 30). The sample ratios R1 and R2 are obtained by dividing the 29 and the 30 current by the sum of the 28, 29 and 30 current. The corresponding reference ratios (obtained from exetainers containing only seawater from the sampling station) are subtracted from the sample ratios. The amount of $^{14}N^{15}N$ and $^{15}N^{15}N$ isotopes (in nmol) was calculated by multiplying R1 and R2 with the total amount of N_2 present in the headspace and the water of the exetainer. The amount of N_2 extracted from the exetainer was determined from the distribution coefficient of N_2 between water and atmosphere (Weiss 1970). Calibration for N_2 took place by injecting 20, 40 and 60 µl of air into the headspace of the exetainers.

Rates of denitrification were calculated from the production of single-labelled $^{14}N^{15}N$ relative to double-labelled $^{15}N^{15}N$ following the calculations of Nielsen (1992). Homogenous mixing of both nitrate species results in a binomial distribution of all dinitrogen species formed, so that $^{14}N^{15}N$ and $^{15}N^{15}N$ are produced with the probability of 2 $N^{14}N^{15}$ and 1 $N^{15}N^{15}$ (Hauck et al. 1958). The denitrification rate of labelled nitrate (D_{15}) is calculated as the sum of all labelled N_2 species formed:

$$D_{15} = (^{14}N^{15}N) + 2(^{15}N^{15}N). \quad (1)$$

The denitrification rate based on unlabelled nitrate (D_{14}), representing *in situ* denitrification, relies on the assumed binomial distribution and is derived from:

$$D_{14} = (^{14}N^{15}N)/2(^{15}N^{15}N) \times D_{15}. \quad (2)$$

The rate of D_{14} is supported by nitrate diffusing into the sediment from the overlying water (Dw) and by nitrate that is produced by nitrification in the oxic layer of the sediment (Dn). The former is calculated as:

$$Dw = (100 - e15)/e15 \times D_{15} \quad (3)$$

where e15 is the percentage of $^{15}NO_3^-$ enrichment of the total nitrate pool in the overlying water. Denitrification coupled to nitrification (Dn) is then simply calculated from the difference:

$$Dn = D_{14} - Dw \quad (4)$$

Oxygen microprofiles and nutrient fluxes. Three sediment cores (25 cm length, 10 cm i.d.) were taken for the determination of oxygen porewater profiles and nutrient fluxes at each denitrification experiment. The cores were preincubated for 2 h prior to measurements. The water column was continuously stirred by a small Teflon coated magnet, switching rotation direction from clockwise to anticlockwise every 5 s. Three to 6 oxygen profiles were made with Clark-type microelectrodes (Diamond Corp., Ann Arbor, USA; type 737) at different horizontal positions at the sediment surface. The average tip diameter of the electrodes was 85 µm. Typical output at 100% O_2 saturation at ambient conditions (9°C, 34.5‰ S) was 250 to 300 pA, while the zero signal in anoxic sediments ranged between 10 and 20 pA. Ninety percent of the output signal was obtained in <3 s. The oxygen concentration in the bottom water was determined by an automated Winkler titration in triplicate. The electrodes were calibrated by assuming a linear relationship between the oxygen concentration and the output signal (Revsbech & Jørgensen 1986). The electrodes were inserted in steps of 100 µm using a motor-driven micromanipulator with computerised depth control. The oxygen uptake of the sediment was calculated by applying a zero-order consumption model according to Bouldin (1968).

Nutrient fluxes were determined simultaneously in these cores by taking 10 ml samples from the overlying water at intervals of 20 min. Ammonium, nitrate and nitrite were determined using standard methods for nitrate (Strickland & Parsons 1972) and ammonium (Helder & de Vries 1979) using a TRAACS-800 autoanalyser. The analytical precision of these measurements was 1% for nitrate and 2% for ammonium.

Porewater profiles. Porewater profiles of dissolved ammonium and nitrate were made by pushing the sediment out of acrylic liners (30 cm length, 3.6 cm i.d.) and sectioning it into intervals of 0–2.5, 2.5–5, 5–7.5, 7.5–10, 10–15, 15–20, 20–25, 25–30, 30–40, 40–50, 50–60 and 60–70 mm. Five to 10 slices were pooled in a centrifuge tube and subsequently centrifuged for 10 min at 1770 × *g* (Saager et al. 1990).

RESULTS

Porewater profiles and fluxes of oxygen and nutrients

A representative oxygen profile is shown in Fig. 1. On average, oxygen penetrated 2.8 ± 0.5 mm into the sediment, indicative for intense mineralisation processes occurring in this continental shelf sediment (Rasmussen & Jørgensen 1992). The diffusive oxygen flux, as calculated by the zero-order model of Bouldin (1968), amounted to 234 ± 20 in Expt A and 254 ± 45 μmol O_2 m^{-2} h^{-1} in Expt B (Table 1). The molecular diffusion coefficient applied (7.2×10^{-5} m^{-2} d^{-1}) was corrected for temperature (Li & Gregory 1974) and porosity (Ullmann & Aller 1982).

A representative nitrate porewater profile (Fig. 2A) shows subsurface nitrate concentrations which were higher than those in the bottom water (0.6 μM). The maximum concentration was observed in the oxic surface layer. In deeper, anoxic layers, nitrate concentrations declined sharply until a depth of ~6 mm. Below that depth down to 70 mm, the nitrate gradient decreased more gradually. Nitrite was a minor component of the NO_x pool (<8%) and was therefore neglected. In agreement with the porewater profile, measured nitrate fluxes were always directed to the water column (Table 1). Nitrate effluxes were consistent with time, but showed large core-to-core variations.

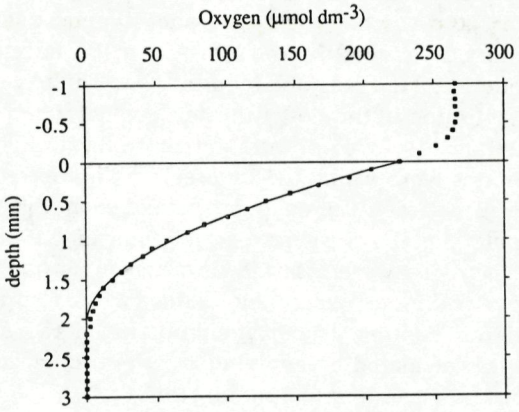


Fig. 1. Representative oxygen profile. Markers indicate the measured profile. Solid line represents the modelled zero-order profile

Table 1. Fluxes (±SD) of oxygen, ammonium and nitrate across the sediment-water interface during all experiments. Negative values denote uptake by the sediment. nd = no data

Experiment	O_2 flux (μmol O_2 m^{-2} h^{-1})	NH_4^+ flux (μmol N m^{-2} h^{-1})	NO_3^- flux (μmol N m^{-2} h^{-1})
Expt A (D1)	−234 ± 20	14.7 ± 13.2	9.8 ± 4.3
B (D2)	−254 ± 45	16.1 ± 5.2	nd
C (D3)	nd	1.9 ± 1.8	11.4 ± 9.6
All measurements	−244 ± 35 (n = 6)	10.9 ± 10.4 (n = 9)	10.6 ± 7.5 (n = 6)

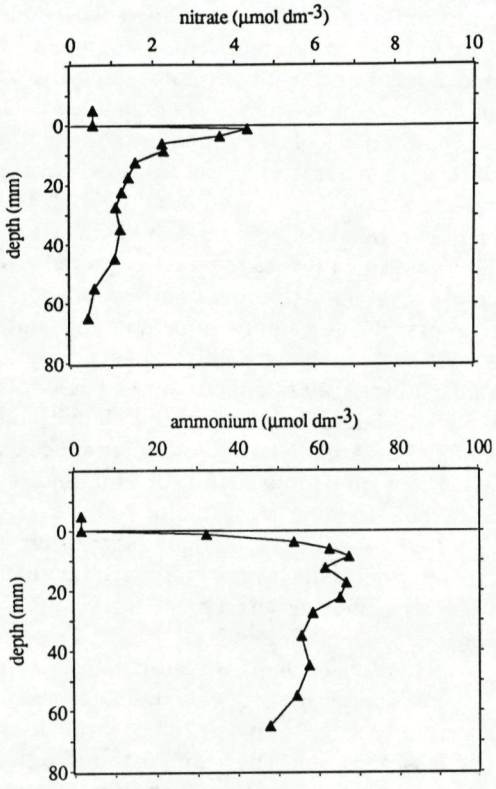


Fig. 2. Representative nitrate (upper panel) and ammonium (lower panel) profiles

The ammonium porewater concentrations increased directly below the sediment-water interface and revealed highest concentrations at ~8 mm (Fig. 2B). Measured effluxes of ammonium across the sediment-water interface were of a similar magnitude as the nitrate fluxes (Table 1).

Denitrification rates

Acetylene inhibition technique (AIT)

Acetylene amended cores showed an elevated content of N_2O compared to the control cores (Fig. 3). In all experiments, the N_2O concentrations in individual cores increased from ~3 nmol at $t = 0$ to ~5–6 nmol per core after 40 to 65 min. No further increase, but instead, a slight decrease in N_2O occurred after 65 min. Consequently, the calculated denitrification rates may depend on the period of their incubation (Fig. 4). The rates were highest in shortly incubated sediment cores ranging between 5.4 and 7.3 μmol N m^{-2} h^{-1} (Table 2).

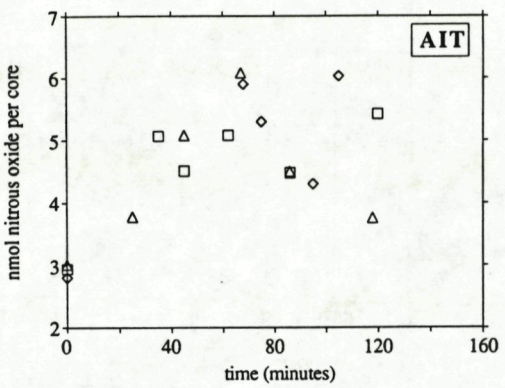


Fig. 3. Pooled N_2O accumulation in individual cores in Expts A (Δ), B (□) and C (◇). N_2O concentrations at $t = 0$ represent the control cores incubated without acetylene

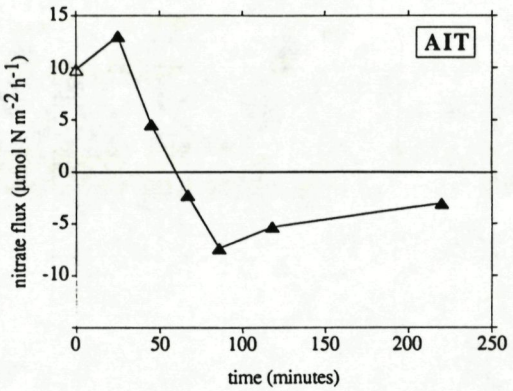


Fig. 5. Development of nitrate fluxes in Expt A in individual acetylene amended sediment cores during the incubation. Open symbol at $t = 0$ denotes the nitrate flux in control cores

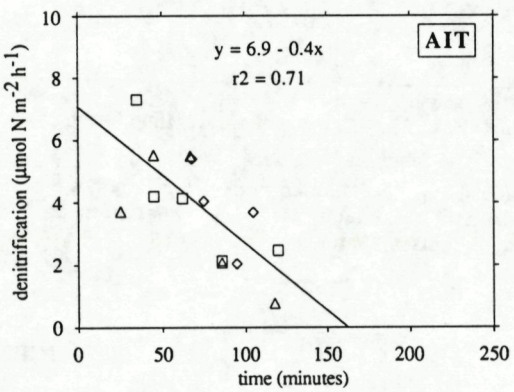


Fig. 4. Pooled denitrification rates in Expts A (Δ), B (□) and C (◇). Solid line indicates linear regression through all denitrification rates

The negative correlation between denitrification rates and incubation time ($y = 6.9–0.4x$, $r^2 = 0.71$) indicates that, when applying the AIT, the calculated denitrification rates become very low after incubations of longer than 150 min. Previous experiments showed that N_2O never accumulated in control cores incubated without acetylene (Lohse et al. 1993).

Nitrate fluxes measured in the acetylene amended cores were also dependent on the period of incubation. Fig. 5 shows the nitrate fluxes in Expt A. The initial nitrate efflux (13.0 µmol N m^{-2} h^{-1}) was similar to the flux measured in the cores without acetylene (Table 1). Continued incubation of the cores revealed decreasing effluxes turning to influxes after ~65 min. Similar influxes were observed for Expts B and C after approximately 1 h of incubation (data not shown).

Isotope pairing method (IPM)

Sediment cores incubated with a uniform concentration of either 61 (Expt A), 83 (B), or 62 µM $^{15}NO_3^-$ (C) showed a regular accumulation of single-labelled ($^{14}N^{15}N$) and double-labelled ($^{15}N^{15}N$) dinitrogen isotopes (Fig. 6, upper panels). More than 75% of the la-

Table 2. $^{15}NO_3^-$ concentration (µmol l^{-1}) and denitrification rates (all in µmol N m^{-2} h^{-1}) based on labelled (D_{15}) and unlabelled (D_{14}) nitrate (± SD). Dn and Dw denote the denitrification rate depending on unlabelled nitrate provided from nitrification and from the overlying water, respectively. Initial AIT denotes highest denitrification rates obtained from acetylene-amended cores analysed within the first 70 min after the start of the incubation

Experiment	IPM					Initial AIT	Ratio D_{14}/AIT
	$[^{15}NO_3^-]$	D_{15}	D_{14}	Dn	Dw		
A	61	55.8 ± 3.6	12.4 ± 2.6	11.6 ± 2.8	0.8 ± 0.3	5.5	2.2
B	83	21.5 ± 4.9	11.6 ± 2.0	11.3 ± 2.0	0.2 ± 0.0	7.3	2.2
C	62	37.0 ± 9.8	13.2 ± 4.4	12.6 ± 4.2	0.8 ± 0.2	5.4	2.4
E	15-180	–	9.8 ± 2.8	9.4 ± 2.4	0.4 ± 0.2		
All measurements	–	38.0 ± 15.6 n = 15	11.3 ± 3.2 n = 28	10.7 ± 3.1 n = 28	0.5 ± 0.2 n = 28	6.1 ± 1.1 n = 3	2.3 ± 0.1

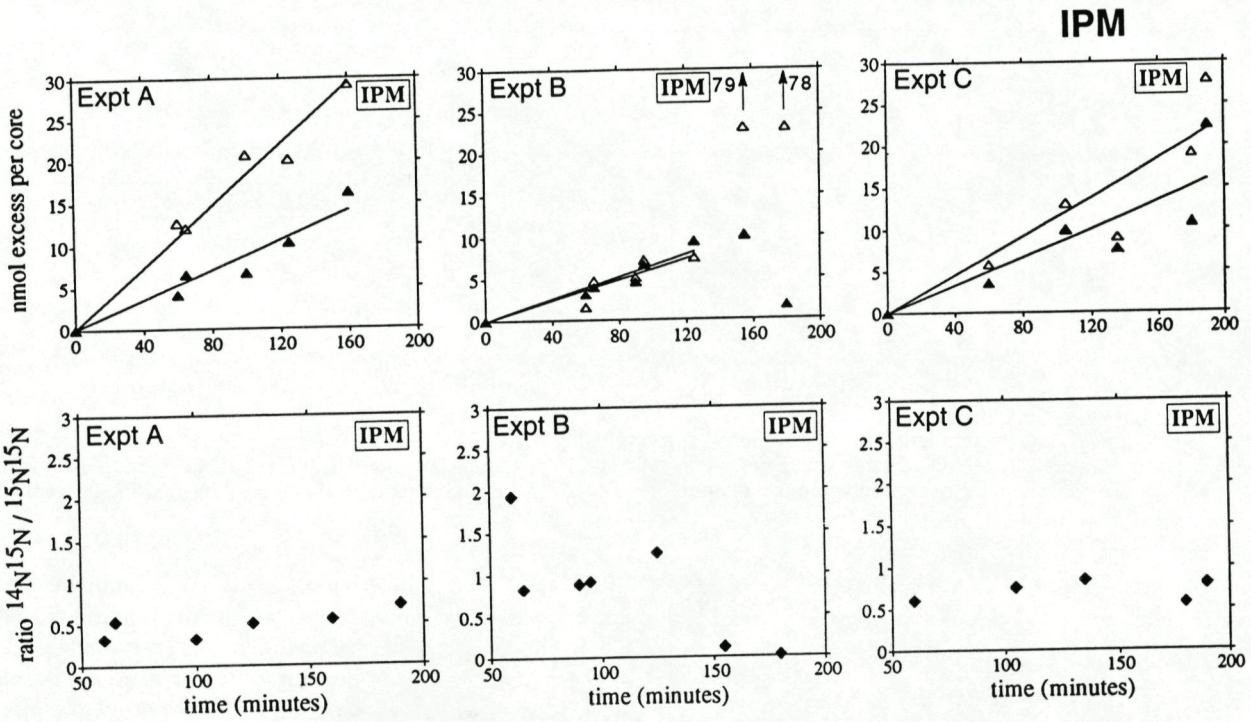


Fig. 6. Upper panels: development of excess of $^{14}N^{15}N$ (closed symbols) and $^{15}N^{15}N$ (open symbols) in Expts A, B and C in individual sediment cores incubated with a uniform $^{15}NO_3^-$ concentration in the overlying water. Lower panels: ratio of $^{14}N^{15}N/^{15}N^{15}N$ produced during the course of Expts A, B and C

belled isotopes produced were found in the sediment; the rest was released to the water column. The slope of the plotted ratios $(^{14}N^{15}N)/(^{15}N^{15}N)$ during the course of the incubation did not show significant differences from zero (Student *t*-test, $p = 0.1$) (Fig. 6, lower panels), indicating that both isotopic nitrate species were denitrified with the same frequency. The low ratios found at the end of incubation B were caused by insufficient $ZnCl_2$ addition, which permitted continued gas production in the exetainers as was observed from the swollen septas of the vacutainer. The denitrification rate of labelled nitrate (D_{15}) was more variable than the rate of unlabelled nitrate (D_{14}) (Table 2). Almost 95% of the denitrification rate based on unlabelled nitrate (D_{14}) was supported by coupled nitrification-denitrification (Dn). Consequently, the downward diffusion of nitrate from the overlying water (Dw) to the anoxic denitrification zone was of minor importance in these particular North Sea sediments.

Denitrification rates obtained from the cores incubated with different concentrations of $^{15}NO_3^-$ in the overlying water (Expt E) are shown in Fig. 7. The D_{15} rates were correlated to the concentration of $^{15}NO_3^-$ in the overlying water. Coupled nitrification-denitrification (Dn) was apparently independent of the $^{15}NO_3^-$ concentration. Within the applied range of 15 to 180 µM $^{15}NO_3^-$ Dn was relatively constant around

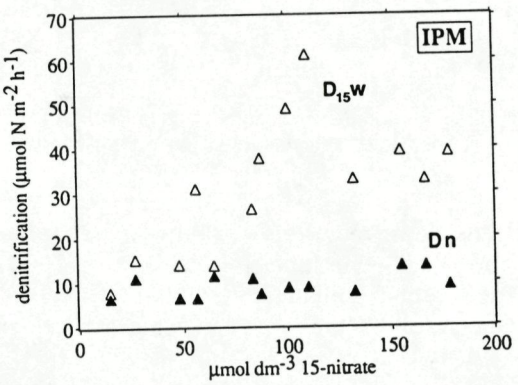


Fig. 7. Denitrification rates in individual sediment cores versus $^{15}NO_3^-$ concentration in the overlying water (Expt E). Denitrification of $^{15}NO_3^-$ coming from the overlying water ($D_{15}w$, △) and produced by nitrification (Dn, ▲)

9.8 ± 2.8 µmol N m^{-2} h^{-1} (Table 2). At all $^{15}NO_3^-$ levels applied, the contribution of unlabelled nitrate in the overlying water (Dw) to the overall denitrification (D_{14}) remained less than 5%.

The *in situ* denitrification rate measured by the IPM, represented by the D_{14} rate in Table 2, exceeded the initial *in situ* denitrification rate obtained with the AIT by a factor of 2.2, 2.2 and 2.4 in Expts A, B and C, respectively (Table 2).

DISCUSSION

Our results indicate that *in situ* denitrification activity can be detected by both the isotope pairing method and the acetylene inhibition technique. However, rates computed from the AIT were always lower and more sensitive to the incubation time than the D_{14} rates measured with IPM. Based on the nitrous oxide accumulation during the first 60 min, the AIT detected ~50% of the D_{14} rate measured by the IPM (Table 2). The non-constant N_2O accumulation with time indicates that the net rate of N_2O production in the sediment changed within the first 2 h of incubation. The levelling off and successive decrease in the N_2O in the sediment cores implies that N_2O was close to zero or was even turned into a consumption after ~60 min.

The efficiency of the AIT in aquatic sediments depends on the availability of nitrate (Oremland et al. 1984, Rudolph et al. 1991). If sedimentary nitrification is the prevailing source of nitrate, a rapid exhaustion of the nitrate porewater pool may lead to underestimation of the true denitrification rate due to the co-inhibition of nitrification by acetylene (Walter et al. 1979, Hyman & Arp 1985). High subsurface nitrate concentrations in the porewater and the net effluxes of nitrate across the sediment-water interface imply that nitrification is the predominant nitrate source in the present study. We found production of nitrous oxide as long as the incubation time was shorter than ~60 min. Evidently, the pool of porewater nitrate was not exhausted during this initial stage of the experiment. This conclusion is supported by the simultaneously measured nitrate effluxes in the first hour of the experiment, which were similar to nitrate effluxes measured in control cores without acetylene (Fig. 5). The maximum nitrate influxes measured after ~70 min were larger than the denitrification rates measured during the initial stage of the experiment. This suggests that the denitrification rate based on the initial N_2O was lower than the true denitrification rate. Probably the inhibition of the N_2O reductase was also incomplete during the initial period of the experiment. This is supported by studies with combined N_2O and O_2 sensors (Christensen et al. 1989, Nielsen et al. 1990). These studies have demonstrated that up to 40% of the accumulated N_2O may be reduced in deeper, anoxic layers, despite the presence of acetylene. Experiments with sediment slurries have shown that nitrous oxide can be reduced in the presence of acetylene as soon as the nitrate concentration decreases below 5 to 10 µM (Slater & Capone 1989). Since the nitrate porewater concentration in the denitrification zone of our sediments was in this range, we conclude that the accumulation of N_2O ceased after 50 to 70 min due to an exhaustion of the nitrate porewater pool. The presupposition for this conclusion is that dissimilative nitrate reduction to ammonia does not play a substantial role in these sediments. Dissimilative nitrate reduction to ammonium normally does not account for more than 5% of the total nitrate uptake in estuarine sediments (Pelegrí et al. 1994, Risgaard-Petersen et al. 1994). The maximum nitrate influx in the acetylene amended cores was close to the denitrification rate measured with the IPM. As denitrification is the only nitrate consuming process in acetylene amended cores, the maximum nitrate influx rather than the nitrous oxide accumulation may give a fairly good estimate for the true denitrification rate.

The major challenge of the isotope pairing technique is to apply an appropriate $^{15}NO_3^-$ concentration in the sediment which on the one hand entraps all $^{14}NO_3^-$ molecules denitrified, but on the other hand does not influence the uptake of $^{14}NO_3^-$ by the denitrifying bacteria. Concentrations of $^{15}NO_3^-$ which are too low may result in a deviation of the assumed binomial distribution of the N_2, and thus in an underestimate of the Dn rate due to a higher formation of unlabelled relative to single- and double-labelled N_2. The ratio between the isotopic species ($^{14}N^{15}N/^{15}N^{15}N$) should remain below 2, since this indicates that all produced $^{14}NO_3^-$ molecules have paired with $^{15}NO_3^-$. The ratio will further decrease as the concentration of added $^{15}NO_3^-$ increases. However, the $^{15}NO_3^-$ concentration cannot be infinitely high, since the first order kinetics of denitrifying bacteria with respect to NO_3^- (Christensen et al. 1990, Jensen et al. 1994) should be maintained to guarantee that the uptake kinetics of $^{14}NO_3^-$ are not affected. The D_{14} rate was independent of the $^{15}NO_3^-$ concentration, whereas D_{15} responded according to first-order kinetics (Fig. 7). This is in line with previous studies using isotope pairing (Pelegrí et al 1994, Rysgaard et al. 1994). From this, we conclude that the major assumptions underlying the IPM were met, and that within the constraints given for this technique (Nielsen 1992), the IPM data (D_{14}) represent a reliable estimate for the *in situ* denitrification rates.

Denitrification in North Sea sediments

Previously reported estimates of denitrification in North Sea sediments were based either on the AIT or on diagenetic modelling of porewater profiles. Investigators using the former approach found rates between 0.6 and 12 (Law & Owens 1990), 1 and 23 (van Raaphorst et al. 1992) and 0 to 8.2 µmol N m^{-2} h^{-1} (Lohse et al. 1993). When only considering rates measured in summer in the direct vicinity of our study site, both the AIT and the IPM/D_{14} in this study gave higher values than those reported in the literature. Law &

Owens (1990), van Raaphorst et al. (1992) and Lohse et al. (1993) found rates of 0.6, 2.1 and 0.5 µmol N m^{-2} h^{-1}, respectively. The average of these estimates (1.1 ± 0.7 µmol N m^{-2} h^{-1}) represents only 18% of our average AIT value. The percentage is as low as 9% when comparing the literature data to the rates obtained from the IPM. Although interannual and spatial variability have probably contributed to the discrepancies among the AIT rates, it is obvious that the incubation times used in previous investigations (up to 16 h) were too long to match initial nitrous oxide accumulation. It thus seems likely that previous data severely underestimated true denitrification rates. This conclusion is confirmed by denitrification rates calculated from diagenetic porewater models, obtained in the same season close to our sampling site (van Raaphorst et al. 1990). Rates based on these diffusive porewater fluxes ranged from 6.3 to 9.8 µmol N m^{-2} h^{-1} and are considerably higher than previous estimates based on the AIT, but differ only by a factor of 1.5 from the IPM values in the present study. These results and the ratio we report between the IPM/D_{14} and the AIT (Table 2) strongly suggest that the D_{14} rates obtained from the IPM represent more accurate values for denitrification than do the AIT rates.

We have previously postulated that the steep diffusive nitrate gradients across the sediment-water interface may favour the release of nitrate to the overlying water column instead of its denitrification in deeper anoxic layers (Lohse et al. 1993). Our data confirm that a substantial amount of nitrate produced by nitrification diffuses to the nitrate-depleted water column. Assuming that the nitrification rate is given by the sum of the nitrate efflux plus the initial AIT denitrification rate, between 64 (Expt A) and 68% (Expt B) of the nitrate produced diffuses to the overlying water. Using the IPM Dn rates as a more accurate estimate, we obtain values between 46 (Expt A) and 48% (Expt C). These results are in line with laboratory experiments (Sloth et. al. 1995) and modelling studies (Blackburn & Blackburn 1993, Ruardij & van Raaphorst 1995). It follows that approximately half of the nitrate produced in the sediment reaches the anoxic layers to be denitrified.

The inorganic nitrogen cycle in these continental shelf sediments of the North Sea can be summarised by assuming that nitrification equals the sum of the average nitrate efflux (Table 1) and the Dn denitrification rate (Table 2). Inferring the total N-mineralisation from the sum of nitrification plus the ammonium efflux (Table 1), we obtain a mineralisation rate of 32 µmol N m^{-2} h^{-1}. About one third of the ammonium produced diffused out of the sediment, while two thirds was nitrified to NO_3^-; about 50% of the nitrate produced diffused out of the sediment, while the other 50% was denitrified. Hence, about 33% of the remineralised nitrogen left the sediment in the form of ammonium, 32% left as nitrate and 35% as gaseous dinitrogen. This high percentage of denitrification points out the important role this process plays in benthic N-cycling. A shift of the anoxic-oxic interface deeper into the sediment due to lower mineralisation activity in winter (as previously observed in Lohse et al. 1995) may result in a relatively higher percentage of ammonium being nitrified and subsequently denitrified, although the absolute rates may be lower due to less intense nitrogen mineralisation.

The results obtained in this study confirm the importance of benthic denitrification but also show that the shallow continental shelf sediments of the North Sea return most of the deposited nitrogen compounds to the water column as ammonium and nitrate. This situation generally holds for shallow sediments overlain by a nitrogen-poor, well-oxygenated water column where nitrification predominantly controls denitrification. In contrast, shelf sediments overlain by water columns with low oxygen and high nitrate concentrations may act as a sink for nitrogen compounds, since here denitrification is also supported by nitrate originating from the overlying water.

Acknowledgements. We express our gratitude to Captain J. C. Groot and the crew of the RV 'Pelagia' who provided a safe and pleasant cruise. We are also indebted to Søren Rysgaard and Preben Sørensen (National Environmental Research Institute, Denmark) for their support and advice during the mass-spectrometric ^{15}N measurements. Porewater and sediment characteristics were measured by Hans Malschaert. Evaline van Weerlee and Annette van Koutrik (nutrient analysis group, Department of Chemical Oceanography) performed the nutrient analysis. This work was partly subsidised by the Dutch Government (BEON grant no. NIOZ 94/95 E-01 RKZ 161/061). This is publication no. 85 of the project Applied Scientific Research (BEWON), at the Netherlands Institute for Sea Research.

LITERATURE CITED

Blackburn TH, Blackburn ND (1993) Coupling of cycles and global significance of sediment diagenesis. Mar Geol 113: 101–110

Blackburn TH, Nedwell DB, Wiebe WJ (1994) Active mineral cycling in a Jamaican seagrass sediment. Mar Ecol Prog Ser 110:233–239

Bouldin DR (1968) Models for describing the diffusion of oxygen and other mobile constituents across the mud-water interface. J Ecol 56:77–87

Christensen PB, Nielsen LP, Revsbech NP, Sørensen J (1989) Microzonation of denitrification activity in stream sediments with a combined oxygen and nitrous oxide microsensor. Appl environ Microbiol 55:1234–1241

Christensen PB, Nielsen LP, Sørensen J, Revsbech NP (1990) Denitrification in nitrate-rich streams: diurnal and seasonal variation related to benthic oxygen metabolism. Limnol Oceanogr 35:640–651

Devol AH, Christensen JP (1993) Benthic fluxes and nitrogen cycling in sediments of the continental margin of the eastern North Pacific. J mar Res 51:345–372

Hauck RD, Melsted SW, Yankwich PE (1958) Use of N-isotope distribution in nitrogen gas in the study of denitrification. Soil Sci 86:287–291

Helder W, de Vries RPT (1979) An automatic phenol-hypochlorite method for the determination of ammonia in sea- and brackish waters. Neth J Sea Res 13:154–160

Hyman MR, Arp DJ (1985) Suicidal labelling and inactivation of ammonia mono-oxygenase by acetylene. Biochem J 227:207–214

Hyman MR, Arp DJ (1987) Quantification and removal of some contaminating gases from acetylene used to study gas-utilizing enzymes and microorganisms. Appl environ Microbiol 53:298–303

Jensen K, Sloth NP, Risgaard-Petersen N, Rysgaard S, Revsbech NP (1994) Estimation of nitrification and denitrification from microprofiles of oxygen and nitrate in model sediment systems. Appl environ Microbiol 60:2094–2100

Jensen MH, Andersen TK, Sørensen J (1988) Denitrification in coastal bay sediment: regional and seasonal variation in Aarhus Bight, Denmark. Mar Ecol Prog Ser 48:155–162

Kemp WM, Sampou P, Caffrey J, Mayer M, Henriksen K, Boynton WR (1990) Ammonium recycling versus denitrification in Chesapeake Bay sediments. Limnol Oceanogr 35:1545–1563

Law CS, Owens NJP (1990) Denitrification and nitrous oxide in the North Sea. Neth J Sea Res 25:65–74

Li YH, Gregory S (1974) Diffusion of ions in sea water and in deep sea sediments. Geochim cosmochim Acta 38: 703–714

Lohse L, Malschaert JFP, Slomp CP, Helder W, van Raaphorst W (1993) Nitrogen cycling in North Sea sediments: interaction of denitrification and nitrification in offshore and coastal areas. Mar Ecol Prog Ser 101:283–296

Lohse L, Malschaert JFP, Slomp CP, Helder W, van Raaphorst W (1995) Sediment-water fluxes of inorganic nitrogen compounds along the transport route of organic matter in the North Sea. Ophelia 41:173–197

Nielsen LP (1992) Denitrification in sediment determined from nitrogen isotope pairing. FEMS Microbiol Ecol 86: 357–362

Nielsen LP, Christensen PB, Revsbech NP, Sørensen J (1990) Denitrification and photosynthesis in stream sediment studied with microsensor and whole-core techniques. Limnol Oceanogr 35:1135–1144

Nishio T, Koike I, Hattori A (1983) Estimates of denitrification and nitrification in coastal and estuarine sediments. Appl environ Microbiol 45:444–450

Nixon SW (1981) Remineralisation and nutrient cycling in coastal marine ecosystems. In: Neilson B, Cronin LE (eds) Nutrient enrichment in estuaries. Humana Press, Clifton, NJ, p 111–138

Nowicki BL (1994) The effect of temperature, oxygen, salinity, and nutrient enrichment on estuarine denitrification rates measured with a modified nitrogen gas flux technique. Estuar coast Shelf Sci 38:137–156

Oremland RS, Umberger C, Culbertson CW, Smith RA (1984) Denitrification in San Francisco Bay intertidal sediments. Appl environ Microbiol 47:1106–1112

Pelegrí SP, Nielsen LP, Blackburn TH (1994) Denitrification in estuarine sediment stimulated by the irrigation activity of the amphipod *Corophium volutator*. Mar Ecol Prog Ser 105:285–290

Rasmussen H, Jørgensen BB (1992) Microelectrode studies of seasonal oxygen uptake in a coastal sediment: role of molecular diffusion. Mar Ecol Prog Ser 81:289–303

Revsbech NP, Jørgensen BB (1986) Microelectrodes: their use in microbial ecology. In: Marshall KC (ed) Advantages in microbial ecology 9. Plenum, New York, p 293–351

Risgaard-Petersen N, Rysgaard S, Nielsen LP, Revsbech NP (1994) Diurnal variation of denitrification and nitrification in sediments colonized by benthic microphytes. Limnol Oceanogr 39:573–579

Rönner U (1985) Nitrogen transformations in the Baltic proper: denitrification counteracts eutrophication. Ambio 14:134–138

Ruardij P, van Raaphorst W (1995) Benthic nutrient regeneration in the ERSEM ecosystem model of the North Sea. Neth J Sea Res 33:453–483

Rudolph J, Frenzel P, Pfennig N (1991) Acetylene inhibition technique underestimates *in situ* denitrification rates in intact sediment cores of freshwater sediment. FEMS Microb Ecol 85:101–106

Rysgaard S, Risgaard-Petersen N, Sloth NP, Jensen K, Nielsen LP (1994) Oxygen regulation of nitrification and denitrification in sediments. Limnol Oceanogr 39: 1643–1652

Saager PM, Sweerts JP, Ellermeijer HJ (1990) A simple porewater sampler for coarse, sandy sediments of low porosity. Limnol Oceanogr 35:747–751

Seitzinger SP (1987) Nitrogen biogeochemistry in an unpolluted estuary: the importance of benthic denitrification. Mar Ecol Prog Ser 37:65–73

Seitzinger SP (1988) Denitrification in freshwater and coastal marine ecosystems: ecological and geochemical evidence. Limnol Oceanogr 33:702–724

Seitzinger SP (1990) Denitrification in aquatic sediments. In: Revsbech NP, Sørensen J (eds) Denitrification in soil and sediment. FEMS Symposium, Plenum Press, New York, p 301–322

Seitzinger SP, Nielsen LP, Caffrey J, Christensen PB (1993) Denitrification in aquatic sediments: a comparison of three methods. Biogeochemistry 23:147–167

Seitzinger SP, Nixon S, Pilson MEQ, Burke S (1980) Denitrification and N_2O production in near-shore marine sediments. Geochim cosmochim Acta 44:1853–1860

Slater JM, Capone DG (1989) Nitrate requirement for acetylene inhibition of nitrous oxide reduction in marine sediments. Microb Ecol 17:143–157

Sloth NP, Blackburn TH, Hansen LS, Risgaard-Petersen N, Lomstein BA (1995) Nitrogen cycling in sediments with different organic loads. Mar Ecol Prog Ser 116:163–170

Sørensen J (1978) Denitrification rates in a marine sediment as measured by the acetylene inhibition technique. Appl environ Microbiol 36:139–143

Strickland JD, Parsons TR (1972) A practical handbook of seawater analysis, 2nd edn. Bull Fish Res Bd Can 167: 71–76

Thompson SA, Paerl HW, Go MC (1995) Seasonal patterns of nitrification and denitrification in a natural and a restored salt marsh. Estuaries 18:399–408

Ullman WJ, Aller RC (1982) Diffusion coefficients in near-shore marine sediments. Limnol Oceanogr 27:552–556

van Raaphorst W, Kloosterhuis HT, Berghuis EM, Gieles AJM, Malschaert JFP, van Noort GJ (1992) Nitrogen cycling in two types of sediments of the southern North Sea (Frisian Front, Broadfourteens): field data and mesocosm results. Neth J Sea Res 28:293–316

van Raaphorst W, Kloosterhuis HT, Cramer A, Bakker KJM (1990) Nutrient early diagenesis in the sediments of the Dogger Bank area, North Sea: pore water results. Neth J Sea Res 26:25–52

Walter HM, Keeney DR, Fillery IR (1979) Inhibition of nitrification by acetylene. Soil Sci Soc Am J 43:195–196

Weiss RF (1970) The solubility of nitrogen, oxygen and argon

in seawater. Deep Sea Res 17:721–735
Weiss RF, Price BA (1980) Nitrous oxide solubility in water and seawater. Mar Chem 8:347–359

Yoshinari T, Knowles R (1976) Acetylene inhibition of nitrous oxide reduction by denitrifying bacteria. Biochem biophys Res Commun 69:705–710

This article was submitted to the editor

Manuscript first received: April 18, 1995
Revised version accepted: August 29, 1995

Reeds verschenen BEON rapporten:

BEON rapport nr.	1.	BEON Meerjarenplan 1988-1993.	1987
BEON rapport nr.	2.	BEON Jaarwerkplan 1988.	1988
BEON rapport nr.	3.	BEON Modellering.	1988
BEON rapport nr.	4.	BEON meerjaren Uitvoeringsprogramma 1988-1993.	1989
BEON rapport nr.	5.	BEON Jaarwerkplan 1989.	1989
BEON rapport nr.	6.	Findings of the BEON Workshop in preparation for the Third North Sea Conference.	1989
BEON rapport nr.	7.	Beleidspresentatie BEON 23 juni 1989 Den Haag.	1989
BEON rapport nr.	8.	Effects of Beamtrawl Fishery on the Bottom Fauna in the North Sea.	1990
BEON rapport nr.	9.	BEON Jaarwerkplan 1990.	1990
BEON rapport nr.	10.	BEON Voortgangsrapport 1988-1989.	1990
BEON rapport nr.	11.	Beleidspresentatie BEON 31 mei 1990 Den Haag.	1990
BEON rapport nr.	12.	Beleidspresentatie BEON 20 juni 1991 Den Haag.	1991
BEON rapport nr.	13.	Effects of Beamtrawl Fishery on the Bottom Fauna in the North Sea. II. The 1990 - studies.	1990
BEON rapport nr.	13 A.	BEON Jaarwerkplan 1991.	1991
BEON rapport nr.	14.	BEON Jaarwerkplan 1992.	1992
BEON rapport nr.	15.	Beleidspresentatie BEON 19 juni 1992 Den Haag.	1992
BEON rapport nr.	16.	Effect of Beamtrawl Fishery on the Bottom Fauna in the North Sea. III. The 1991 - studies.	1992
BEON rapport nr.	17.	Beleidspresentatie BEON 12 december 1991.	1992
BEON rapport nr.	18.	Trace Element Geochemistry at the Sediment Water Interface in the North Sea and the Western Wadden Sea.	1993
BEON rapport nr.	19.	Effecten van met benzo(a)pyreen verontreinigd sediment op de Helmkrab (Corystes cassivelaunus). Rapportage Project BEONADD I/II.I	1993
BEON rapport nr.	20.	Scavenging seabirds behind fishing vessels in the Northeast Atlantic. (With emphasis on the Southern North Sea).	1993
BEON rapport nr.	21	Brug tussen Beleid en Onderzoek (Rapportage over het eerste BEON Meerjarenprogramma 1988-1992).	1993
BEON rapport nr.	93-1	Naar een duurzame ontwikkeling van de Noordzee. (Tweede Meerjarenprogramma BEON1993-1997).	1993
BEON rapport nr.	93-2	The appearance of scars on the shell of Arctica Islandica L. (Mollusca, Bivalvia) and their relation to bottom trawl fishery.	1993
BEON rapport nr.	93-3	BEON Jaarwerkplan 1993.	1993
BEON rapport nr.	93-4	BEON Beleidspresentatie "Zee en Wadvogels. "Voorkomen en invloeden daarop" d.d. 10 december 1993.	1993

1994

BEON rapport nr. 94-1	Philippart, C.J.M. & Groodt, E.G. de & Brinkman, A.G. & Jak, R.G. & Scholten, M.C.Th., Effecten van verschuivingen van nutriëntenconcentraties op biota in de Nederlandse kustwateren (IBN 93 E 02).
BEON rapport nr. 94-2	Kaag, N.H.B.M. et al., BENTOX: Toxische effecten van microverontreinigingen in sediment:- deel 1, Verkennend onderzoek met natuurlijke verontreinigde sedimenten (TNO 93 M 04/TNO 94 M 06).
BEON rapport nr. 94-3	Jaarwerkplan 1994.
BEON rapport nr. 94-4	Riegman, R., jaarverslag 1993: Algenonderzoek in mesocosms en modelleringlering (NIOZ 93 E 01).
BEON rapport nr. 94-5	Veer, H.W. van der, Impact of anthropogenic activities on the productivity of the western Wadden Sea ecosystem (NIOZ 93 E 02).
BEON rapport nr. 94-6.1	Ruardij, P. and W. van Raaphorst. Bentic nutriënt generation in the ERSEM ecosystem model of the North Sea. (NIOZ 93 E 03)
BEON rapport nr. 94-6.2	J.P.C. Smit, A.G. Brinkman, E.G.M. Embsen, P. Ruardij, and W. van Raaphorst. The Eco-Wasp model and it's environment. (NIOZ 93 E 03).
BEON rapport nr. 94-7	Risico-analyse Mariene Systemen (RAM*2 project) Eindrapport van de RAM-Auditgroep.
BEON rapport nr. 94-8	Michielsen, H & Berg, A. van den & Joordens, J., et al. Comparison of models describing species composition of marine phytoplankton (project MANS-FYFY, WL 93 E 01).
BEON rapport nr. 94-9	Verslag BEON Workshop Risico-analyse, d.d. 27 april 1994, Den Haag.
BEON rapport nr. 94-10	BEON Beleidspresentatie "Microverontreinigingen: effecten en trends", d.d. 21 juni 1994.
BEON rapport nr. 94-11	De epi- en endofauna van de Nederlandse, Duitse en Deense kustzone: een analyse van 20 jaar bijvangsgegevens. J. Buijs, J.A. Craeymeersch, P. van Leeuwen, A.D. Rijnsdorp. (BEONADD IIV/V)
BEON rapport nr. 94-12	De inductie van cytochroom P450 1 A in platvis door blootstelling aan polyaromatische koolwaterstoffen in de Noordzee. INP-programma 1991- 1992. (NIOZ 93 M 05).
BEON rapport nr. 94-13	Bergman, M.J.N. en J.W. van Santbrink. Directe effecten van de visserij met de 12m en 4m boomkorren op het bodemleven in de Nederlandse sector van de Noordzee. (NIOZ 93 V 07).
BEON rapport nr. 94-14	Camphuysen, C.J. Scavenging seabirds at beamtrawlers in the southern North Sea, distribution, relative abundance, behaviour, prey selection, feeding efficiency, kleptoparastism and the possible effects of the establishment of protected areas'. (BEONADD IIV/V).
BEON rapport nr. 94-15	Spaans, A.L., M. BukaciÑska, D. BukaciÑska. the relationship between food supply, reproductive parameters and population dynamics in Dutch Lesser Black-backed Gulls Larus fuscus: a pilot study. (BEONADD IV/V)
BEON rapport nr. 94-16	Brenninkmeijer, A. & E.W. M. Stienen. Pilot study on the influence of feeding conditions at the North Sea on the breeding results of the Sandwich Tern Sterna sandvicensis. (BEONADD IV/V)
BEON rapport nr. 94-17	Boddeke, R. en P. Hagel. BEON-studie naar de effecten van de teruglopende nutriëntenbelasting van de Nederlandse kustzone. (RIVO 93 E 03).

1995

BEON rapport nr. 95-1	Effecten van de schelpdiervisserij op het bodemleven in de Voordelta (RIVO 94 V 06).
BEON rapport nr. 95-2	Jaarwerkplan 1995.
BEON rapport nr. 95-3	Trends in het voorkomen van vissen en epibenthische evertebraten in de Noordzee: Een vergelijking van datasets. (NIOZ 93 A 04)
BEON rapport nr. 95-4	De ontwikkeling van een in vitro assay voor de bepaling van de invloed van biotransformatie op de bioaccumulatie van lipofiele organohalogeen verbindingen in mariene toppredatoren. I. Validatie van de assay met PCBS en de eerste resultaten met Toxafeen. Boon, J.P., van Schanke, A., Roex, E., de Boer, J., Wester, P. (NIOZ 94 M 01).
BEON rapport nr. 95-5	BEON beleidspresentatie "Ontwikkelingen in het beleid", d.d. 9 december 1994.

BEON rapport nr. 95-6 BEON beleidspresentatie "Modellering: de stand van zaken en het belang voor beleid en beheer", d.d. 31 maart 1995.

BEON rapport nr. 95-7 De visserij-intensiteit van de Nederlandse boomkorvisserij op de Noordzee, mede in het licht van de milieu-effecten en gesloten gebieden. Wetenschappelijke discussie BEON 18 mei 1995 Den Haag.

BEON rapport nr. 95-8 Antropogene eutrofiëring en natuurlijke variaties. Consequenties voor de produktiviteit van de Noordzee. INP-MOORING/PELAGIC FOOD WEB/STED/ STRAECOS. (NIOZ 94 E 01).

BEON rapport nr. 95-9 Effecten van antropogene aktiviteiten op de produktiviteit van het ecosysteem in de Westelijke Waddenzee. (NIOZ 93 E 02).

BEON rapport nr. 95-11 Biomarkers of Toxic effects chemoreceprion: effects of contaminated dredge spoil on chemo-reception acuity in whelks. Ten Hallers-Tjabbes, C. and C.V. Fisher, 1994. (NIOZ 93 M 05).

BEON rapport nr. 95-12 Habitatkarakteristieken van de Nederlandse kustzone, Wintermans, C. et al. (IBN 94 H 02).

BEON rapport nr. 95-13 BEON Tweejaarverslag 1993-1994. Onderzoek en beleid kiezen samen het ruime sop; PB-BEON; augustus 1995.

BEON rapport nr. 95-14 Toxische algen tussen Noordwijk- en Terschelling-raai. Peperzak, L. et al. (RIKZ 94 E 05; RKZ-040).

BEON rapport nr. 95-15 ELTEVIER (voorlopige titel). Bergman, M. et al (NIOZ 94 V 01).

BEON rapport nr. 95-16 Intercallibratie en toepassing Noordzee-modellen (MANS-FYFY) fase 2. (WL 94 E 04).

1996

BEON rapport nr. 96-1 De ontwikkeling van een in-vitro assay voor de bepaling van de invloed van biotransformatie op de bioaccumulatie en de mutageniteit van lipofiele organohalogeenverbindingen in mariene top-predatoren. II. Toxafeen. J.P. Boon, H.M. Sleiderink, J. De Boer, P. Wester, H.J. Klamer, B. Govers. (NIOZ 95 M 03).

BEON rapport nr. 96-2 Spisula subtruncata als voedselbron voor Zeeëenden in Nederland. Leopold, M.F. (IBN 95 V 29).

BEON rapport nr. 96-3 BENTOX . Toxische effecten van verontreinigde sedimenten voor marien benthos. 1e fase: Verkennend onderzoek met "natuurlijk' verontreinigde sedimenten, 2e fase: Benzo(a)pyreen en fluoranteen, 3e fase: BaP concentratiereeks (TNO 93 M 04, TNO 94 M 06, TNO 95 M 16).

BEON rapport nr. 96-4 Algenbegrazing: Een nadere analyse van de invloed van toxicanten op het ontstaan van eutro-fiëringsproblemen. Jak, R.G., Michielsen, B.F. (TNO 95 E 07).

BEON rapport nr. 96-5 Habitatkartering en beschrijving Nederlandse kustwateren (IBN 95 H 36).

BEON rapport nr. 96-6 Onderzoek naar de invloed van fluctuaties in de lokale voedselbeschikbaarheid op de populatie-dynamiek van de grote stern Sterna sandvicensis: tussentijdse resultaten. Stienen, E.W.M. & A. Brenninkmeijer. (IBN 95 H 24).

BEON rapport nr. 96-7 Verslag van de BEON Workshop in het kader van de voorbereiding van de vierde Nota waterhuishouding (NW4). Gehouden op 30 november en 1 december 1995 bij het NIOZ op Texel.

BEON rapport nr. 96-8 Thema bijeenkomst Boomkorvisserij.

BEON rapport nr. 96-9 Jaarwerkplan 1996.

BEON rapport nr. 96-10 SCREMOTOX (WL 95 M 21).

BEON rapport nr. 96-11 Effecten van de schelpdiervisserij op het bodemleven in de Voordelta: De schelpdierbestanden in de Voordelta in 1995. Van der Land, M.A. (RIVO 95 V 30).

BEON rapport nr. 96-12 Verslag van de BEON workshop ter voorbereiding van de Nederlandse inbreng van de tussen-conferentie van Noordzee- en Visserijministers (IMM 97).

BEON rapport nr. 96-13 BEON thema bijeenkomst polycyclische aromatische koolwaterstoffen (PAK's). 22 februari 1996 Den Haag.

BEON rapport nr. 96-14 Evaluatierapport BEON 1996. Tussentijdse evaluatie Tweede Meerjarenprogramma BEON 1993-1997. Rapport naar aanleiding van de BEON evaluatieworkshop d.d. 2 februari 1996, Den Haag.

BEON rapport nr. 96-15 Onderzoek naar de mogelijkheden tot vermindering van discard productie door technische aanpassing van boomkornetten (NIOZ 95 V 05).

Informatie BEON:

PROGRAMMA BUREAU BEON
p/a Directoraat-Generaal Rijkswaterstaat
Rijks Instituut voor Kust en Zee
Kortenaerkade 1
2518 AX Den Haag
Postbus 20907
2500 EX Den Haag
070- 3114257/3114258/3114259/3114260
Telefax: 070- 311432

e-mail: beon@rikz.rws.minvenw.nl.

